UNCLASSIFIED

AD NUMBER
AD912980
LIMITATION CHANGES
TO: **Approved for public release; distribution is unlimited.**
FROM: **Distribution authorized to U.S. Gov't. agencies only; Test and Evaluation; AUG 1973. Other requests shall be referred to Air Force Armament Laboratory, Attn: DLTI, Eglin AFB, FL 32542.**
AUTHORITY
AFATL ltr, 24 Oct 1975

THIS PAGE IS UNCLASSIFIED

AEDC-TR-73-145
AFATL-TR-73-169

SEP 26 1973
APR 3 1979
JUN 27 1989

Cy 2

SEPARATION CHARACTERISTICS OF SEVERAL MUNITIONS FROM THE F-4C AND F-111E AIRCRAFT AT MACH NUMBERS FROM 0.9 TO 1.6

J. B. Carman

ARO, Inc.

TECHNICAL REPORTS
FILE COPY

PROPERTY OF U.S. AIR FORCE
AEDC TECHNICAL LIBRARY

August 1973

This document has been approved for public release
Per TAB 76-4
13 Feb, 1976

Distribution limited to U.S. Government agencies only; this report contains information on test and evaluation of military hardware; August 1973; other requests for this document must be referred to Air Force Armament Laboratory (AFATL/DLJA), Eglin AFB, FL 32542.

PROPULSION WIND TUNNEL FACILITY
ARNOLD ENGINEERING DEVELOPMENT CENTER
AIR FORCE SYSTEMS COMMAND
ARNOLD AIR FORCE STATION, TENNESSEE

Property of U. S. Air Force
AEDC LIBRARY
F40600-74-C-0001

NOTICES

When U. S. Government drawings specifications, or other data are used for any purpose other than a definitely related Government procurement operation, the Government thereby incurs no responsibility nor any obligation whatsoever, and the fact that the Government may have formulated, furnished, or in any way supplied the said drawings, specifications, or other data, is not to be regarded by implication or otherwise, or in any manner licensing the holder or any other person or corporation, or conveying any rights or permission to manufacture, use, or sell any patented invention that may in any way be related thereto.

Qualified users may obtain copies of this report from the Defense Documentation Center.

References to named commercial products in this report are not to be considered in any sense as an endorsement of the product by the United States Air Force or the Government.

SEPARATION CHARACTERISTICS OF SEVERAL MUNITIONS FROM THE F-4C AND F-111E AIRCRAFT AT MACH NUMBERS FROM 0.9 to 1.6

J. B. Carman
ARO, Inc.

This document has been approved for public release its distribution is unlimited. Per TAB 76-4
13 Feb, 1976

Distribution limited to U.S. Government agencies only; this report contains information on test and evaluation of military hardware; August 1973; other requests for this document must be referred to Air Force Armament Laboratory (AFATL/DLJA), Eglin AFB, FL 32542.

FOREWORD

The work reported herein was done by the Arnold Engineering Development Center (AEDC), Air Force Systems Command (AFSC), and sponsored by the Air Force Armament Laboratory (AFATL/DLJA), Air Force Systems Command (AFSC), under Program Element 64602F, Project 5613.

The test results presented were obtained by ARO, Inc. (a subsidiary of Sverdrup & Parcel and Associates, Inc.), contract operator of the AEDC, AFSC, Arnold Air Force Station, Tennessee. The tests were conducted from September 18 through 29, 1972 and June 12 through 14, 1973, under ARO Project No. PA013. The manuscript was submitted for publication on July 11, 1973.

This technical report has been reviewed and is approved.

L. R. KISSLING
Lt Colonel, USAF
Chief Air Force Test Director, PWT
Directorate of Test

FRANK J. PASSARELLO
Colonel, USAF
Director of Test

ABSTRACT

Wind tunnel tests were conducted using 0.05- and 0.0416-scale models to study the separation characteristics of several munitions from the F-4C and F-111E aircraft, respectively. For the F-4C tests, separation trajectories of the MK-82 GPB, SUU-30H/B, MK-20 "Rockeye," MK-84 GPB, MK-84 LGB, and MK-84 EOGB stores were initiated from a multiple ejection rack (MER) on the right wing outboard and centerline pylons or from the right wing outboard and inboard pylons alone. Data were obtained at Mach numbers from 1.05 to 1.6 at simulated altitudes of 5,000 to 30,000 ft. Other simulated flight variables included dive angle (0 to 60 deg), parent aircraft acceleration (1 to 3g), and store cg position. For the F-111E tests, separation trajectories of the SUU-30H/B store were inititated from a multiple rack (BRU-3A/A) on the numbers 3 and 6 pylons or from pylon numbers 4 and 6 alone. Data were obtained at Mach numbers from 0.9 to 1.3 at simulated altitudes of 5,000 to 20,000 ft. Other simulated flight variables included parent-aircraft wing sweep angle (50 and 72.5 deg) and different ejector forces.

This document has been approved for public release its distribution is unlimited. Per TAB 76-4 13 Feb, 1976

Distribution limited to U.S. Government agencies only; this report contains information on test and evaluation of military hardware; August 1973; other requests for this document must be referred to Air Force Armament Laboratory (AFATL/DLJA), Eglin AFB, FL 32542.

CONTENTS

APPENDIXES

NOMENCLATURE

a_Z — Aircraft acceleration along the Z_F axis, positive direction is down as viewed by the pilot, ft/sec^2

BL — Aircraft buttock line from plane of symmetry, in., model scale

b — Store reference dimension, ft, full scale

C_A — Store axial-force coefficient, axial force/$q_\infty S$

C_ℓ — Store rolling-moment coefficient, rolling moment/$q_\infty Sb$

C_{ℓ_p} — Store roll-damping derivative, $dC_\ell/d(pb/2V_\infty)$

C_m Store pitching-moment coefficient, referenced to the store cg, pitching moment/$q_\infty Sb$

C_{m_q} Store pitch-damping derivative, $dC_m/d(qb/2V_\infty)$

C_n Store yawing-moment coefficient, referenced to the store cg, yawing moment/$q_\infty Sb$

C_{n_r} Store yaw-damping derivative, $dC_n/d(rb/2V_\infty)$

FS Aircraft fuselage station, in., model scale

F_{Z_1} Forward ejector force, lb

F_{Z_2} Aft ejector force, lb

H Pressure altitude, ft

I_{xx} Full-scale moment of inertia about the store X_B axis, slug-ft^2

I_{yy} Full-scale moment of inertia about the store Y_B axis, slug-ft^2

I_{zz} Full-scale moment of inertia about the store Z_B axis, slug-ft^2

M_∞ Free-stream Mach number

$\overline{m}$ Full-scale store mass, slugs

p Store angular velocity about the X_B axis, radians/sec

q Store angular velocity about the Y_B axis, radians/sec

q_∞ Free-stream dynamic pressure, psf

r Store angular velocity about the Z_B axis, radians/sec

S Store reference area, ft^2, full scale

t Real trajectory time from initiation of trajectory, sec

V_∞ Free-stream velocity, ft/sec

WL Aircraft waterline from reference horizontal plane, in., model scale

X Separation distance of the store cg parallel to the flight axis system X_F direction, ft, full scale measured from the prelaunch position

X_{cg} Full-scale cg location, ft, from nose of store

X_{L_1} Forward ejector piston location relative to the store cg, positive forward of store cg, ft, full scale

X_{L_2} Aft ejector piston location relative to the store cg, positive forward of store cg, ft, full scale

Y Separation distance of the store cg parallel to the flight axis system Y_F direction, ft, full scale measured from the prelaunch position

Z Separation distance of the store cg parallel to the flight-axis system Z_F direction, ft, full scale measured from the prelaunch position

α_p Parent-aircraft model angle of attack relative to the free-stream velocity vector, deg

γ Simulated parent-aircraft dive angle; angle between the flight direction and the earth horizontal, deg, positive for decreasing altitude

θ Angle between the store longitudinal axis and its projection in the X_F-Y_F plane, positive when store nose is raised as seen by pilot, deg

Λ_{LE} Wing leading edge sweep angle, deg

ϕ Angle between the projection of the store lateral axis in the Y_F-Z_F plane and the Y_F axis, positive for clockwise rotation when looking upstream, deg

ψ Angle between the projection of the store longitudinal axis in the X_F-Y_F plane and the X_F axis, positive when the store nose is to the right as seen by the pilot, deg

ψ_p Parent-aircraft model angle of yaw relative to the free-stream velocity vector, deg

FLIGHT-AXIS SYSTEM COORDINATES

Directions

X_F Parallel to the free-stream wind vector, positive direction is forward as seen by the pilot

Y_F Perpendicular to the X_F and Z_F directions, positive direction is to the right as seen by the pilot

Z_F In the aircraft plane of symmetry, perpendicular to the free-stream wind vector, positive direction is downward

The flight-axis system origin is coincident with the aircraft cg and remains fixed with respect to the parent aircraft during store separation. The X_F, Y_F, and Z_F coordinate axes do not rotate with respect to the initial flight direction and attitude.

STORE BODY-AXIS SYSTEM COORDINATES

Directions

X_B Parallel to the store longitudinal axis, positive direction is upstream in the prelaunch position

Y_B Perpendicular to the store longitudinal axis, and parallel to the flight-axis system X_F-Y_F plane when the store is at zero roll angle, positive direction is to the right looking upstream when the store is at zero yaw and roll angles

Z_B Perpendicular to both the X_B and Y_B axes, positive direction is downward as seen by the pilot when the store is at zero pitch and roll angles.

The store body-axis system origin is coincident with the store cg and moves with the store during separation from the parent airplane. The X_B, Y_B, and Z_B coordinate axes rotate with the store in pitch, yaw, and roll so that mass moments of inertia about the three axes are not time-varying quantities.

SECTION I
INTRODUCTION

Wind tunnel store separation data for six munitions launched from the F-4C aircraft and one munition launched from the F-111E aircraft were obtained using a six-degree-of-freedom captive trajectory store separation system (CTS). The tests were conducted in the Aerodynamic Wind Tunnel (4T) of the Propulsion Wind Tunnel Facility (PWT) using 0.05-scale models for the F-4C test phase and 0.0416-scale models for the F-111E test phase. All trajectory data were obtained using simulated full-scale store parameters.

For the F-4C tests, separation trajectories for three stores (MK-82 GPB, SUU-30H/B, and MK-20 "Rockeye") were initiated from a multiple ejection rack (MER) mounted on either the right wing outboard pylon or centerline pylon while separation trajectories for the MK-84 GPB, MK-84 LGB, and MK-84 EOGB stores were initiated from either the inboard or outboard pylons of the right wing. Mach number was varied from 1.05 to 1.6 and simulated flight variables included altitude and store cg position along with parent aircraft angles of attack, dive angle, and acceleration.

For the F-111E tests, separation trajectories of the SUU-30H/B store were initiated from a multiple rack (BRU-3A/A) mounted on the number 3 or 6 pylon and from the numbers 4 and 6 pylons alone. Mach number was varied from 0.9 to 1.3 and simulated flight variables included altitude and ejector forces along with parent-aircraft angles of attack and wing sweep angles.

SECTION II
APPARATUS

2.1 TEST FACILITY

The Aerodynamic Wind Tunnel (4T) is a closed-loop, continous flow, variable-density tunnel in which the Mach number can be varied from 0.1 to 1.3, and operated at Mach 1.6 and 2.0 by placing nozzle inserts over the present nozzle configuration. At all Mach numbers, the stagnation pressure can be varied from 300 to 3700 psfa. The test section is 4 ft square and 12.5 ft long with perforated, variable porosity (0.5- to 10-percent open) walls. It is completely enclosed in a plenum chamber from which the air can be evacuted, allowing part of the tunnel airflow to be removed through the perforated walls of the test section.

For store separation testing, two separate and independent support systems are used to support the models. The parent aircraft model is inverted in the test section and supported by an offset sting attached to the main pitch sector. The store model is supported by the CTS which extends down from the tunnel top wall and provides store movement (six degreees of freedom) independent of the parent-aircraft model. An isometric drawing of a typical store separation installation is shown in Fig. 1, Appendix I.

Also shown in Fig. 1 is a block diagram of the computer control loop used during captive trajectory testing. The analog system and the digital computer work as an integrated unit and, utilizing required input information, control the store movement during a trajectory. Store positioning is accomplished by use of six individual d-c electric motors. Maximum translational travel of the CTS is ±15 in. from the tunnel centerline in the lateral and vertical directions and 36 in. in the axial direction. Maximum angular displacements are ±45 deg in pitch and yaw and ±360 deg in roll. A more complete description of the test facility can be found in Ref. 1. A schematic showing the test section details and the location of the models in the tunnel is shown in Fig. 2.

2.2 TEST ARTICLES

The basic dimensions of the 0.05-scale F-4C parent model and 0.0416-scale F-111E parent model are presented in Figs. 3a and b, respectively. The parent models are geometrically similar to the full-scale airplanes except that the tail sections are removed to minimize interference with CTS support movement.

Details of the F-4C pylons and MER are shown in Figs. 4 and 5, respectively, and the F-111E TAC pylon and BRU-3A/A rack details are presented in Fig. 6. The MER was aligned with the 30-in. suspension lug positions on the pylons and the BRU-3A/A was mounted as indicated. Fuel tanks for the F-4C are shown in Fig. 7. Details of the store models are given as follows: ALQ-119 (Fig. 8), AGM-65 (Fig. 9), MK-82 GPB (Fig. 10), SUU-30H/B (Figs. 11 and 12), MK-20 Rockeye (Fig. 13), MK-84 GPB (Fig. 14), MK-84 LGB (Fig. 15), and MK-84 EOGB (Fig. 16). The numbering sequence and roll orientation of the stores for the MER and BRU-3A/A stations are shown in Fig. 17. Typical tunnel installation photographs showing parent aircraft, store model, and CTS are shown in Fig. 18.

2.3 INSTRUMENTATION

Internal strain-gage balances of four, five, and six components were used to obtain store aerodynamic force and moment data. Translational and angular positions of the store were obtained from CTS analog inputs, and parent-model angle of attack was determined using the main pitch sector. The pylons, BRU-3A/A, and MER contained a touch wire system which enabled the store to be accurately positioned for launch. The system was also wired to automatically stop the CTS motion and give visual indication should the store or sting support make contact with any surface other than the touch wire.

SECTION III
TEST DESCRIPTION

3.1 TEST CONDITIONS

Separation trajectory data were obtained at the wind tunnel test conditions listed in the table below. Simulated pressure altitude for each wind tunnel test condition is also shown.

M_∞	p_t,psf	T_t,°F	q_∞,psf	Parent Aircraft	Λ_{LE}	H,ft
1.05	1300	100	500	F-4C	—	5,000
1.15	1230	↓	↓	↓	↓	10,000
1.25	1180	↓	↓	↓	↓	15,000
1.30	1170	↓	↓	↓	↓	20,000
1.60	1200	↓	↓	↓	↓	30,000
0.90	1490	100	500	F-111E	50	5,000
0.95	1410	↓	↓	↓	50, 72.5	
1.05	1300	↓	↓	↓	↓	
1.10	1260	↓	↓	↓	72.5	10,000
1.15	1230	↓	↓	↓	50, 72.5	12,000*
1.15	1230	↓	↓	↓	72.5	15,000
1.20	1200	↓	↓	↓	↓	20,000
1.30	1170	↓	↓	↓	↓	18,000

*BRU-3A/A racks off for this condition

Tunnel conditions were held constant at the desired Mach number and stagnation pressure while data for each trajectory were obtained. The trajectories were terminated when the store or sting contacted the parent-aircraft model or when a CTS limit was reached.

3.2 TRAJECTORY DATA ACQUISITION

To obtain a trajectory, test conditions were established in the tunnel and the parent model was positioned at the desired angle of attack. The store model was then oriented to a position corresponding to the store carriage location. After the store was set at the desired initial position, operational control of the CTS was switched to the digital computer which controlled the store movement during the trajectory through commands to the CTS analog system (see block diagram, Fig. 1). Data from the wind tunnel, consisting of measured model forces and moments, wind tunnel operating conditions, and CTS rig positions, were input to the digital computer for use in the full-scale trajectory calculations.

The digital computer was programmed to solve the six-degree-of-freedom equations to calculate the angular and linear displacements of the store relative to the parent aircraft pylon (Ref. 2). In general, the program involves using the last two successive measured values of each static aerodynamic coefficient to predict the magnitude of the coefficients over the next time interval of the trajectory. These predicted values are used to calculate the new position and attitude of the store at the end of the time interval. The CTS is then commanded to move the store model to this new position and the aerodynamic loads are measured. If these new measurements agree with the predicted values, the process is continued over another time interval of the same magnitude. If the measured and predicted values do not agree within the desired precision, the calculation is repeated over a time interval one-half the previous value. This process is repeated until a complete trajectory has been obtained.

In applying the wind tunnel data to the calculations of the full-scale store trajectories, the measured forces and moments are reduced to coefficient form and then applied with proper full-scale store dimensions and flight dynamic pressure. Dynamic pressure was calculated using a flight velocity equal to the free-stream velocity component plus the components of store velocity relative to the aircraft, and a density corresponding to the simulated altitude.

The initial portion of each launch trajectory incorporated simulated ejector forces in addition to the measured aerodynamic forces acting on the store. The ejector force was considered to act perpendicularly to the rack mounting surface. The ejector forces and locations along with other full-scale store parameters used in the trajectory calculations are listed in Table I, Appendix II.

3.3 CORRECTIONS

Balance, sting, and support deflections caused by the aerodynamic loads on the store models were accounted for in the data reduction program to calculate the true store-model angles and coordinates. Corrections were also made for model weight tares to calculate the net aerodynamic forces on the store model.

3.4 PRECISION OF DATA

The trajectory data are subject to error from several sources including tunnel conditions, balance measurements, extrapolation tolerances allowed in the predicted coefficients, computer inputs, and CTS positioning control. Maximum error in the CTS position control was ±0.05 in. for the translational settings and ±0.15 deg for the angular settings in pitch and yaw. Extrapolation tolerances were ±0.10 for the aerodynamic coefficients. The estimated uncertainty in setting Mach number was ±0.005, and uncertainty in parent-model angle of attack was estimated to be ±0.1 deg. The maximum uncertainties in the full-scale position data caused by the balance inaccuracies are given below:

Store	t,sec	X,ft	Y,ft	Z,ft	θ,deg	ψ,deg	ϕ,deg
MK-82 GPB	0.2	±0.1	±0.1	±0.1	±0.8	±0.6	—
SUU-30H/B (5 percent)	0.2	±0.1	±0.1	±0.1	±1.3	±1.3	—
MK-20	0.2	±0.1	±0.1	±0.1	±1.6	±1.5	—
MK-84 GPB	0.2	±0.1	±0.1	±0.1	±0.1	±0.1	±0.9
MK-84 LGB	0.2	±0.1	±0.1	±0.1	±0.1	±0.1	±1.0
MK-84 EOGB	0.2	±0.1	±0.1	±0.1	±0.1	±0.1	±0.9
SUU-30H/B (4.16 percent)	0.2	±0.1	±0.1	±0.1	±0.5	±0.4	—

SECTION IV
RESULTS AND DISCUSSION

All trajectories obtained were for use in the determination of safe separation envelopes of the respective munitions from the F-4C and F-111E aircraft. No attempt will be made in this report to establish these envelopes or to qualify the store as safe or unsafe for aircraft separation. The trajectory data are presented as obtained from the wind tunnel along with comments regarding the aerodynamics of the store in the aircraft flow field.

Data taken during these tests consisted of ejector-separated trajectories simulating release from multiple carriage racks or from pylons alone. Data showing the linear displacements of stores relative to the carriage position and the angular displacements relative to the flight-axis system are presented as functions of full-scale trajectory time. Positive X, Y, and Z displacements (as seen by the pilot) are forward, to the right and down, respectively. Positive changes in θ, ψ, and ϕ (as seen by the pilot) are nose up, nose to the right, and clockwise, respectively. Table I lists the full-scale store parameters used in trajectory calculations and Tables II and III describe the aircraft load configuration nomenclature.

Launch trajectories for the MK-82 GPB are presented in Figs. 19 and 20 with all separations being initiated from a MER on the right wing outboard pylon of the F-4C. At all Mach numbers for the parent in level flight (Fig. 19), the MK-82 GPB tended to pitch down when released from the bottom and aft shoulder stations (MER positions 1, 2, 3, and 5) but to pitch up when released from the forward shoulder stations (MER positions 4 and 6). Separations from all MER stations almost always resulted in an initial positive yaw of the store. When compared with the level flight case, the trajectories obtained at simulated parent dive angles of 45 and 60 deg generally showed increased pitch down (or decreased pitch up) and increased yaw. For parent accelerations of -2 g, yaw angle was generally reduced and the store separated at a slightly faster rate. Removal of the ALQ-119 ECM pod (configuration 2, Fig. 20) from the right wing inboard pylon generally introduced increased pitch and decreased yaw for the trajectories at MER station 4 (inboard, forward shoulder). For the forward outboard shoulder (MER station 6), little influence on pitch was noted.

Separations of the SUU-30H/B from the F-4C aircraft are presented in Figs. 21, 22, and 23. All trajectories were initiated from a MER on the aircraft centerline pylon. For the parent in level flight (Fig. 21), the SUU-30H/B tended to pitch down when released from MER stations 1, 2, 3, and 5 and pitch up when released from MER stations 4 and 6. Trends in both pitch and yaw were quite similar for parent-aircraft dive angles (45 and 60 deg) and accelerations (-2 g). However, the store did separate at a much faster rate when the parent was accelerating. Placement of the external stores produced enough differences in the aircraft flow field to significantly vary the trajectories (Fig. 22) from MER station 6 as would be expected. Aft movement of the store cg position (Fig. 23) reduced pitchup but increased yaw negatively for the one configuration tested.

Trajectories for the MK-20 Rockeye, shown in Figs. 24 and 25, were also initiated from an MER on the centerline pylon of the F-4C. Trends in the MK-20 data for level flight, dive angle, parent acceleration, and movement of the external stores were quite similar to those of the SUU-30H/B.

Separations of the MK-84 GPB from the right wing outboard pylon of the F-4C are presented in Fig. 26. The store pitched down and yawed positively at all test conditions and removal of the ALQ-119 ECM pod (configuration 11) from the right wing inboard pylon had little effect on the trajectories. However, the accelerated flight case did produce a much faster store separation from the parent.

Shown in Fig. 27 are the MK-84 LGB launch trajectories from the right wing inboard pylon of the F-4C. For both level and diving flight, pitch of the store changed from up to down as Mach number increased from 1.05 to 1.6. Yaw behavior was substantially influenced by both changes in Mach number and arrangement of the fuel tanks (configuration 14). Separations of the MK-84 EOGB (Fig. 28) generally indicated only small pitch excursions and the yawing characteristics were quite similar to those of the MK-84 LGB.

The aerodynamic characteristics of the MK-84 stores in the carriage position are presented in Figs. 29 and 30 with varying parent angle of attack and in Fig. 31 with varying parent angle of yaw. These data were obtained with the CTS by adjusting the store to the correct attitude and position for each parent aircraft attitude. For all three munitions, the trends in the data with angle of attack were not greatly affected by a change in Mach number (Fig. 29), although the levels of the data did change considerably in some cases. Generally, only the lateral coefficient variations with angle of attack were greatly affected by the arrangement of the fuel tanks (Fig. 30), which substantiated the trajectory data of Figs. 27 and 28. The variation of the lateral coefficients with angle of yaw were similarly affected (Fig. 31).

Launch trajectories of the SUU-30H/B from the F-111E aircraft are presented in Figs. 32 and 33. The separations were initiated from a BRU-3A/A rack on the number 3 or number 6 pylons or from the number 4 and number 6 pylons alone. Ejectors are identified on the figures as 1, 2, or 3, corresponding to the ejector forces listed in Table I. With Λ_{LE} at 50 deg (Fig. 32), the SUU-30H/B tended to pitch down when launched from the bottom and aft shoulder rack positions as well as the pylons alone and to pitch up when launched from the forward shoulder positions for simulated ejector forces of 900 and 500 lb on the forward and aft feet, respectively (ejector 1). Using an ejector force of 1300 lb on the aft foot (ejector 2), decreased pitch down, whereas an ejector force of 1300 lb on the forward foot (ejector 3) decreased pitch up as would be expected. Yaw of the store was almost always nose away from the aircraft centerline. Separation characteristics of the munition for Λ_{LE} = 72.5 deg (Fig. 33) were quite similar to those for Λ_{LE} = 50 deg.

REFERENCES

1. Test Facilities Handbook (Ninth Edition). "Propulsion Wind Tunnel Facility, Vol. 4." Arnold Engineering Development Center, July 1971.

2. Christopher, J. P. and Carleton, W. E. "Captive-Trajectory Store-Separation System of the AEDC-PWT 4-Foot Transonic Tunnel." AEDC-TR-68-200 (AD839743), September 1968.

APPENDIXES

I. ILLUSTRATIONS

II. TABLES

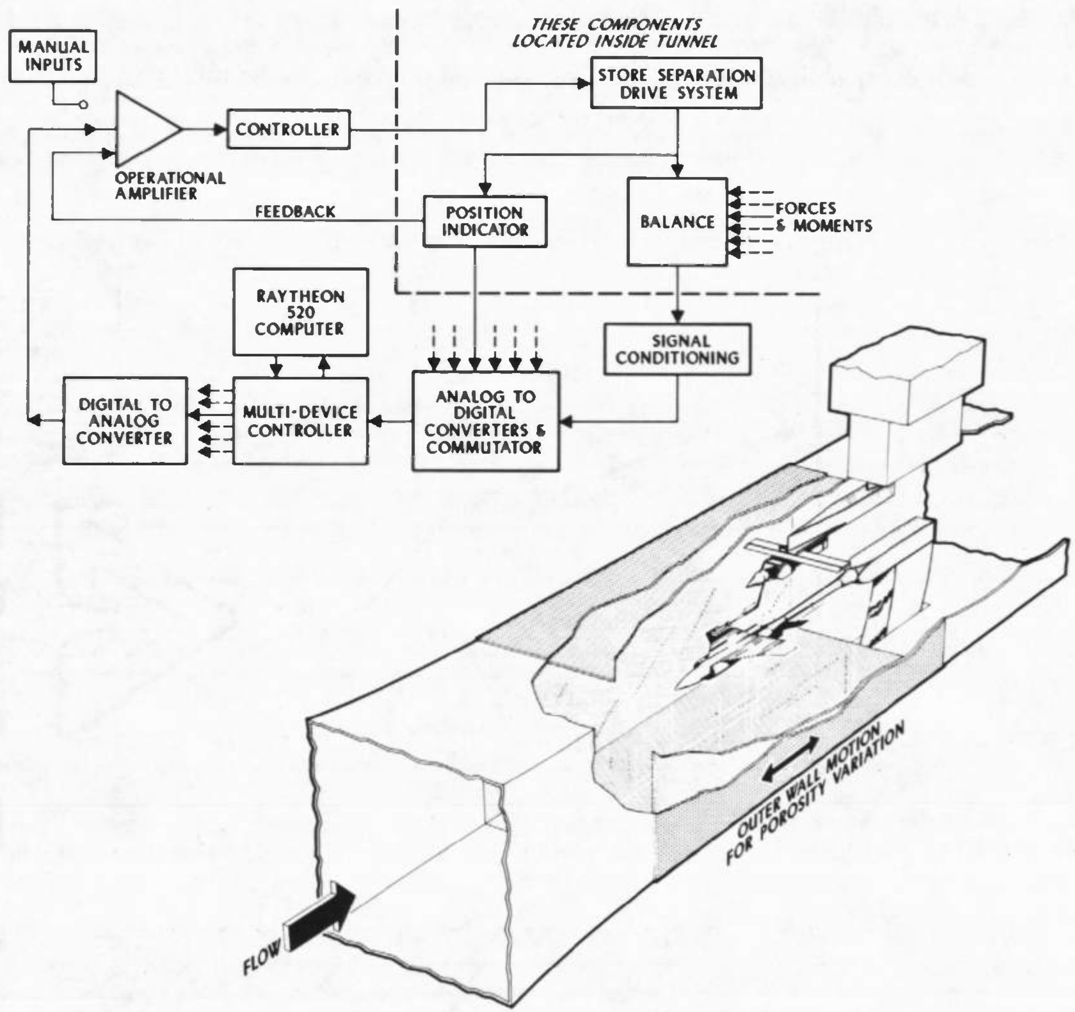

Fig. 1 Isometric Drawing of a Typical Store Separation Installation and a Block Diagram of the Computer Control Loop

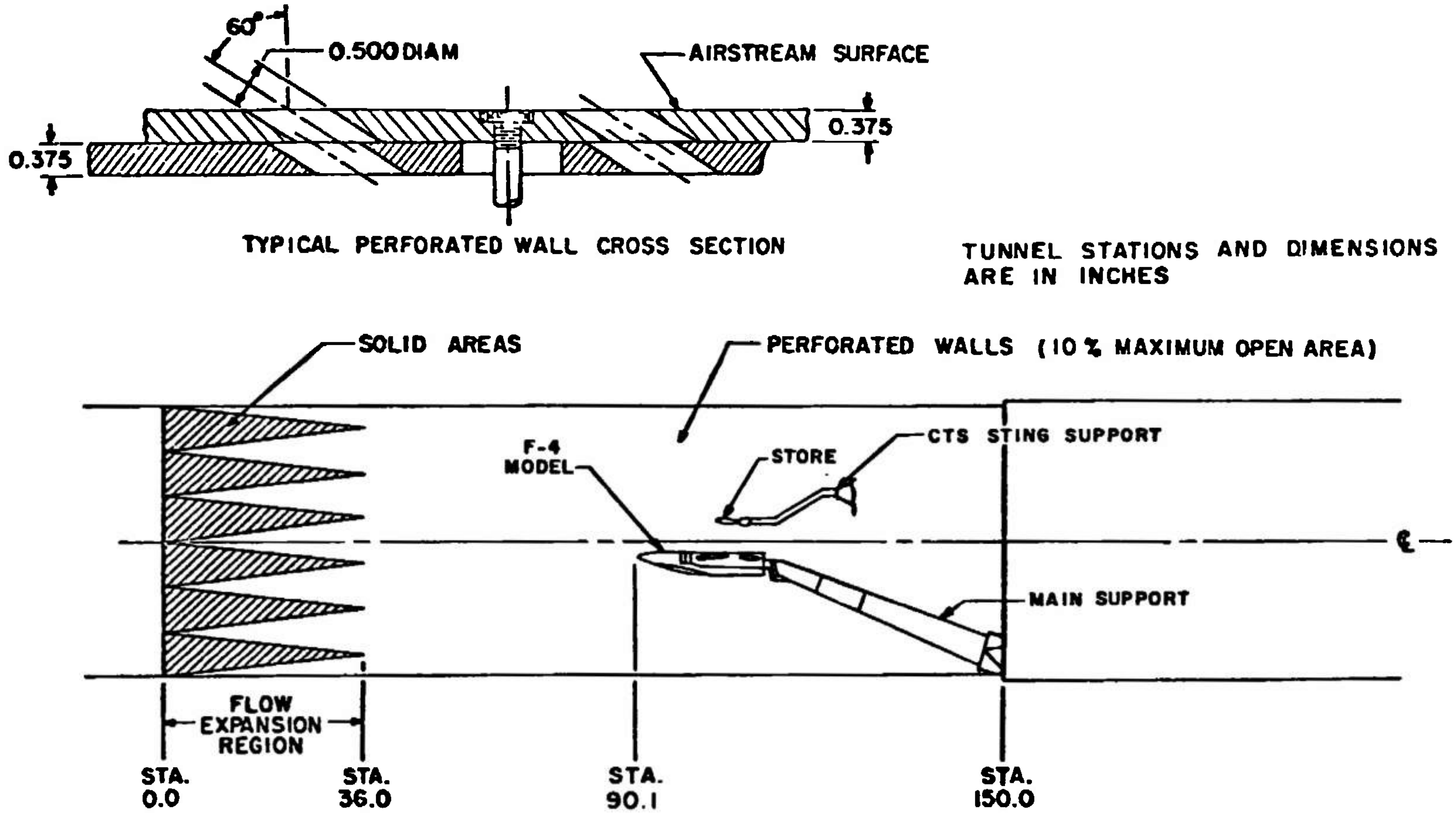

a. F-4C Aircraft

Fig. 2 Schematic of the Tunnel Test Section Showing Model Locations

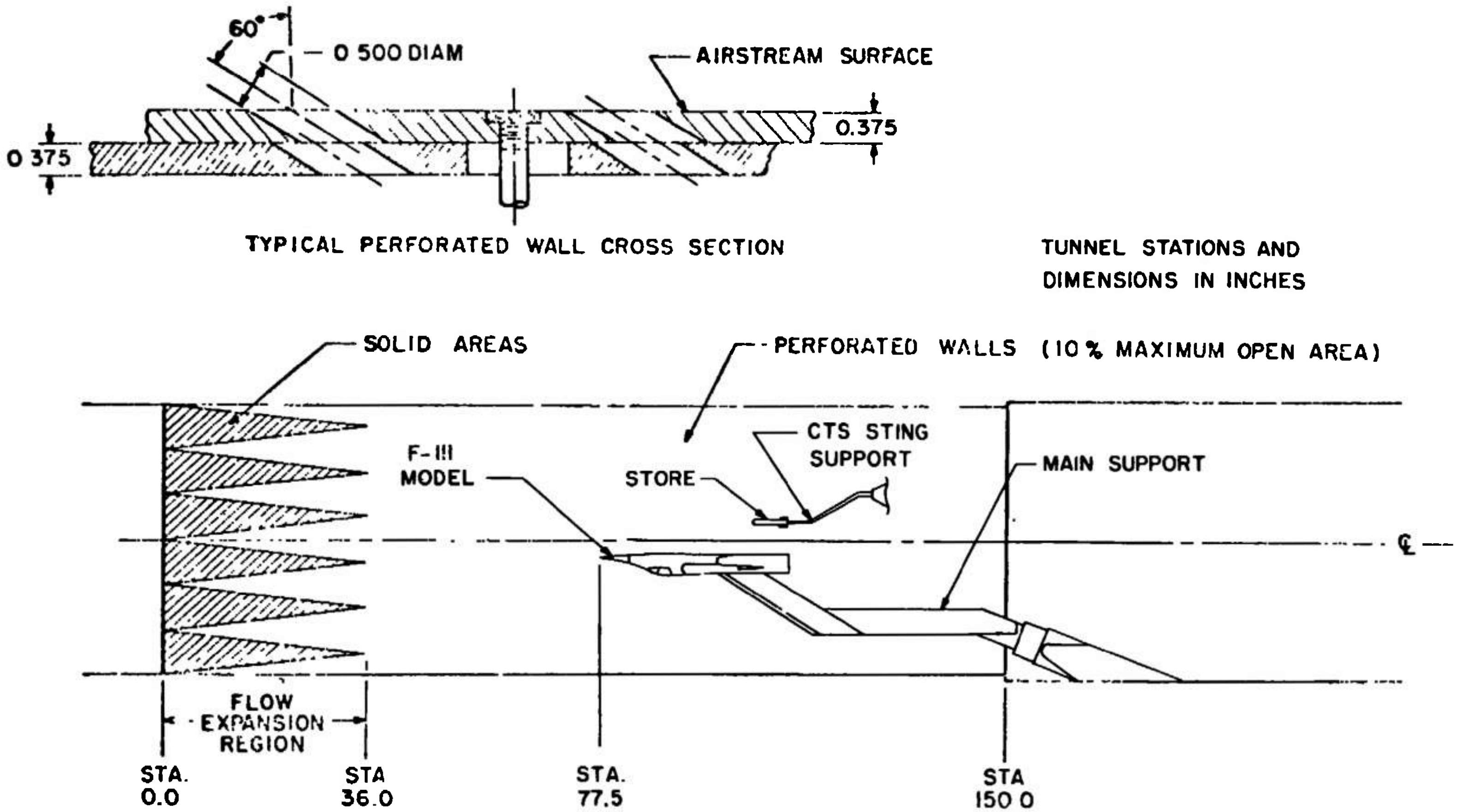

b. F-111E Aircraft
Fig. 2 Concluded

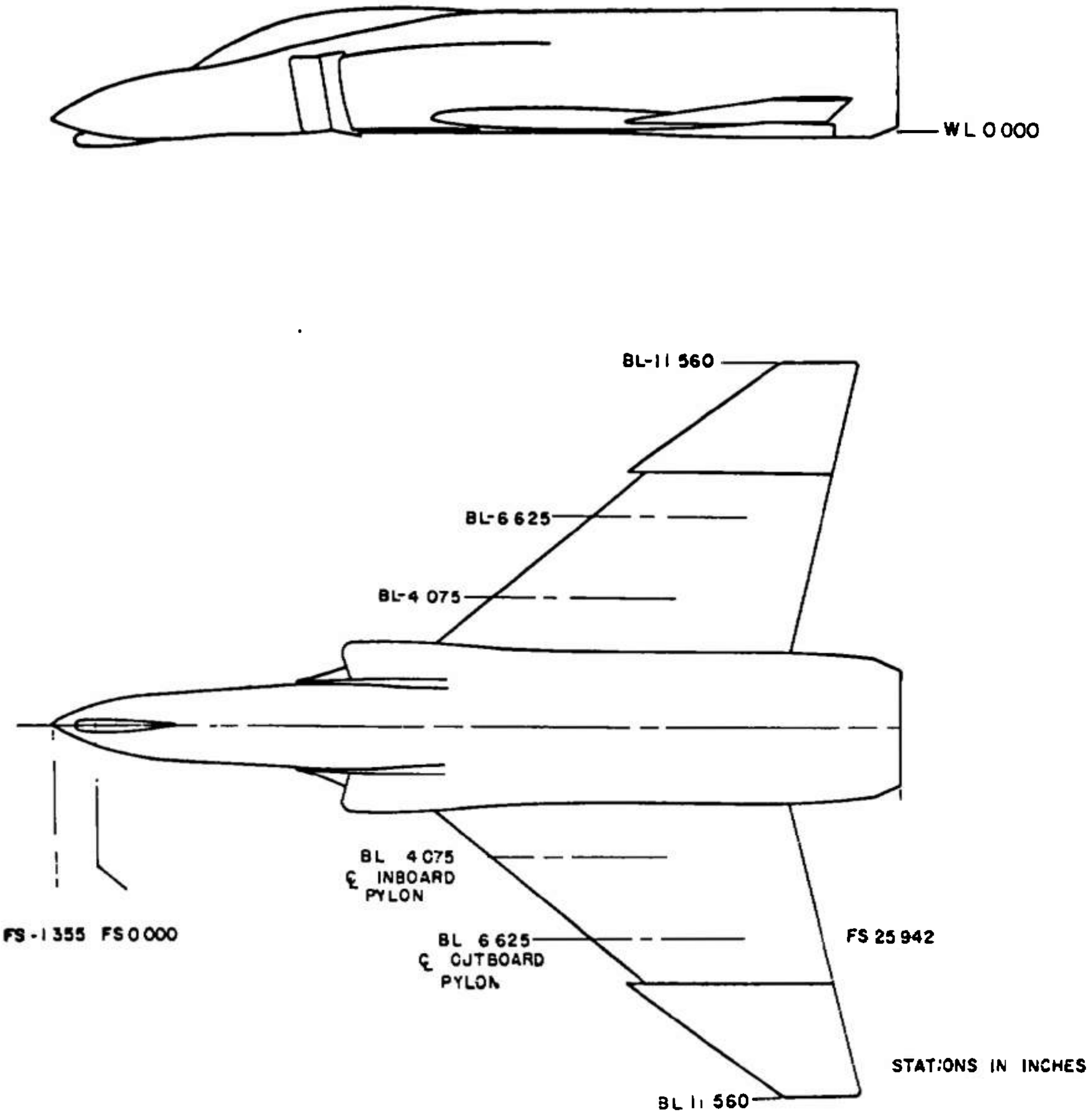

a. F-4C (1/20 Scale)
Fig. 3 Sketch of the Parent-Aircraft Models

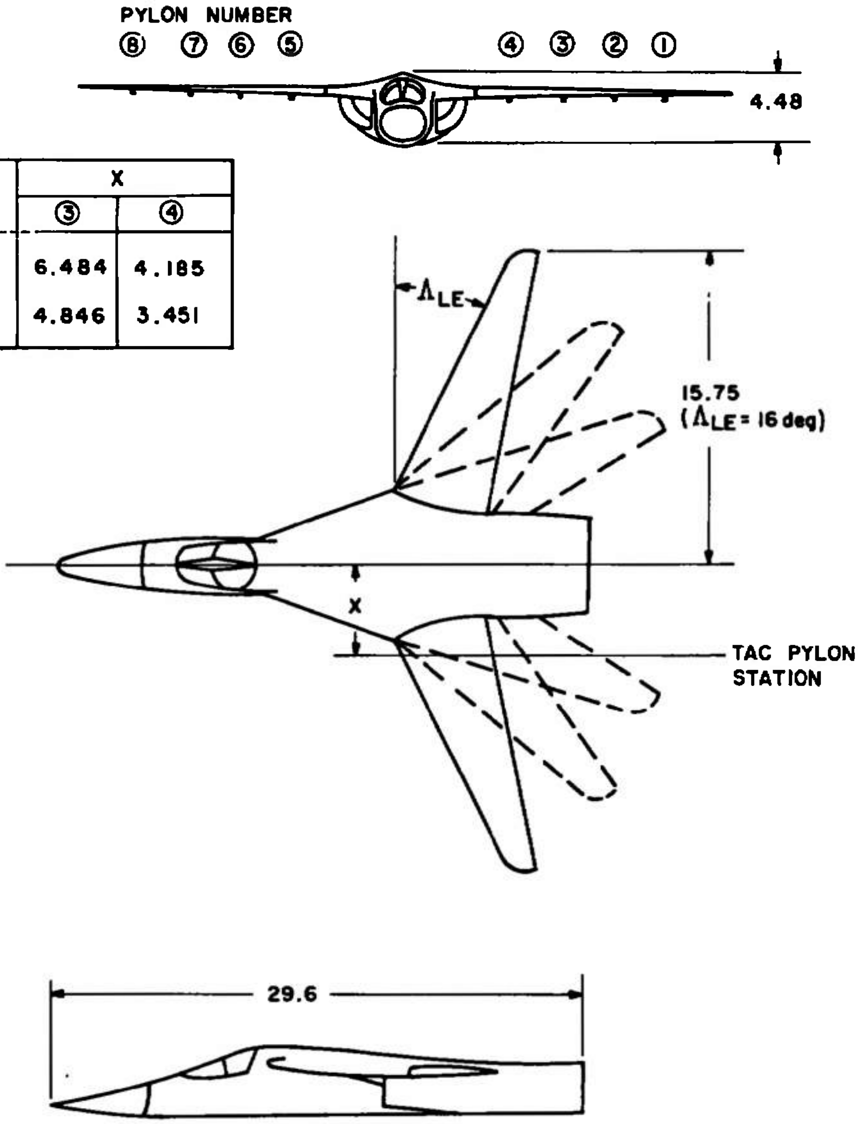

Λ_{LE}	X	
	③	④
50.0	6.484	4.185
72.5	4.846	3.451

b. F-111E (1/24 Scale)
Fig. 3 Concluded

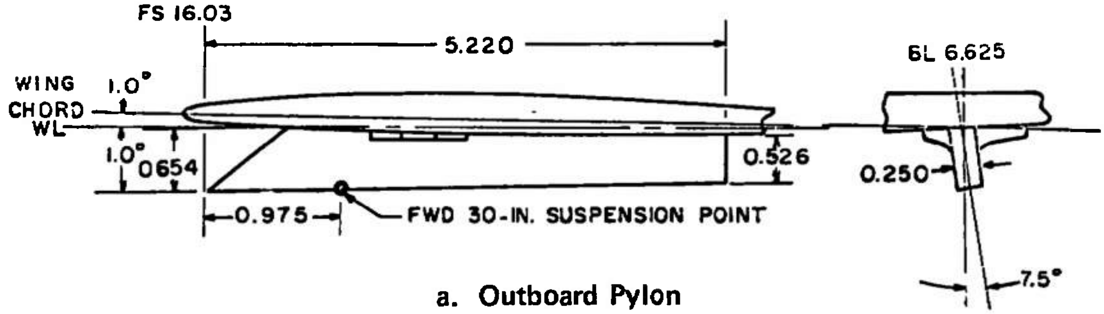

a. Outboard Pylon

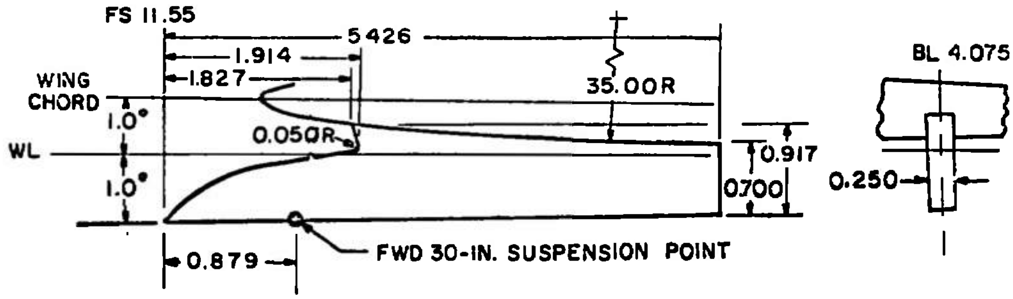

b. Inboard Pylon

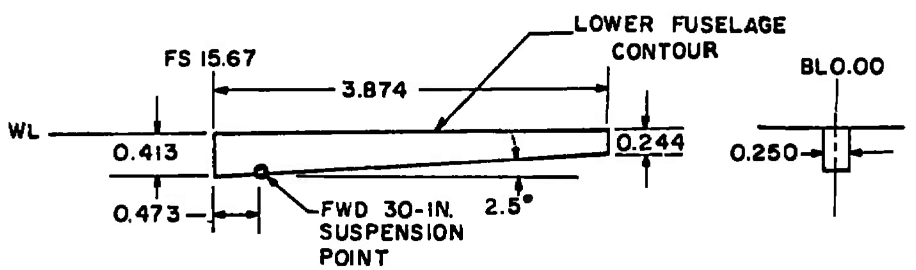

ALL DIMENSIONS IN INCHES

c. Centerline Pylon

Fig. 4 Details of the 1/20-Scale F-4 Pylon Models

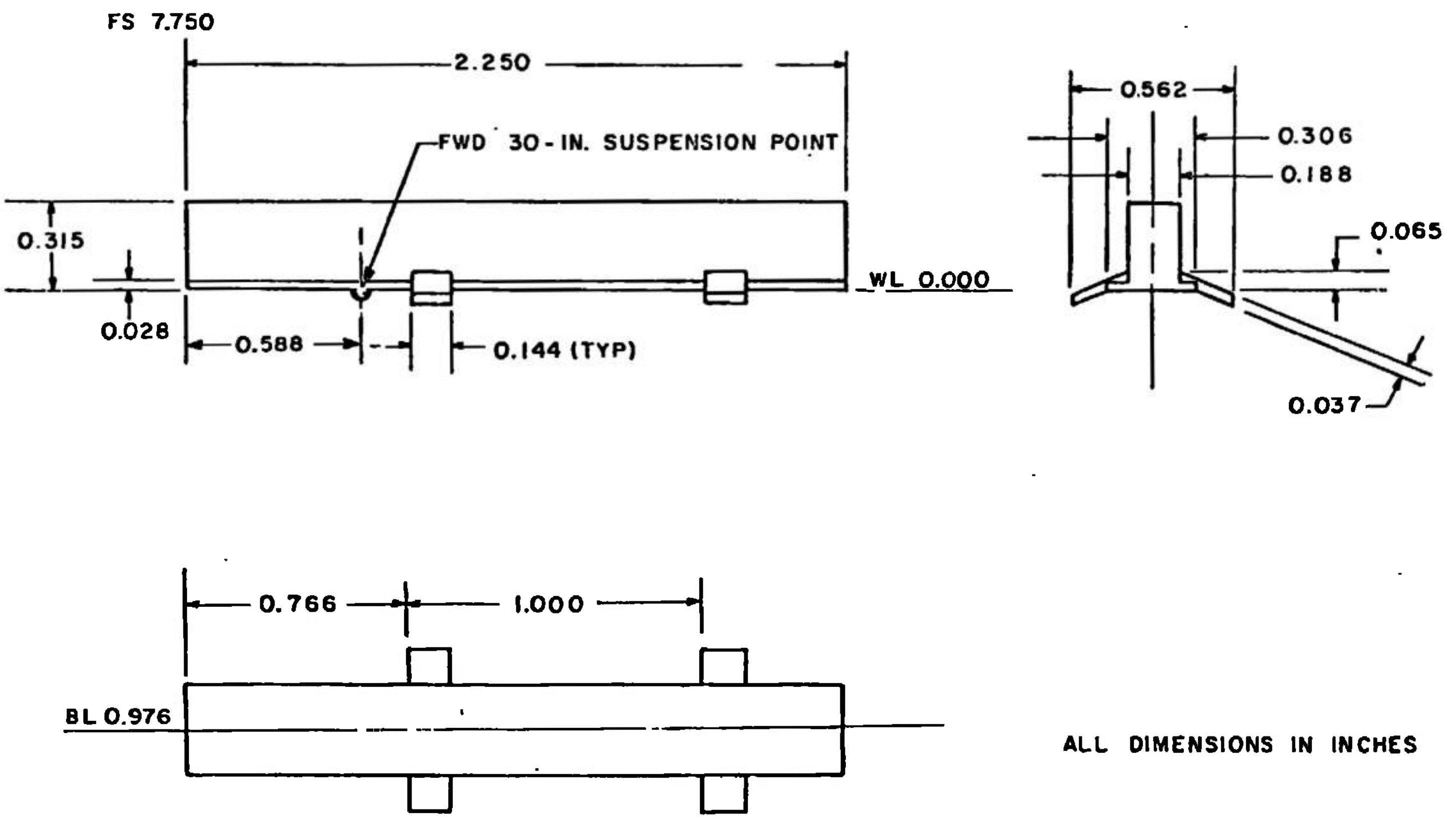

d. Missile Well Pylon
Fig. 4 Concluded

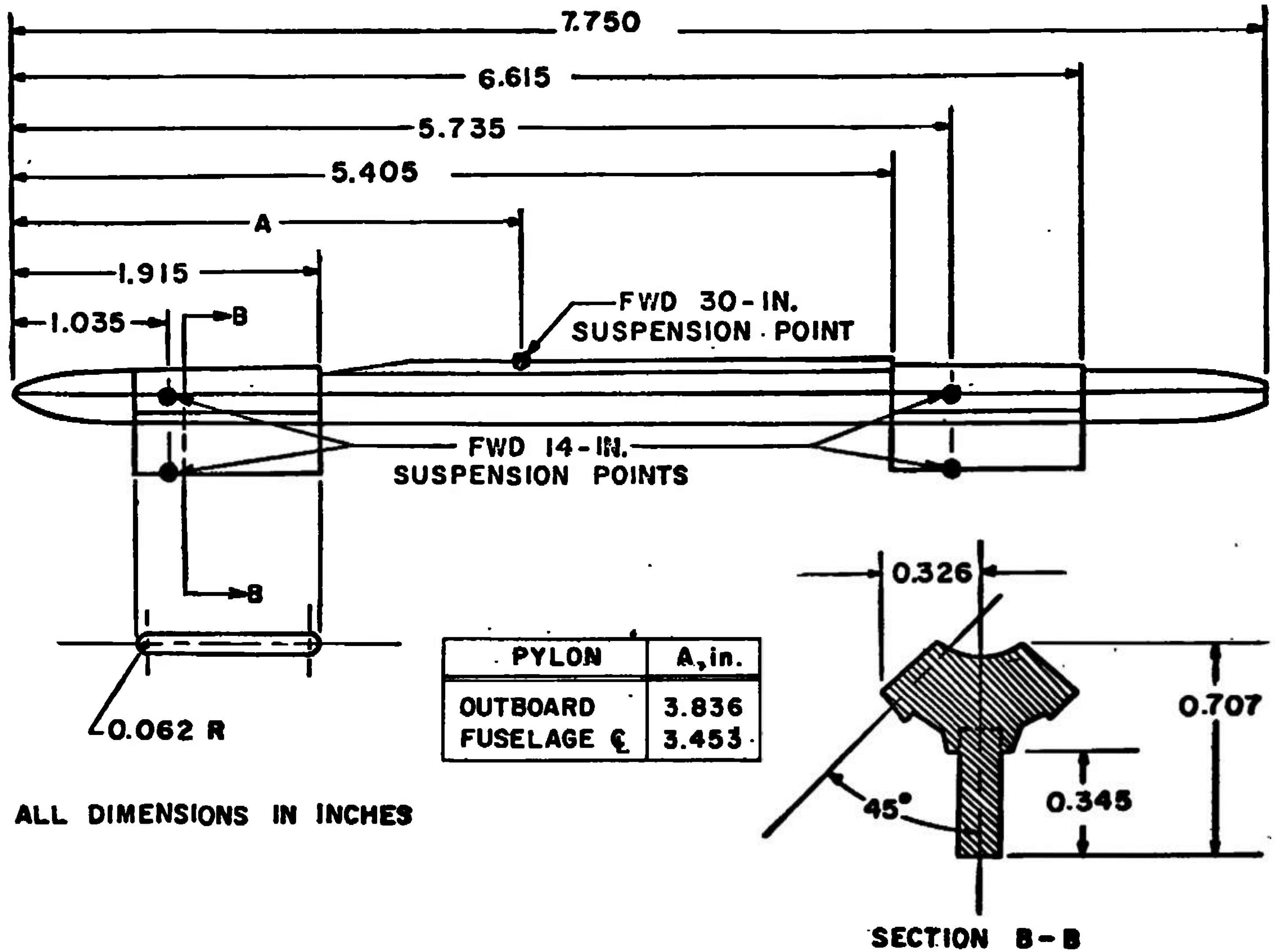

PYLON	A, in.
OUTBOARD	3.836
FUSELAGE ℄	3.453

Fig. 5 Details of the 1/20-Scale F-4 MER Model

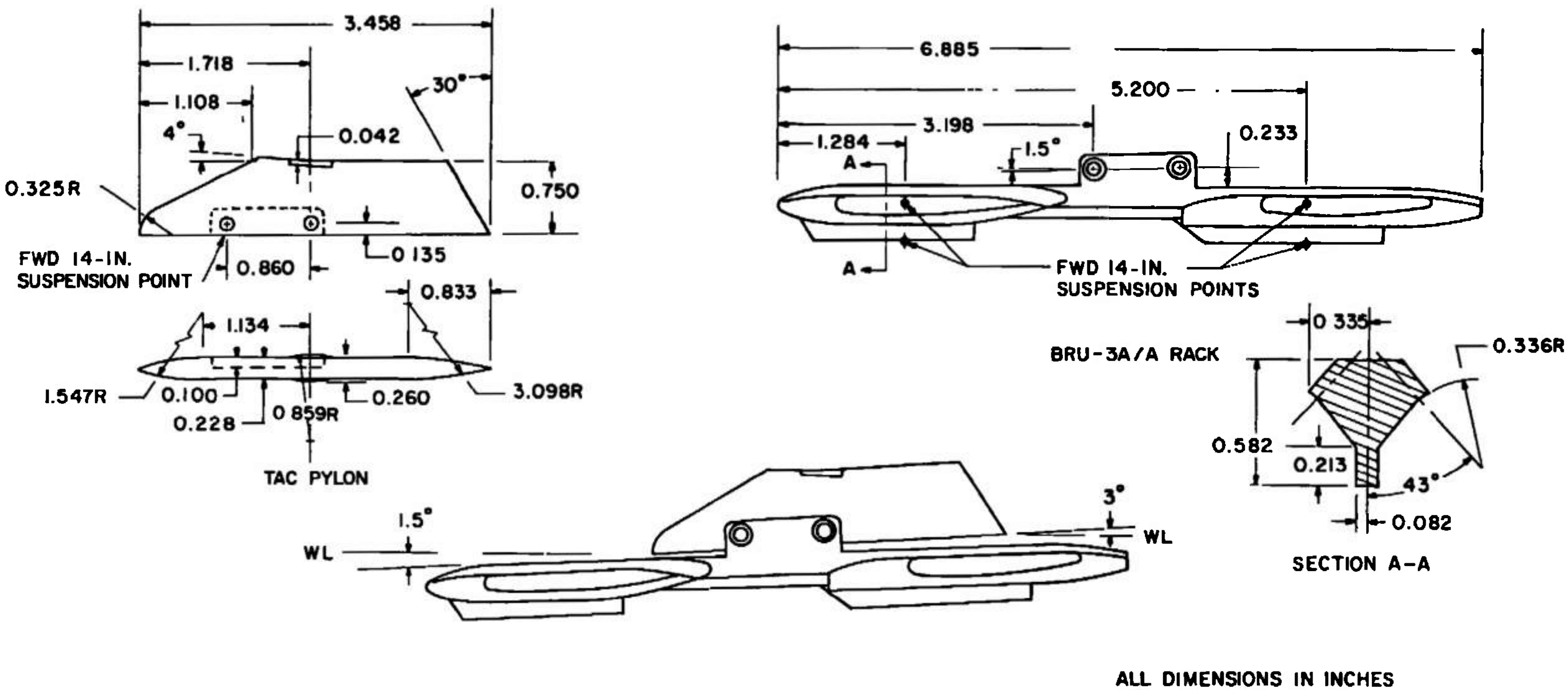

Fig. 6 Details of the 1/24-Scale F-111 TAC Pylon and BRU-3A/A Rack

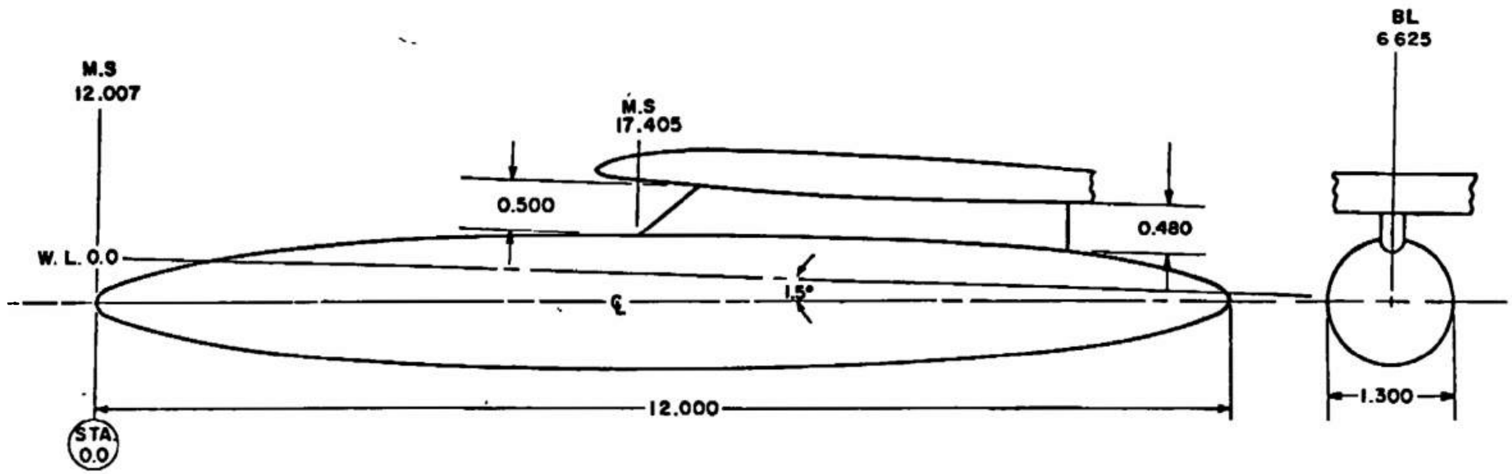

BODY CONTOUR, TYPICAL BOTH ENDS

STATION	BODY DIAM	STATION	BODY DIAM
0.000	0.000	2.500	1.116
0.025	0.100	2.750	1.156
0.050	0.144	3.000	1.190
0.150	0.258	3.250	1.218
0.250	0.340	3.500	1.242
0.500	0.498	3.750	1.260
0.750	0.622	4.000	1.274
1.000	0.724	4.250	1.286
1.250	0.812	4.500	1.294
1.500	0.890	4.750	1.298
1.750	0.958	5.000	1.300
2.000	1.016	6.000	1.300
2.250	1.070		

NOTE: MODEL STATIONS AND DIMENSIONS IN INCHES

a. 370 gal
Fig. 7 Details of the 1/20-Scale F-4 Fuel Tank Models

BODY CONTOUR

Y	R	Y	R
0.000	0.000	4.250	0.827
0.050	0.049	4.500	0.838
0.100	0.077	4.750	0.847
0.150	0.101	5.000	0.854
0.200	0.122	5.250	0.859
0.250	0.143	5.500	0.860
0.500	0.232	6.250	0.860
0.750	0.308	6.500	0.859
1.000	0.376	6.750	0.856
1.250	0.438	7.000	0.852
1.500	0.494	7.250	0.846
1.750	0.546	7.500	0.839
2.000	0.593	7.750	0.830
2.250	0.637	8.000	0.820
2.500	0.679	8.250	0.809
2.750	0.713	8.500	0.796
3.000	0.740	8.750	0.781
3.250	0.762	9.000	0.765
3.500	0.782	9.250	0.745
3.750	0.799	13.000	0.400
4.000	0.814		

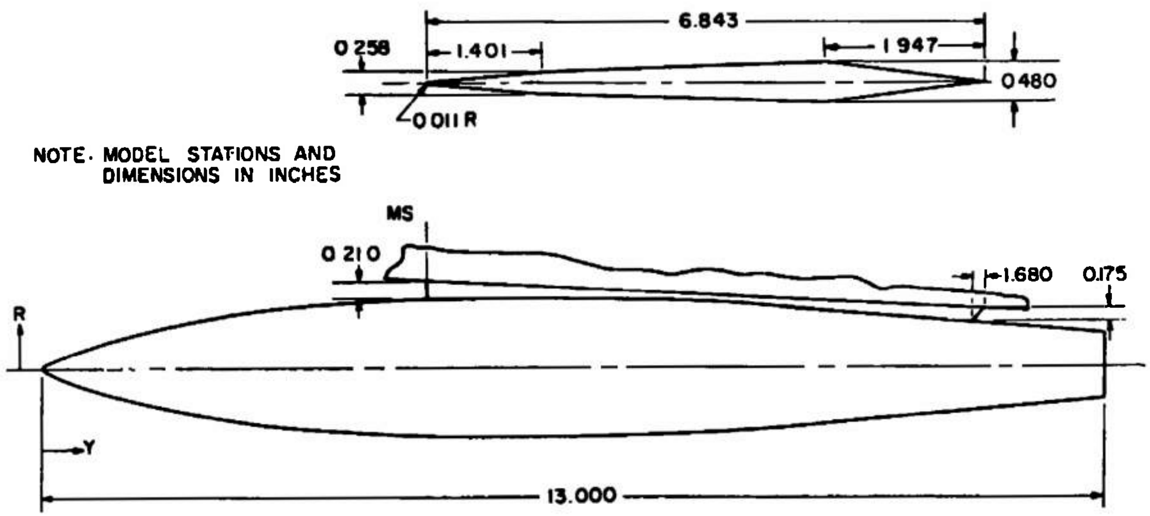

b. 600 gal
Fig. 7 Concluded

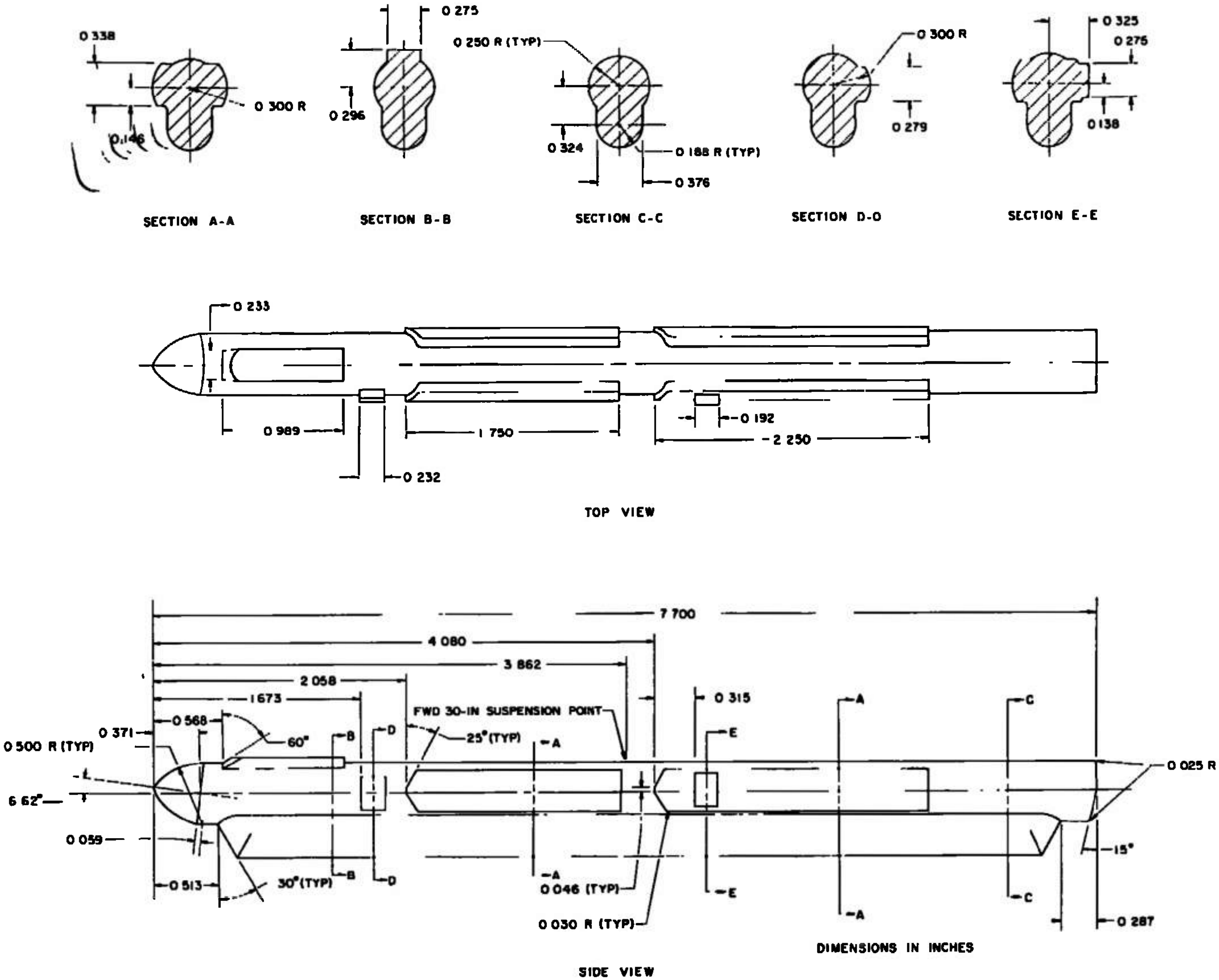

Fig. 8 Details of the 1/20-Scale ALQ-119 Model

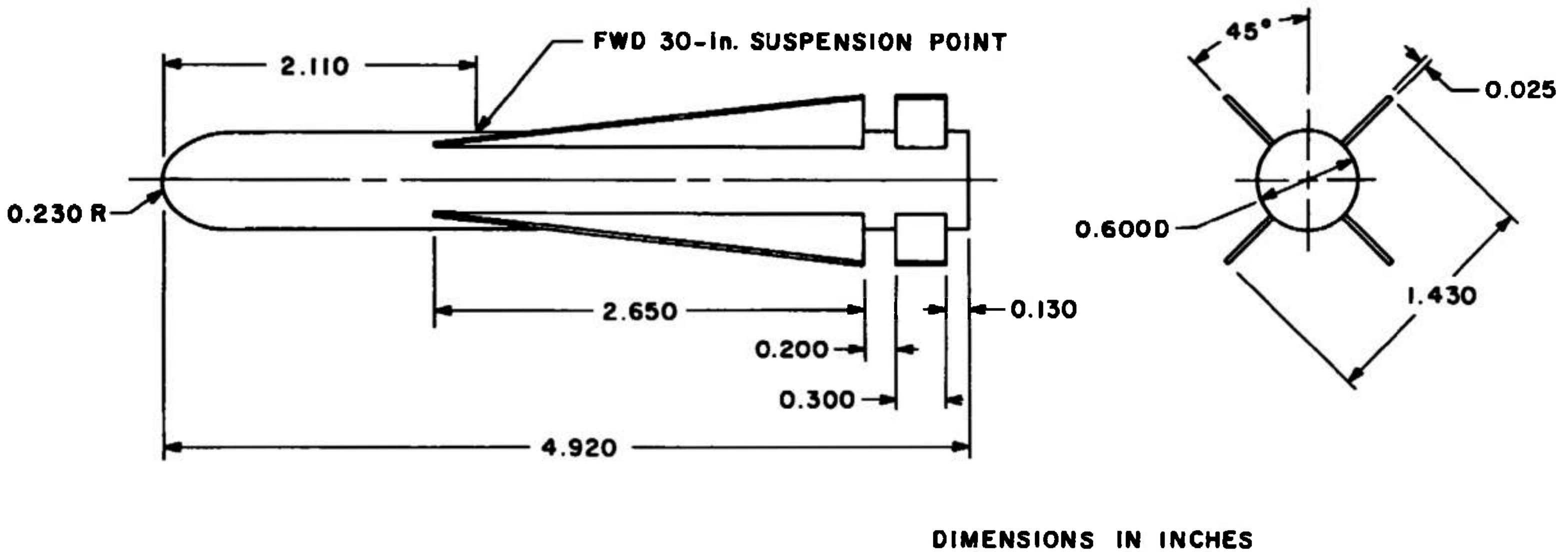

Fig. 9 Details of the 1/20-Scale AGM-65 Model

STA.	DIAM
0.000	0.150
0.210	0.150
0.212	0.231
0.312	0.282
0.412	0.322
0.512	0.361
0 612	0.391
0.712	0 421
0.812	0 445
0.912	0.465
1.012	0.483
1.112	0.497
1.212	0 510
1.312	0 520
1.412	0 525
1.512	0 530
1.612	0 532
1.712	0 533
1.812	0 535
1.912	0.537
2.312	0 537
2.412	0.535
2.512	0.525
2.612	0 520
2.712	0 510
2 812	0.497
2.912	0 483
3.012	0 465
3 173	0 438

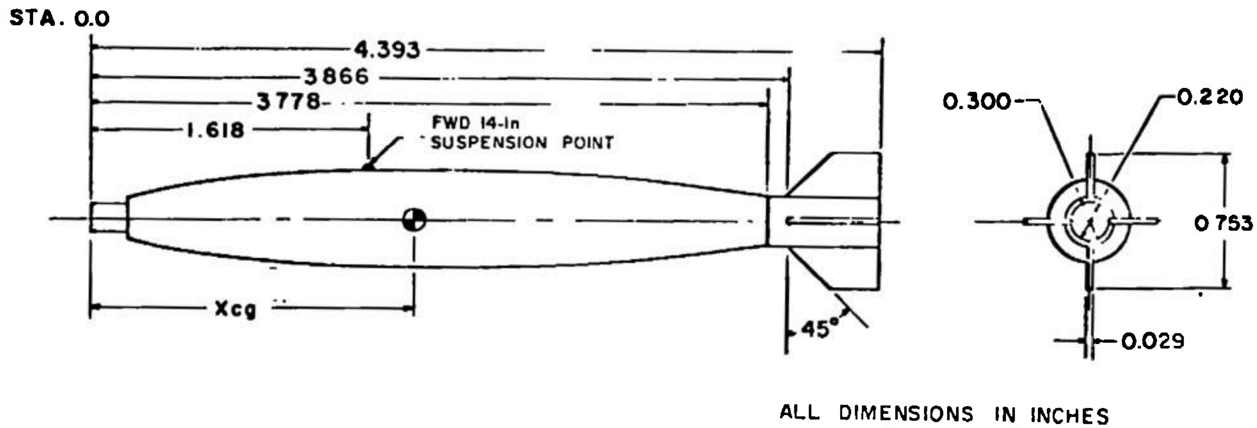

Fig. 10 Details of the 1/20-Scale MK-82 GPB Model

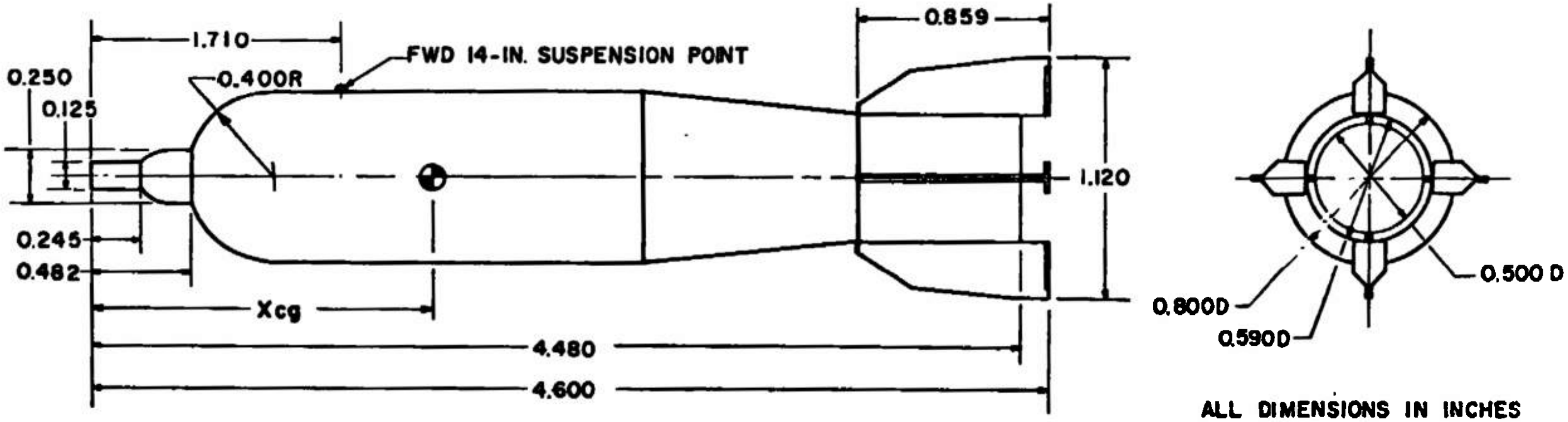

Fig. 11 Details of the 1/20-Scale SUU-30H/B Model

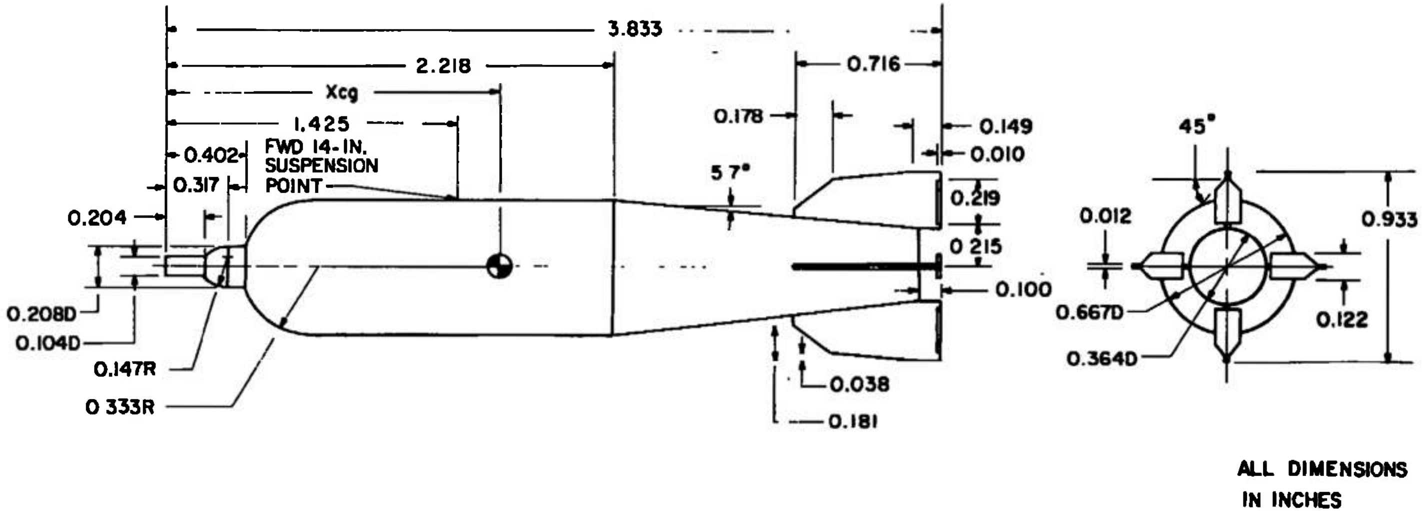

Fig. 12 Details of the 1/24-Scale SUU-30H/B Model

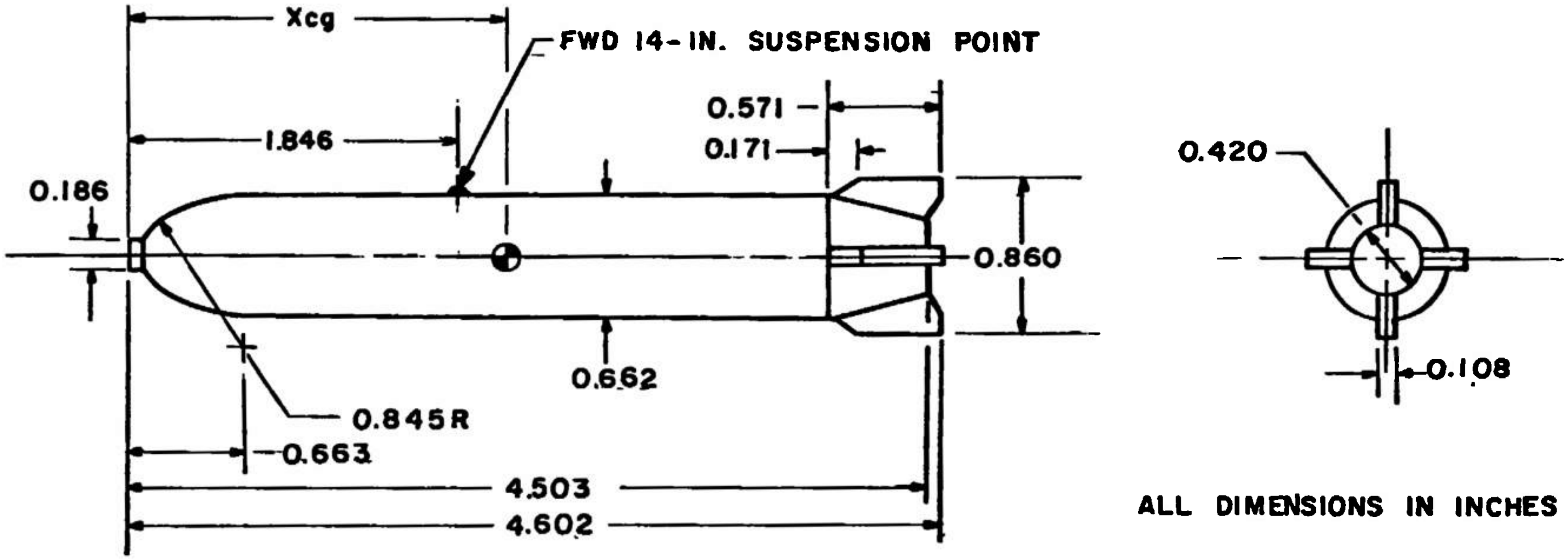

Fig. 13 Details of the 1/20-Scale MK-20 "Rockeye" Model

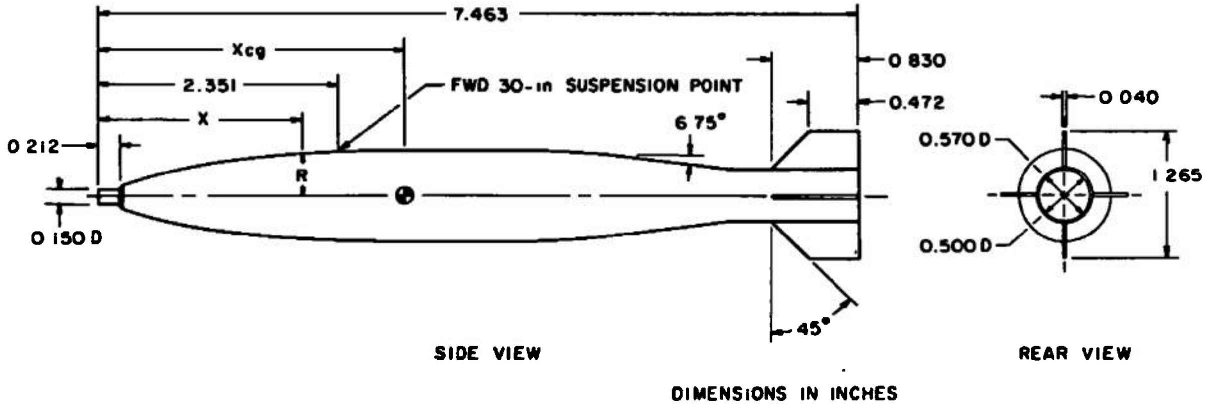

X, in	R, in
0.238	0 116
0.412	0 177
0 612	0 234
0 812	0.278
1 012	0.312
1.212	0.340
1.412	0 365
1 612	0 385
1 812	0.403
2 012	0 419
2 212	0 434
2.412	0.444
2.707	0 450
3.000	0 450
3.500	0.450
3.821	0 450
4 021	0.448
4 221	0.444
4 421	0 437
4 621	0 428
4.821	0 416
5.045	0 400

Fig. 14 Details of the 1/20-Scale MK-84 GPB Model

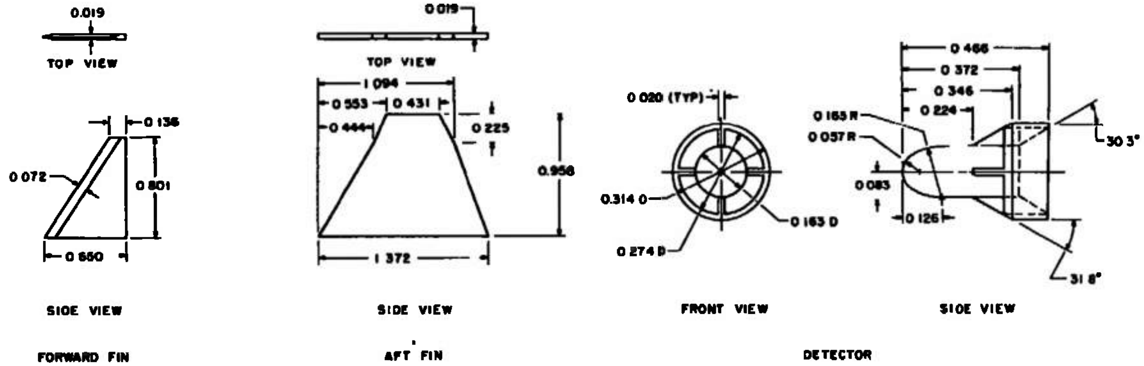

X, in	R, in
2 464	0 200
2 622	0 243
2 793	0 260
2 964	0 310
3 136	0 335
3.307	0 356
3 479	0 375
3 650	0 392
3 622	0 407
3 993	0 420
4 164	0 432
4 336	0.441
4 507	0 448
4 679	0 450
3 230	0 450
3 793	0 450
5 964	0 449
6.136	0 446
6 307	0 441
6 479	0 434
6 650	0 425
6 822	0 414
7 141	0 400

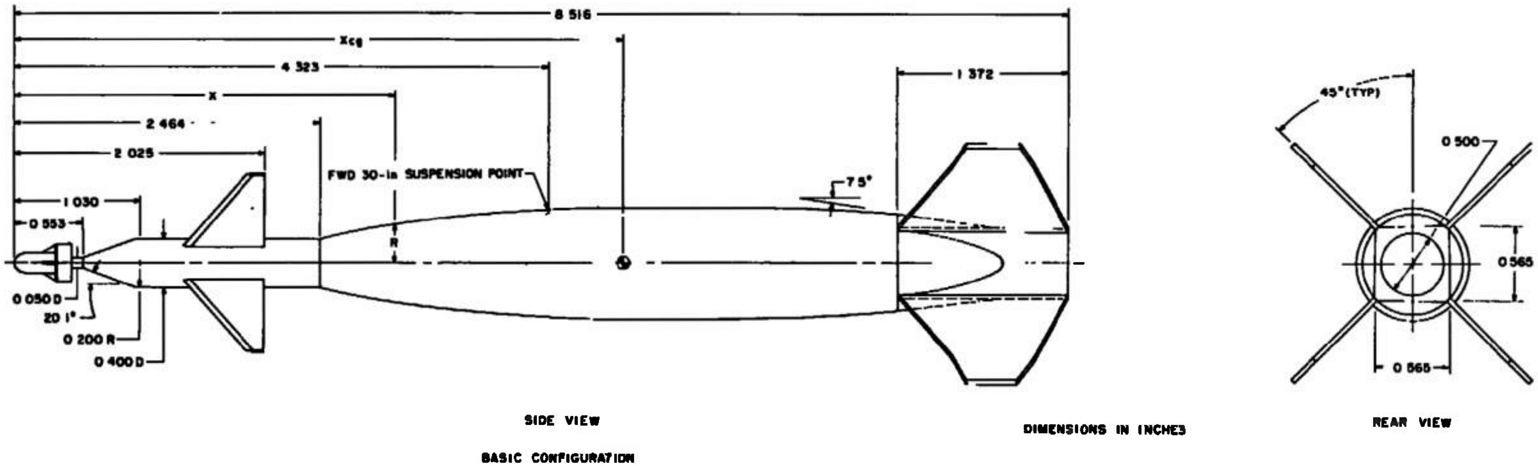

Fig. 15 Details of the 1/20-Scale MK-84 LGB Model

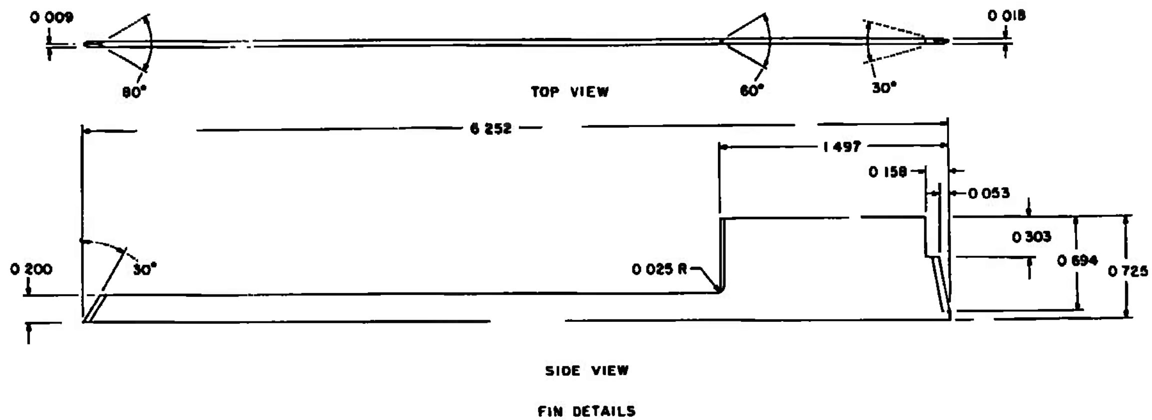

X, in	R, in
2 273	0 364
2 385	0 376
2 585	0 394
2 785	0 412
2 985	0 426
3 185	0 438
3 385	0 446
3 580	0 450
4 000	0 450
4 250	0 450
4 500	0 450
4 694	0 450
4 894	0 448
5 094	0 444
5 294	0 437
5 494	0 428
5 694	0 416
5 894	0 401
5 918	0 400

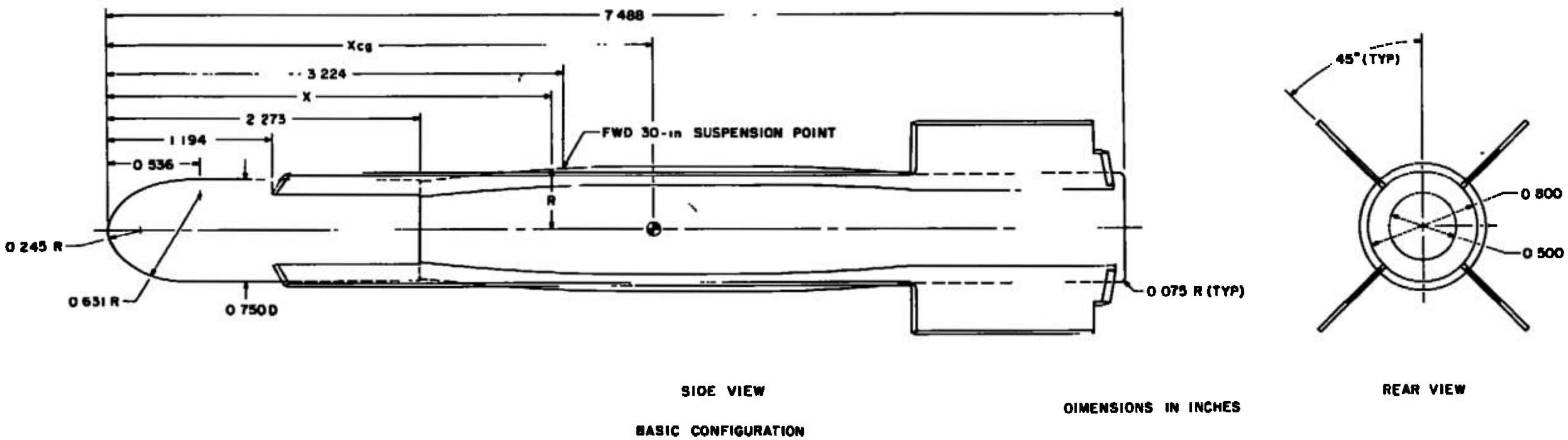

Fig. 16 Details of the 1/20-Scale MK-84 EOGB Model

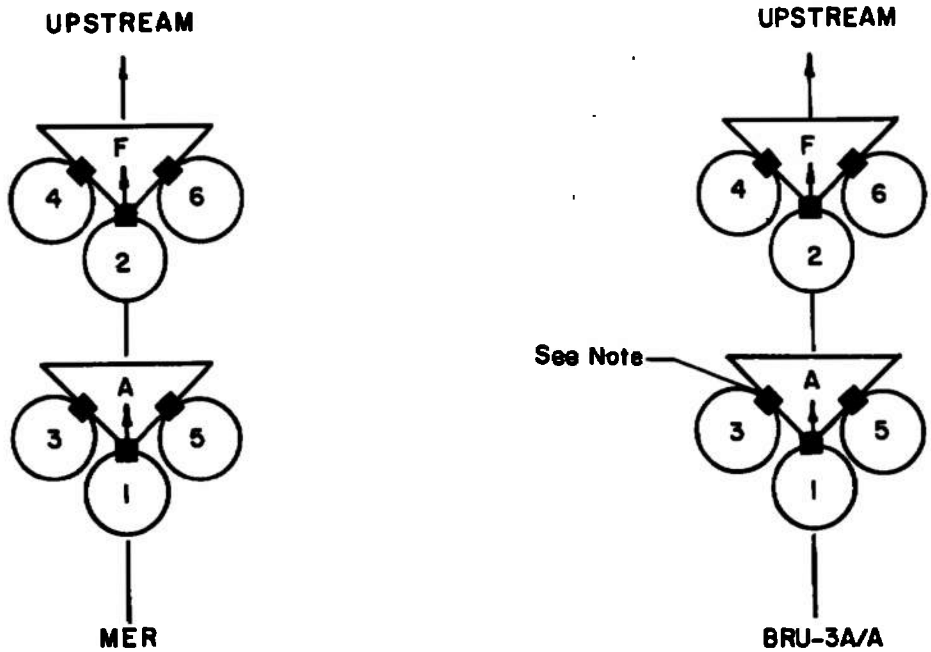

NOTE: The square indicates the orientation of the suspension lugs

TYPE RACK	STATION	ROLL ORIENTATION, deg
MER	1	0
	2	0
	3	45
	4	45
	5	-45
	6	-45
BRU-3A/A	1	0
	2	0
	3	43
	4	43
	5	-43
	6	-43

Fig. 17 Schematic of the MER and BRU-3A/A Store Stations and Orientations

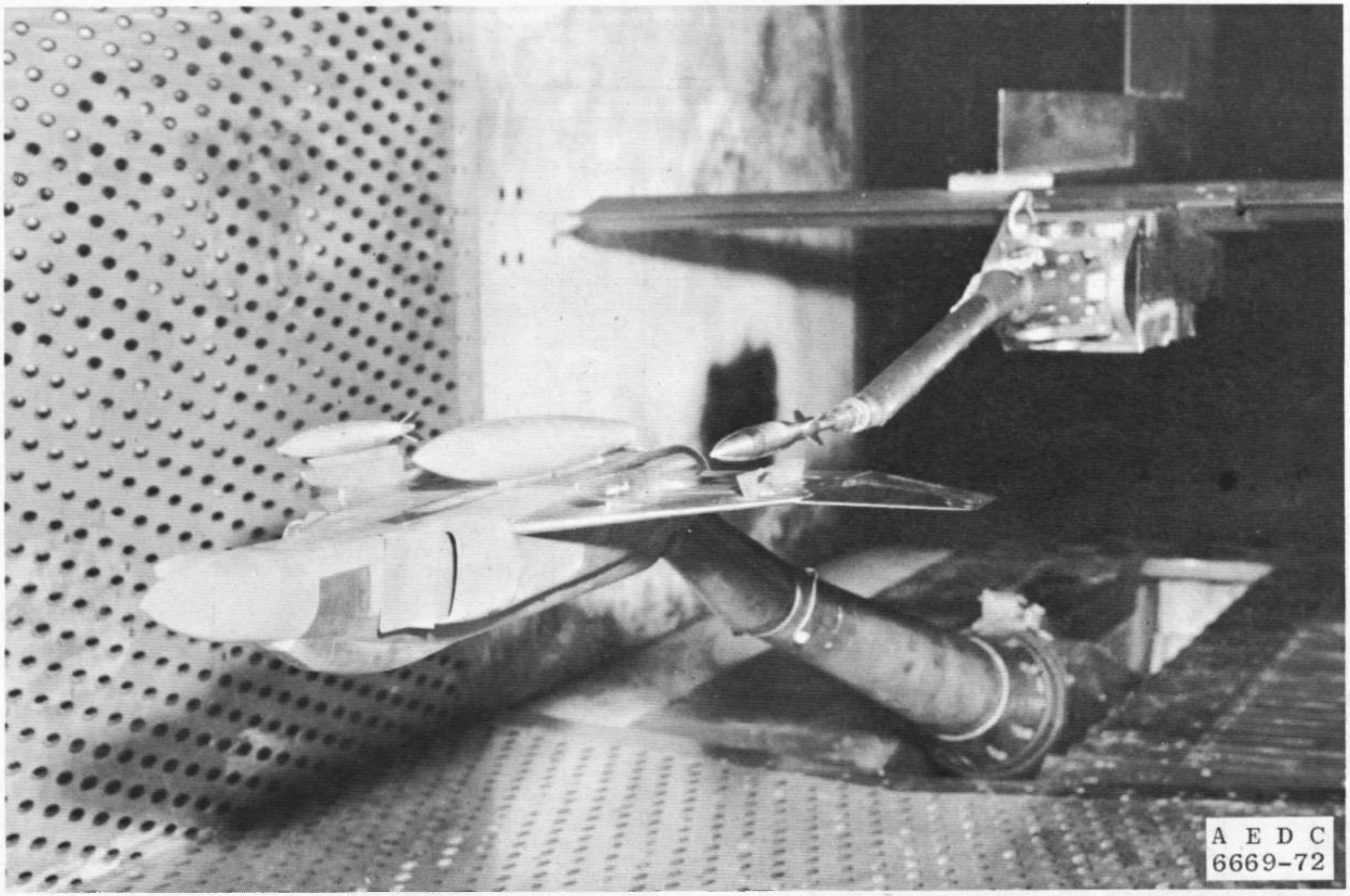

a. F-4C
Fig. 18 Tunnel Installation Photographs Showing Parent Aircraft, Store, and CTS

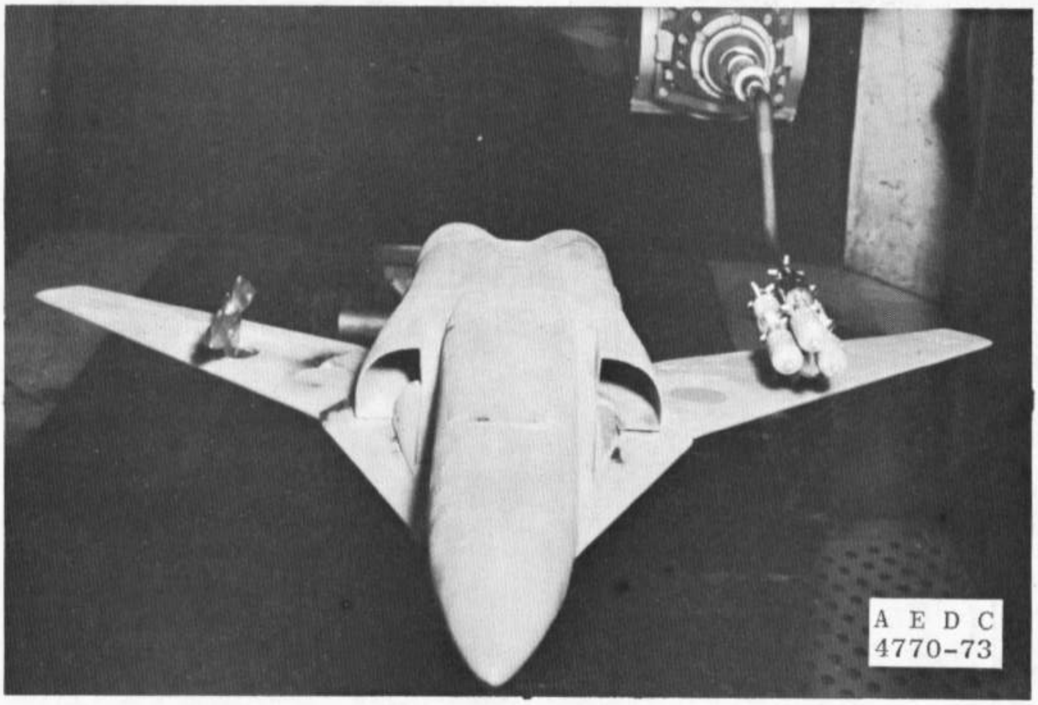

Λ_{LE} = 50 deg

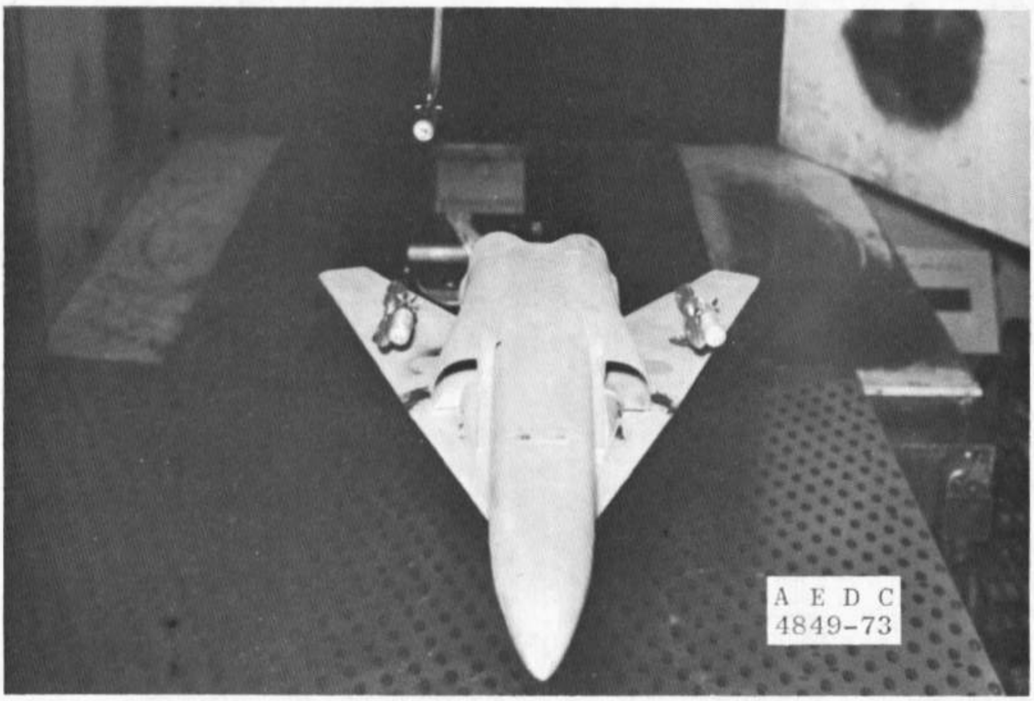

Λ_{LE} = 72.5 deg

b. F-111E
Fig. 18 Concluded

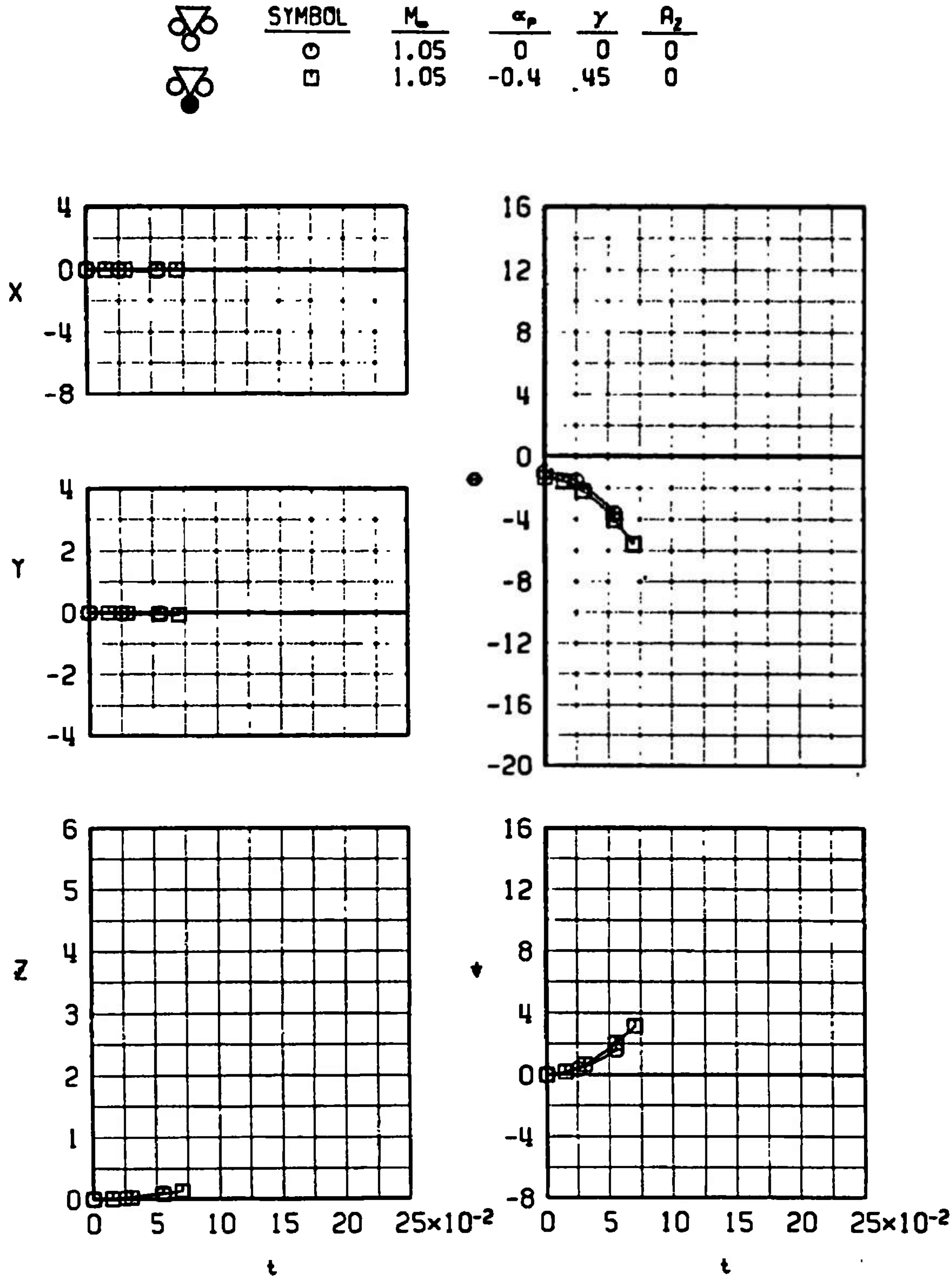

a. Configuration 1-1, M_∞ = 1.05
Fig. 19 Dive Angle Comparison of the MK-82 GPB Launch Trajectories from the MER for Different Mach Numbers

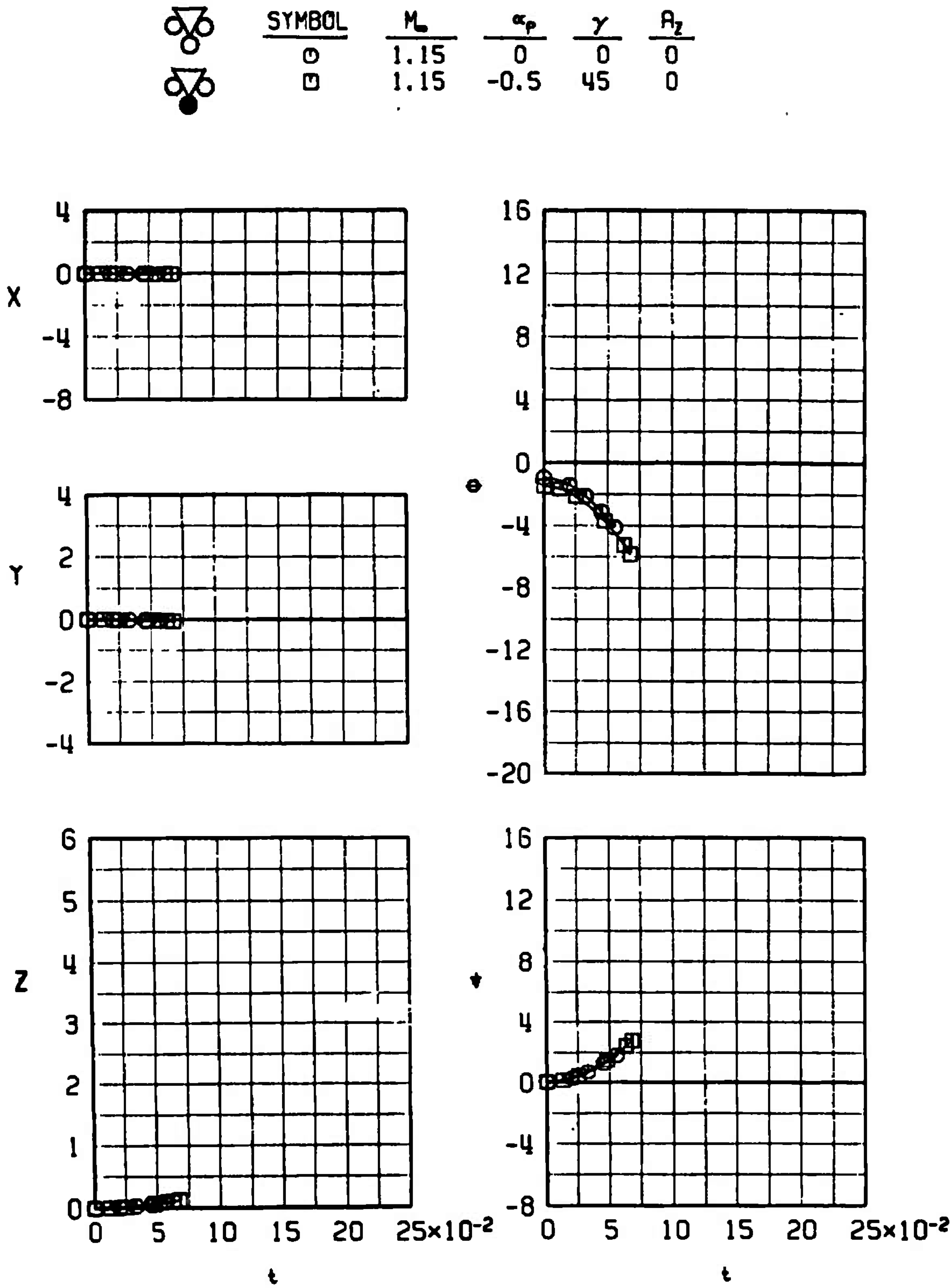

b. Configuration 1-1, M_∞ = 1.15
Fig. 19 Continued

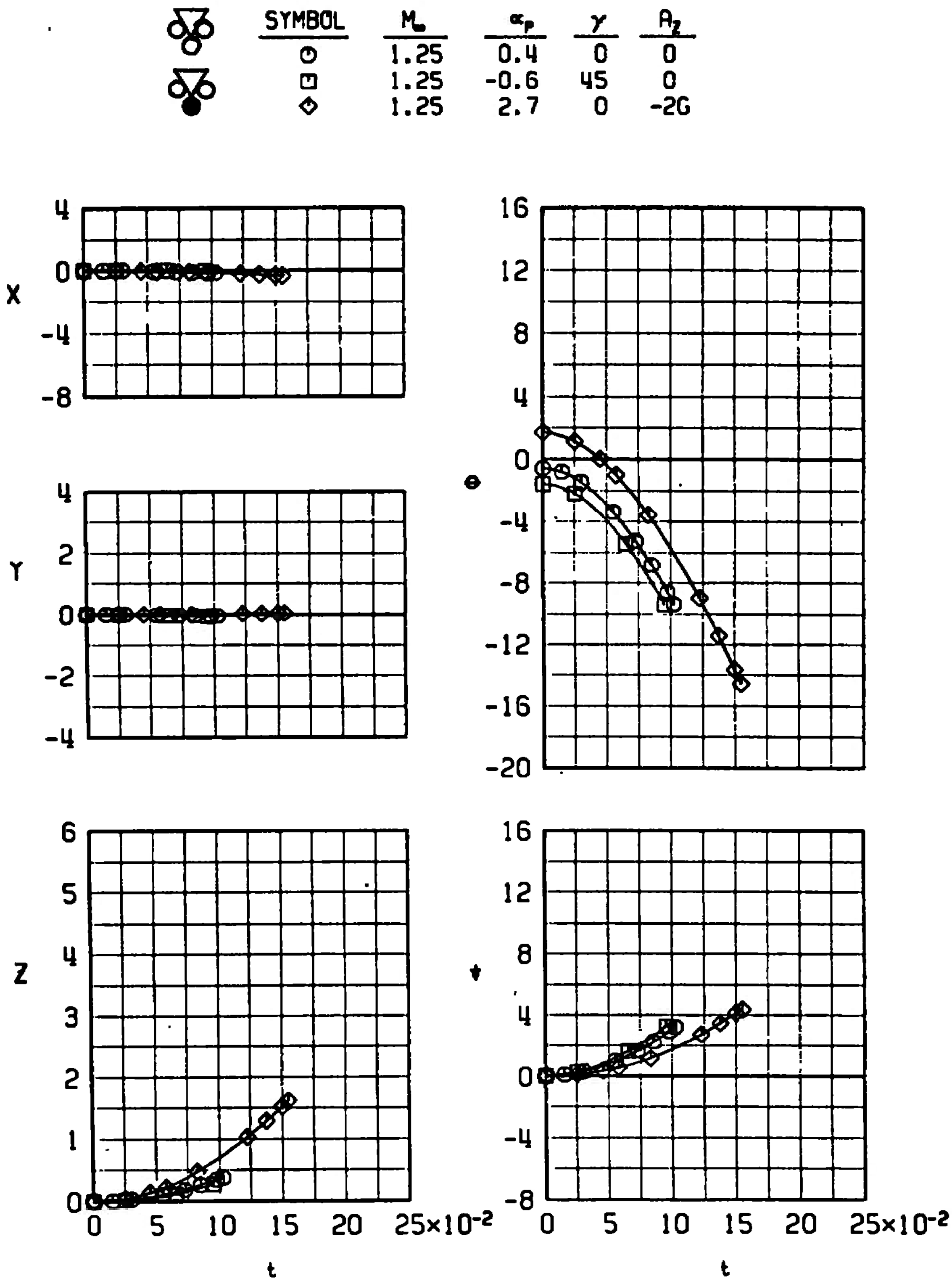

c. Configuration 1-1, M_∞ = 1.25
Fig. 19 Continued

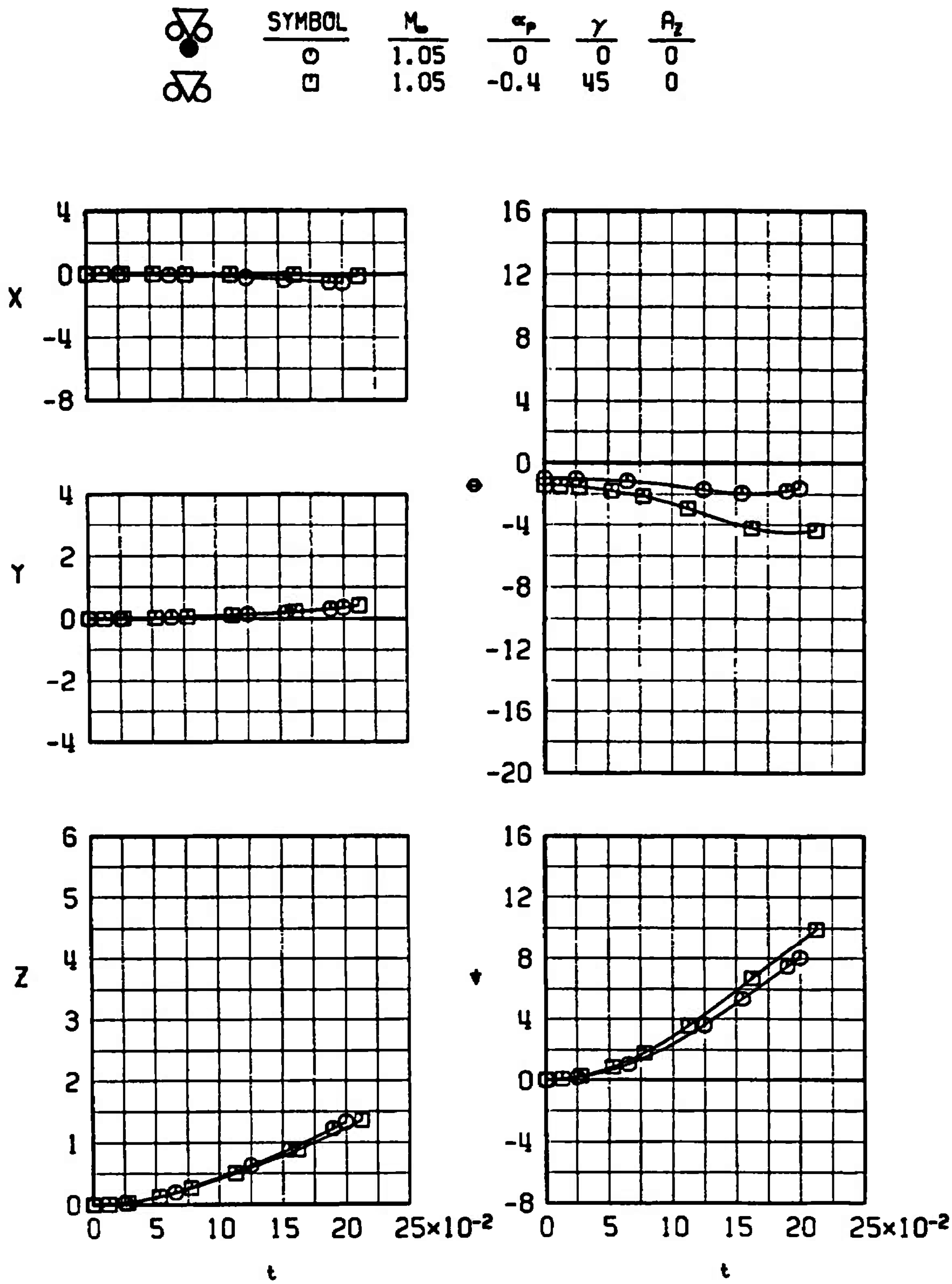

d. Configuration 1-2, M_∞ = 1.05
Fig. 19 Continued

SYMBOL	M_∞	α_p	γ	A_z
○	1.15	0	0	0
□	1.15	-0.5	45	0

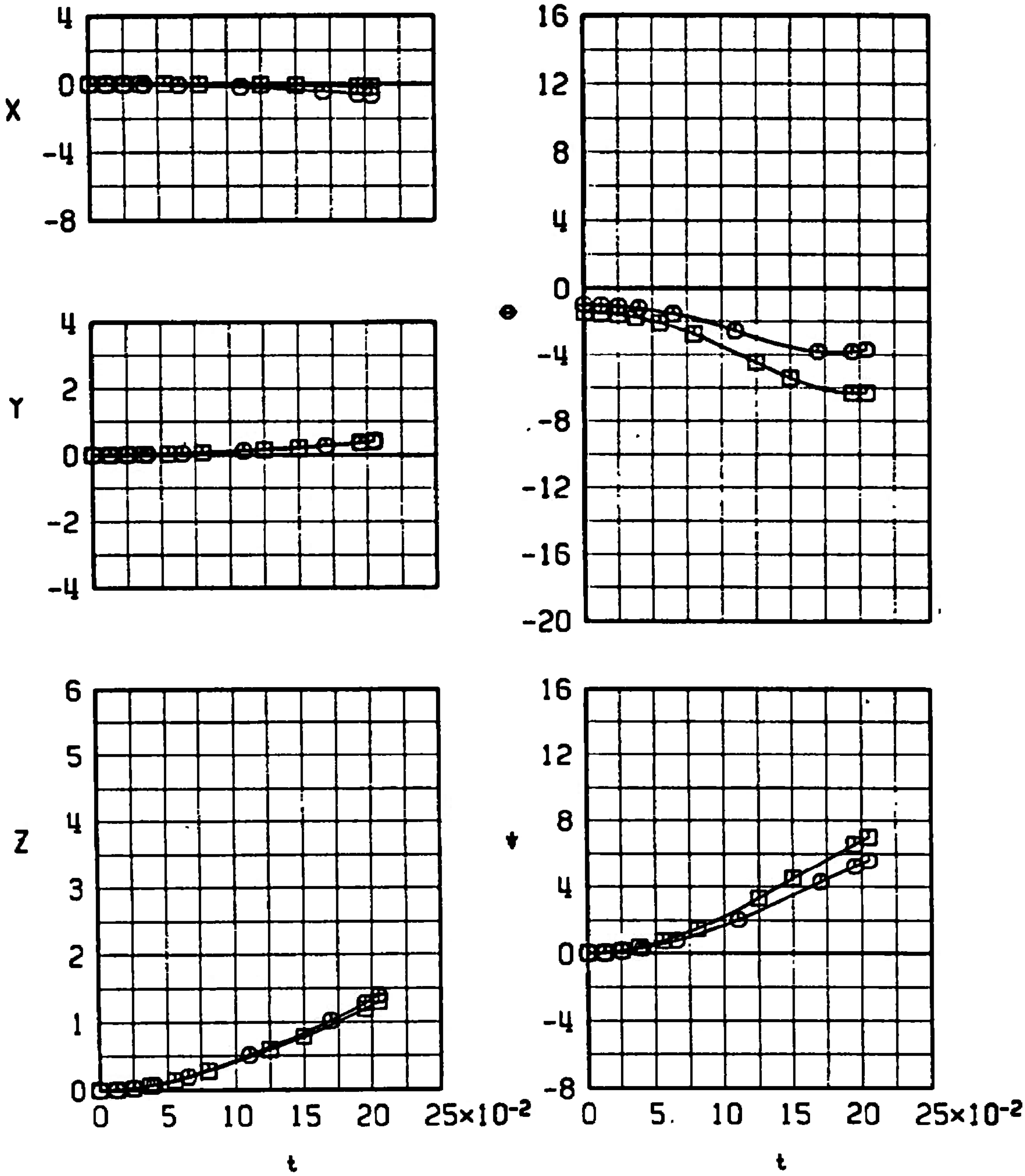

e. Configuration 1-2, M_∞ = 1.15
Fig. 19 Continued

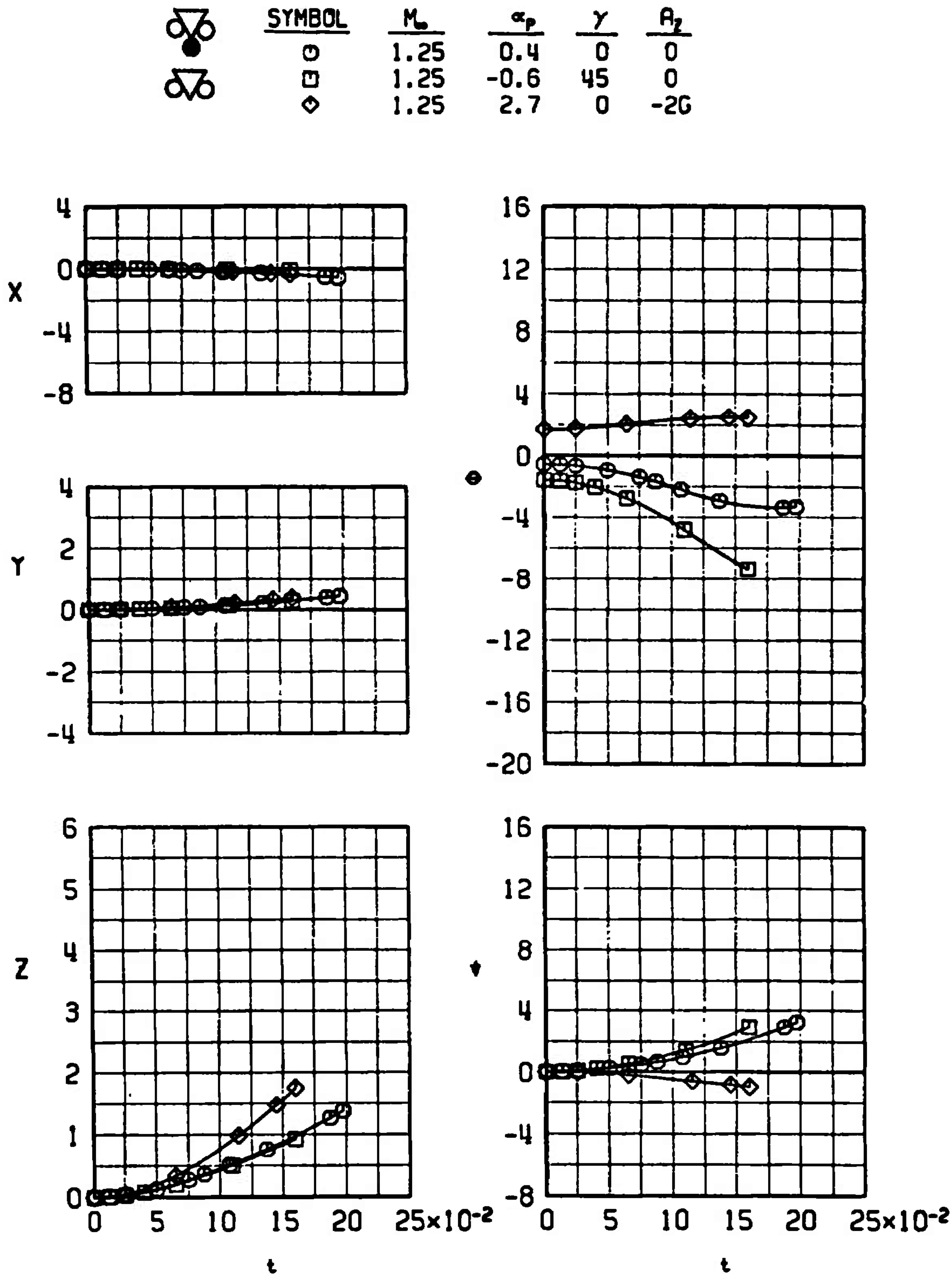

f. Configuration 1-2, M_∞ = 1.25
Fig. 19 Continued

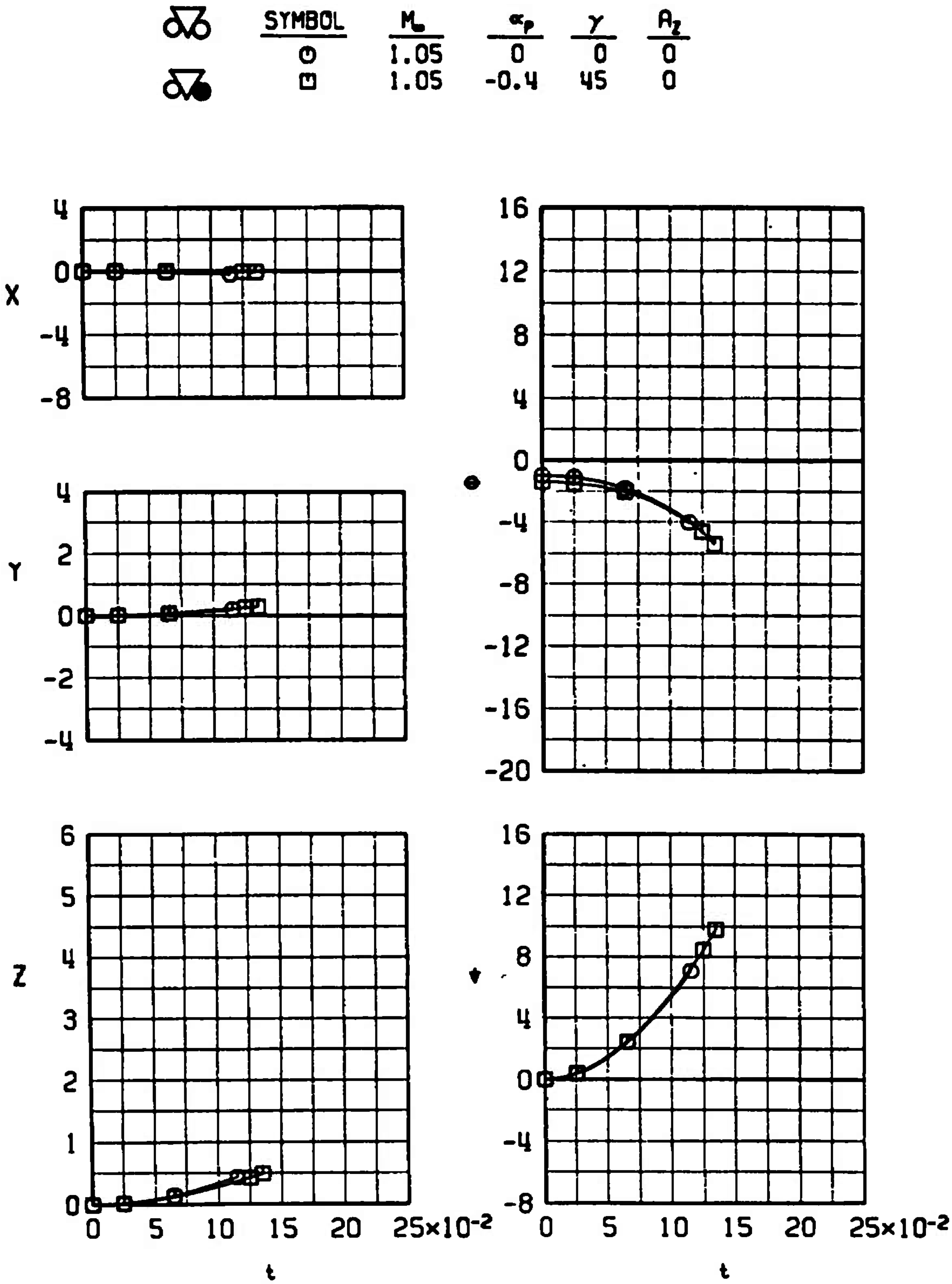

g. Configuration 1-3, M_∞ = 1.05
Fig. 19 Continued

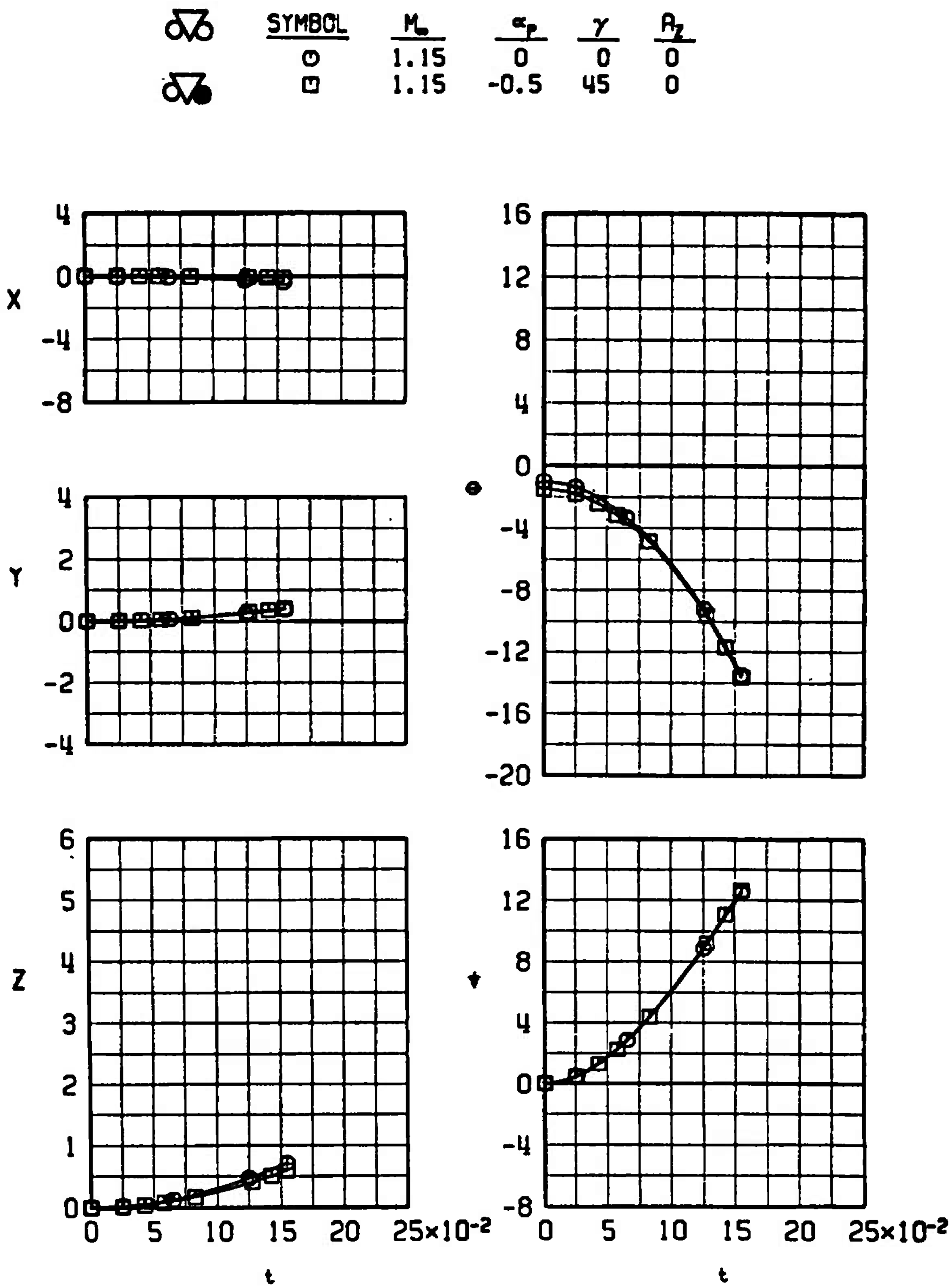

h. Configuration 1-3, M_∞ = 1.15
Fig. 19 Continued

SYMBOL	M_∞	α_p	γ	A_z
○	1.25	0.4	0	0
□	1.25	-0.6	45	0
◇	1.25	2.7	0	-2G

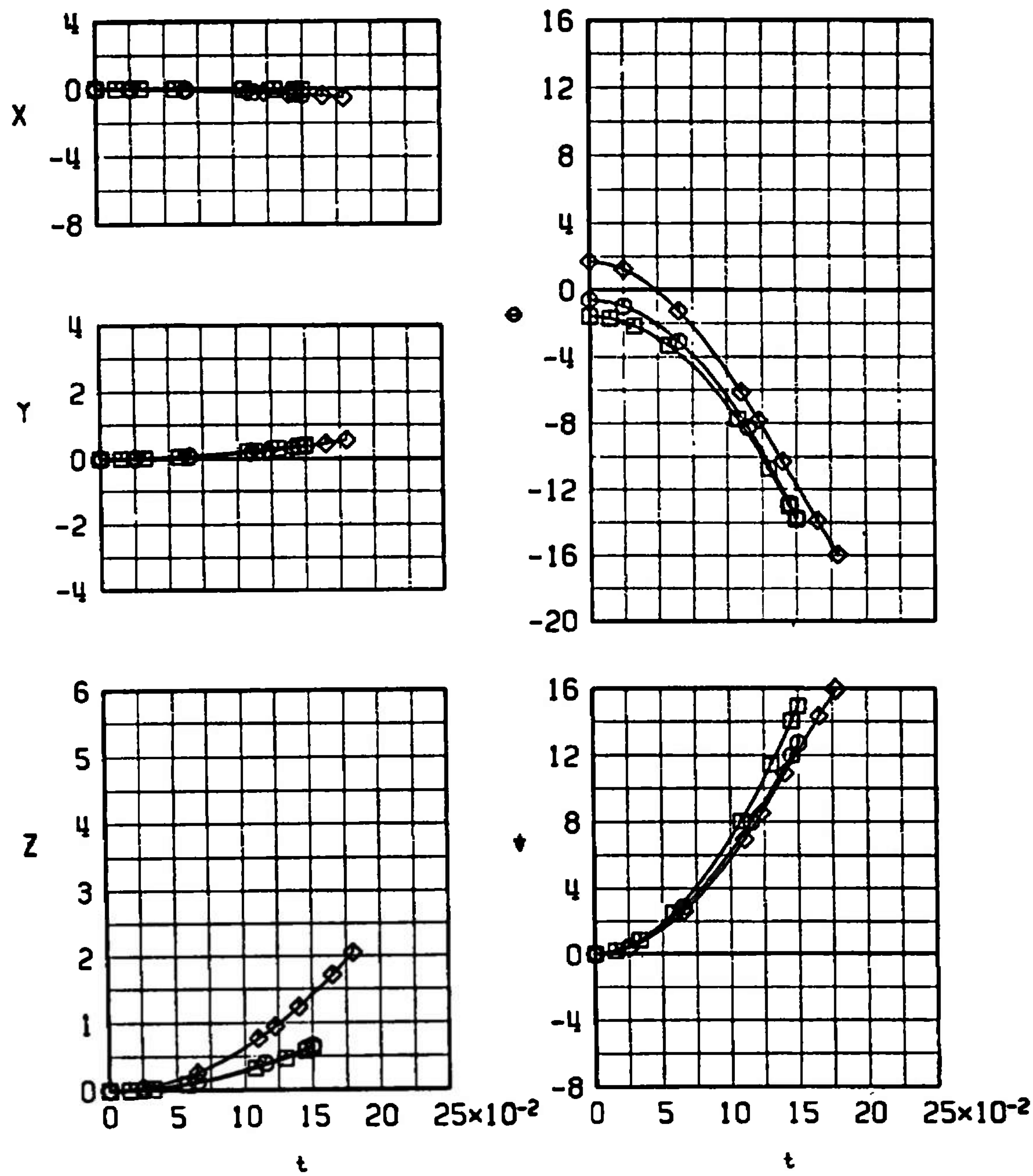

i. Configuration 1-3, M_∞ = 1.25
Fig. 19 Continued

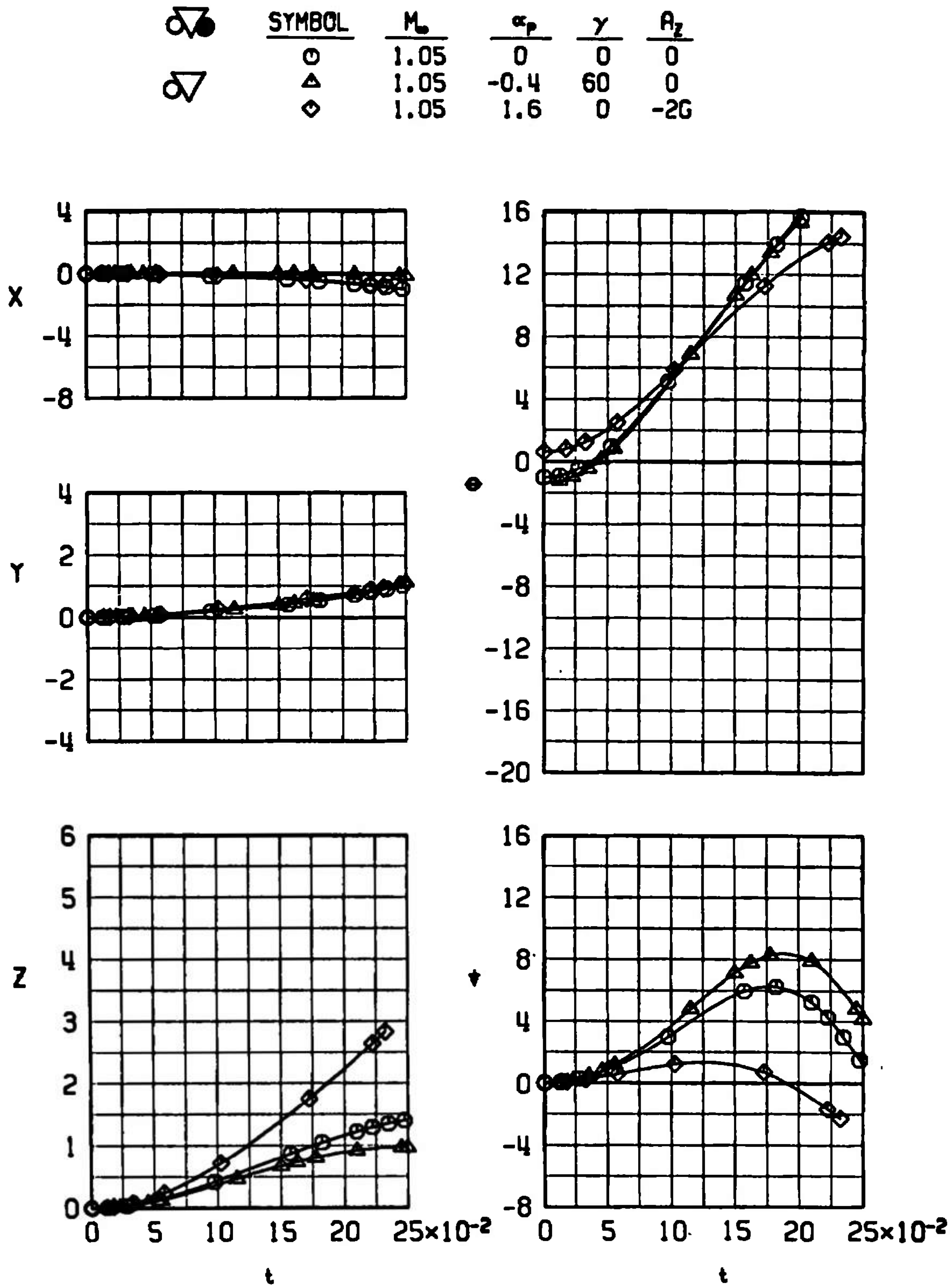

j. Configuration 1-4, M_∞ = 1.05
Fig. 19 Continued

SYMBOL	M_∞	α_p	γ	A_z
⊙	1.15	0	0	0
△	1.15	-0.5	60	0

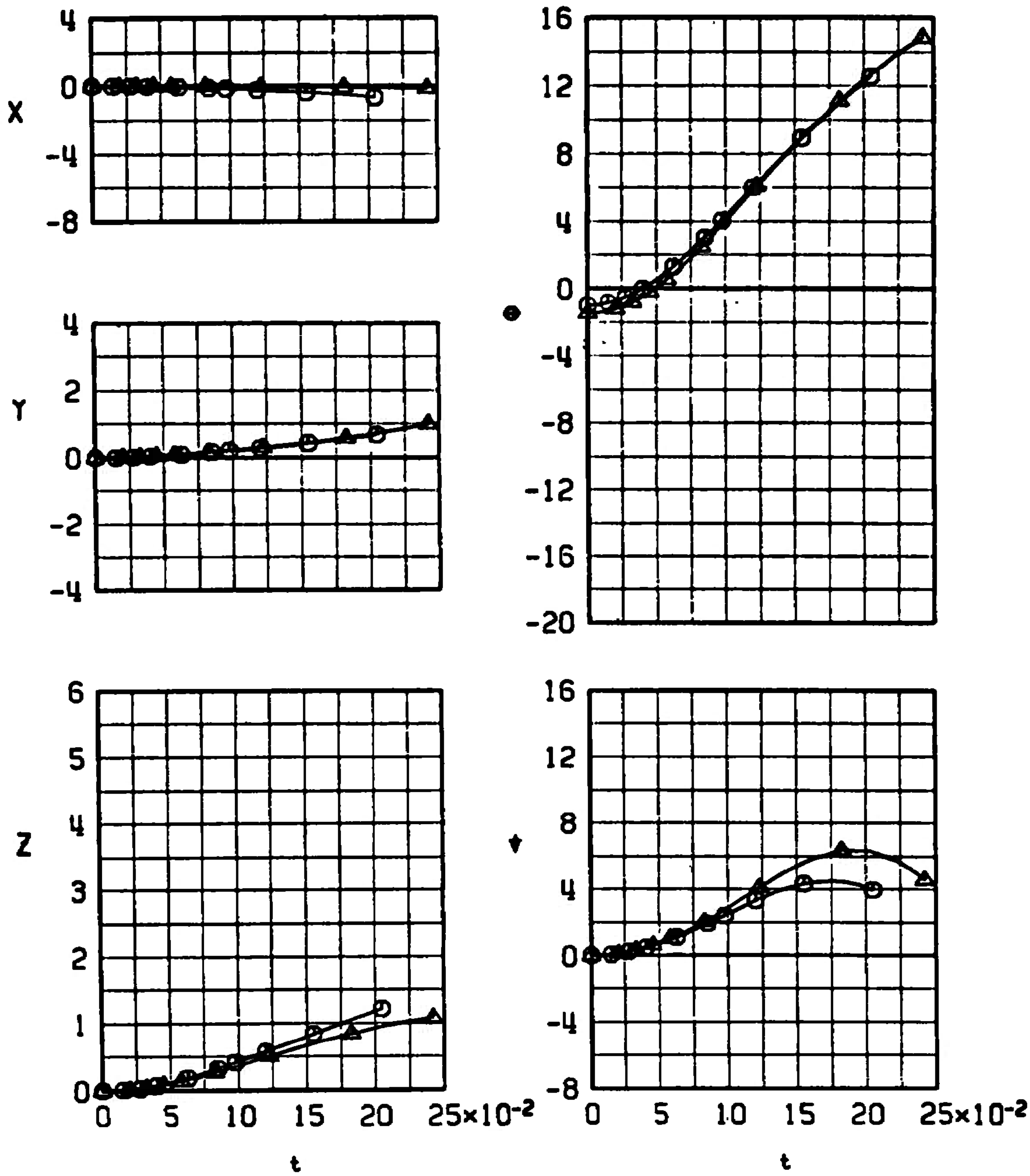

k. Configuration 1-4, M_∞ = 1.15
Fig. 19 Continued

	SYMBOL	M_∞	α_p	γ	A_z
	⊙	1.25	0.4	0	0
	△	1.25	-0.6	60	0

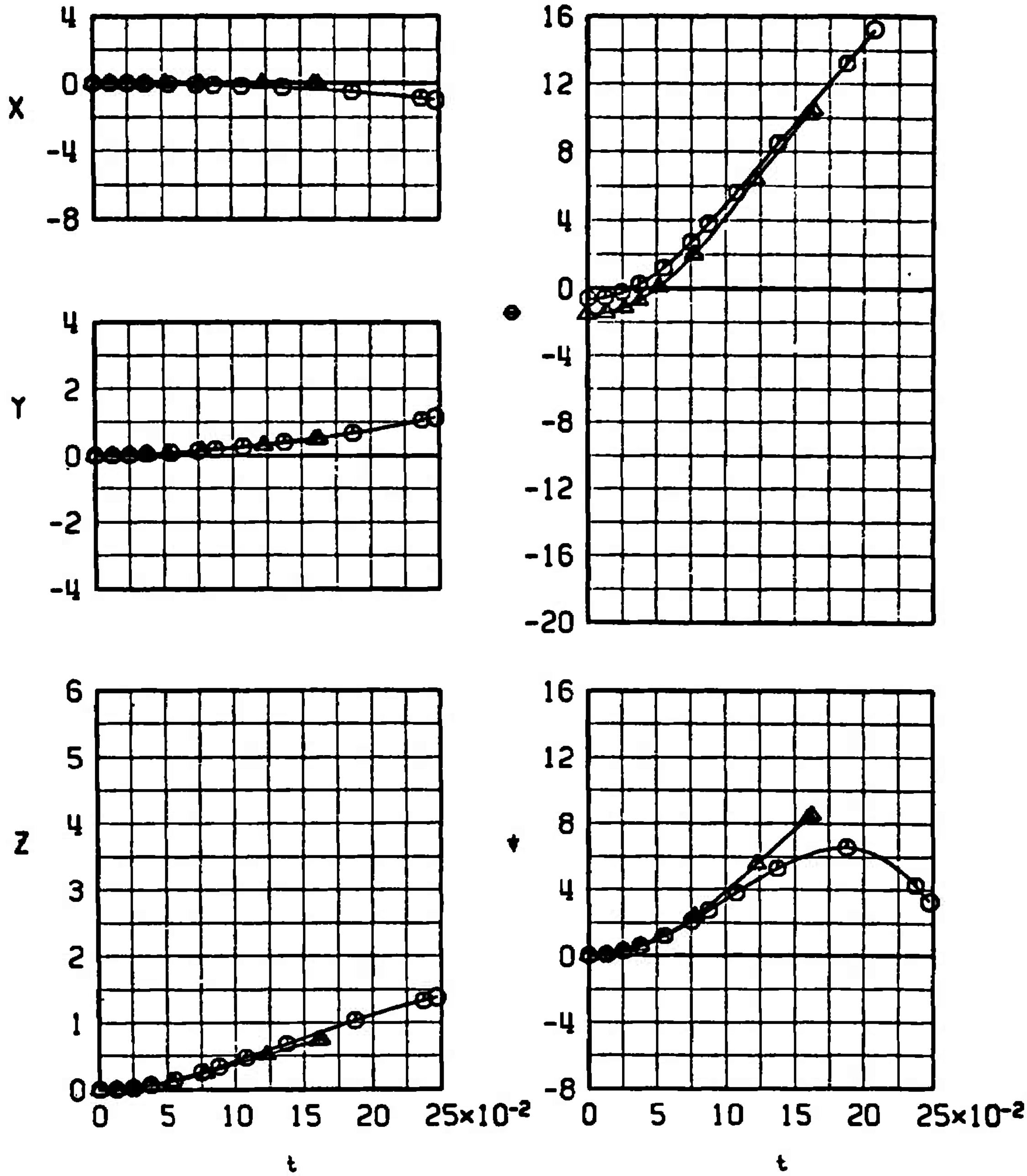

I. Configuration 1-4, M_∞ = 1.25
Fig. 19 Continued

	SYMBOL	M_∞	α_p	γ	R_Z
○▽	○	1.05	0	0	0
●▽	□	1.05	-0.4	45	0

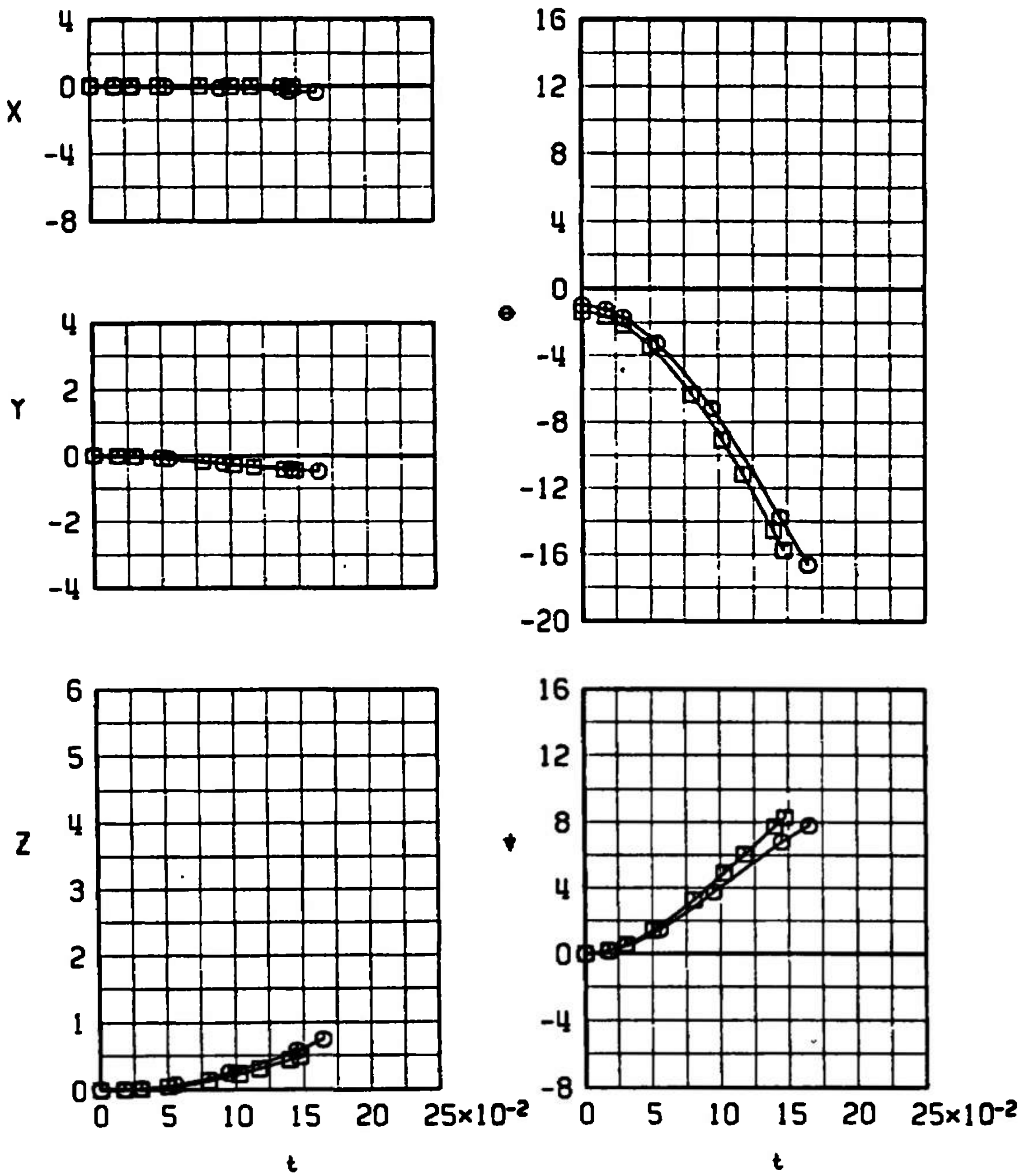

m. Configuration 1-5, M_∞ = 1.05
Fig. 19 Continued

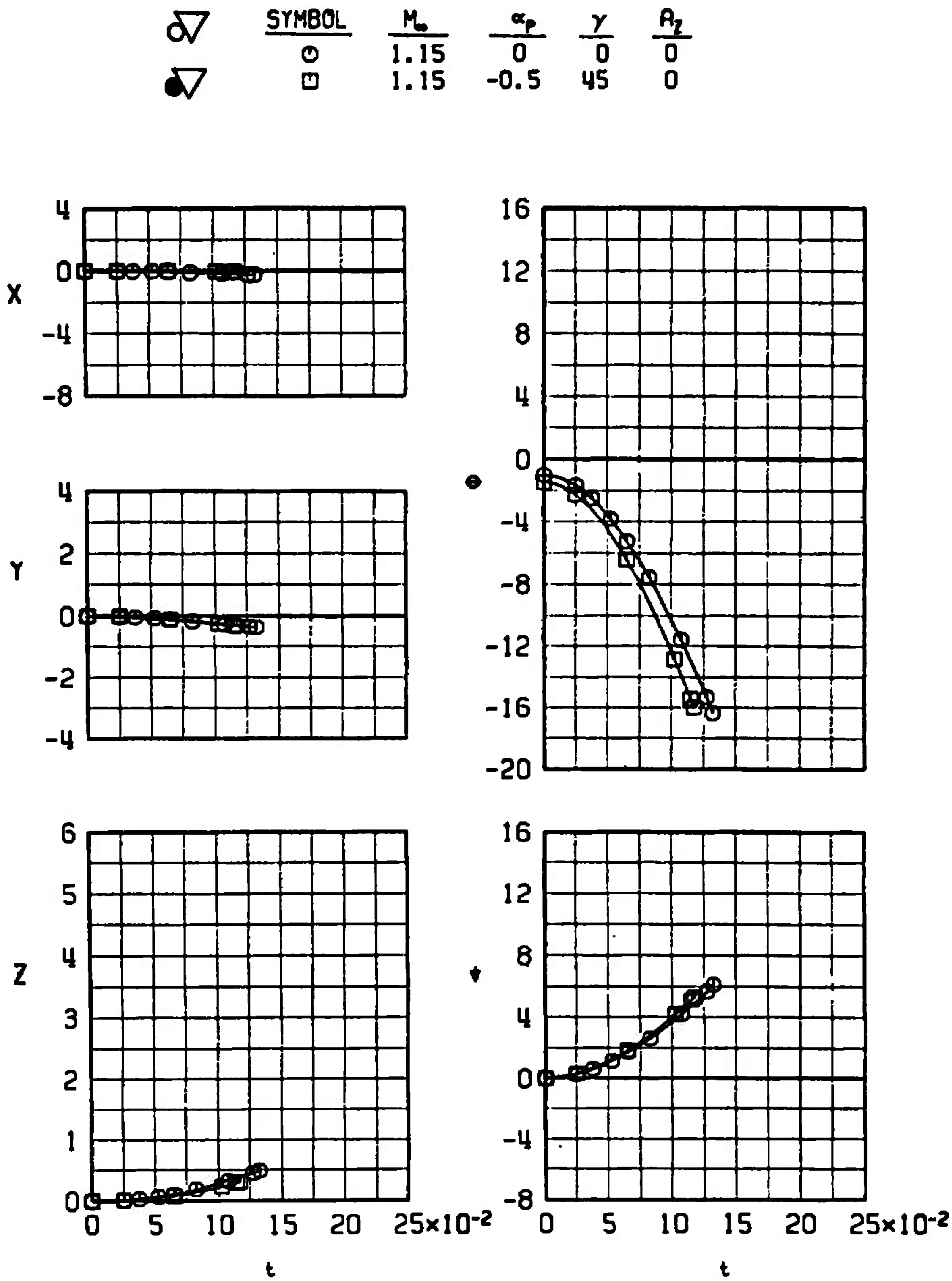

n. Configuration 1-5, M_∞ = 1.15
Fig. 19 Continued

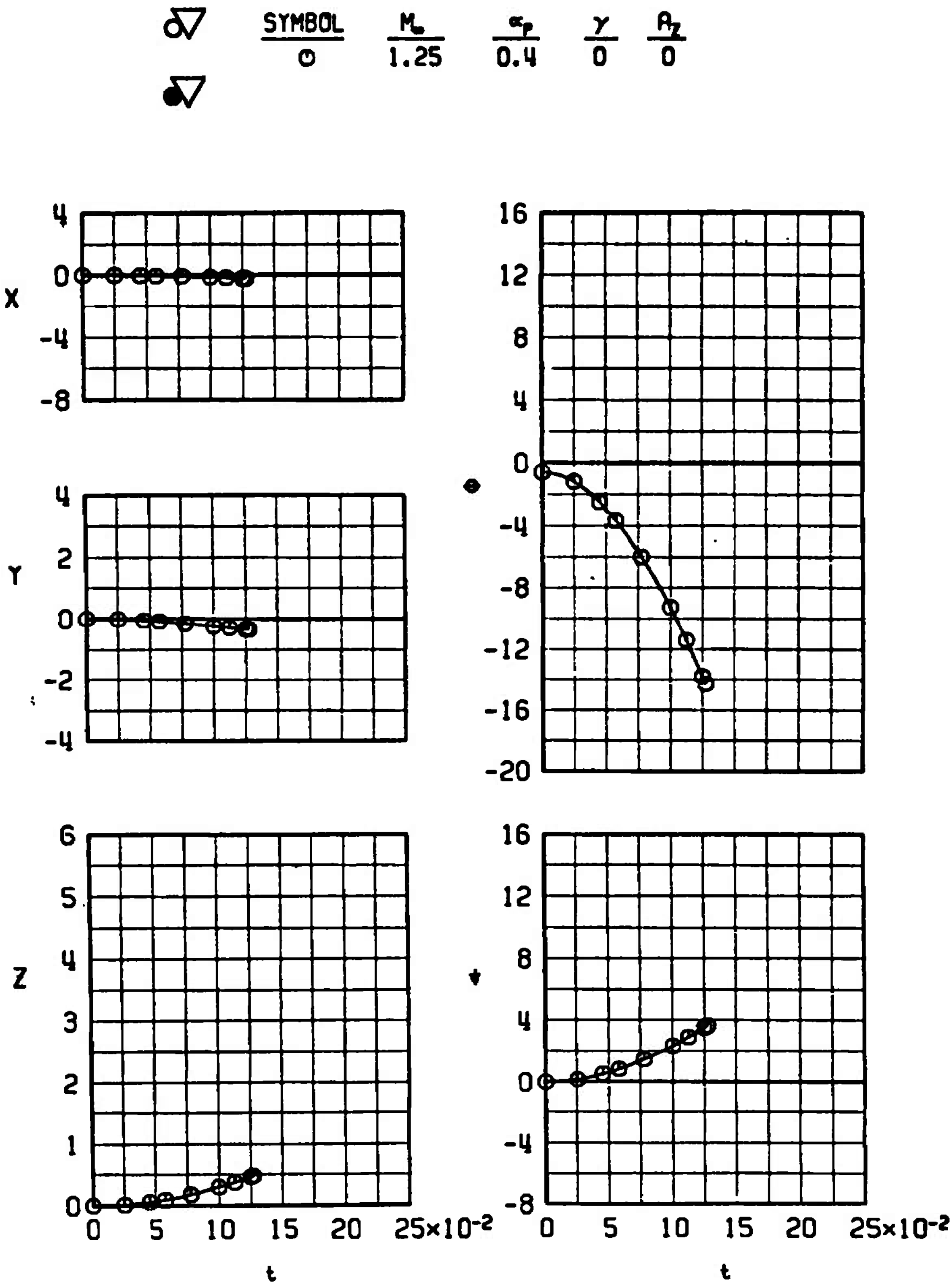

o. Configuration 1-5, M_∞ = 1.25
Fig. 19 Continued

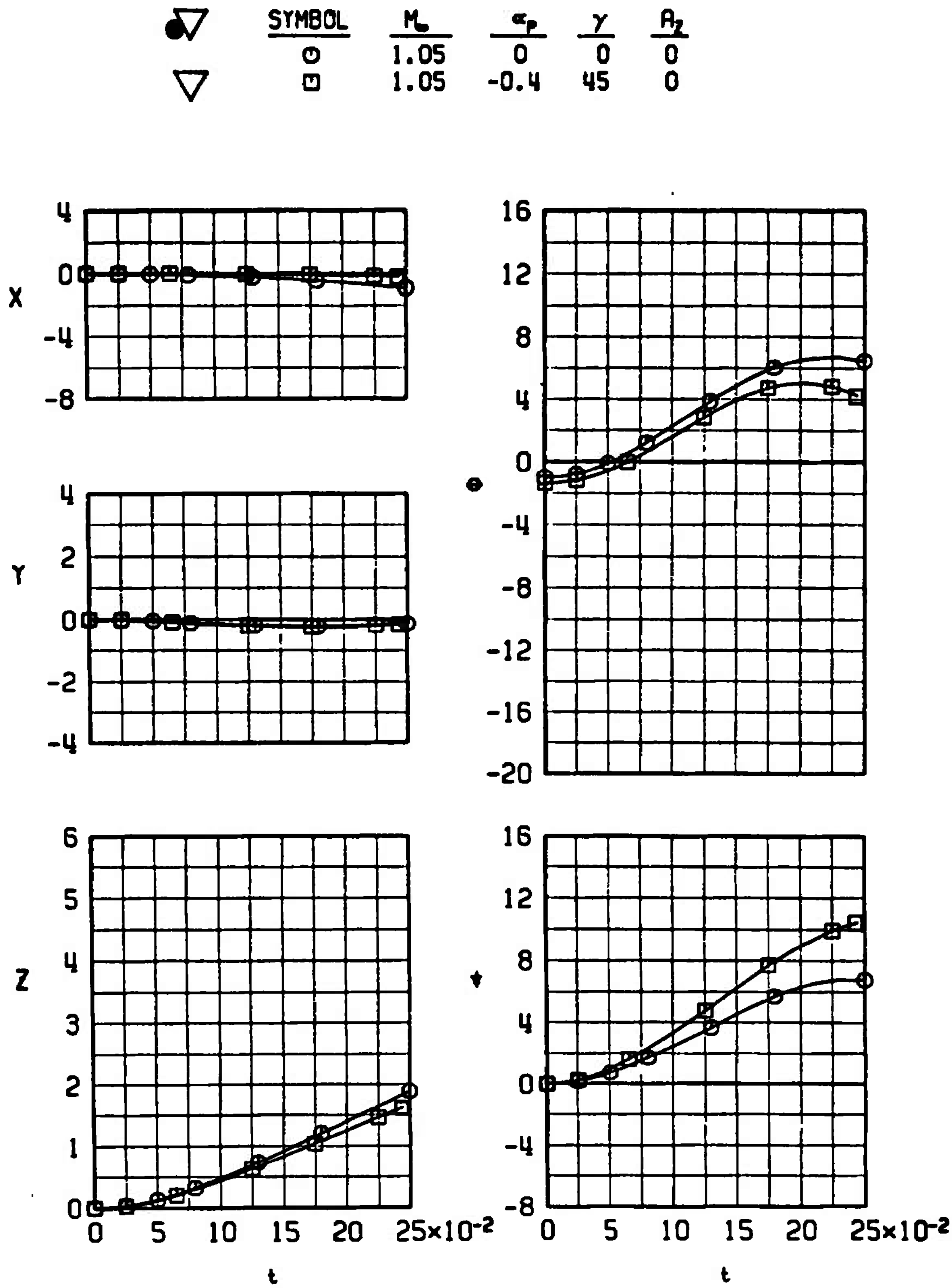

p. Configuration 1-6, M_∞ = 1.05
Fig. 19 Continued

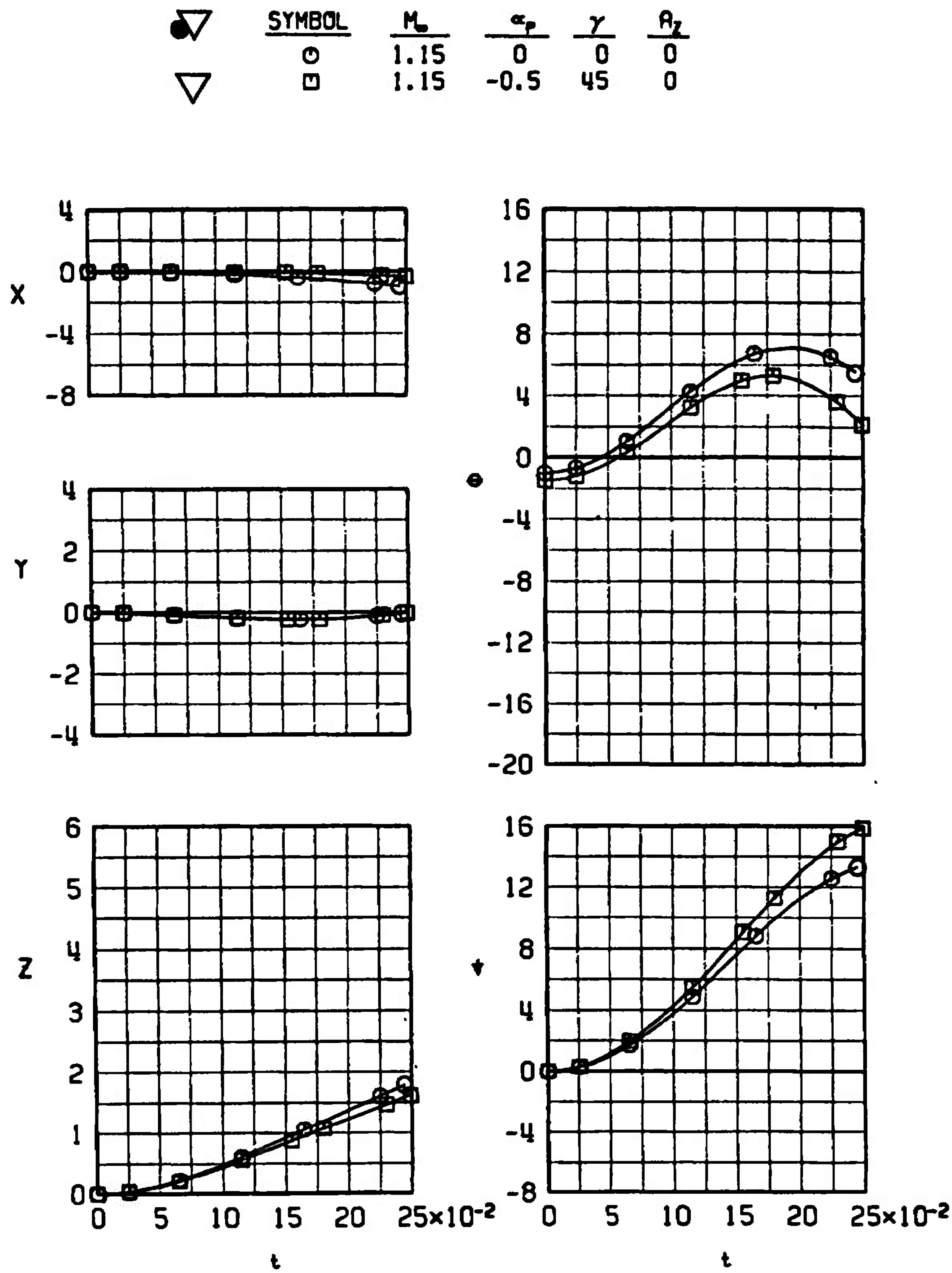

q. Configuration 1-6, M_∞ = 1.15
Fig. 19 Continued

SYMBOL	M_∞	α_p	γ	A_Z
○	1.25	0.4	0	0
□	1.25	-0.6	45	0
◇	1.25	2.7	0	-2G

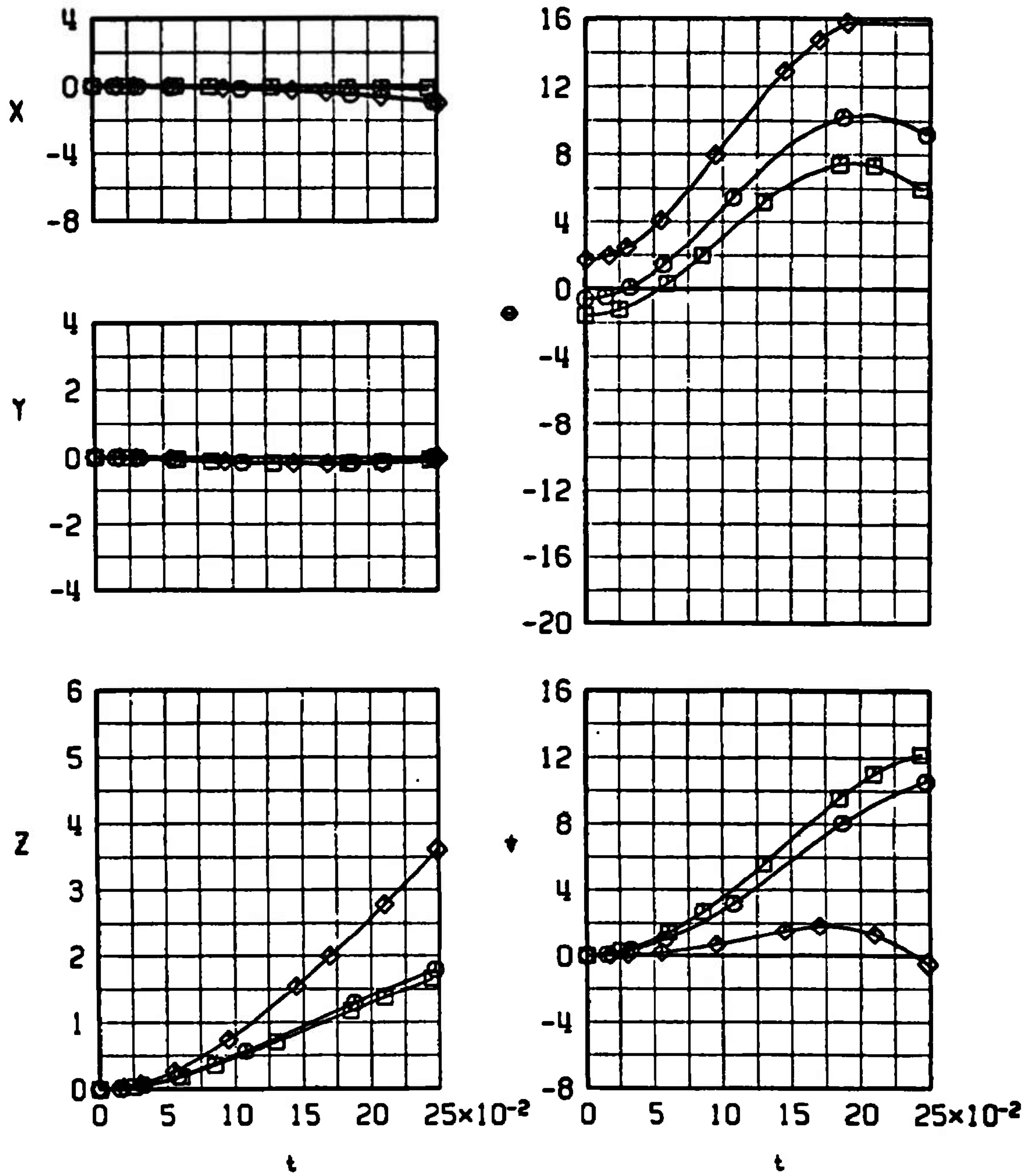

r. Configuration 1-6, M_∞ = 1.25
Fig. 19 Continued

SYMBOL	M_∞	α_p	γ	A_z
⊙	1.05	0	0	0
⊡	1.05	-0.4	45	0

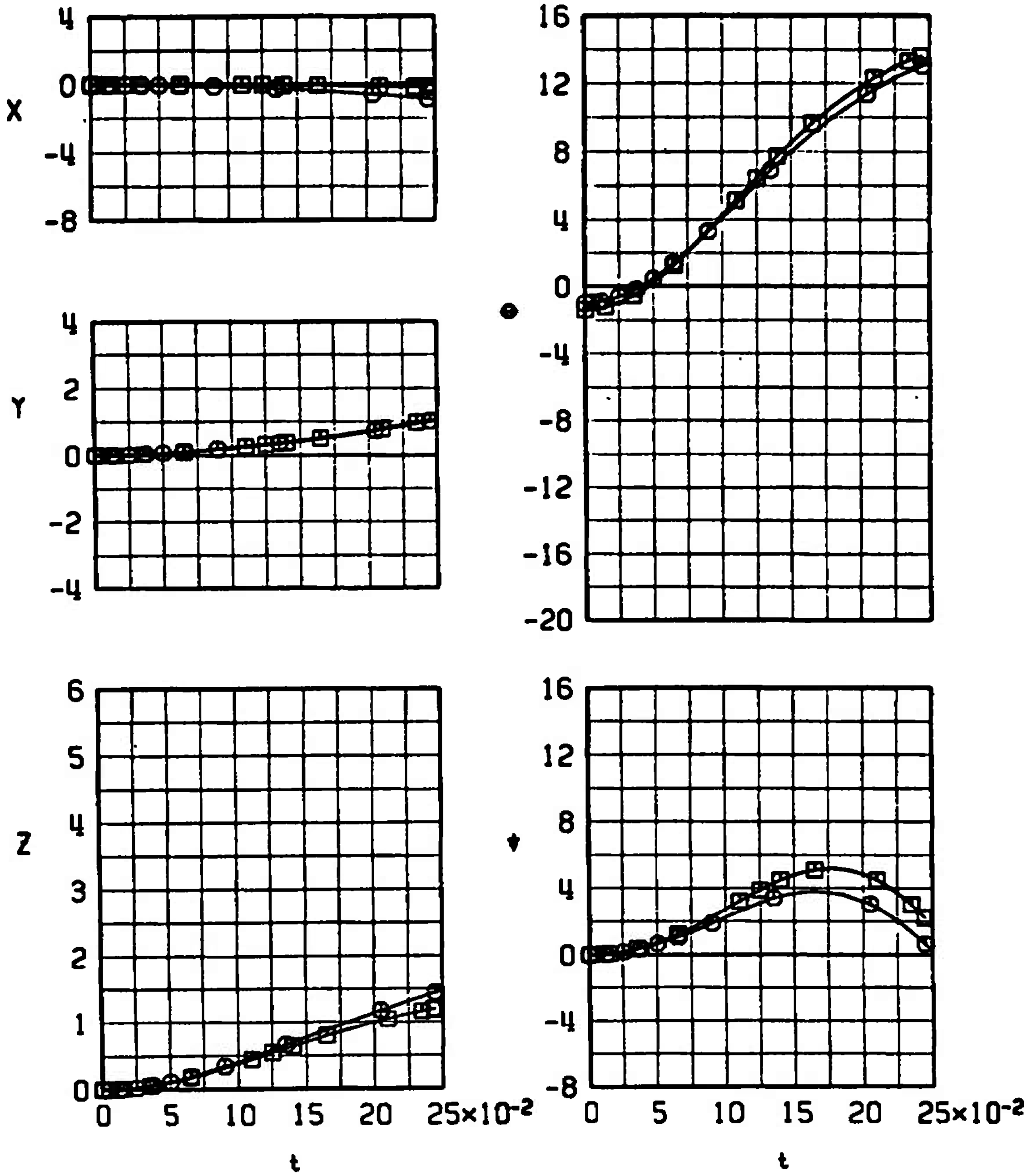

s. Configuration 1-7, M_∞ = 1.05
Fig. 19 Continued

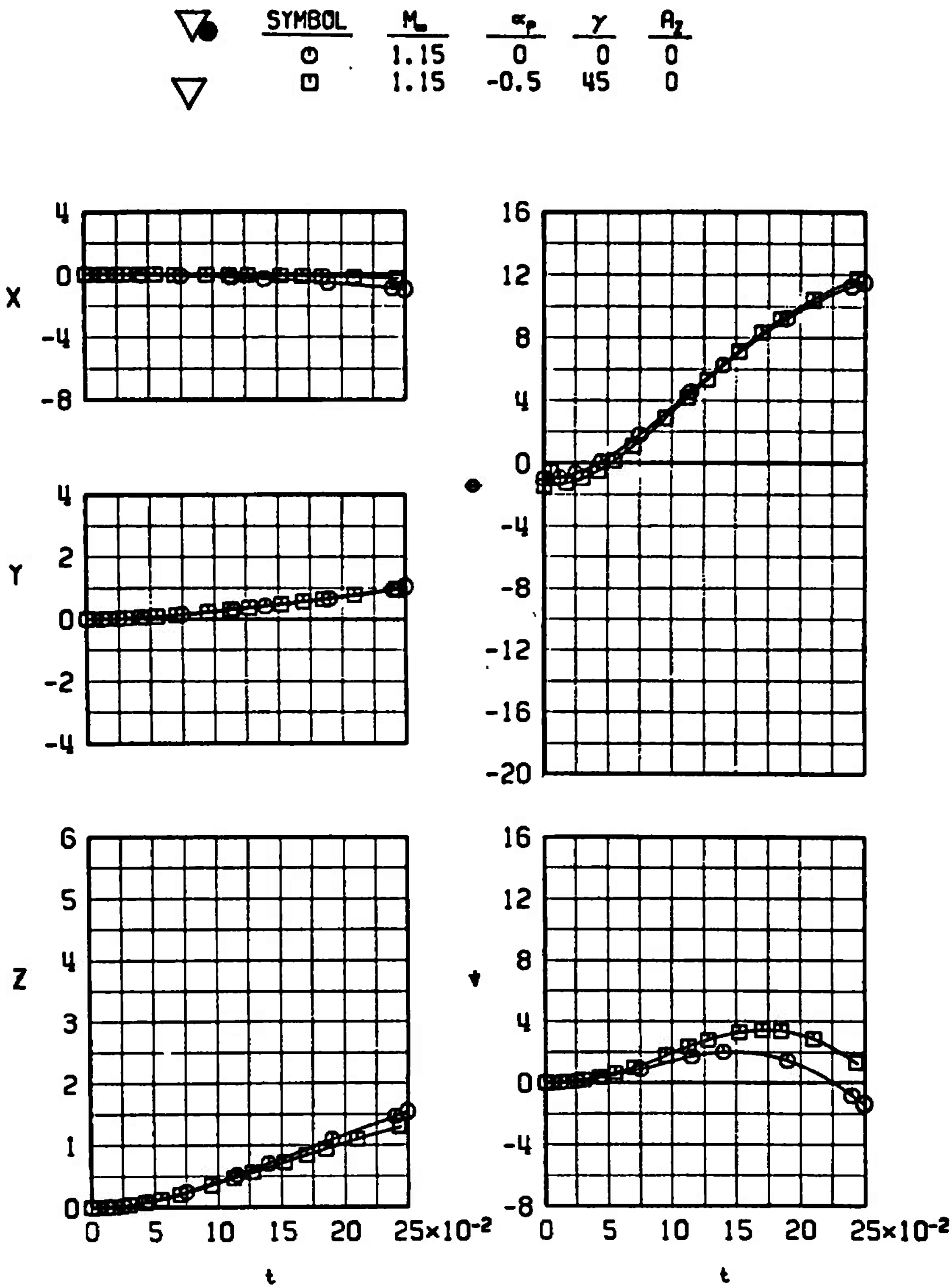

t. Configuration 1-7, M_∞ = 1.15
Fig. 19 Continued

SYMBOL	M_∞	α_p	γ	A_Z
○	1.25	0.4	0	0
□	1.25	-0.6	45	0
◇	1.25	2.7	0	-2G

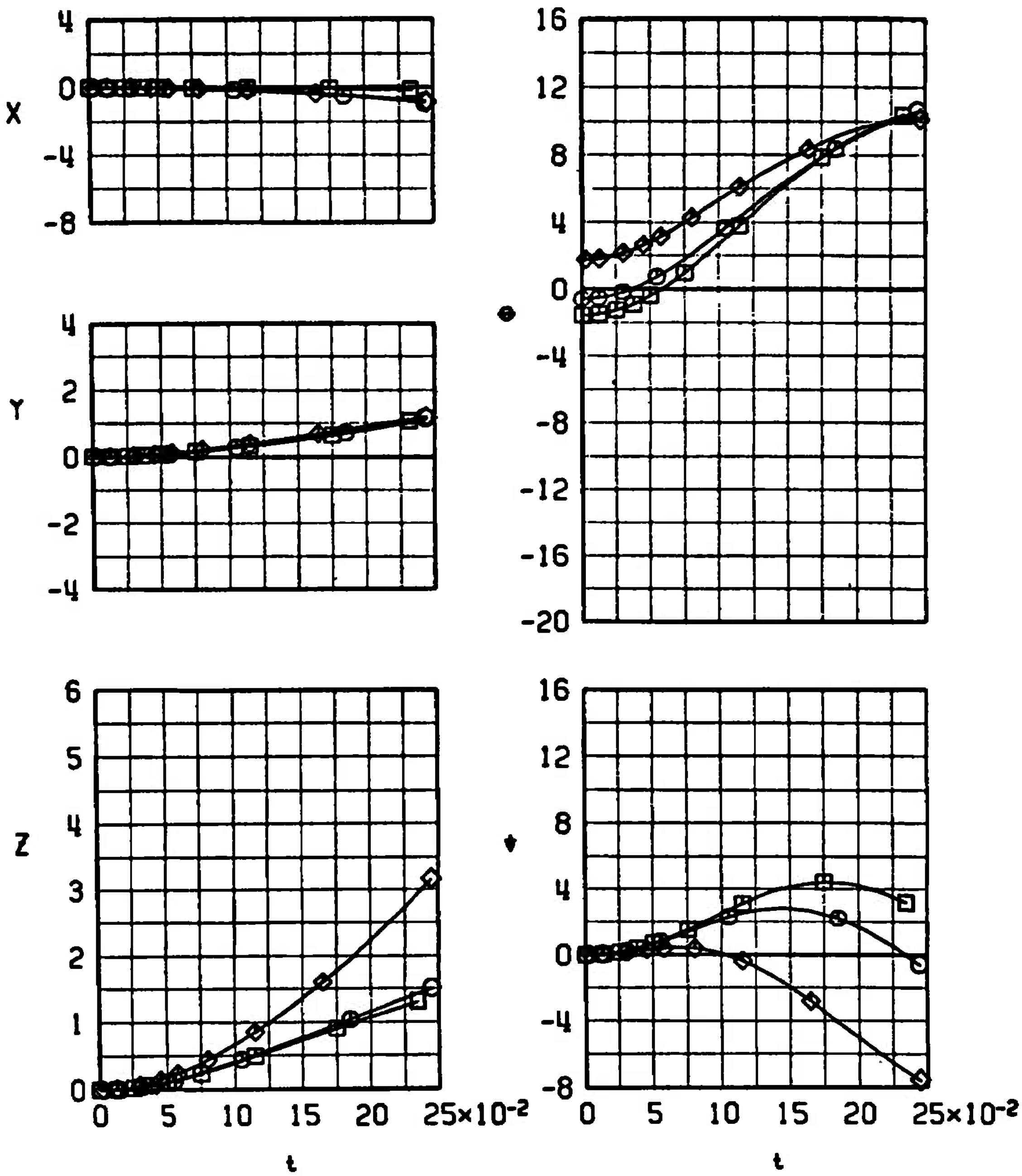

u. Configuration 1-7, M_∞ = 1.25
Fig. 19 Continued

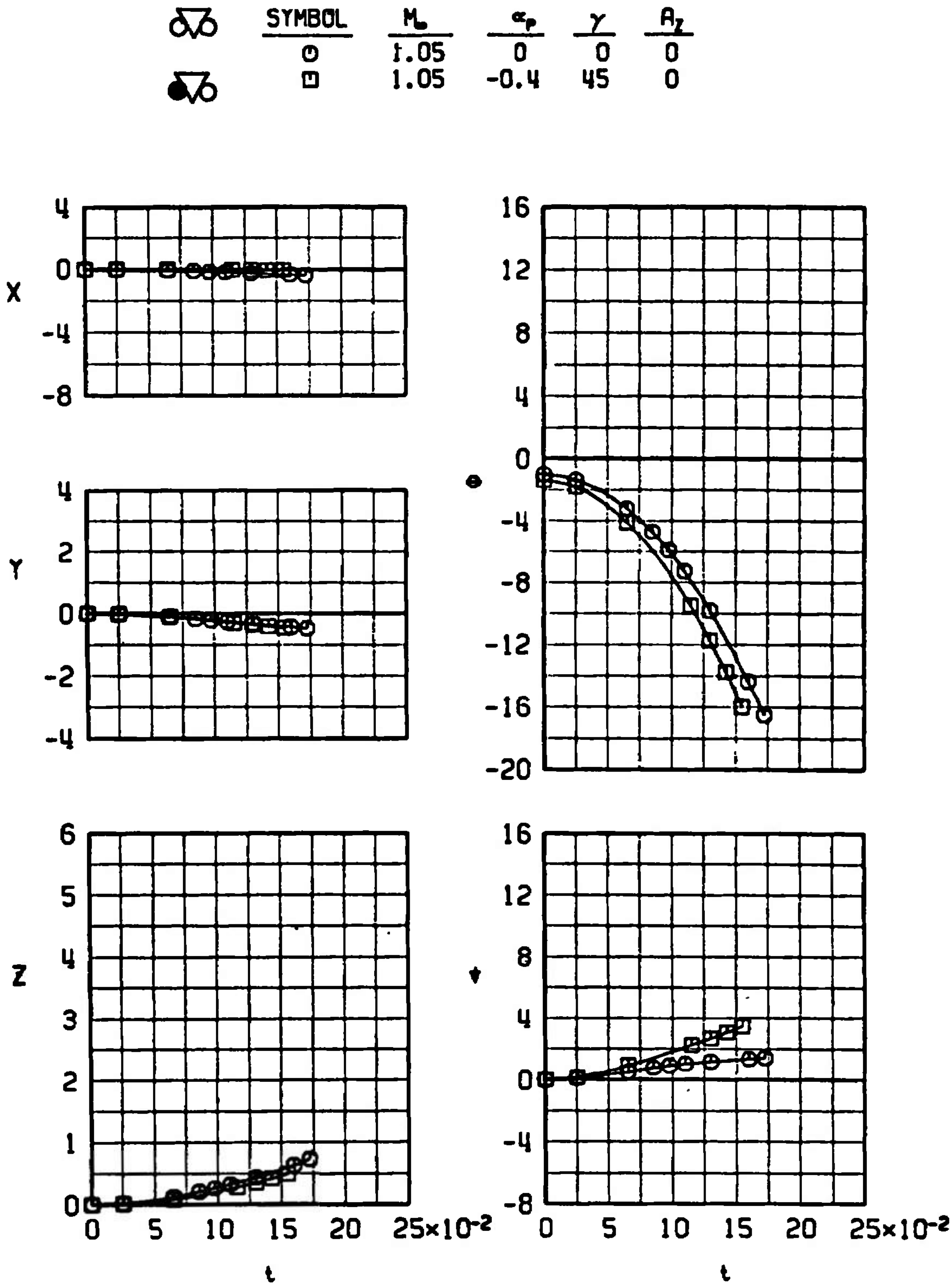

v. Configuration 1-10, $M_\infty = 1.05$
Fig. 19 Continued

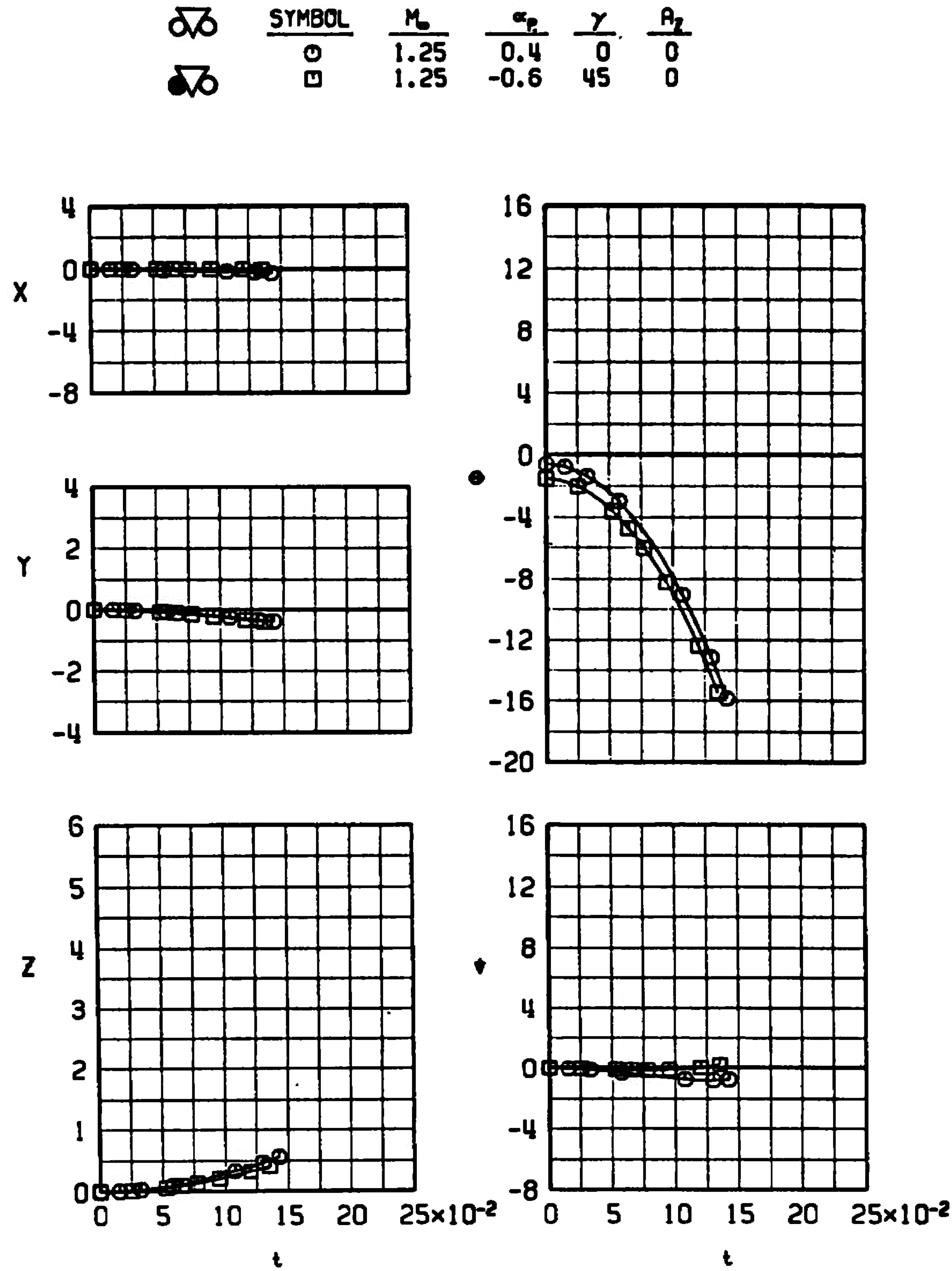

w. Configuration 1-10, M_∞ = 1.25
Fig. 19 Concluded

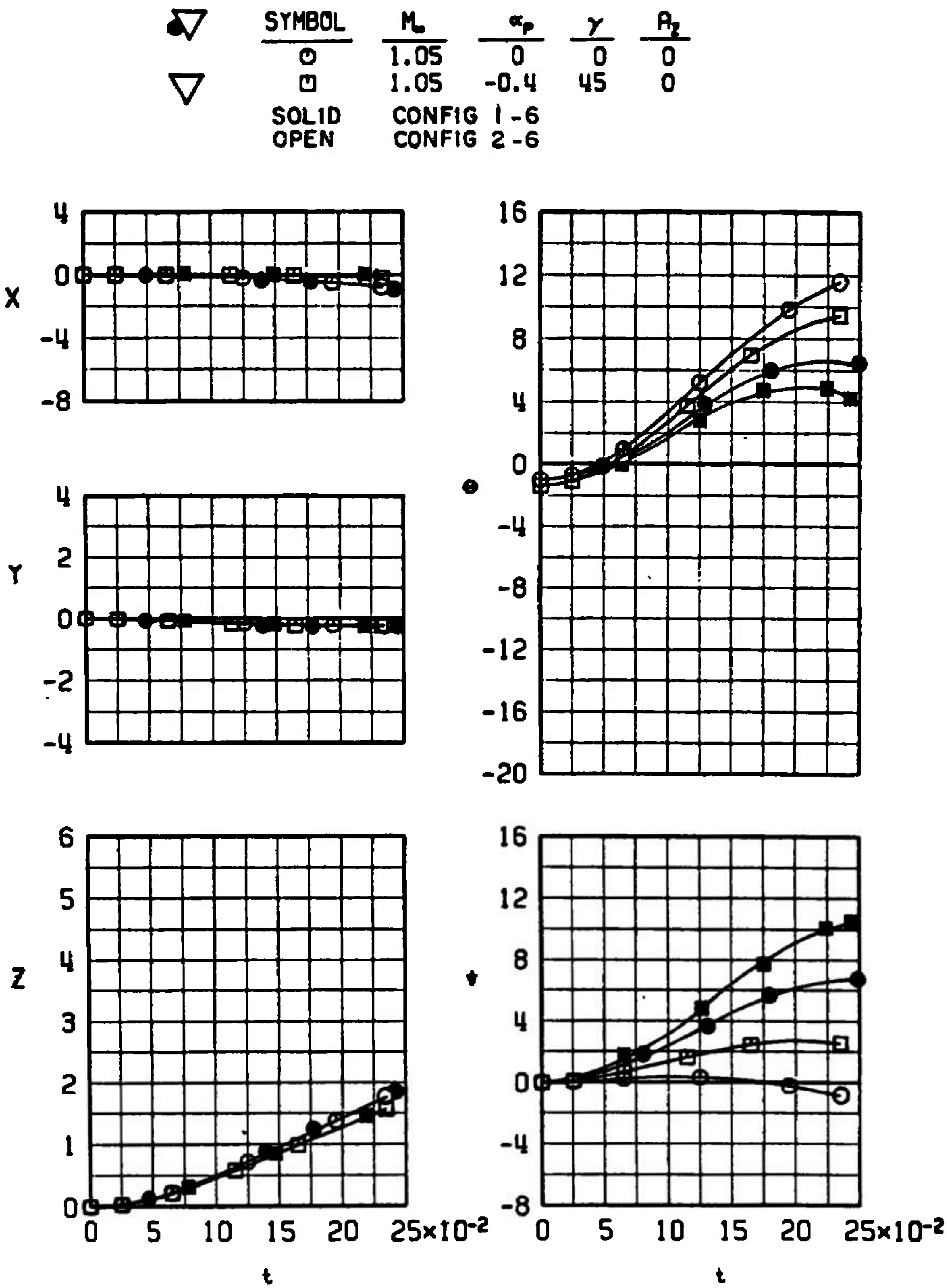

e. M_∞ = 1.05, MER Station 4

Fig. 20 Effects of External Store Configuration on the MK-82 GPB Launch Trajectories from the MER

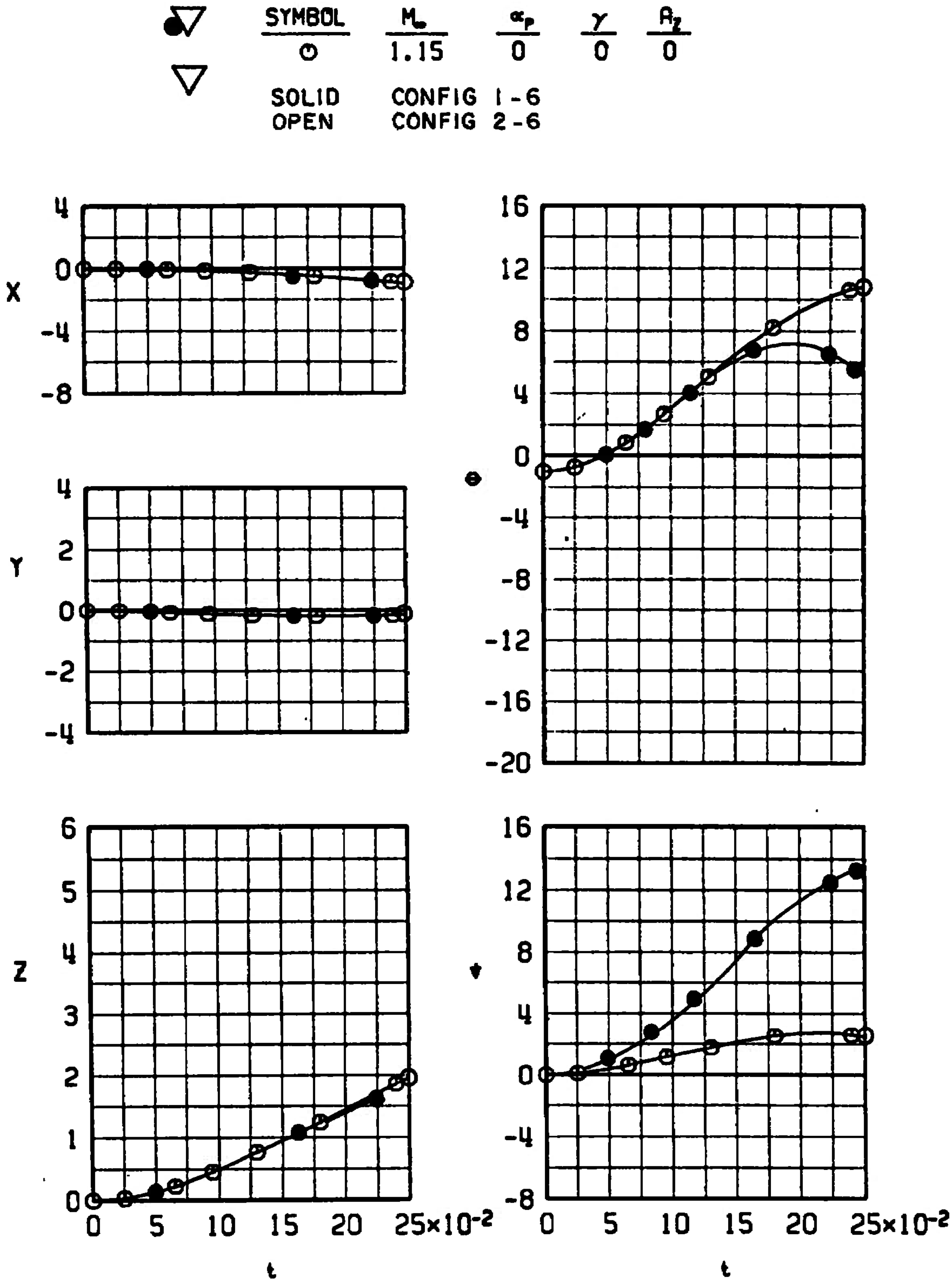

b. M_∞ = 1.15, MER Station 4
Fig. 20 Continued

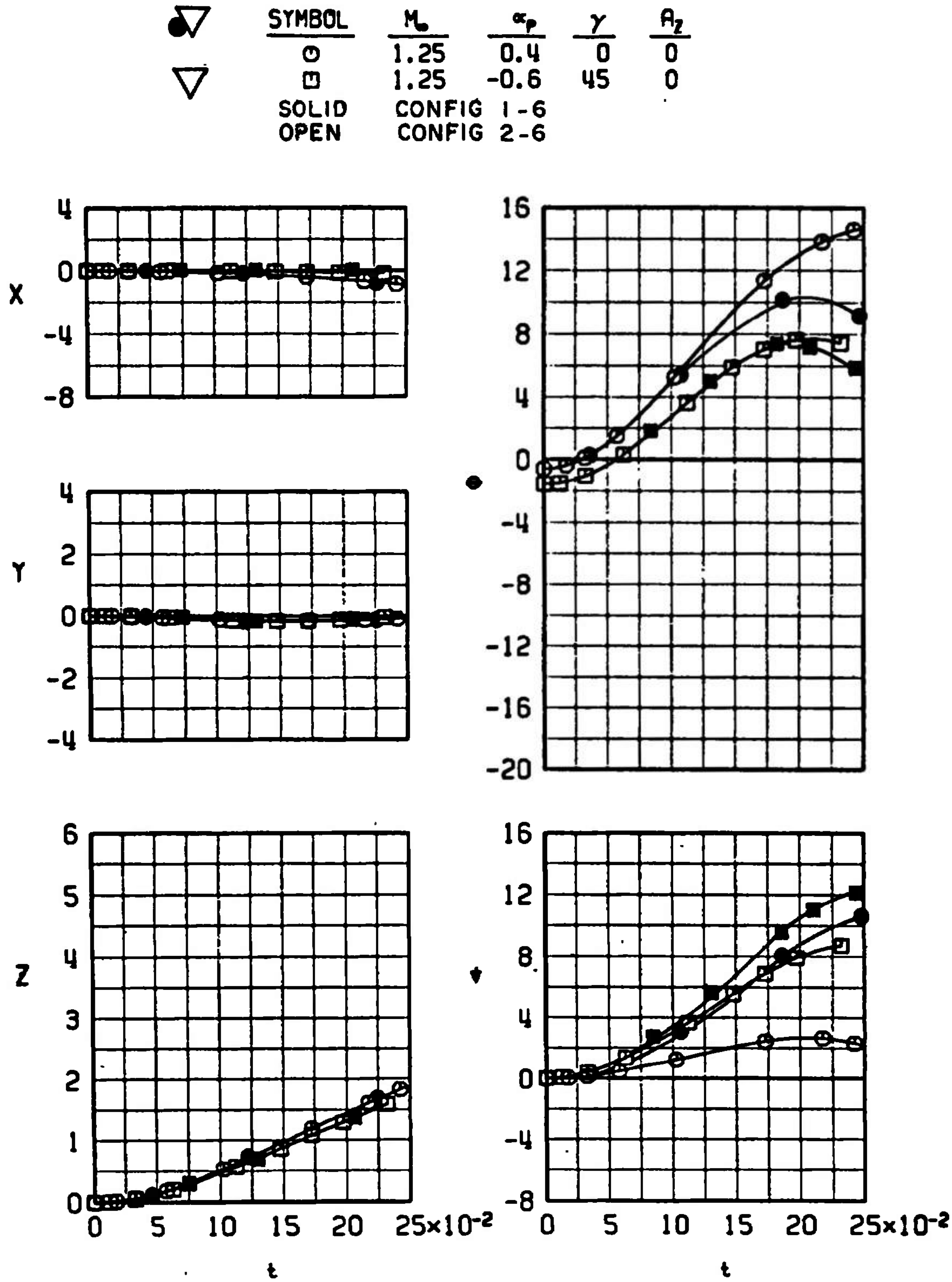

c. M_∞ = 1.25, MER Station 4
Fig. 20 Continued

SYMBOL	M_∞	α_p	γ	A_z
○	1.05	0	0	0
□	1.05	-0.4	45	0

SOLID CONFIG 1-6
OPEN CONFIG 2-6

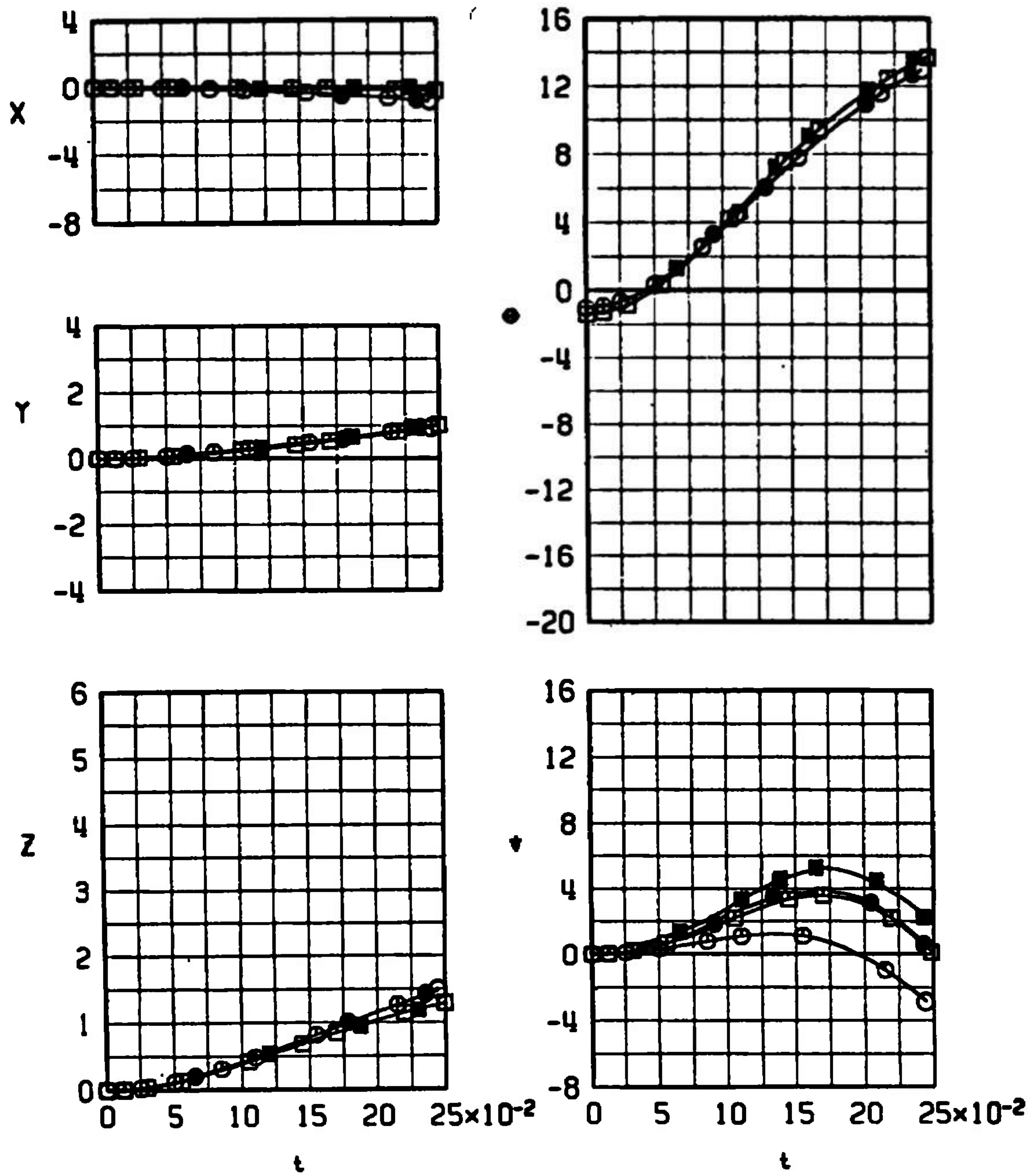

d. M_∞ = 1.05, MER Station 6
Fig. 20 Continued

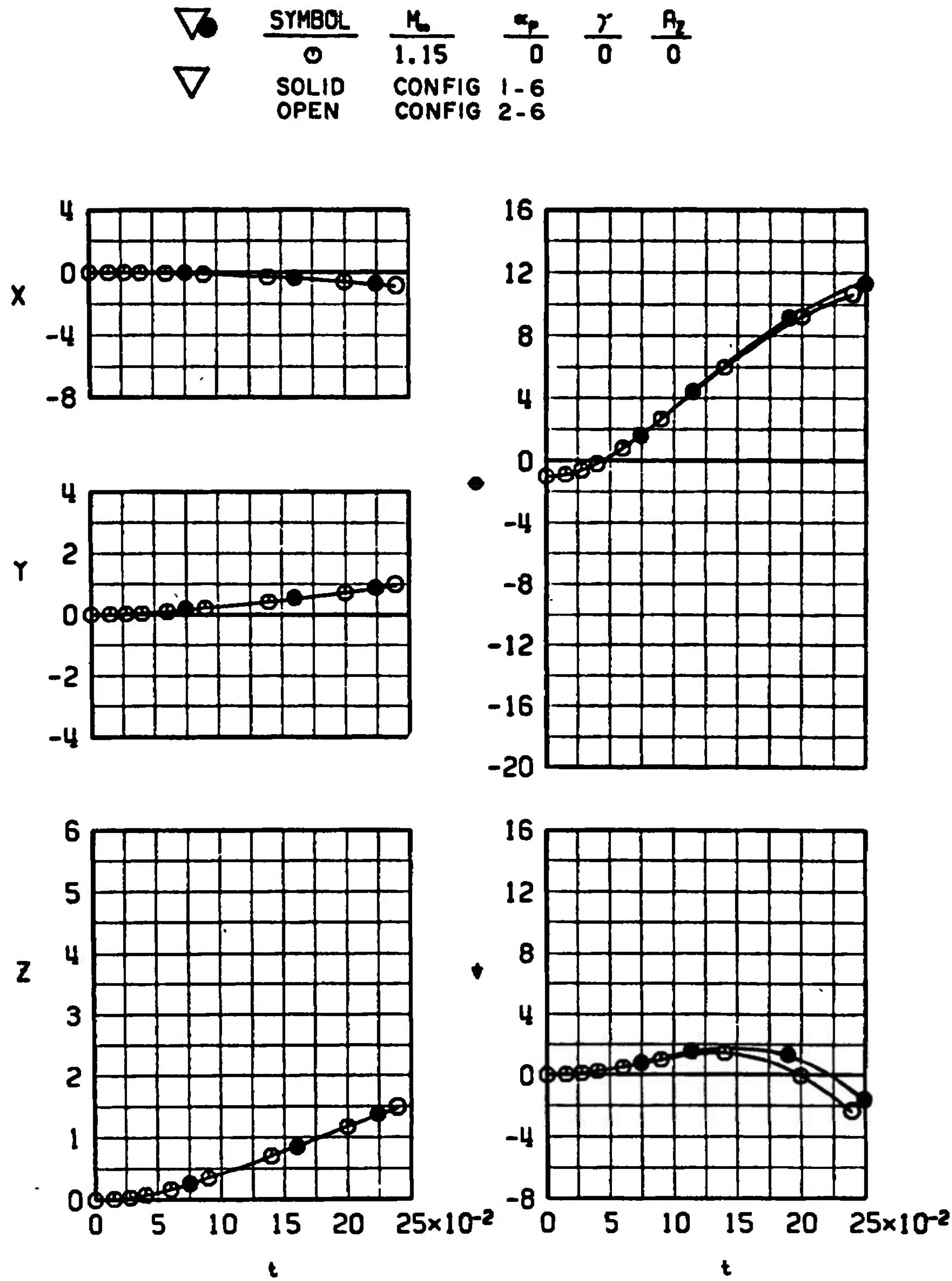

e. M_∞ = 1.15, MER Station 6
Fig. 20 Continued

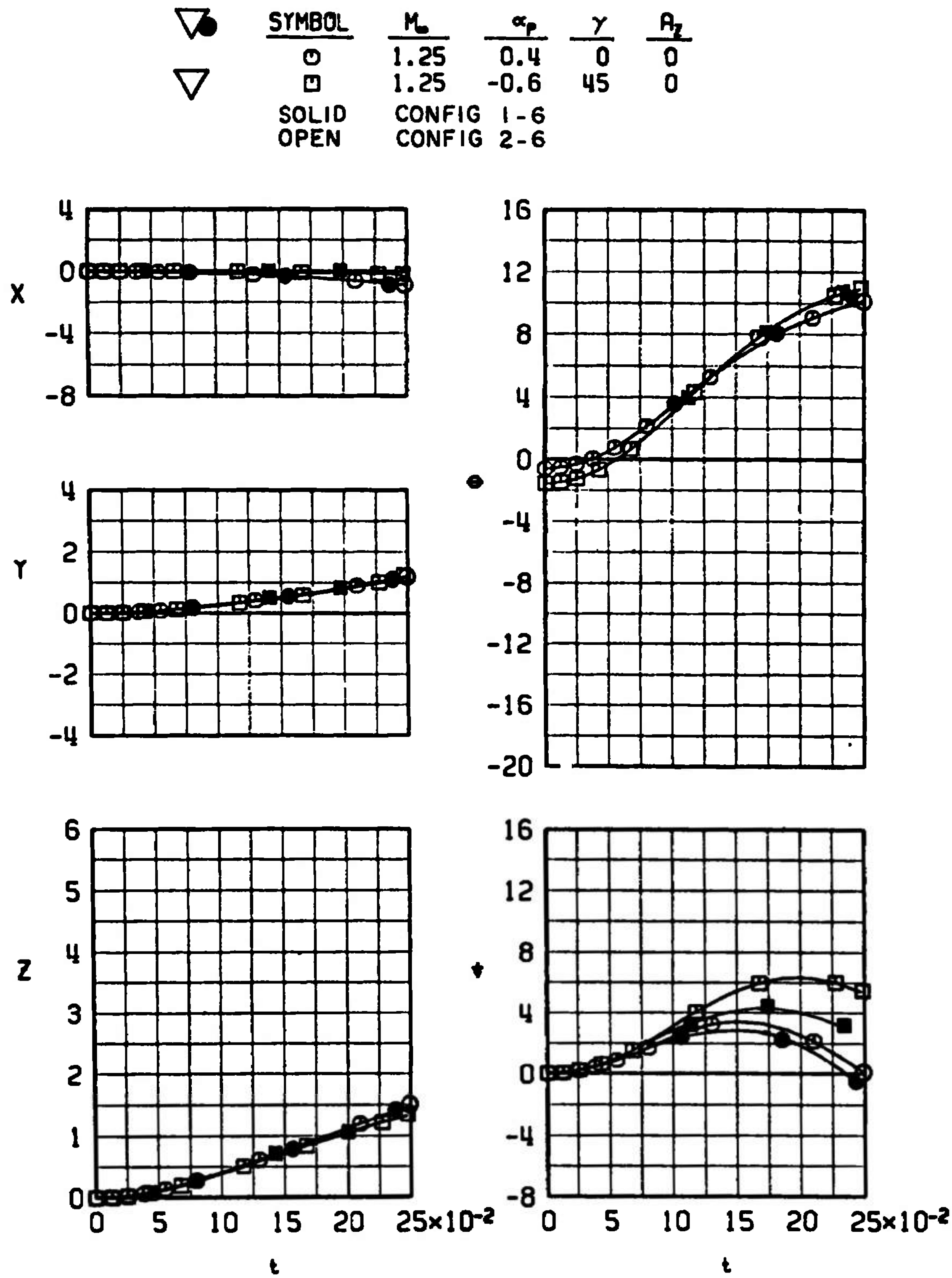

f. M_∞ = 1.25, MER Station 6
Fig. 20 Concluded

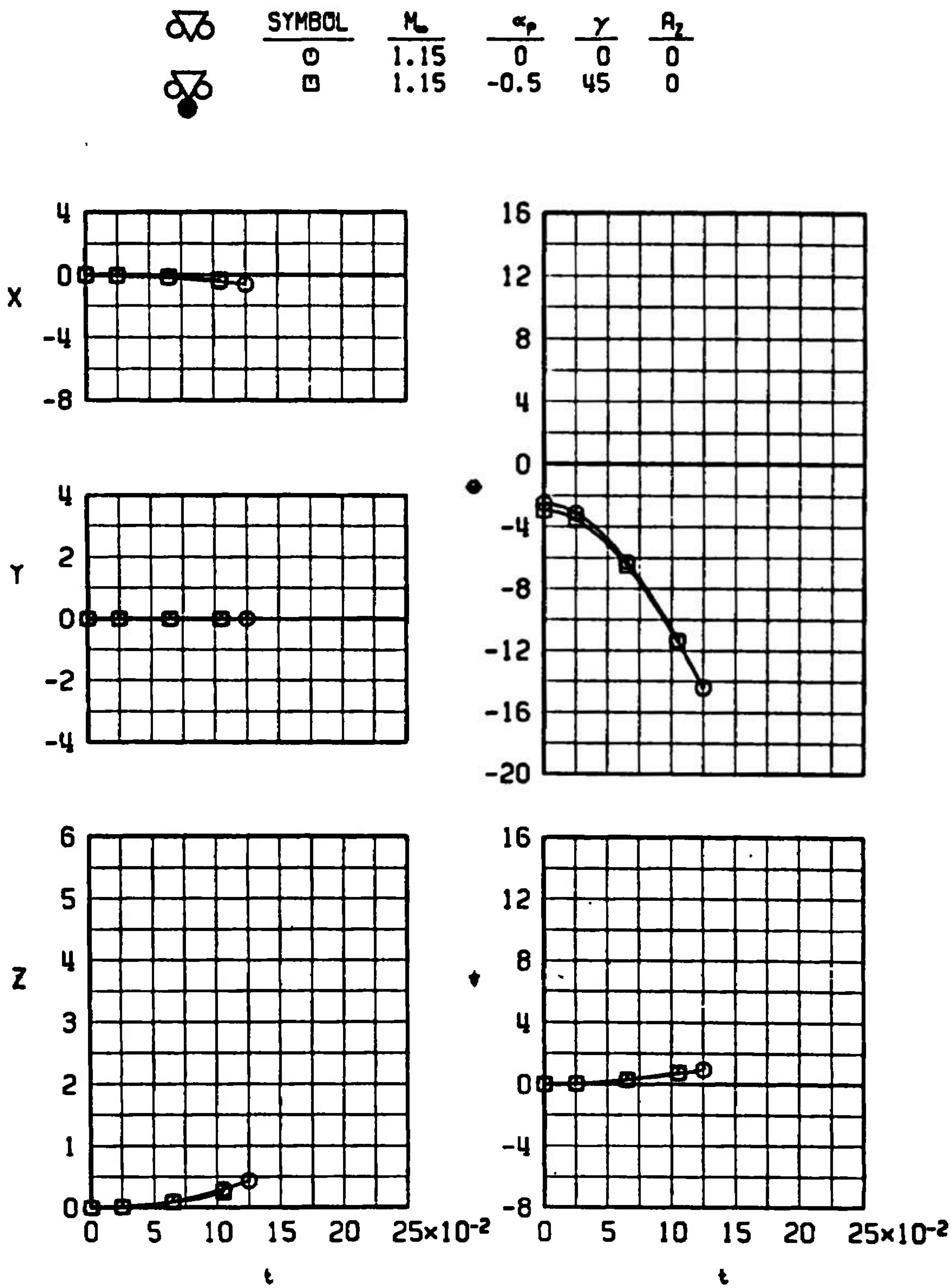

a. Configuration 5-2, M_∞ = 1.15

Fig. 21 Dive Angle Comparison of the SUU-30H/B Launch Trajectories from the MER for Different Mach Numbers

SYMBOL	M_∞	α_p	γ	A_z
○	1.30	0.8	0	0
□	1.30	-0.6	45	0
◇	1.30	3.3	0	-2G

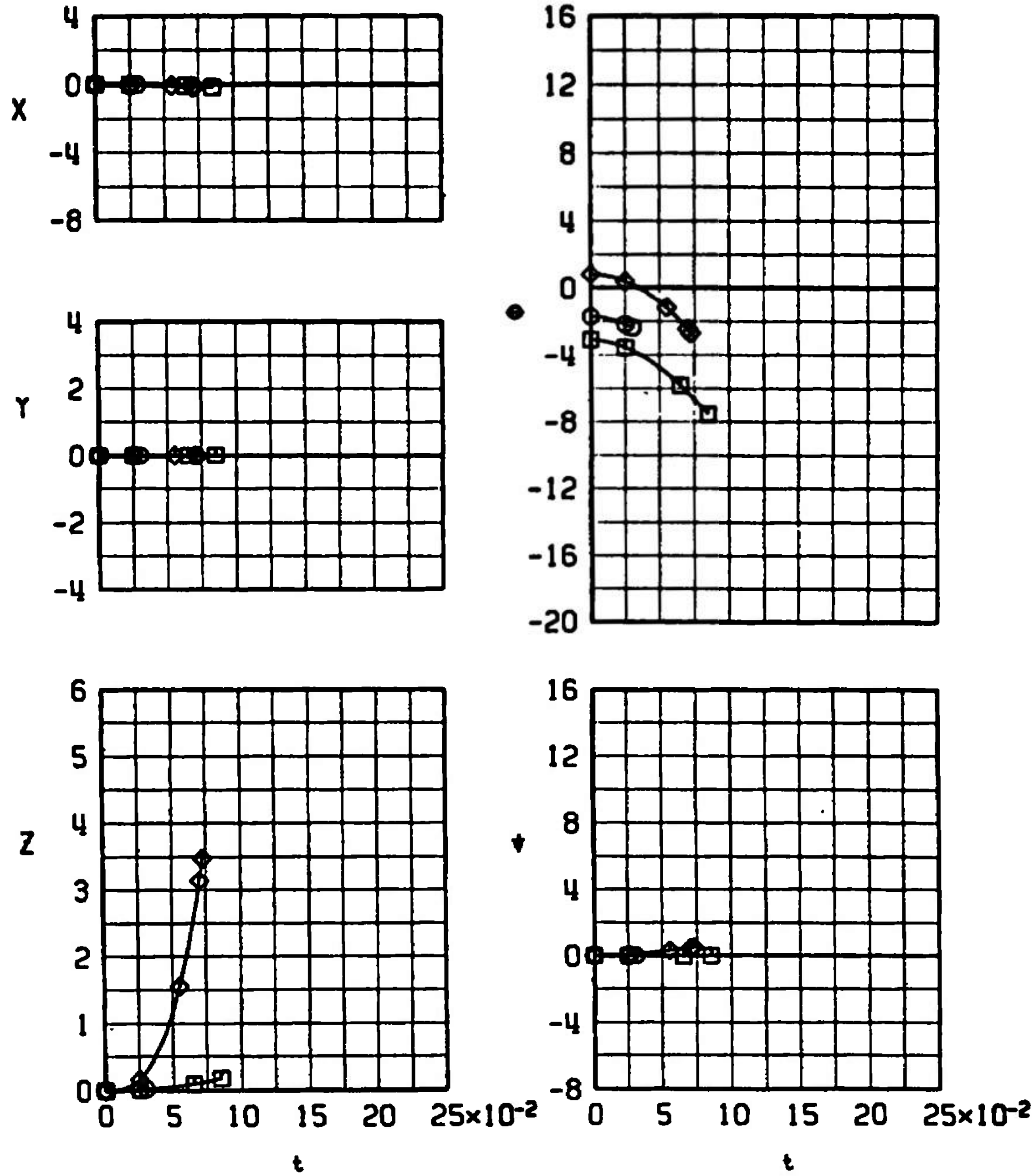

b. Configuration 5.2, M_∞ = 1.30
Fig. 21 Continued

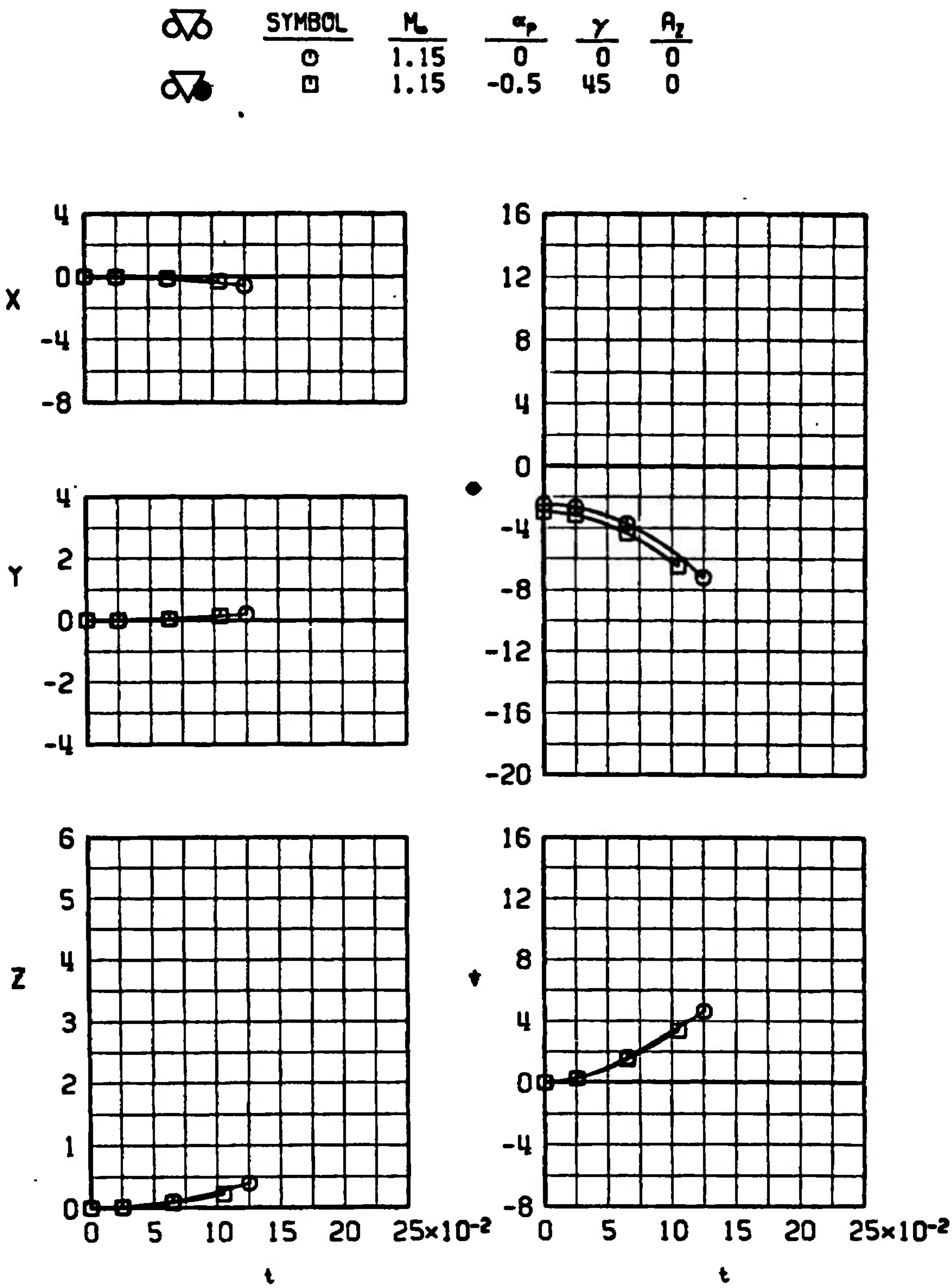

c. Configuration 5-3, M∞ = 1.15
Fig. 21 Continued

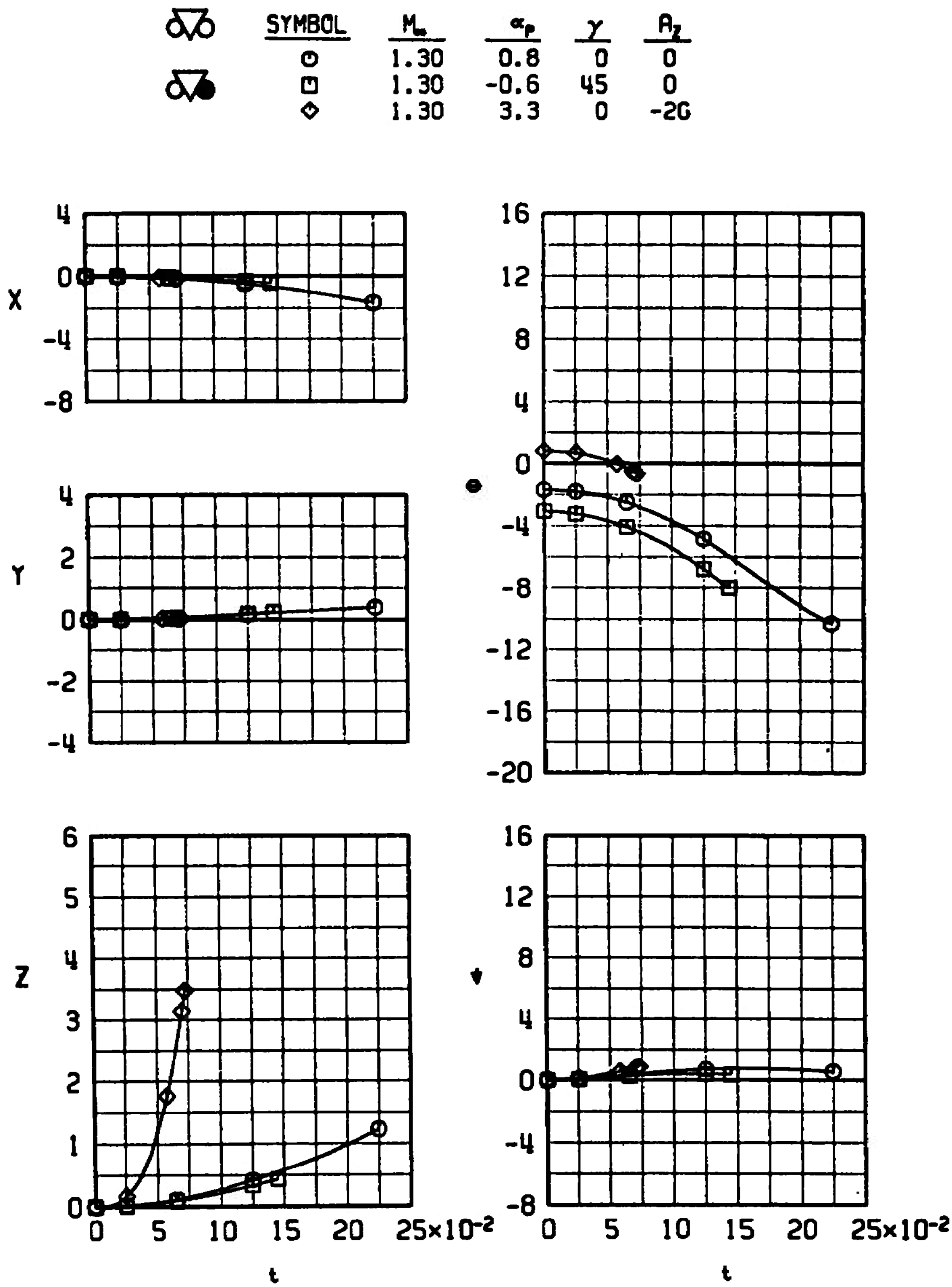

d. Configuration 5-3, M_∞ = 1.30
Fig. 21 Continued

SYMBOL	M_∞	α_p	γ	θ_z
○	1.15	0	0	0
△	1.15	-0.5	60	0

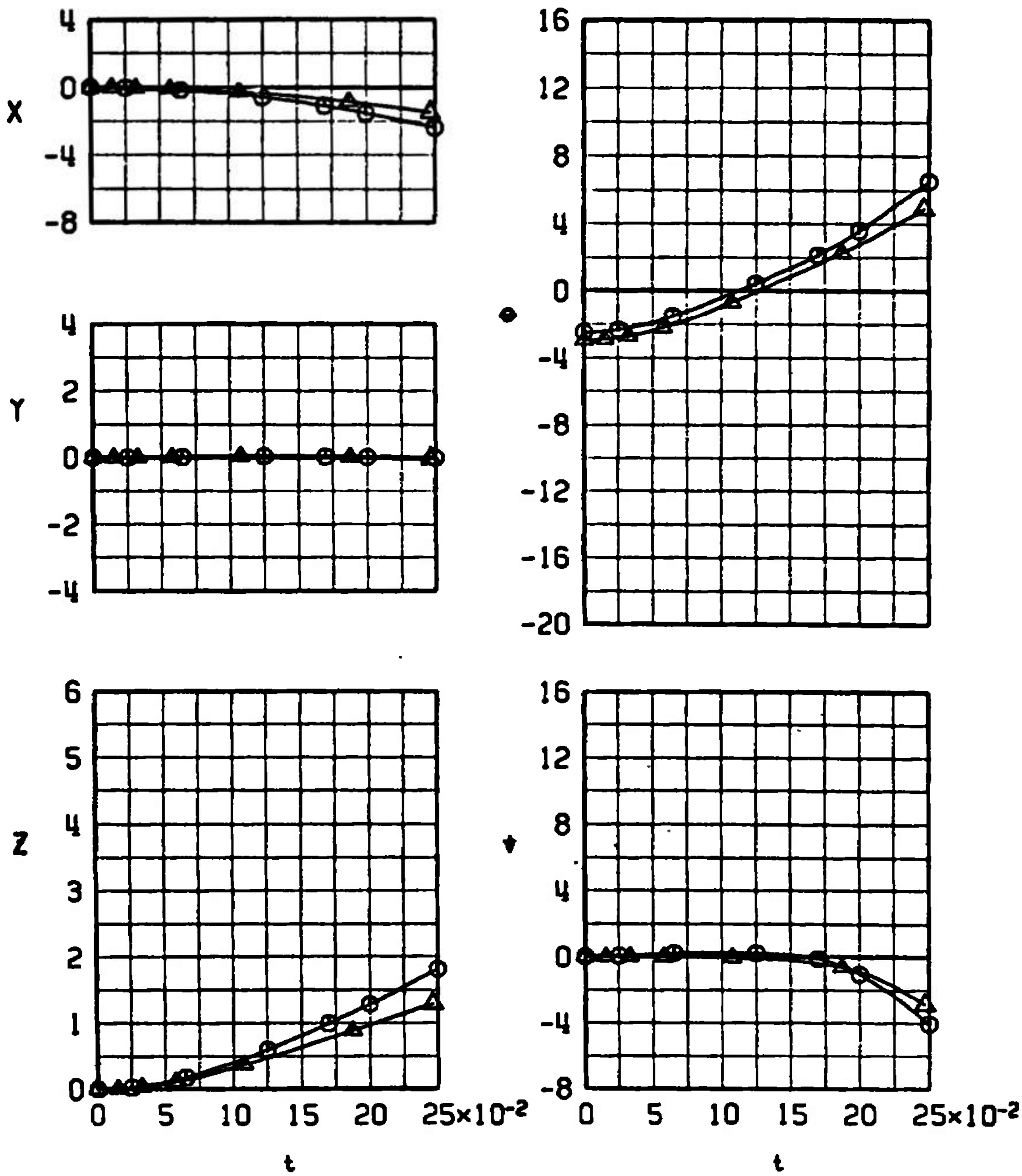

e. Configuration 5-4, M_∞ = 1.15
Fig. 21 Continued

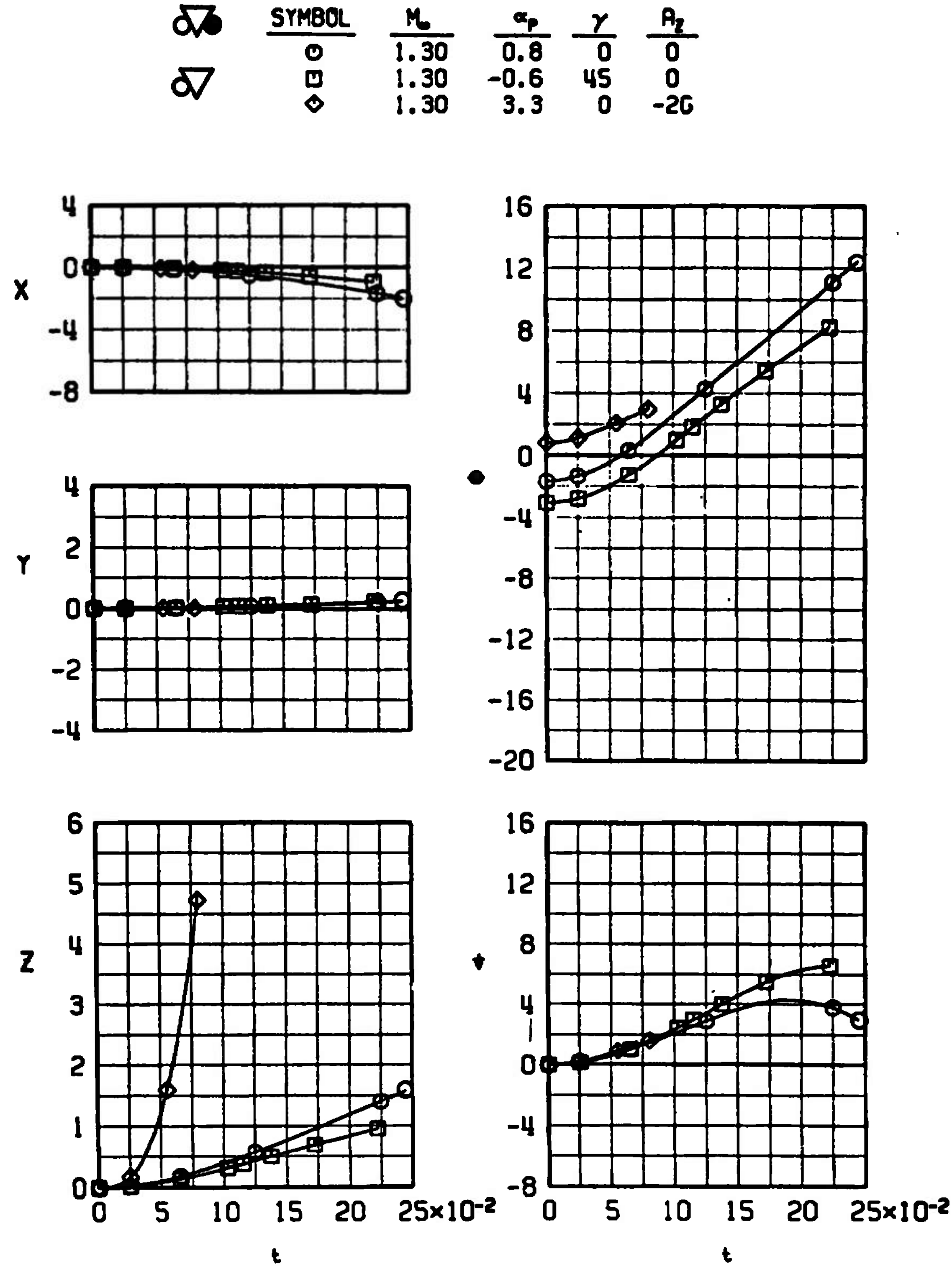

f. Configuration 5-4, M_∞ = 1.30
Fig. 21 Continued

SYMBOL	M_∞	α_p	γ	A_z
○	1.15	0	0	0
□	1.15	-0.5	45	0

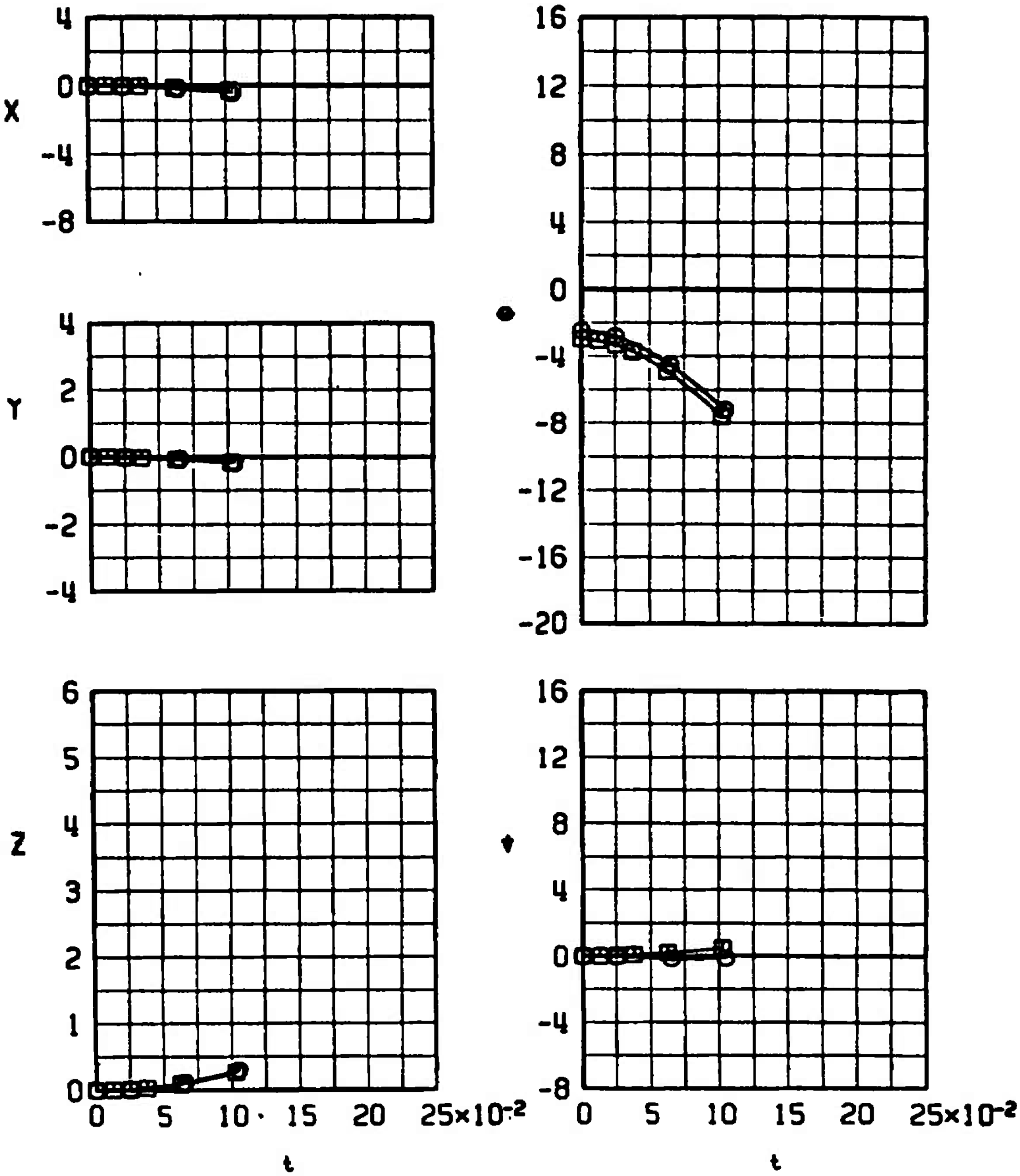

g. Configuration 5-5, M_∞ = 1.15
Fig. 21 Continued

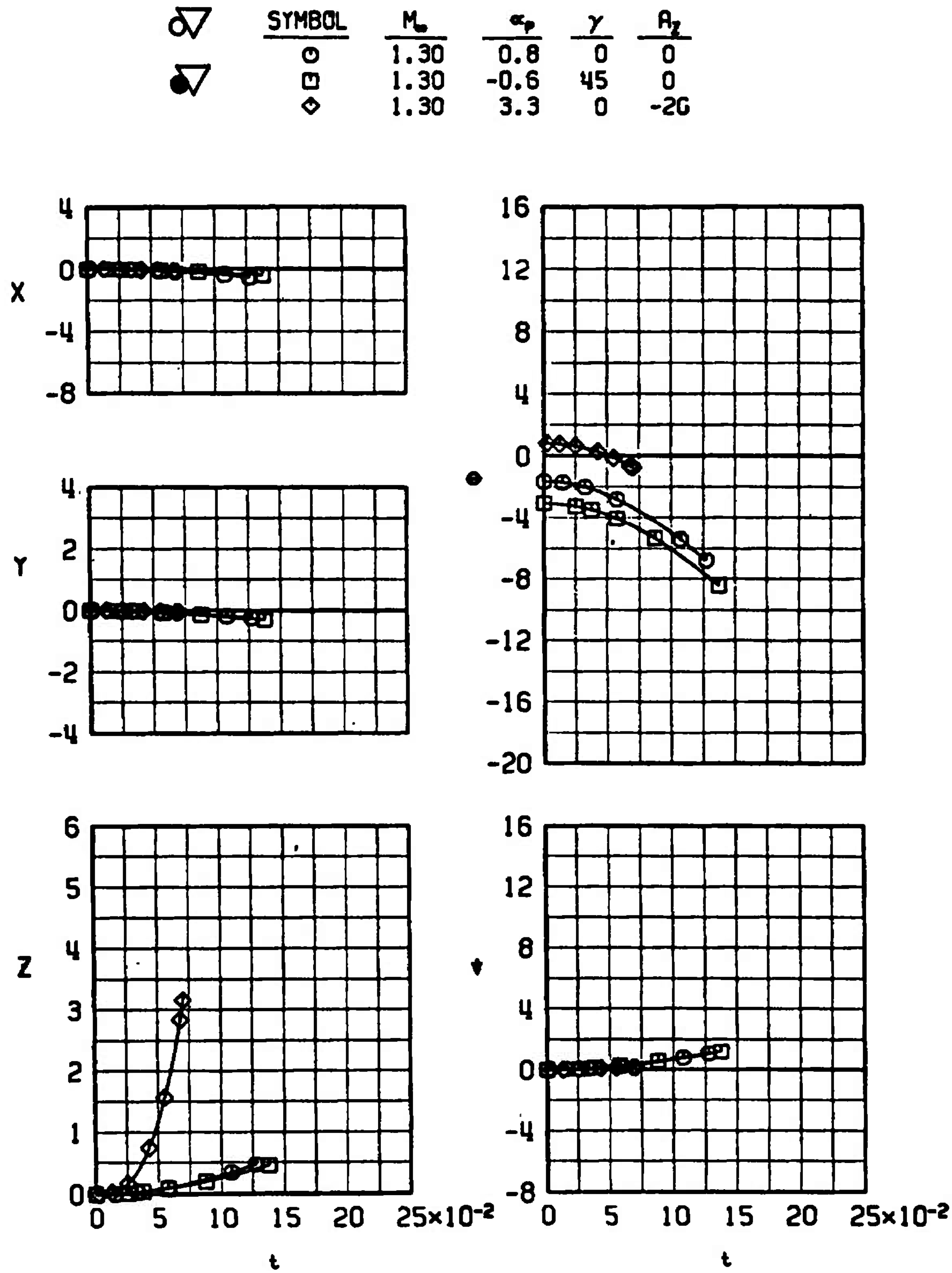

h. Configuration 5-5, M_∞ = 1.30
Fig. 21 Continued

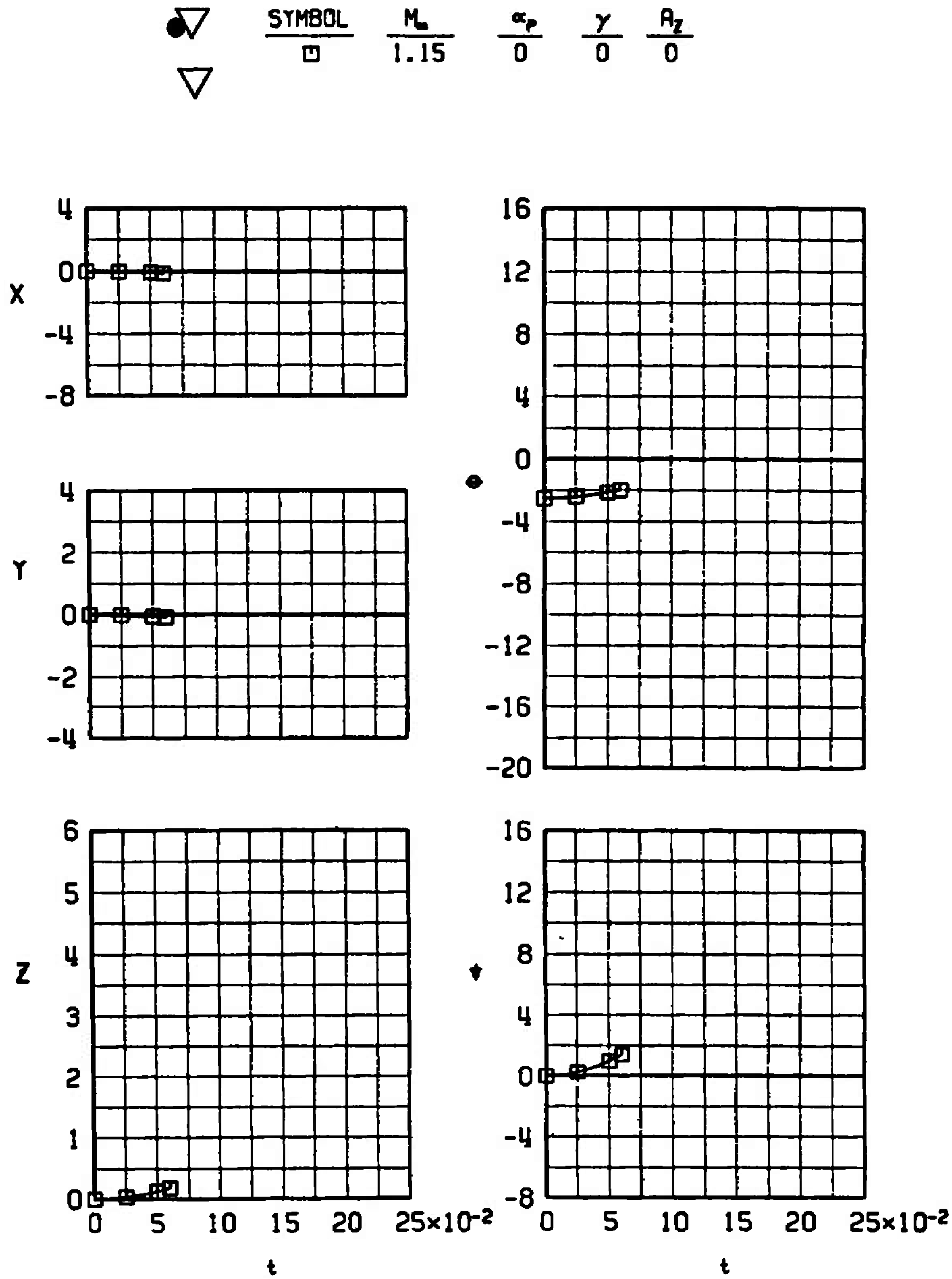

i. Configuration 5-6, M_∞ = 1.15
Fig. 21 Continued

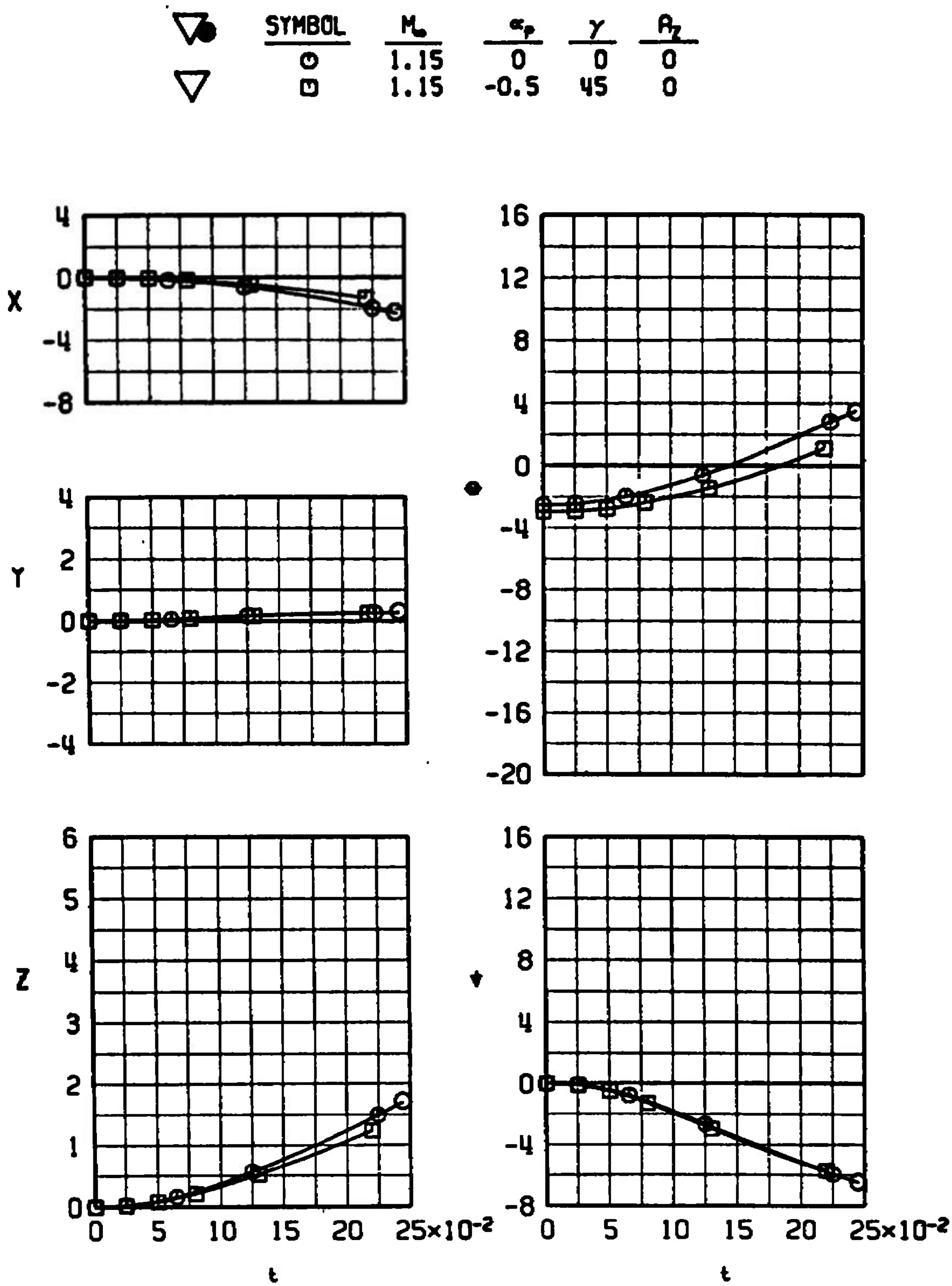

j. Configuration 5-7, M_∞ = 1.15
Fig. 21 Continued

SYMBOL	M_∞	α_P	γ	A_Z
○	1.30	0.8	0	0
□	1.30	-0.6	45	0

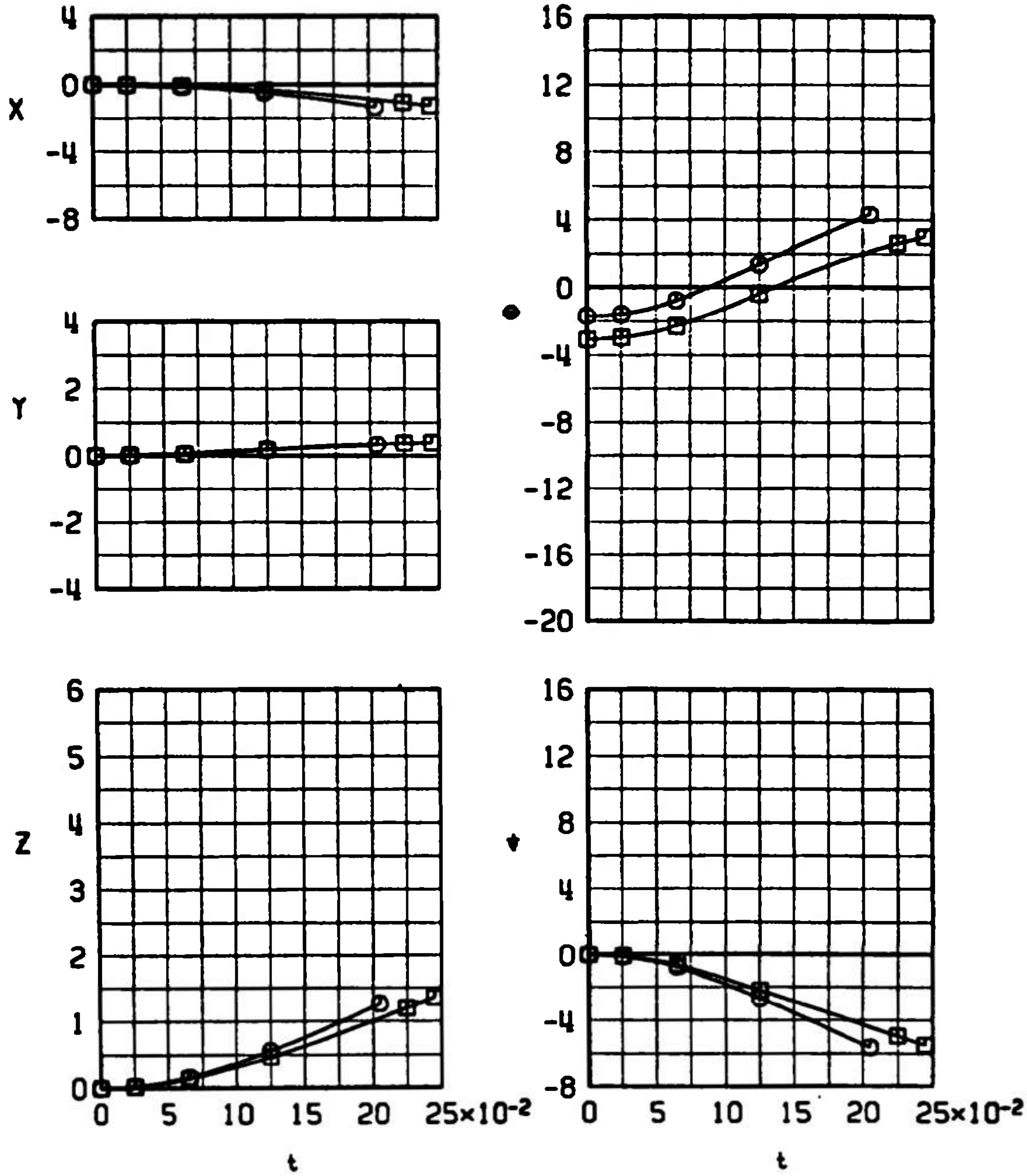

k. Configuration 5-7, M_∞ = 1.30
Fig. 21 Concluded

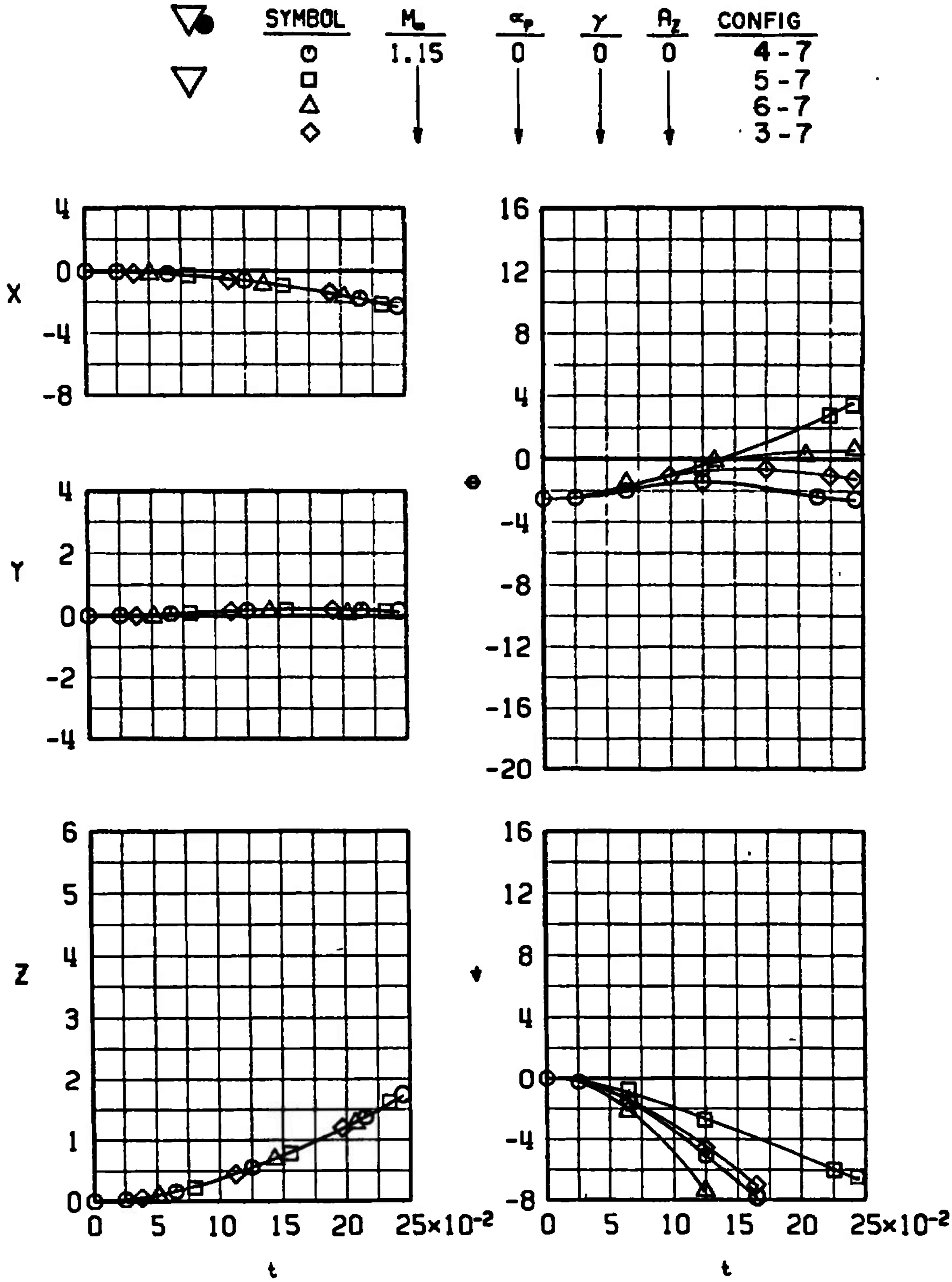

a. M_∞ = 1.15
Fig. 22 Effects of External Store Configuration on the SUU-30H/B Launch Trajectories from the MER, Station 6

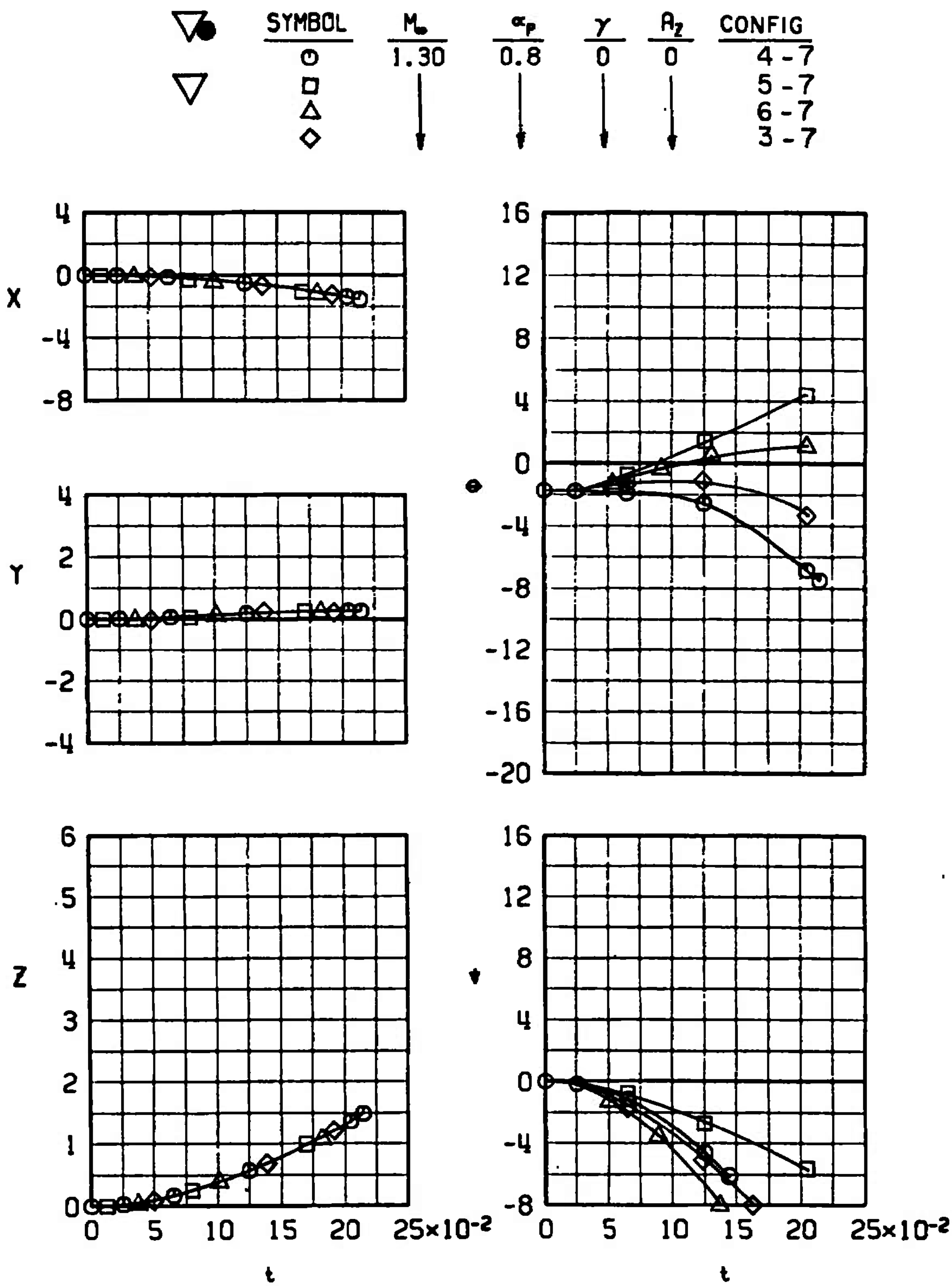

b. M_∞ = 1.30
Fig. 22 Concluded

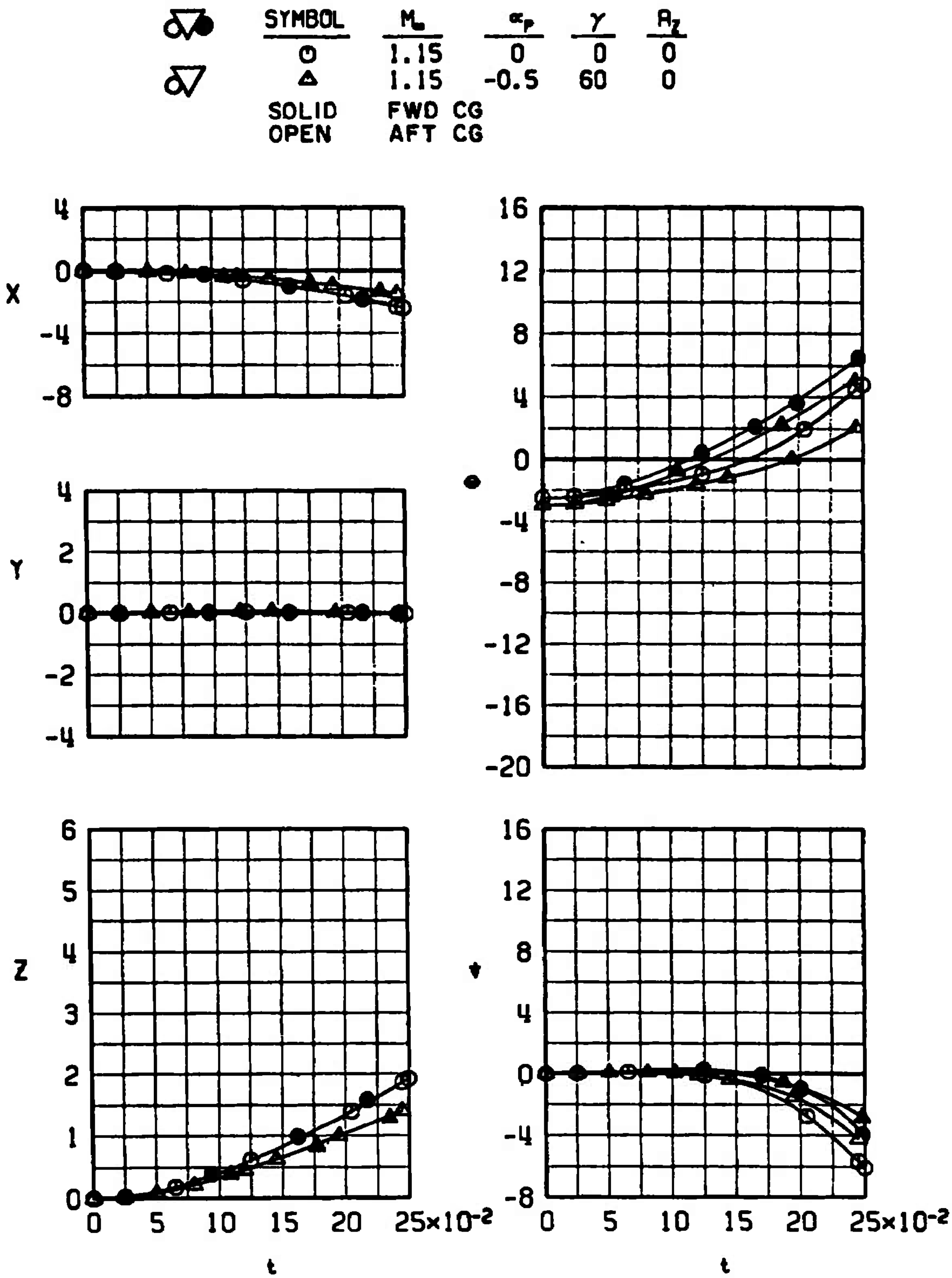

Fig. 23 Effect of Store cg Location on the SUU-30H/B Launch Trajectories from the MER, Configuration 5-4

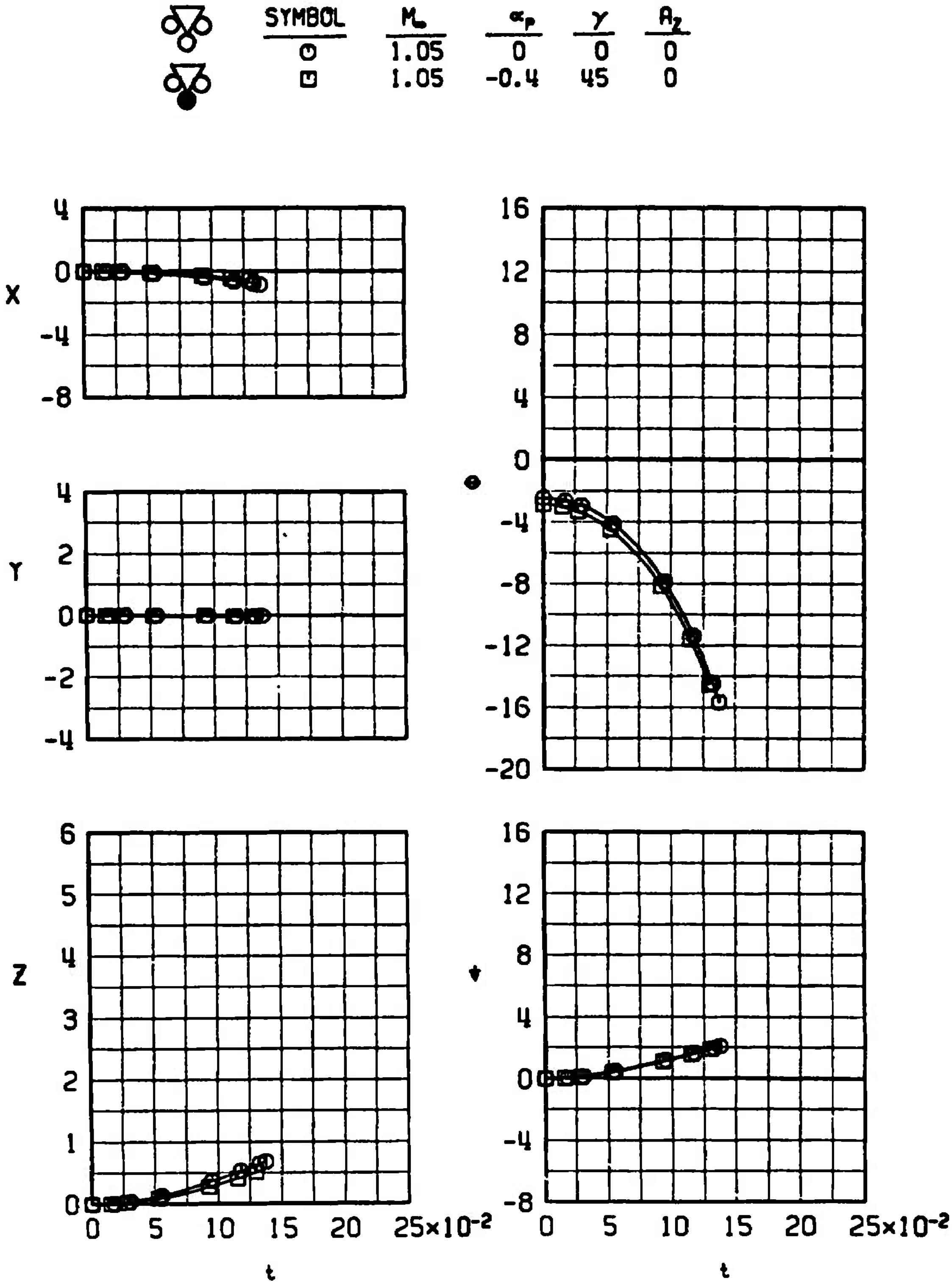

a. Configuration 8-1, M_∞ = 1.05
Fig. 24 Dive Angle Comparison of the MK-20 "Rockeye" Launch Trajectories from the MER for Different Mach Numbers

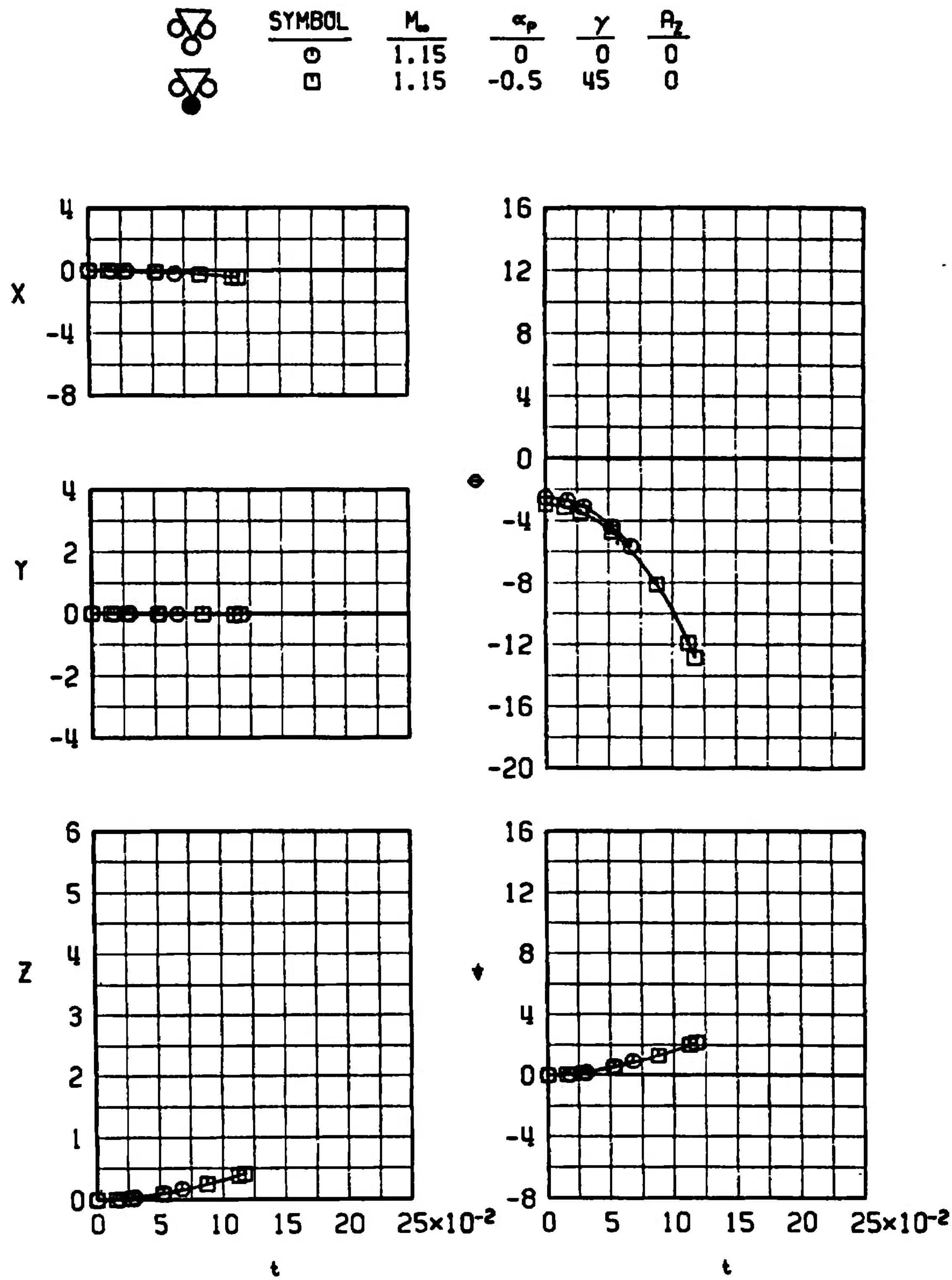

b. Configuration 8-1, M_{∞} = 1.15
Fig. 24 Continued

SYMBOL	M_∞	α_p	γ	A_z
○	1.30	0.8	0	0
□	1.30	-0.6	45	0
◇	1.30	3.3	0	-2G

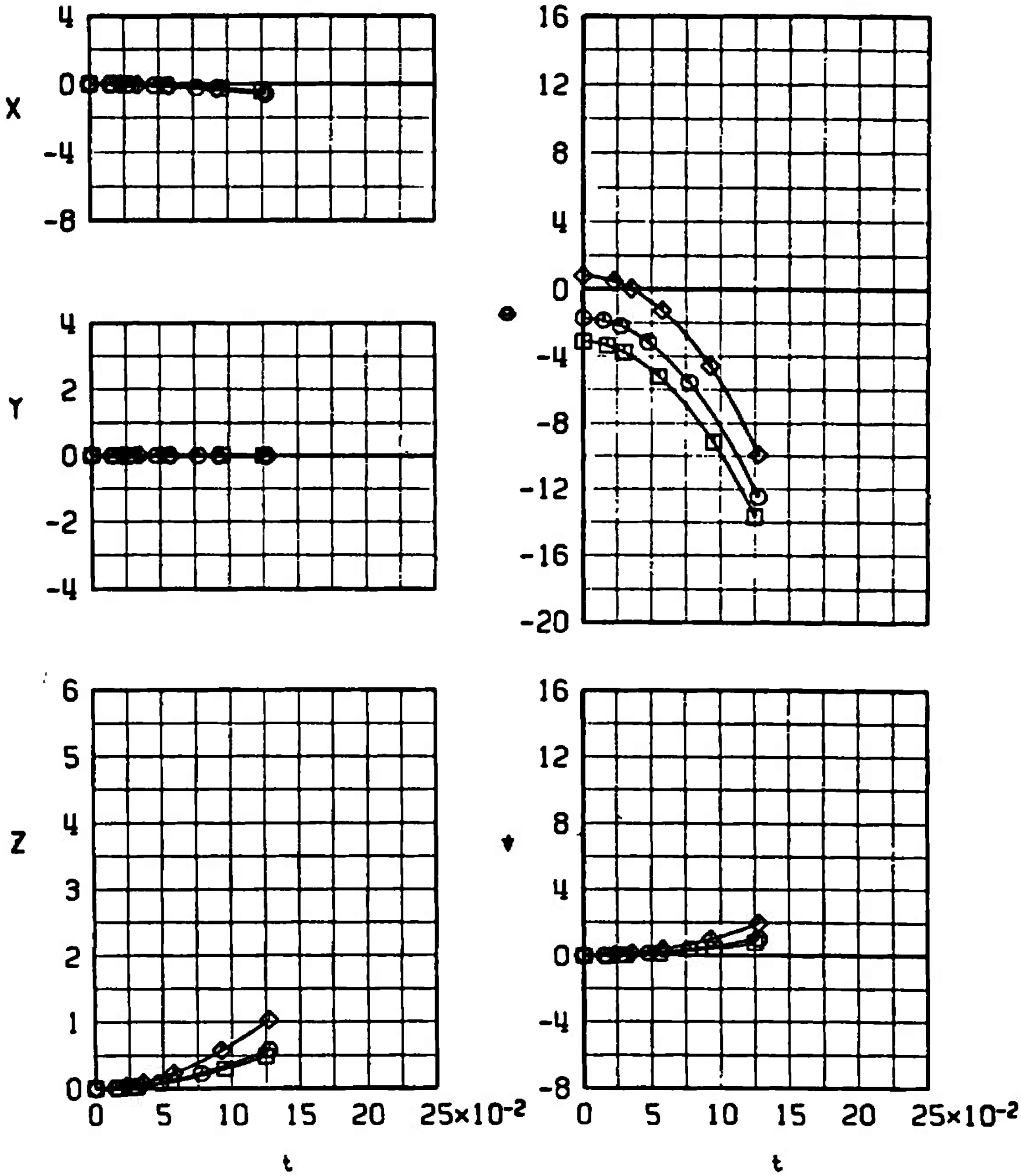

c. Configuration 8-1, M_∞ = 1.30
Fig. 24 Continued

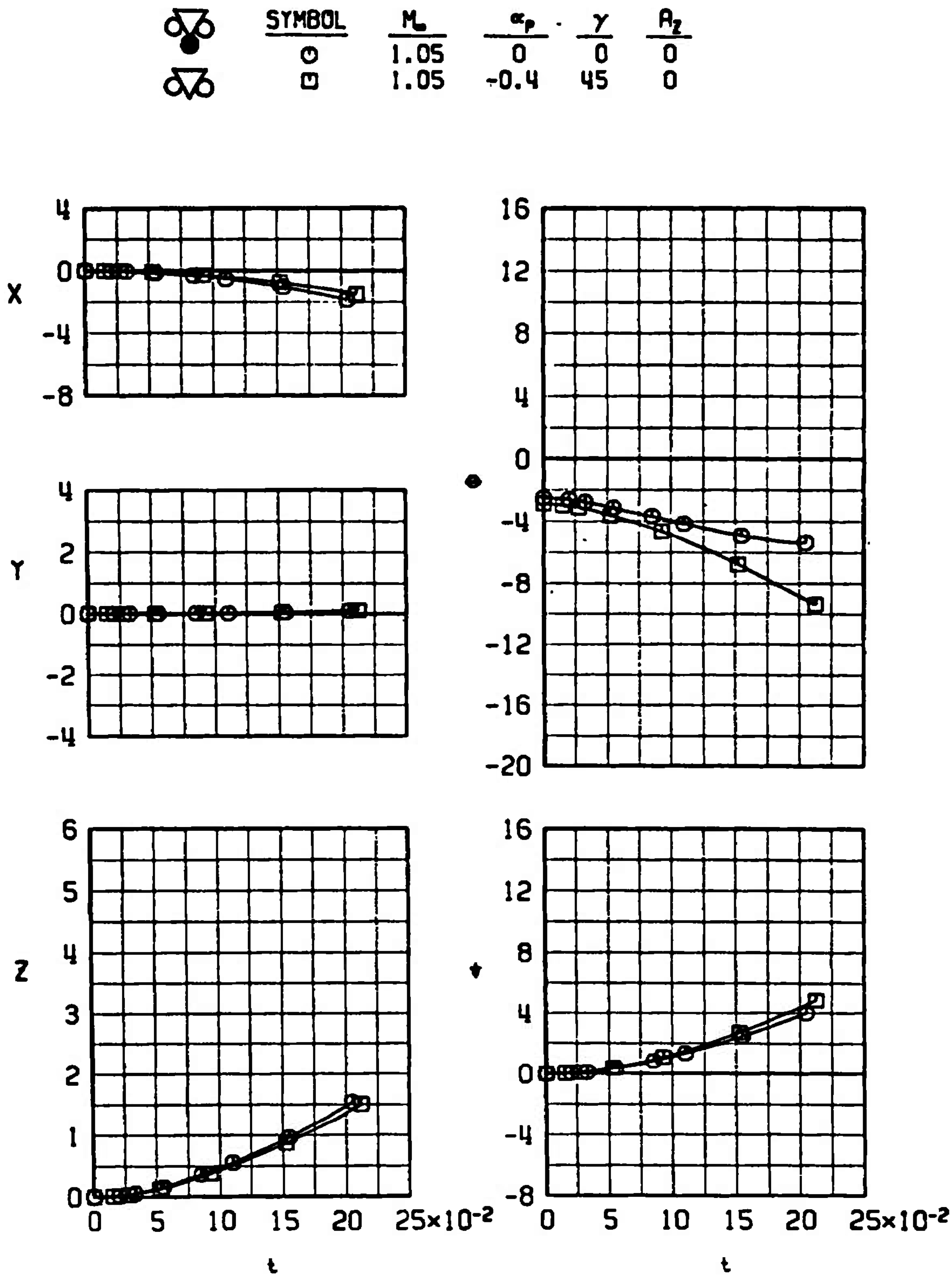

d. Configuration 8-2, M_∞ = 1.05
Fig. 24 Continued

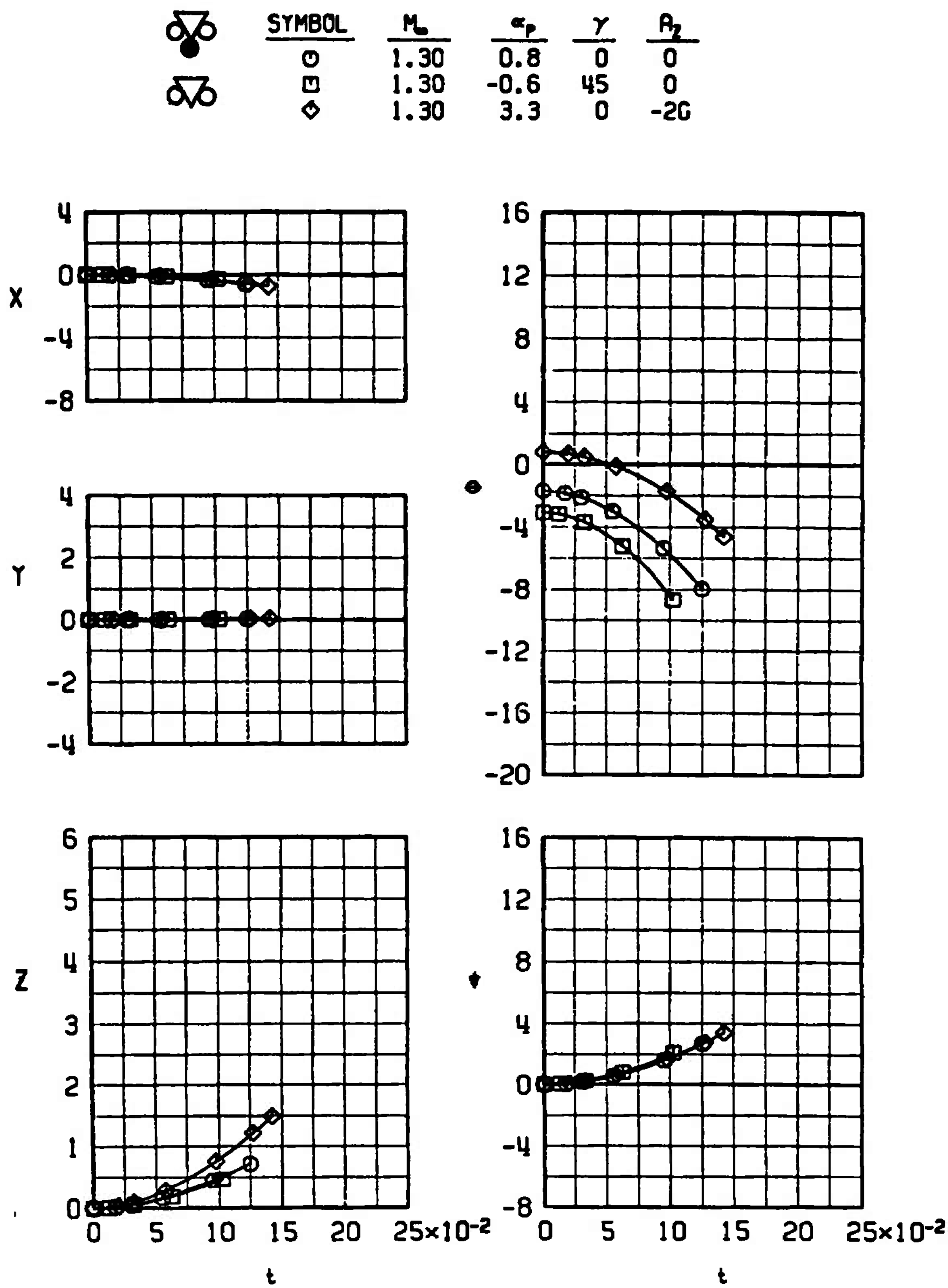

e. Configuration 8-2, M_∞ 1.30
Fig. 24 Continued

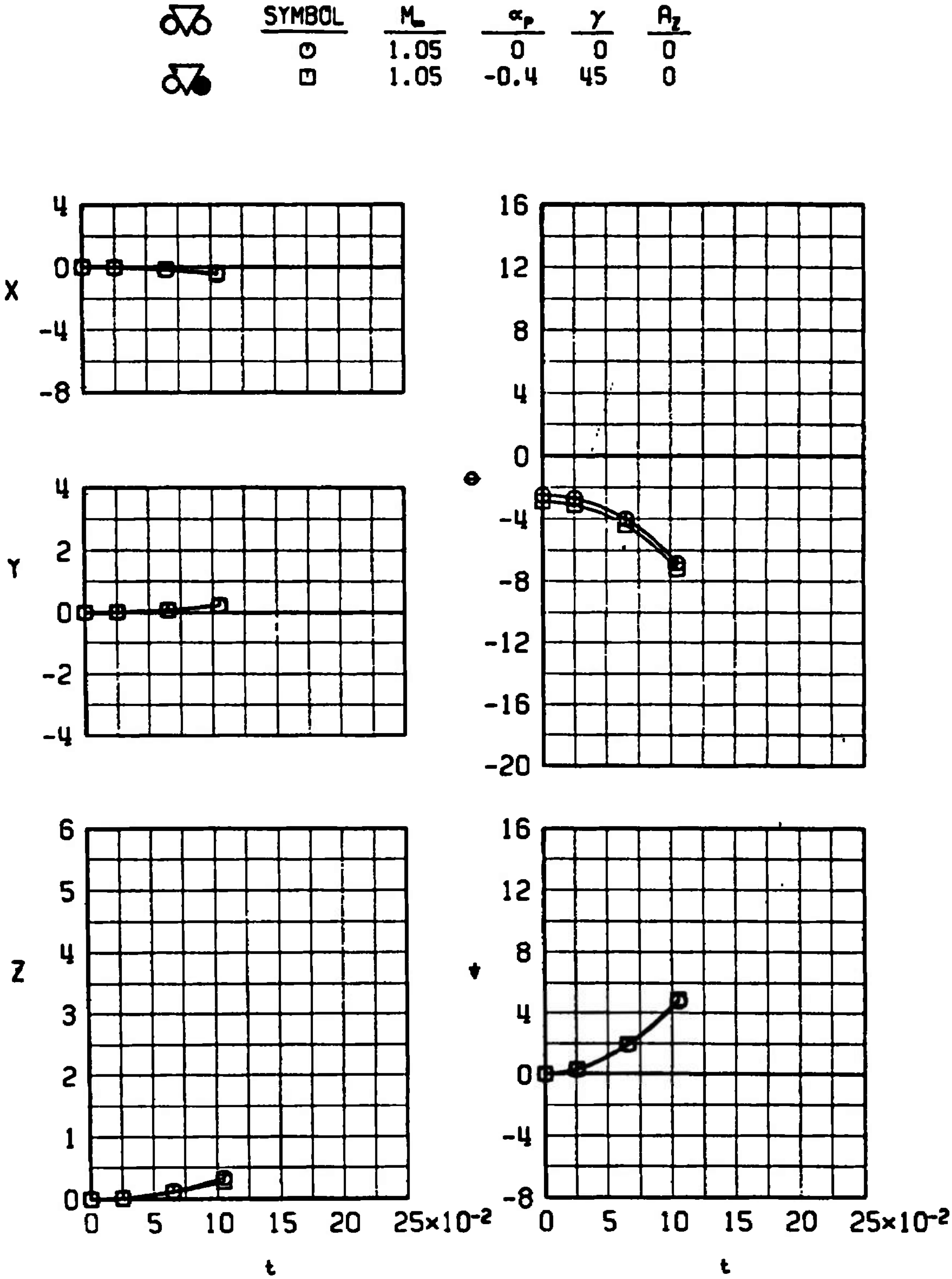

f. Configuration 8-3, M_{∞} = 1.05
Fig. 24 Continued

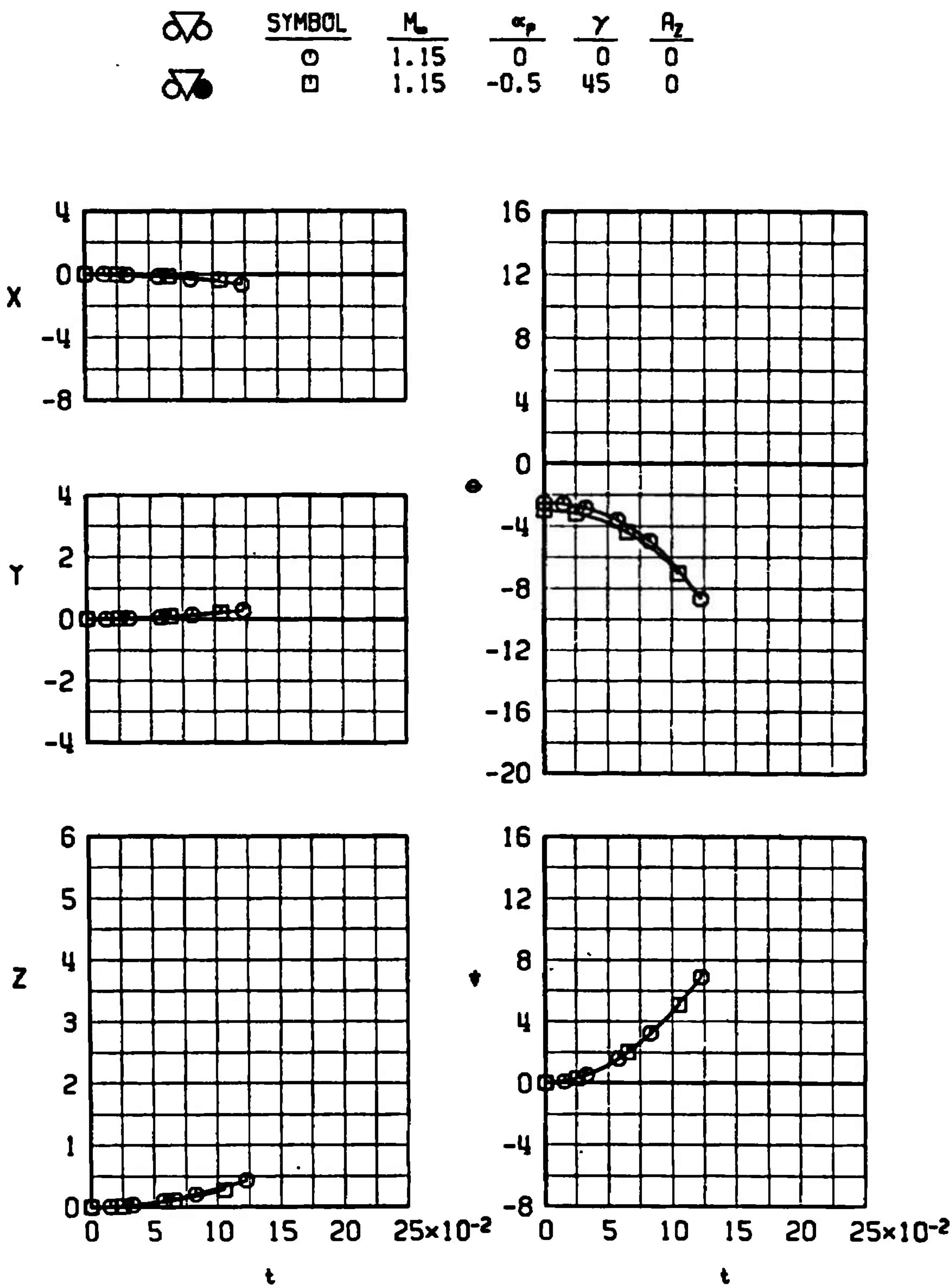

g. Configuration 8-3, M_∞ = 1.15
Fig. 24 Continued

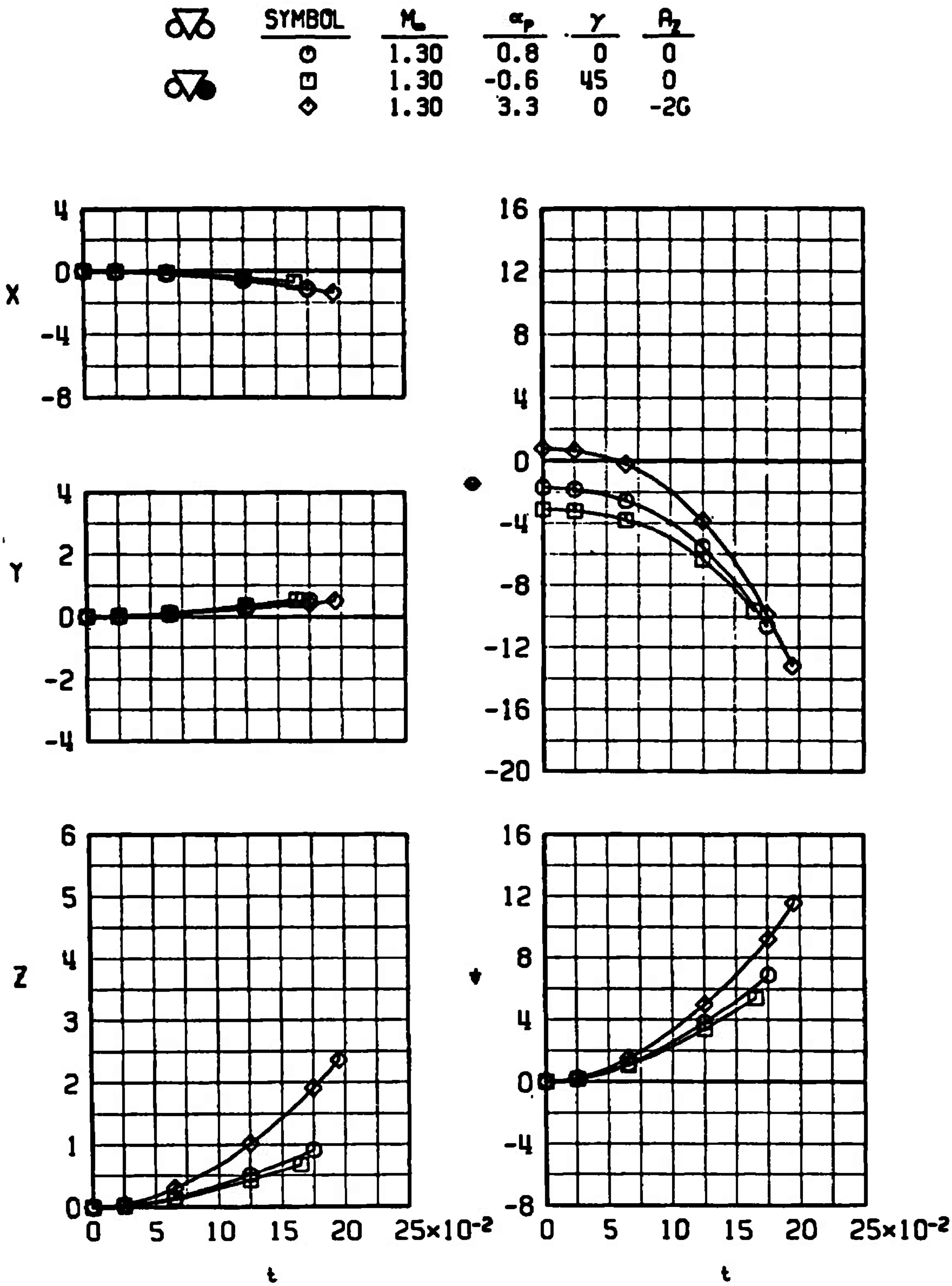

h. Configuration 8-3, M_∞ = 1.30
Fig. 24 Continued

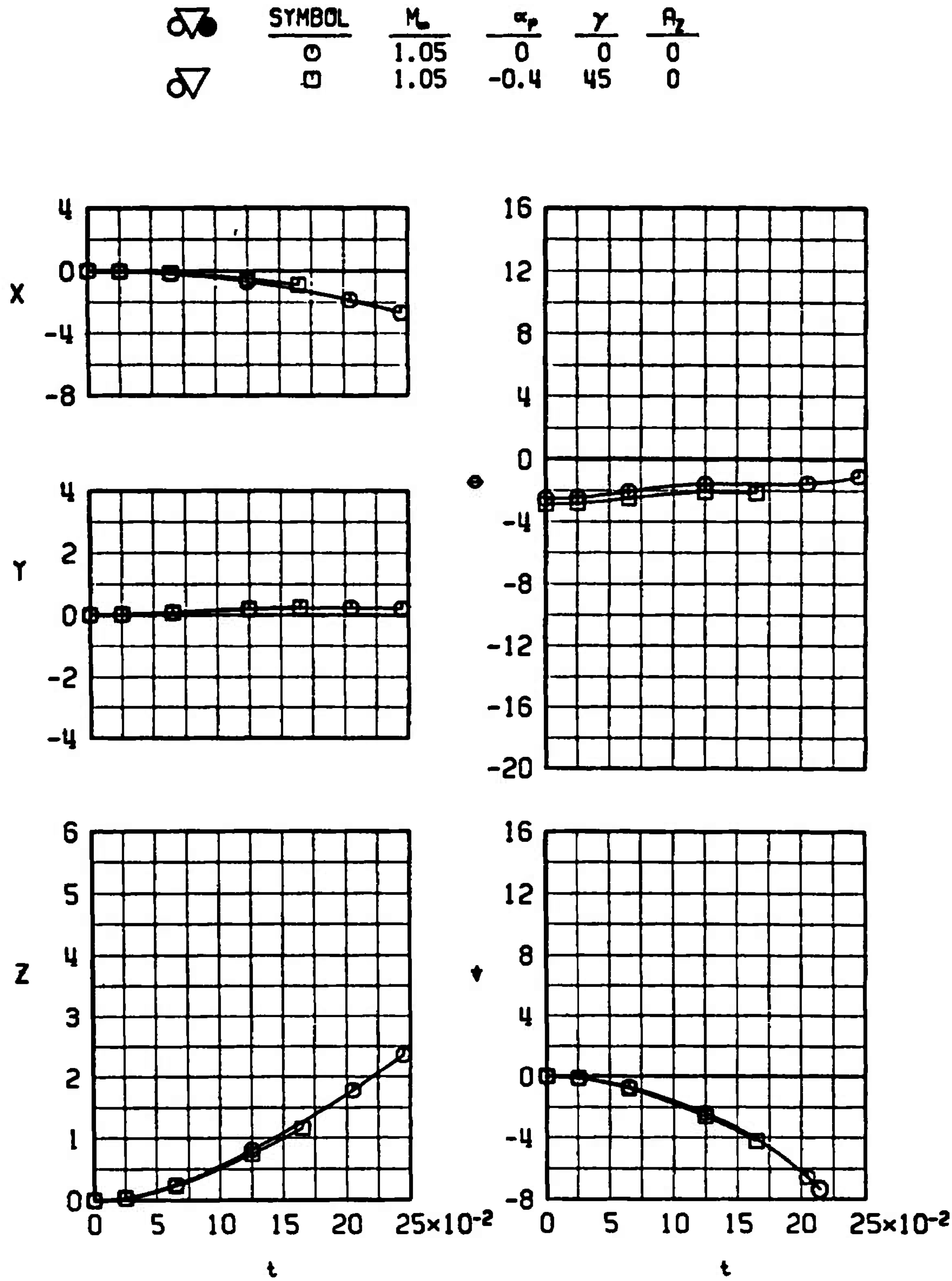

i. Configuration 8-4, M_∞ = 1.05
Fig. 24 Continued

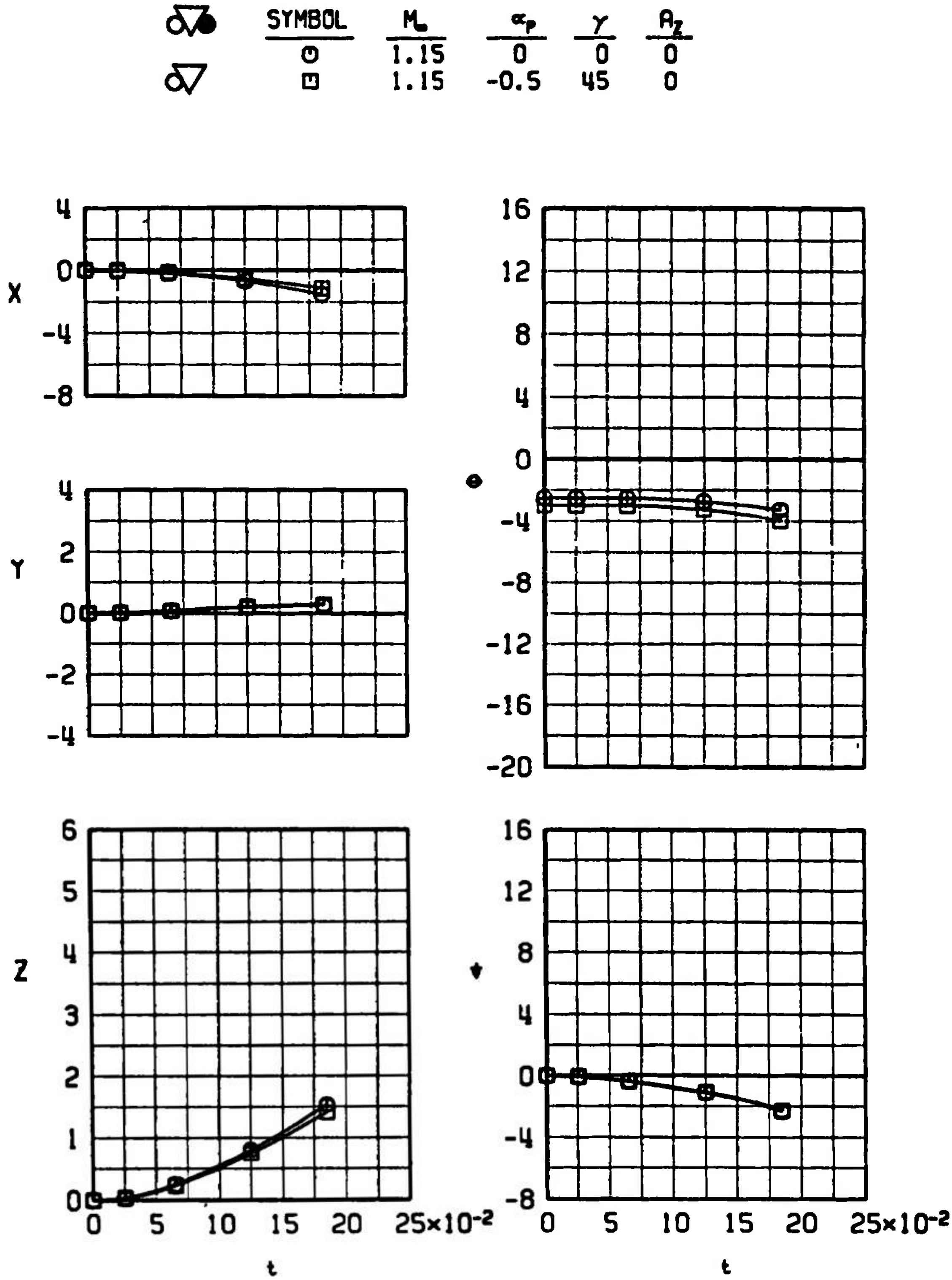

j. Configuration 8-4, M_∞ = 1.15
Fig. 24 Continued

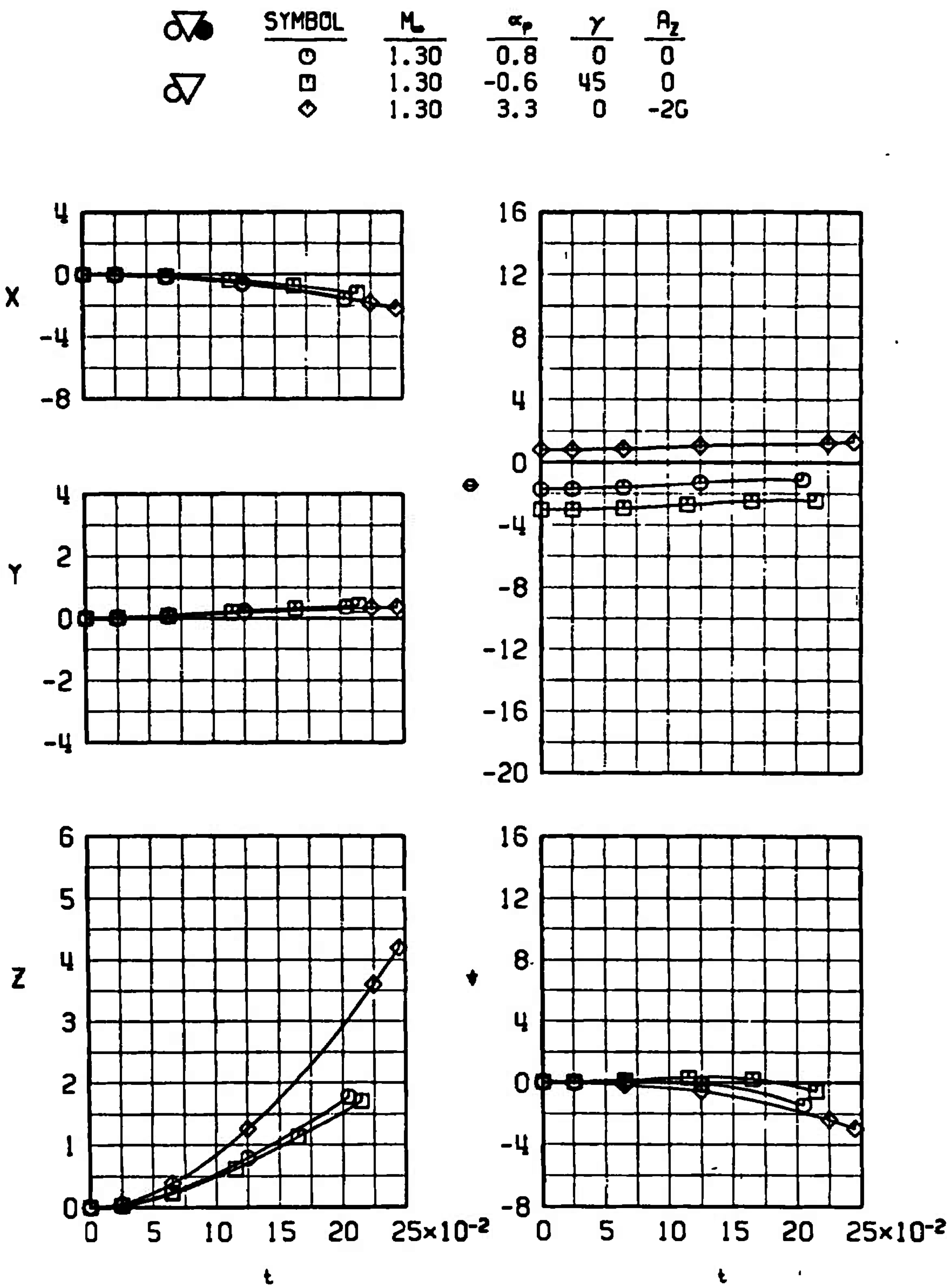

k. Configuration 8-4, M_∞ = 1.30
Fig. 24 Continued

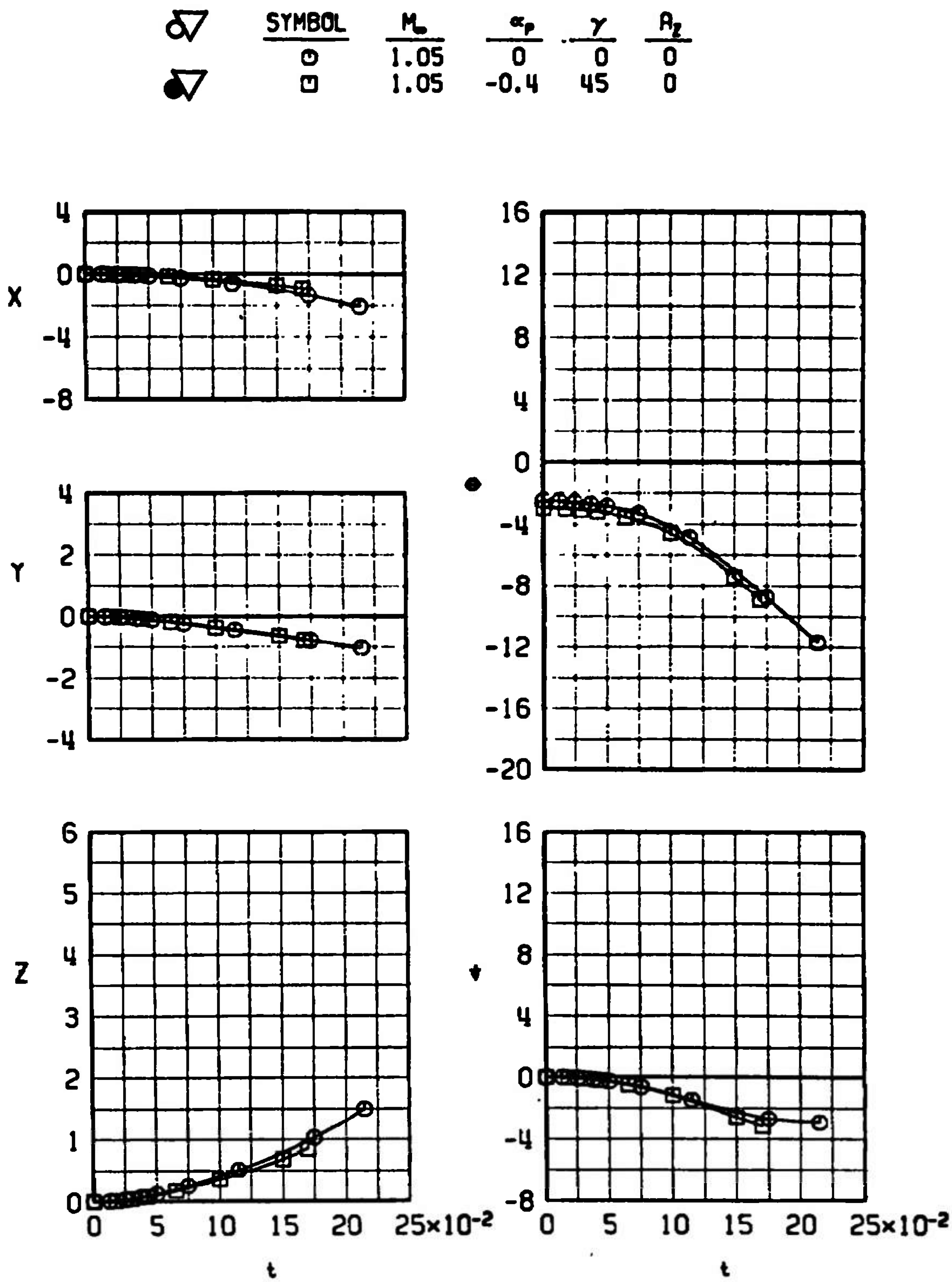

I. Configuration 8-5, M_∞ = 1.05
Fig. 24 Continued

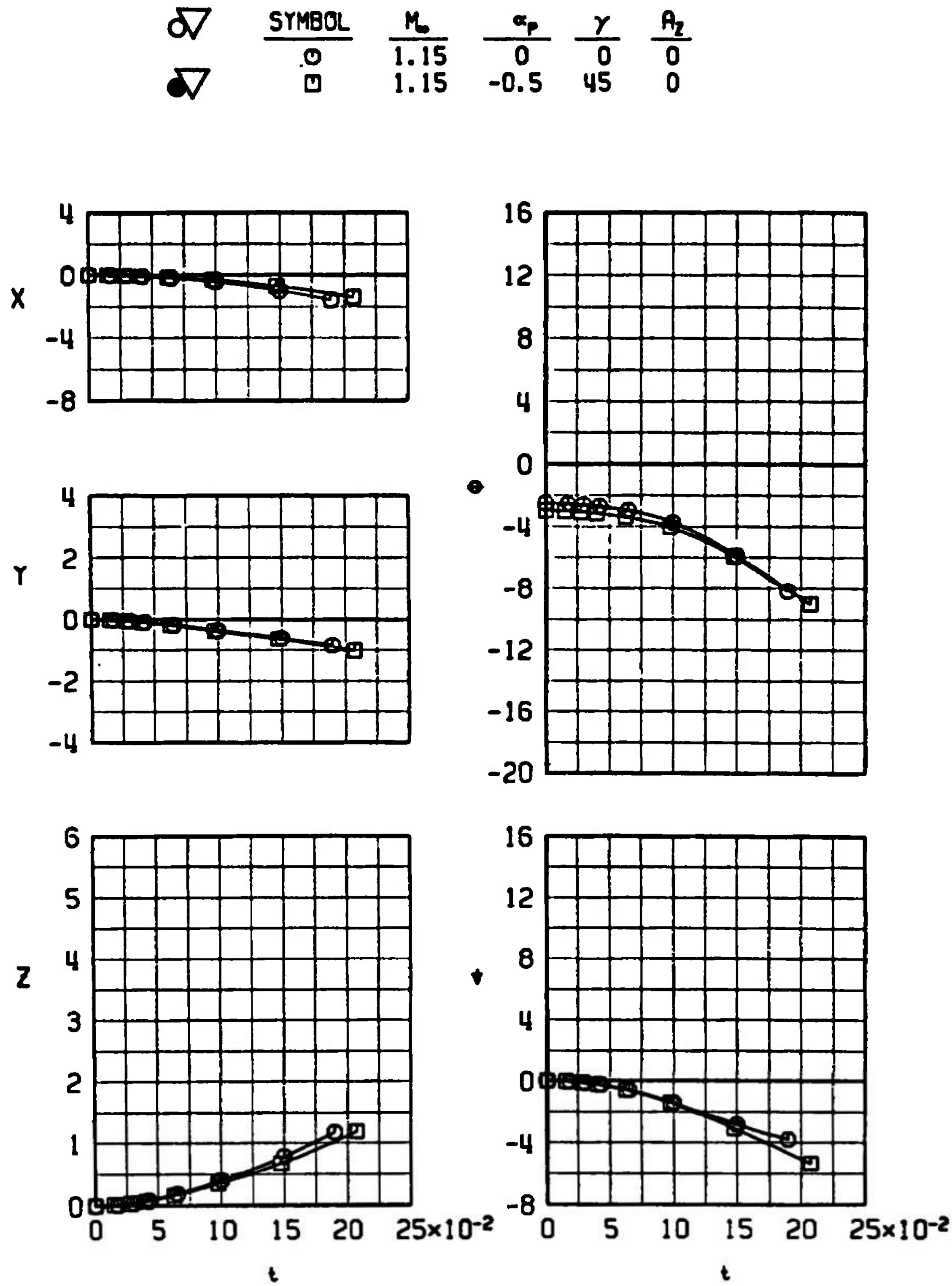

m. Configuration 8-5, M_∞ = 1.15

Fig. 24 Continued

SYMBOL	M_∞	α_p	γ	A_z
○	1.30	0.8	0	0
□	1.30	-0.6	45	0
◇	1.30	3.3	0	-2G

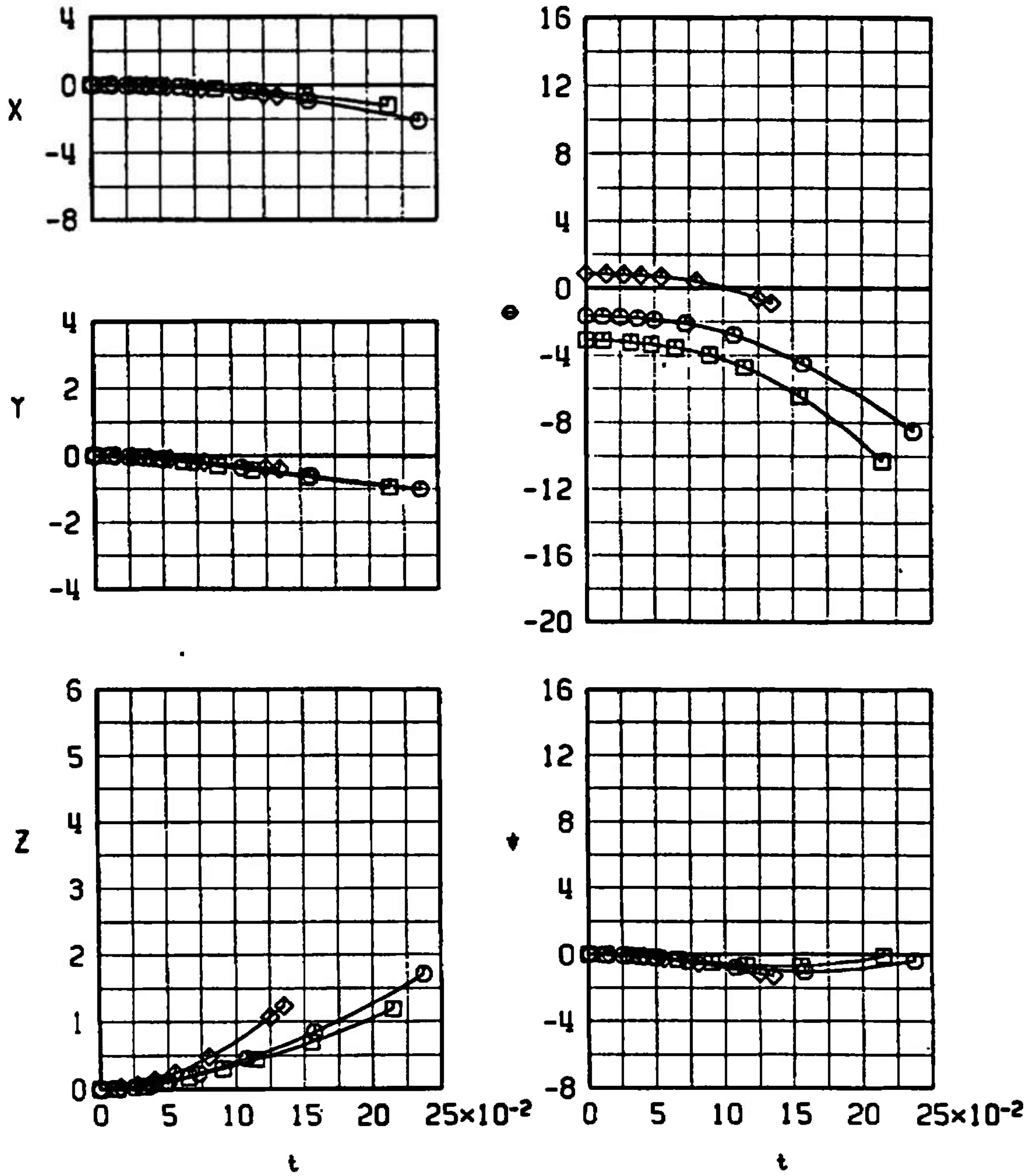

n. Configuration 8-5, M_∞ = 1.30
Fig. 24 Continued

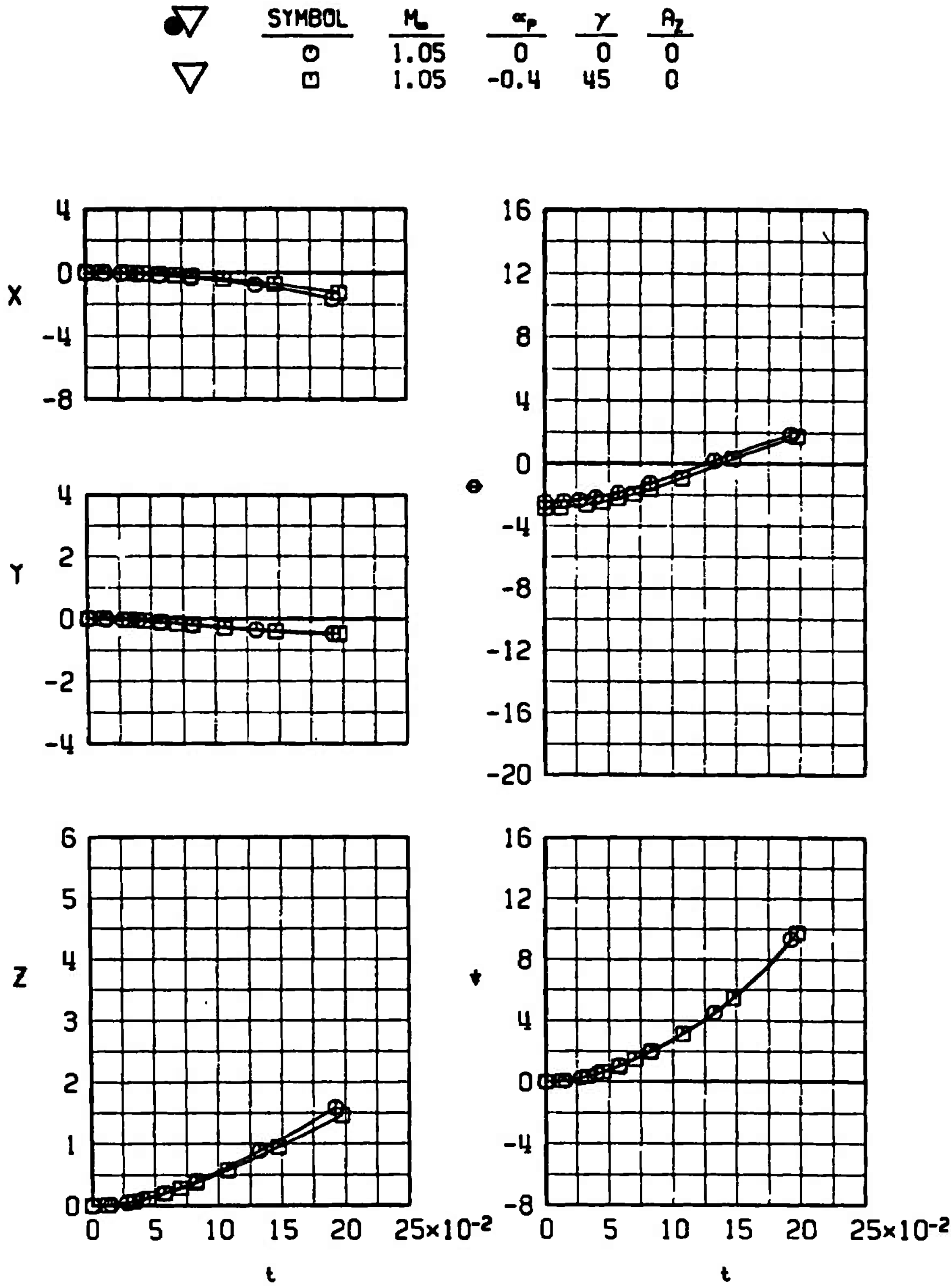

o. Configuration 8-6, M_∞ = 1.05
Fig. 24 Continued

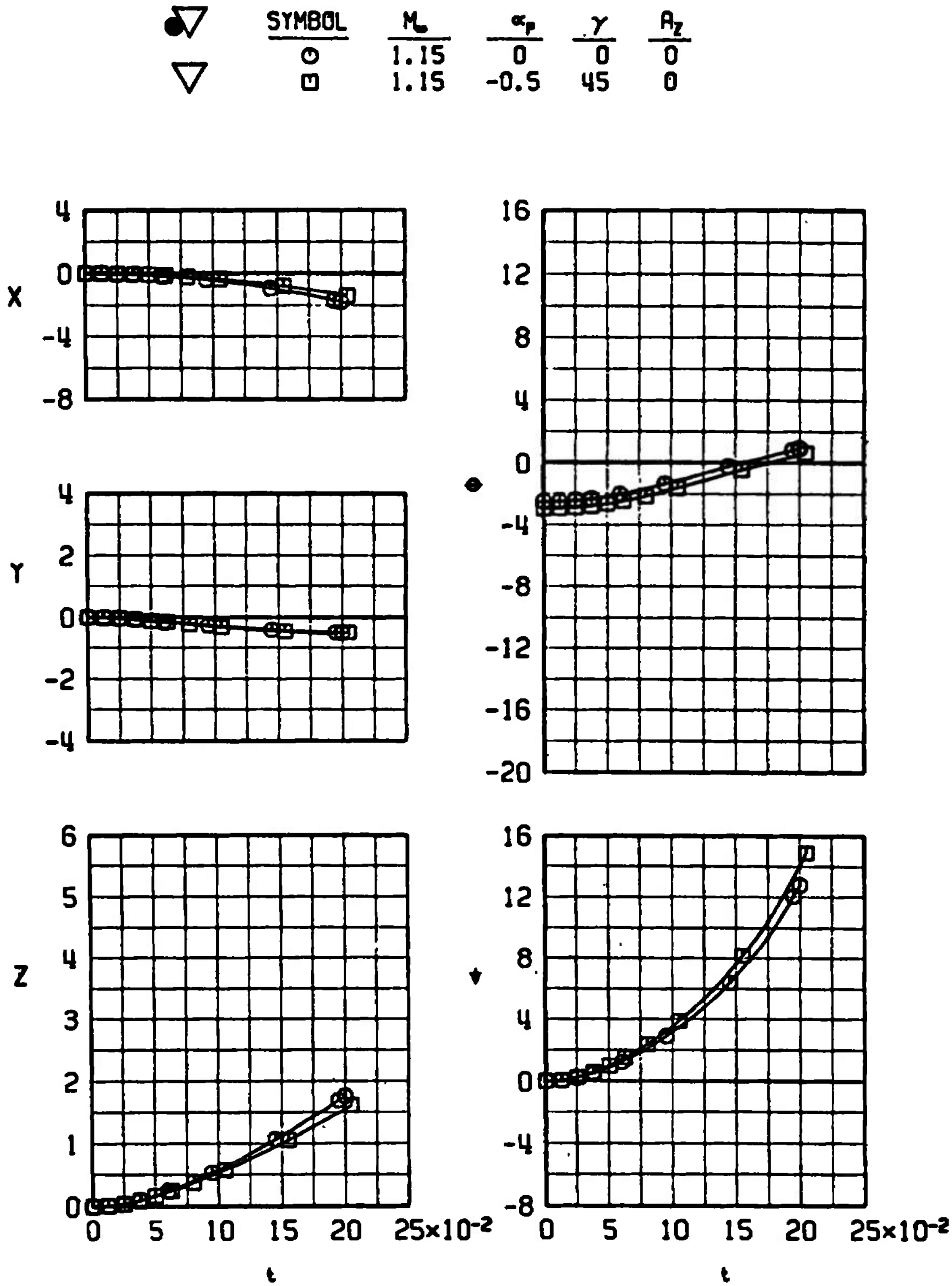

p. Configuration 8-6, M_∞ = 1.15
Fig. 24 Continued

SYMBOL	M_∞	α_p	γ	A_z
○	1.30	0.8	0	0
□	1.30	-0.6	45	0
◇	1.30	3.3	0	-2G

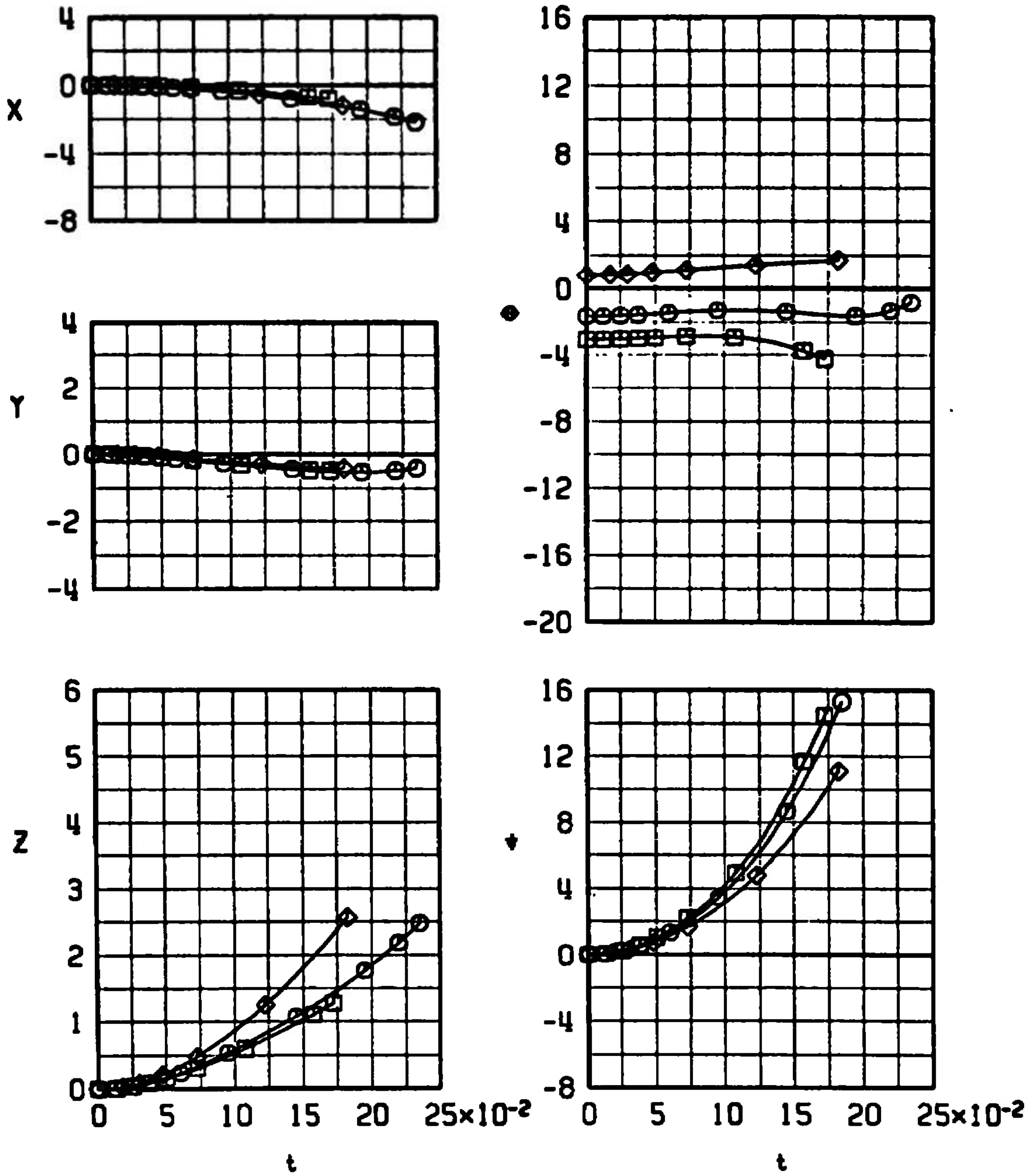

q. Configuration 8-6, M_∞ = 1.30
Fig. 24 Continued

SYMBOL	M_∞	α_p	γ	A_z
□	1.05	0	0	0
○	1.05	-0.4	45	0

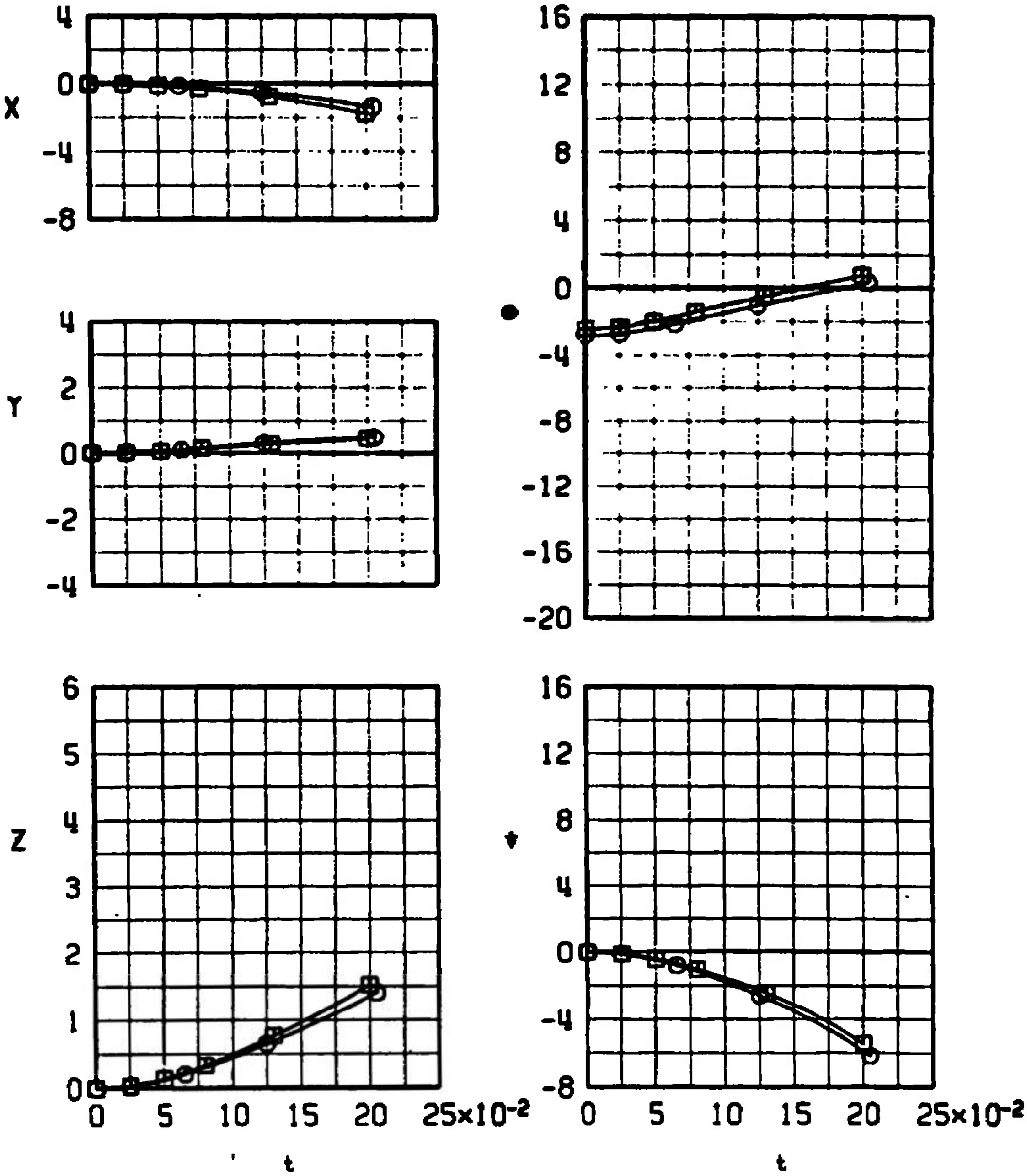

r. Configuration 8-7, M_∞ = 1.05
Fig. 24 Concluded

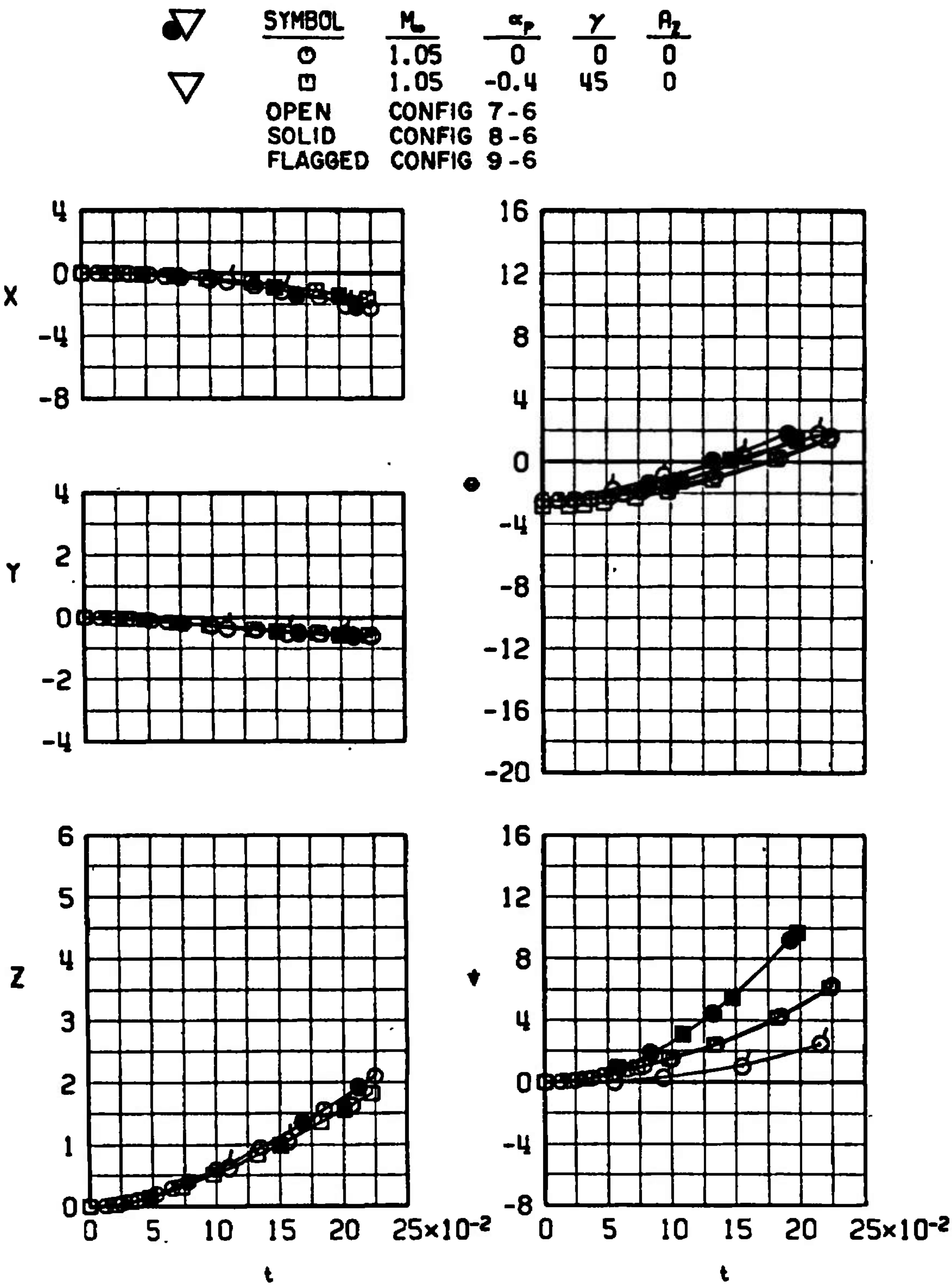

a. $M_\infty = 1.05$
Fig. 25 Effects of External Store Configuration on the MK-20 "Rockeye" Launch Trajectories from the MER, Station 4

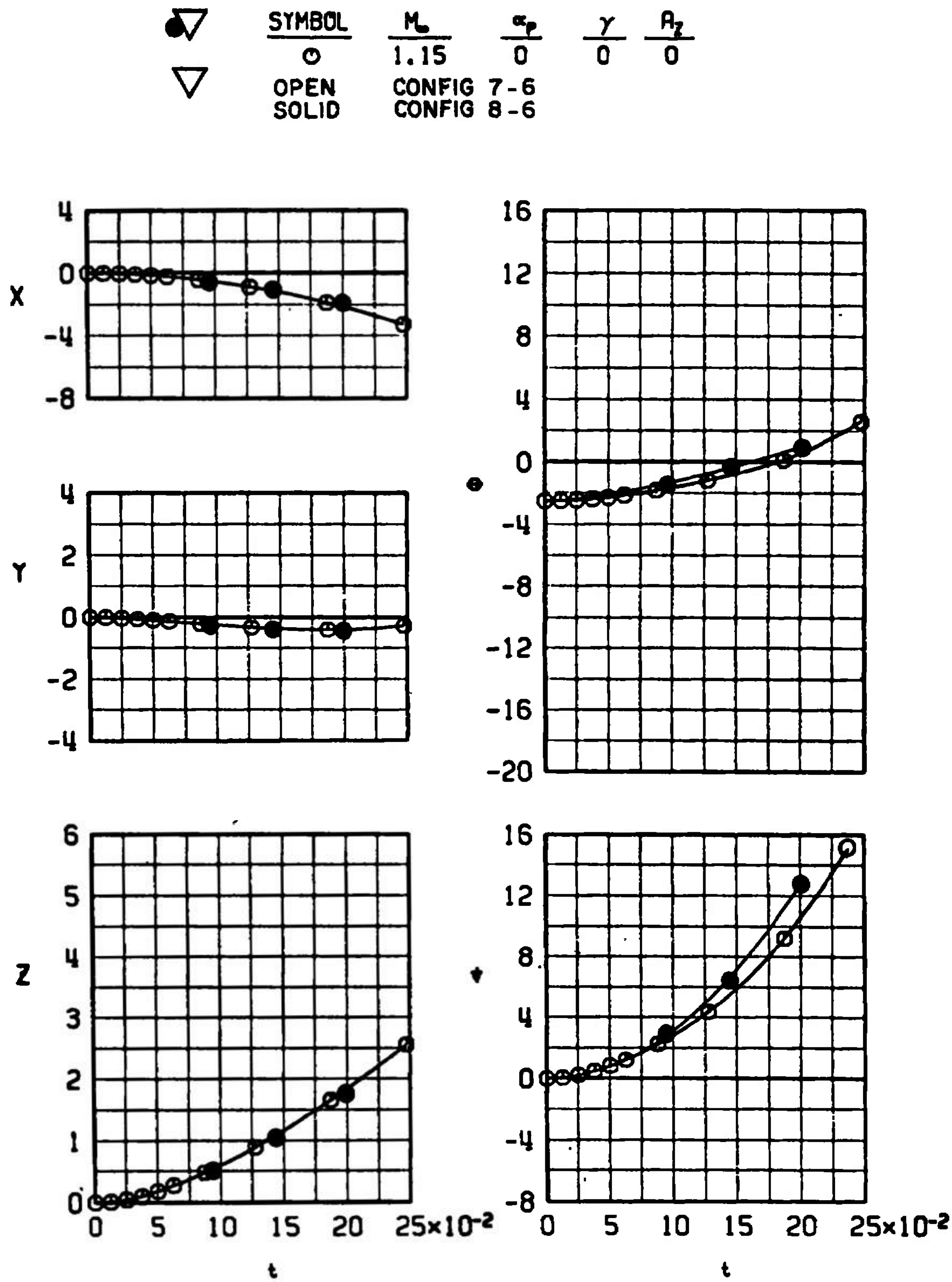

b. $M_\infty = 1.15$
Fig. 25 Continued

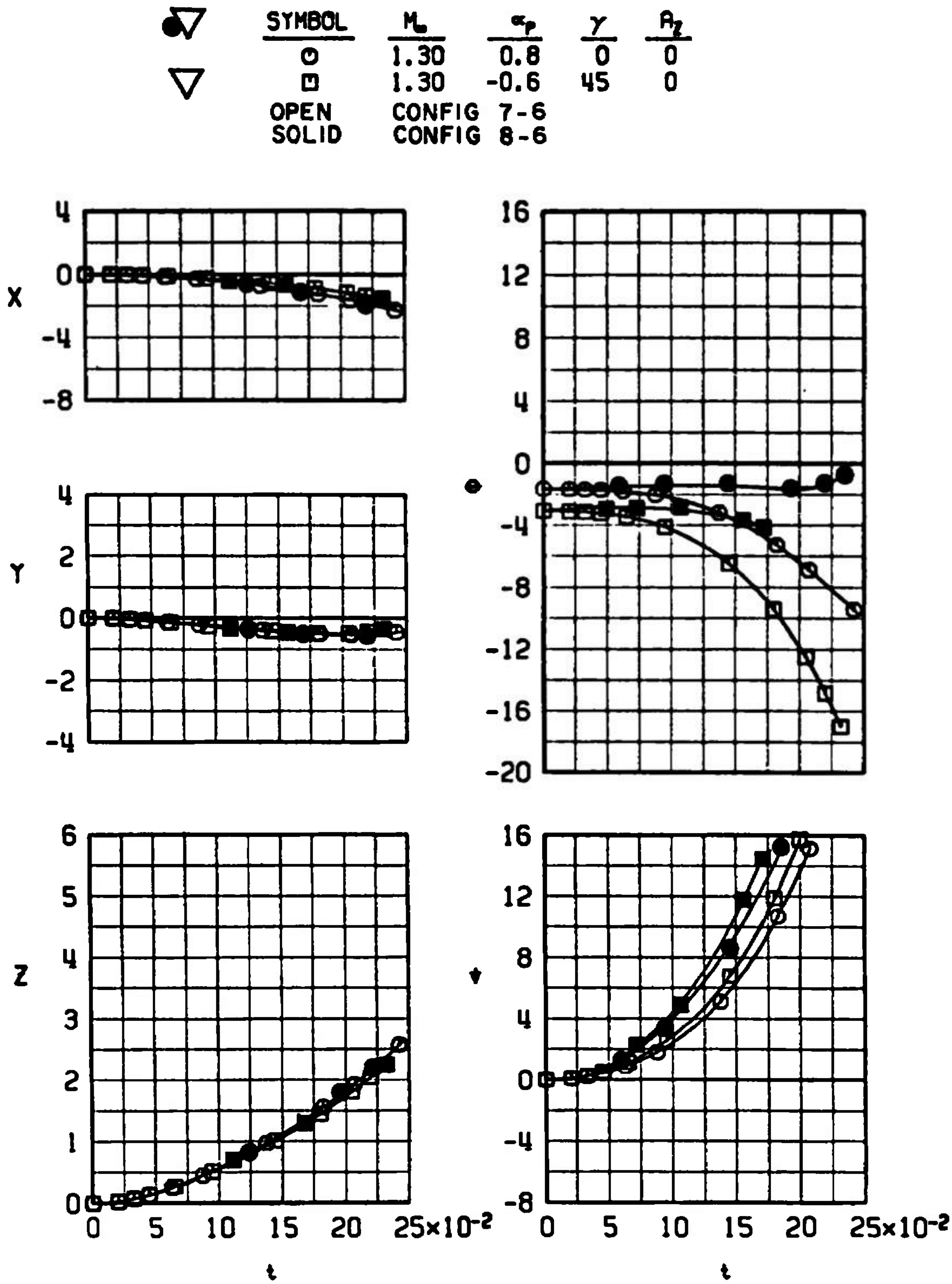

c. $M_\infty = 1.30$
Fig. 25 Concluded

SYMBOL	M_∞	α_p	γ	A_z
○	1.15	0	0	0
□	1.15	-0.5	45	0
△	1.15	-0.5	60	0

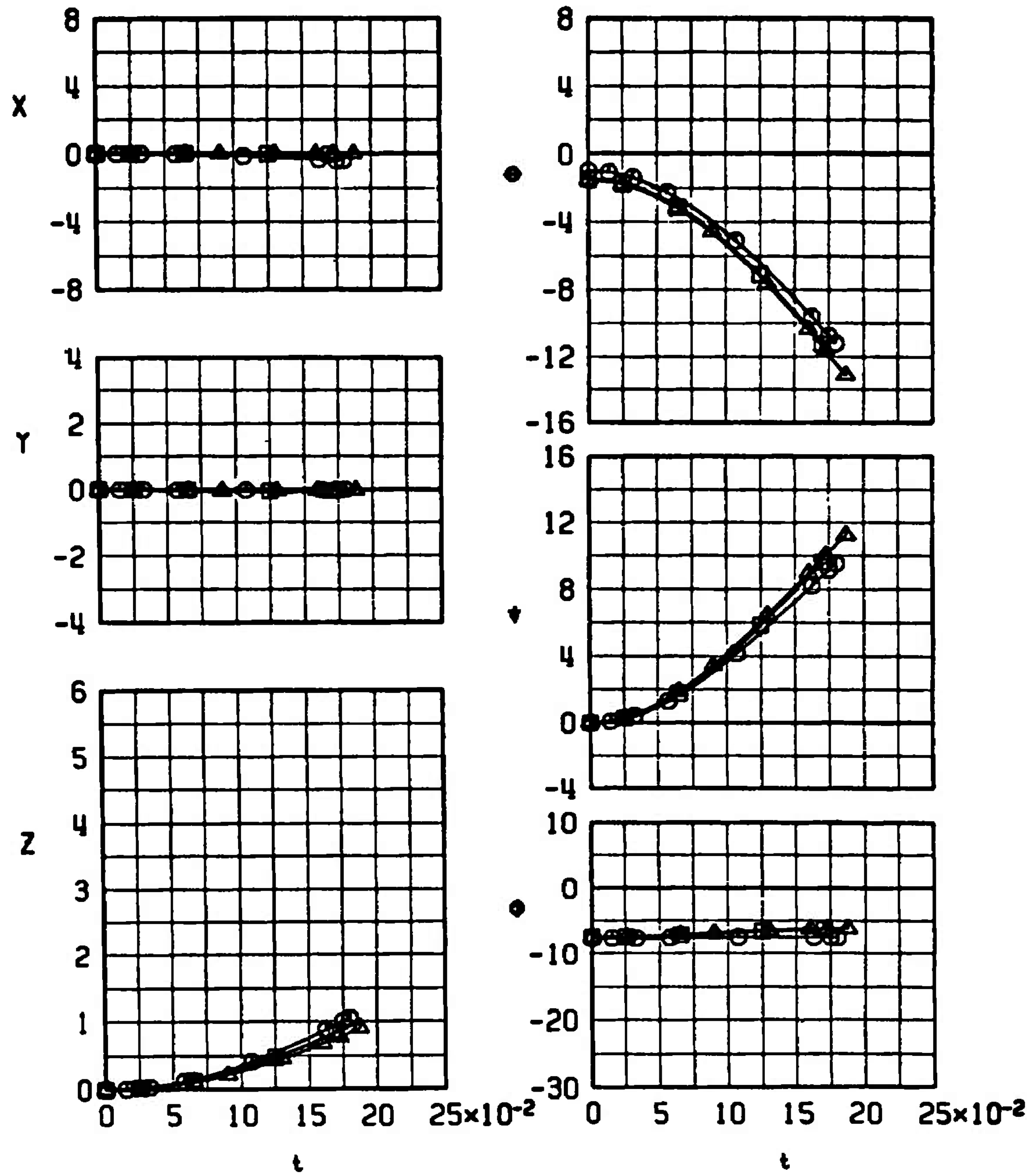

a. Configuration 10, M_∞ = 1.15
Fig. 26 Dive Angle Comparison of the MK-84 GPB Launch Trajectories from the Outboard Pylon for Different Mach Numbers

SYMBOL	M_∞	α_p	γ	A_z
○	1.25	0.4	0	0
□	1.25	-0.6	45	0
△	1.25	-0.6	60	0
◇	1.25	2.7	0	-2G

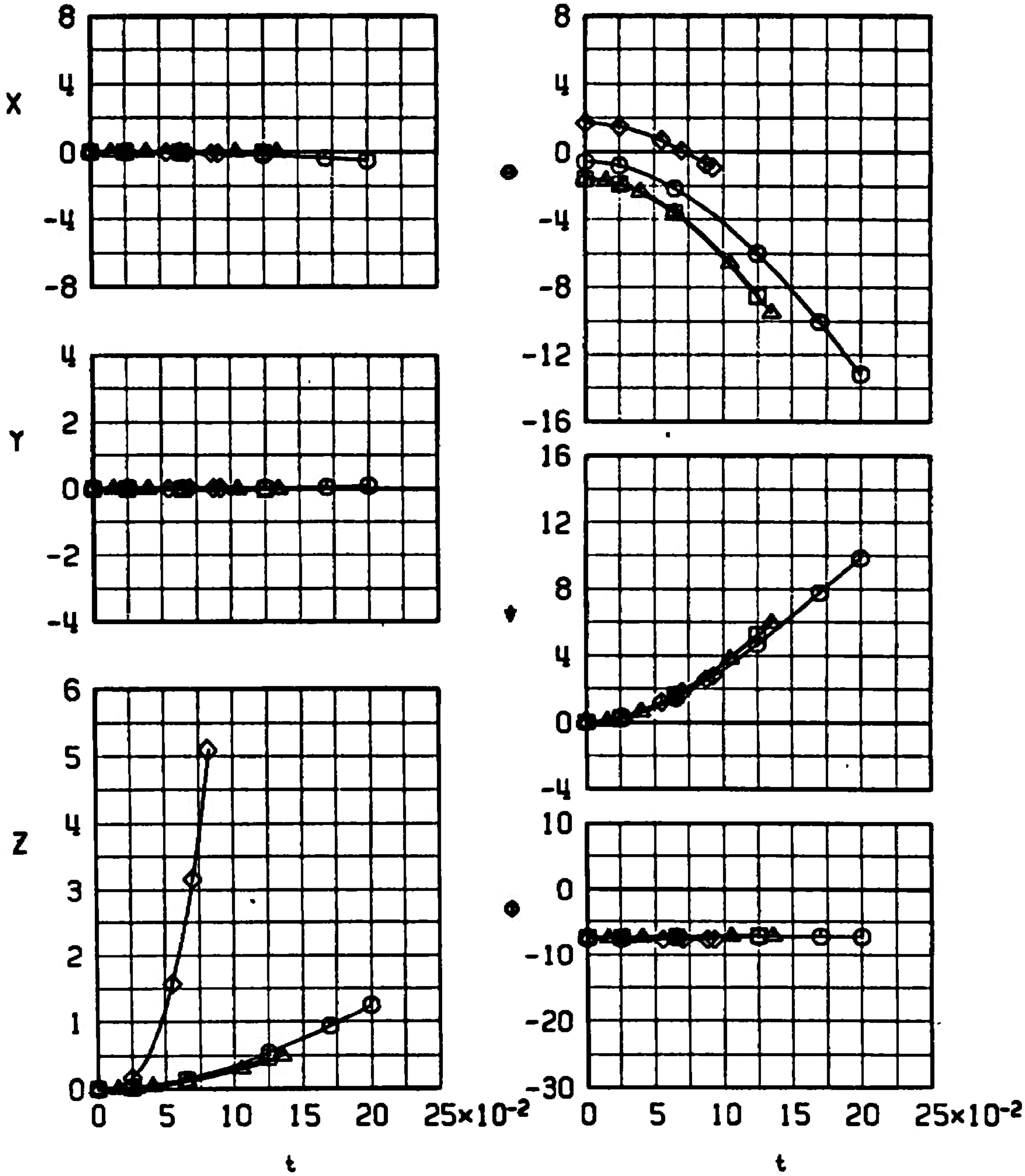

b. Configuration 10, 1.25
Fig. 26 Continued

SYMBOL	M_∞	α_p	γ	R_z
○	1.60	1.2	0	0
△	1.60	-0.3	60	0

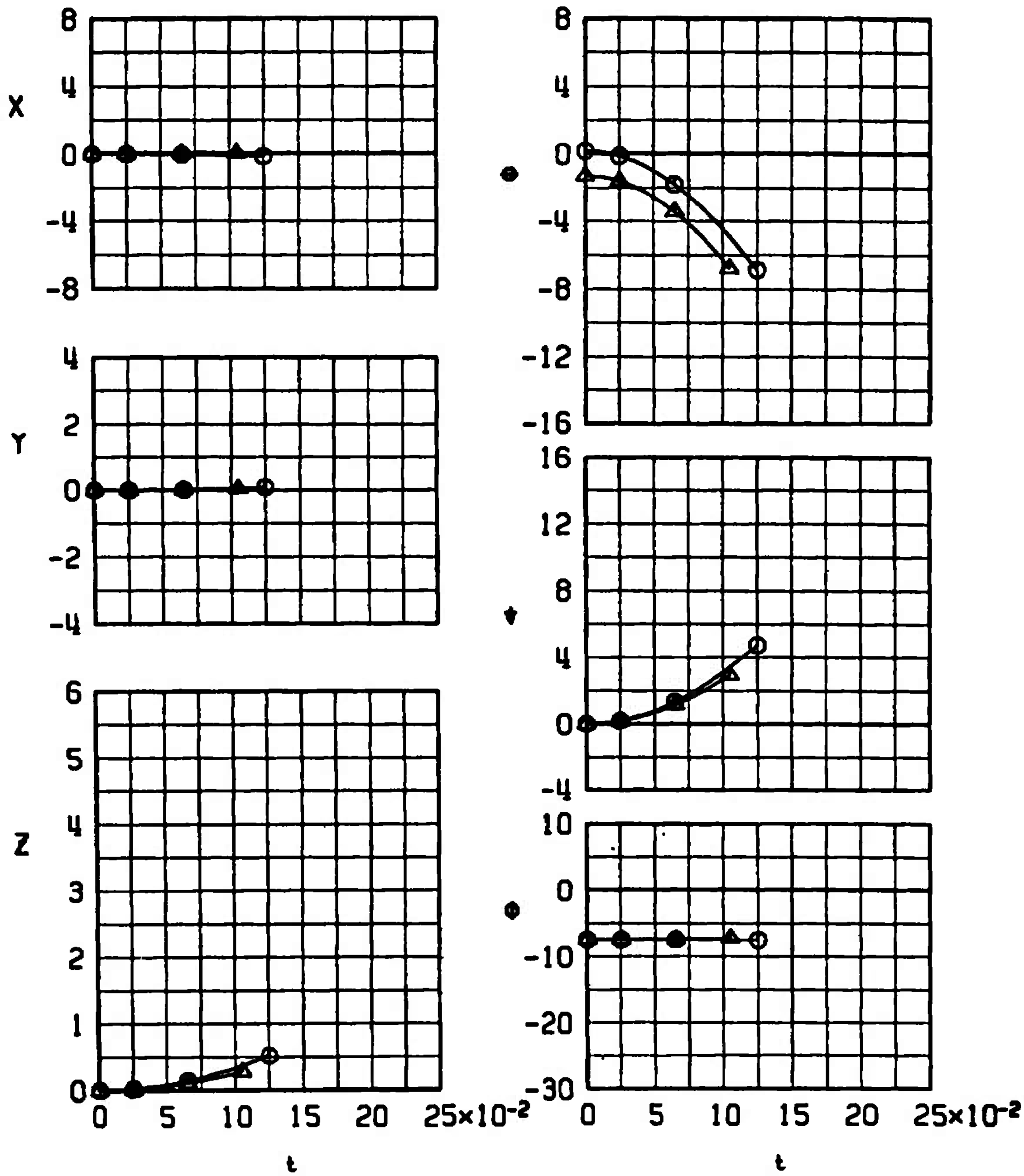

c. Configuration 10, M_∞ = 1.60
Fig. 26 Continued

SYMBOL	M_∞	α_p	γ	A_z
○	1.15	0	0	0
△	1.15	-0.5	60	0

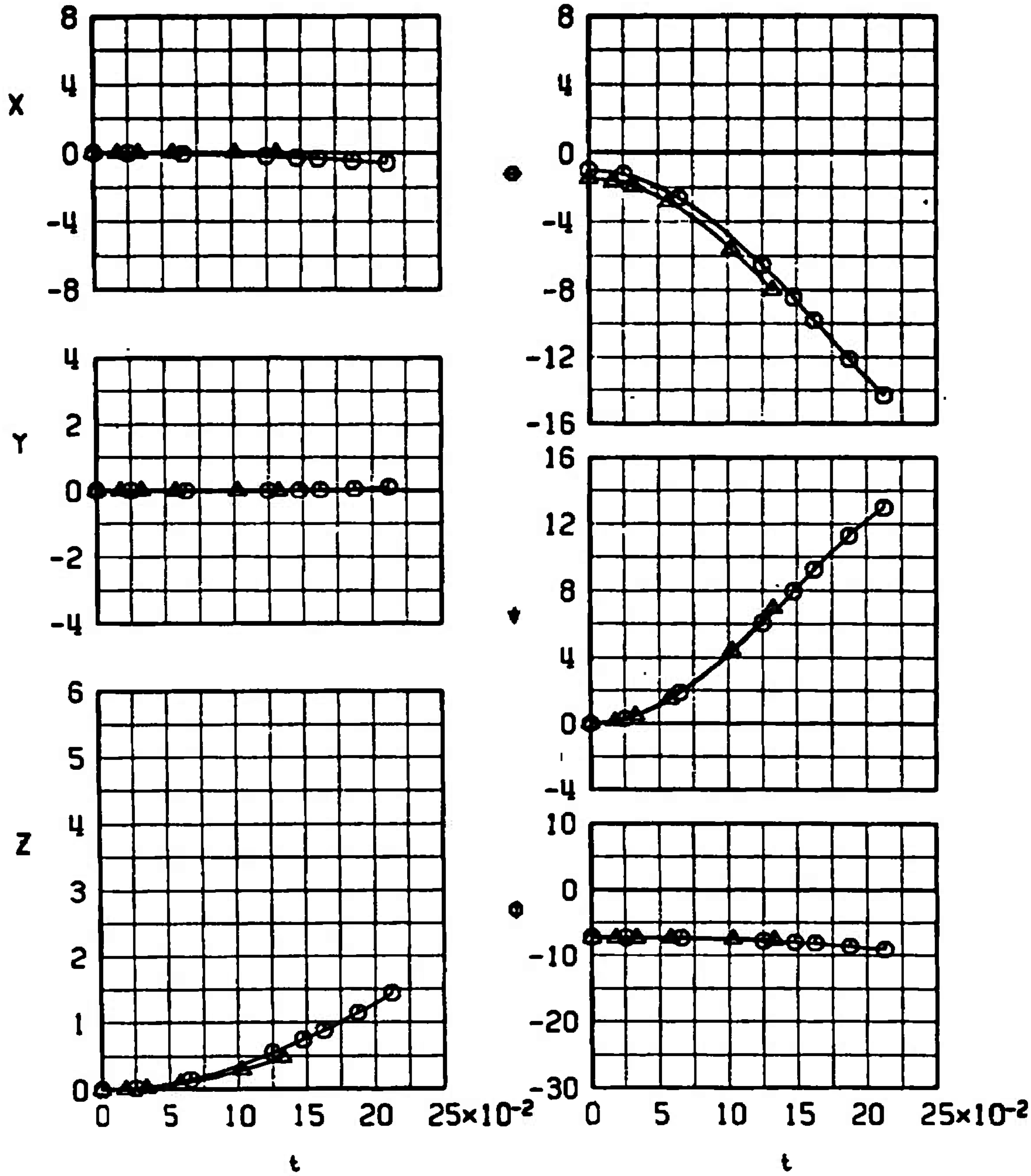

d. Configuration 11, M_∞ = 1.15
Fig. 26 Continued

SYMBOL	M_∞	α_p	γ	R_z
○	1.25	0.4	0	0
△	1.25	-0.6	60	0

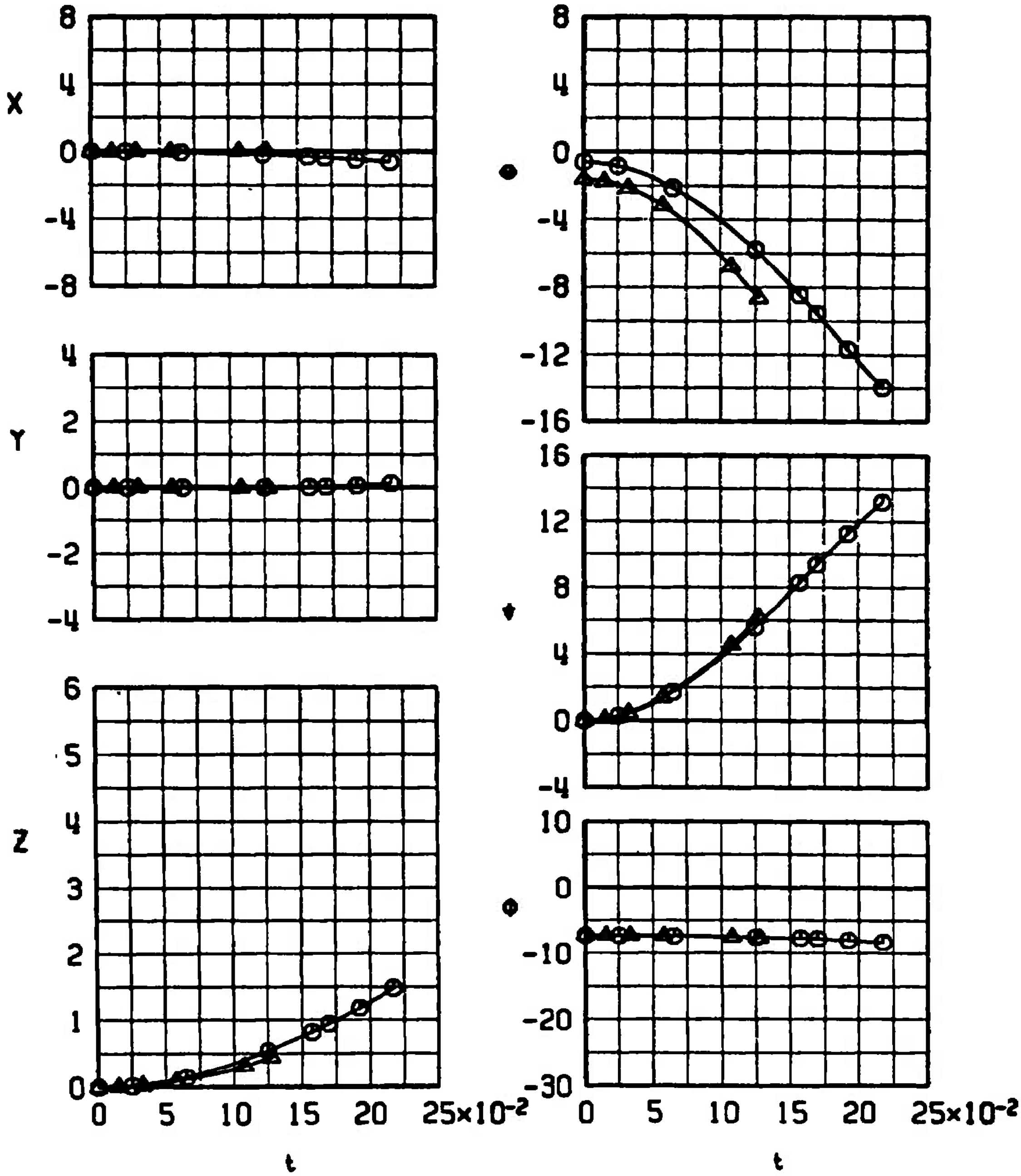

e. Configuration 11, M_∞ = 1.25
Fig. 26 Continued

SYMBOL	M_∞	α_p	γ	A_Z
○	1.60	1.2	0	0
△	1.60	-0.3	60	0

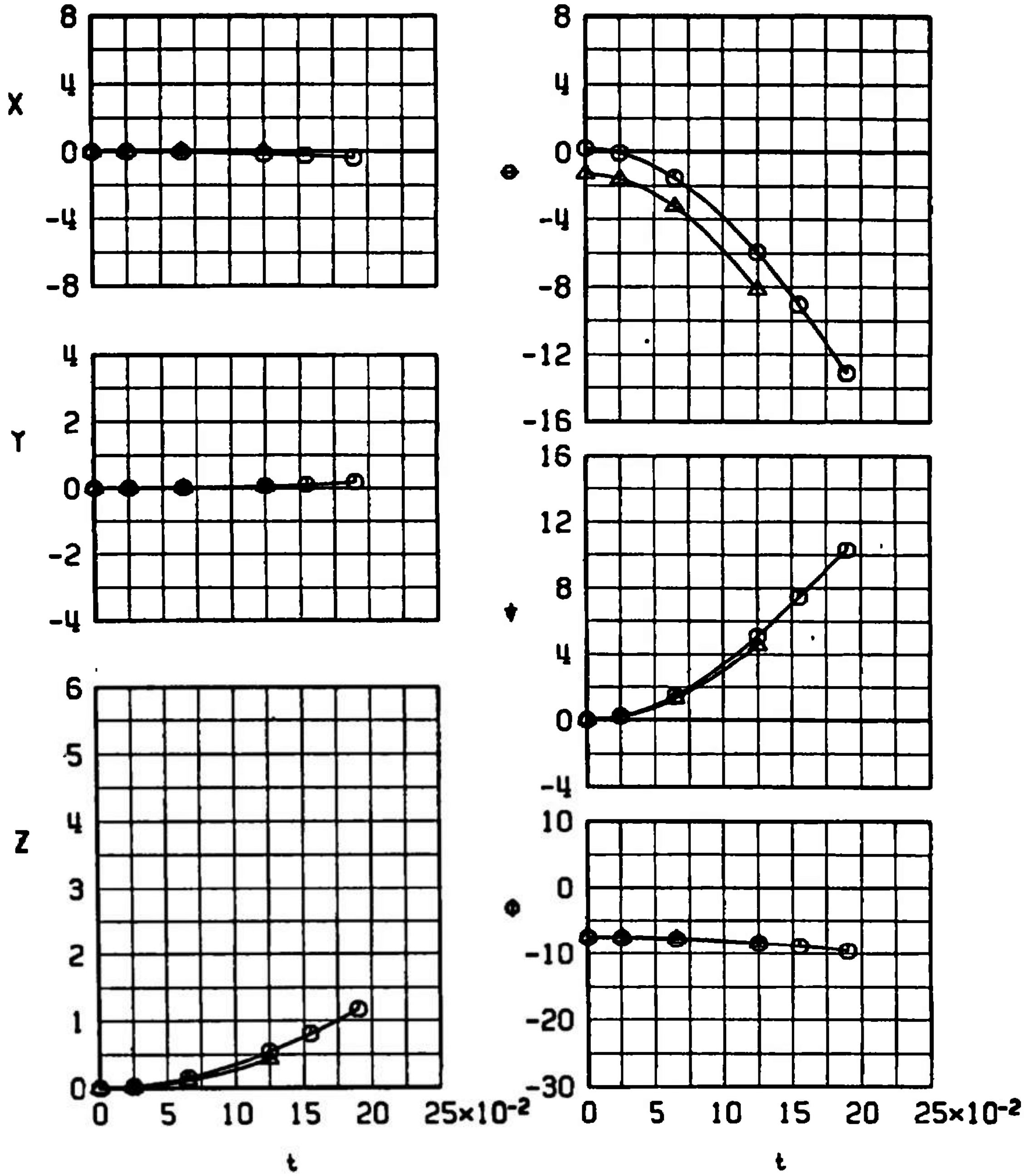

f. Configuration 11, M_∞ = 1.60
Fig. 26 Concluded

SYMBOL	M_∞	α_p	γ	A_z
○	1.05	0	0	0
△	1.05	-0.4	60	0

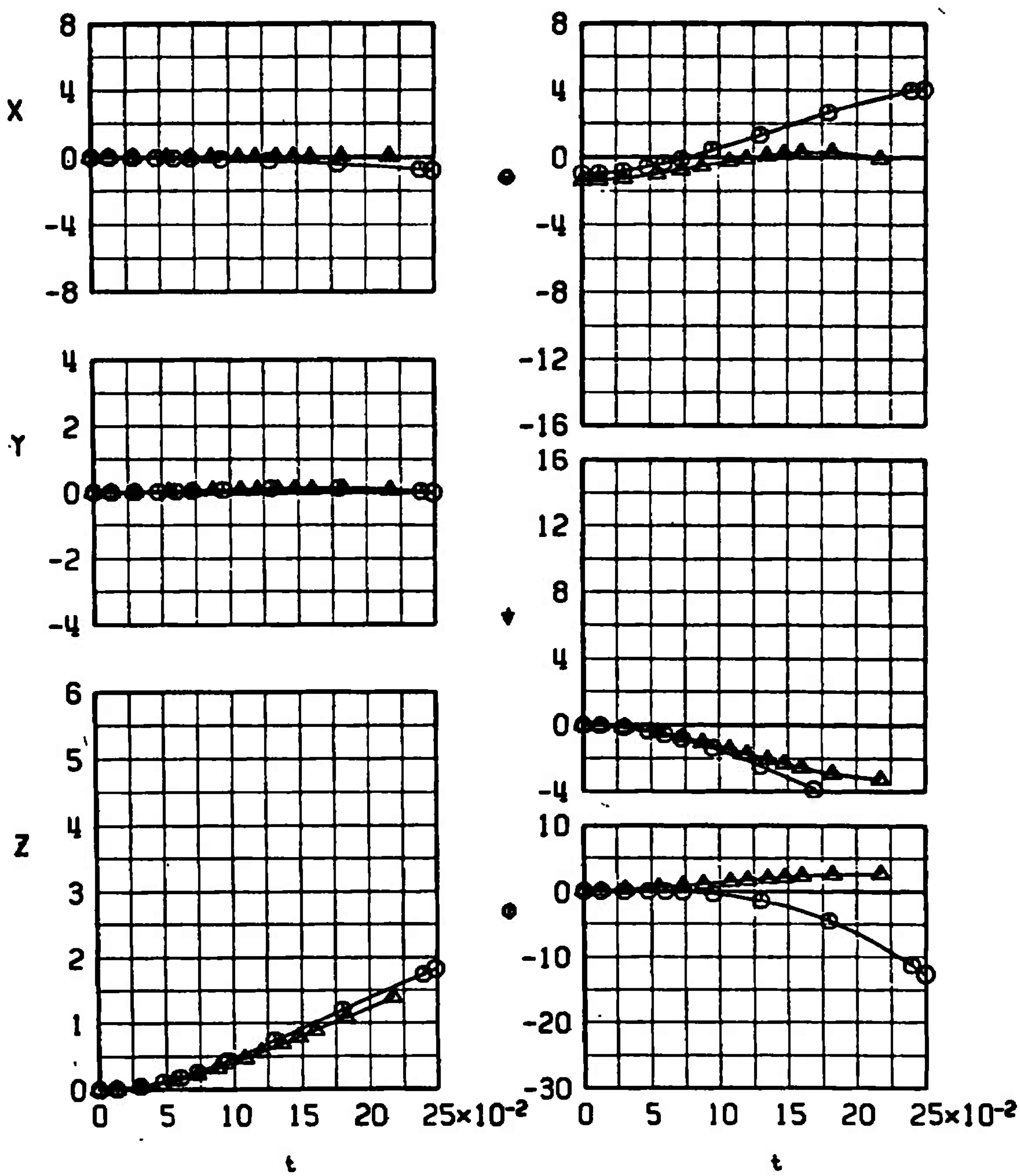

a. Configuration 12, M_∞ = 1.05

Fig. 27 Dive Angle Comparison of the MK-84 LGB Launch Trajectories from the Inboard Pylon for Different Mach Numbers

SYMBOL	M_∞	α_p	γ	θ_z
○	1.25	0.4	0	0
△	1.25	-0.6	60	0

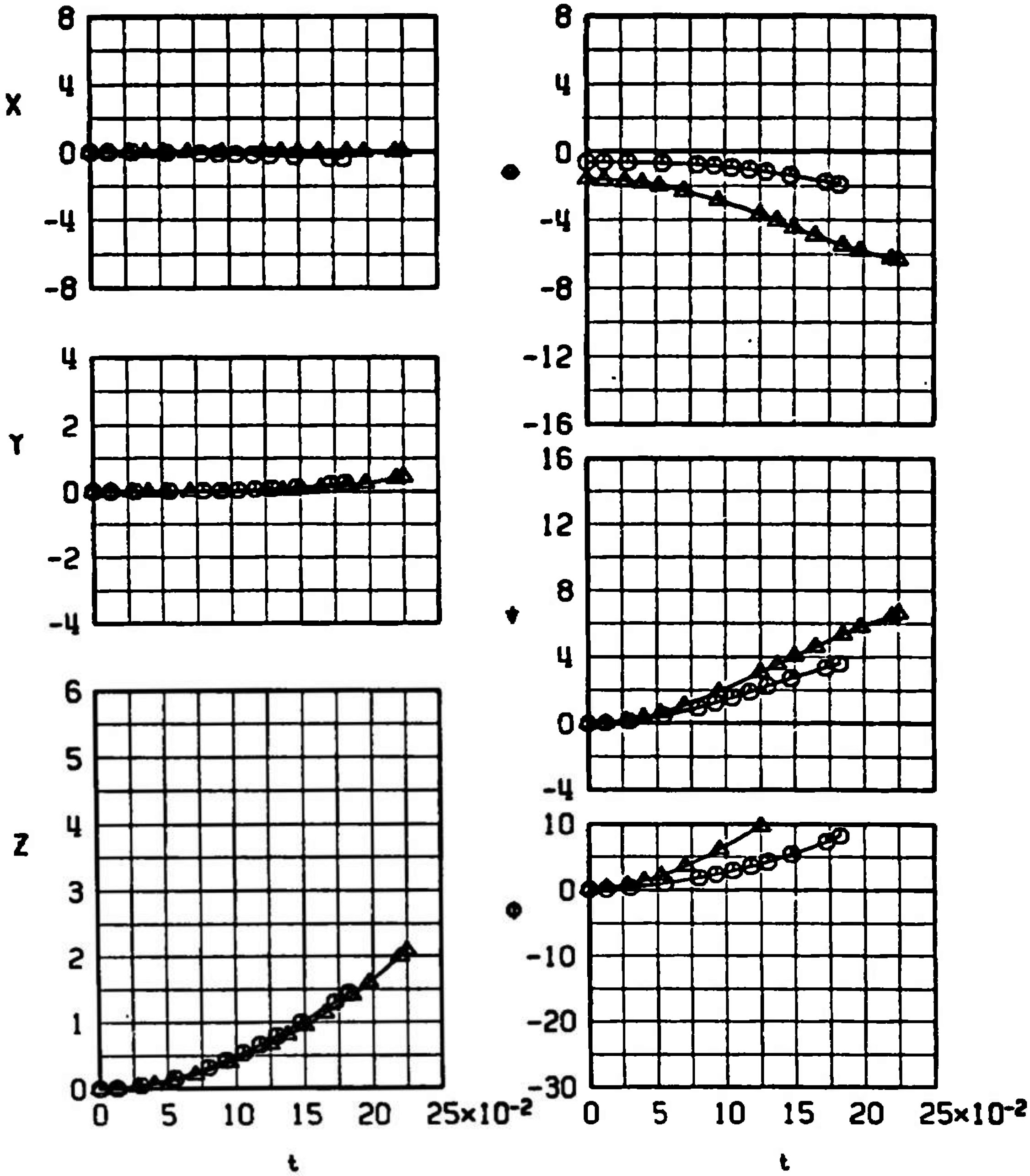

b. Configuration 12, M_∞ = 1.25
Fig. 27 Continued

SYMBOL	M_∞	α_p	γ	A_z
○	1.05	0	0	0
△	1.05	-0.4	60	0

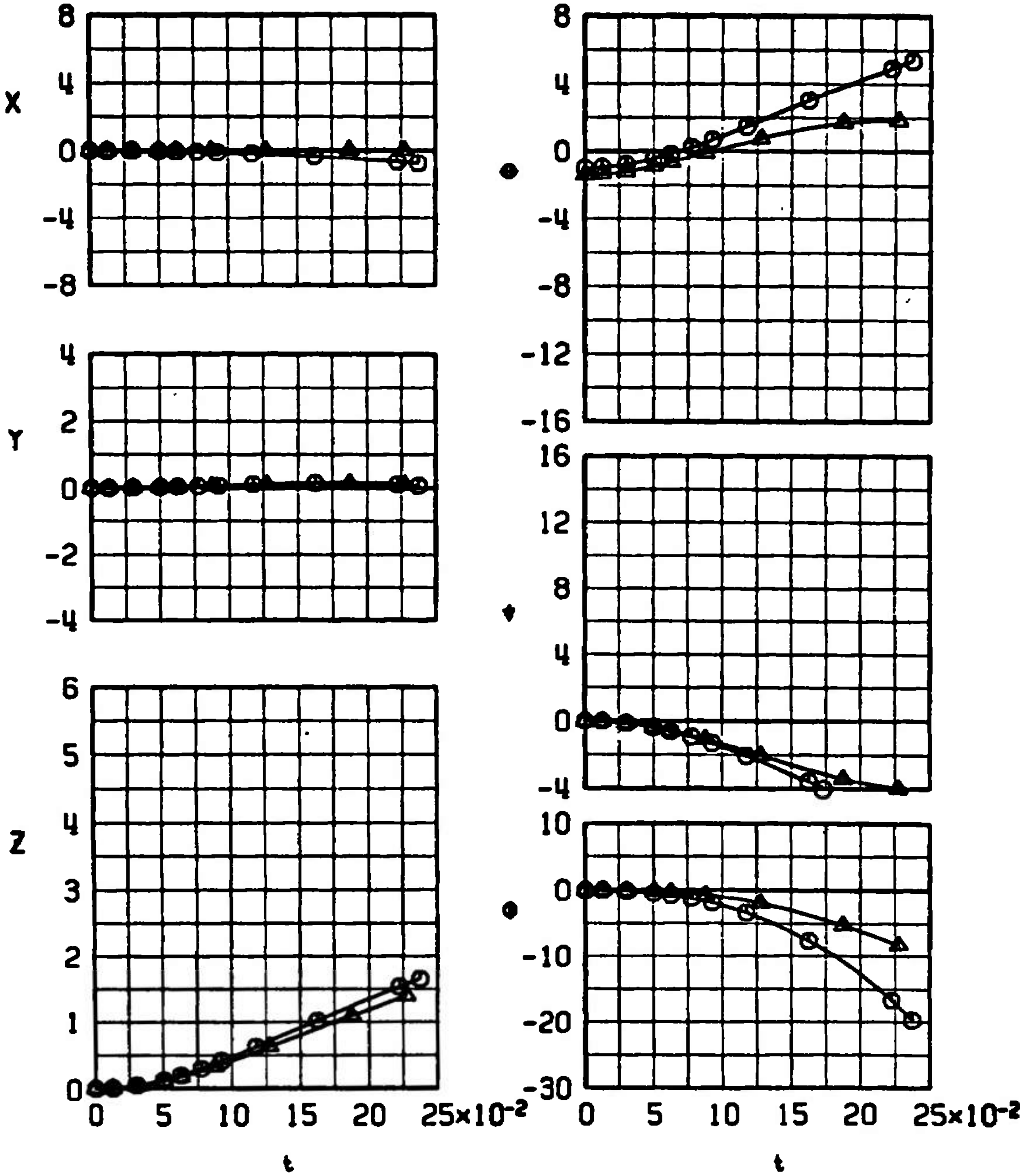

c. Configuration 13, M_∞ = 1.05
Fig. 27 Continued

SYMBOL	M_∞	α_p	γ	R_z
○	1.15	0	0	0
△	1.15	-0.5	60	0

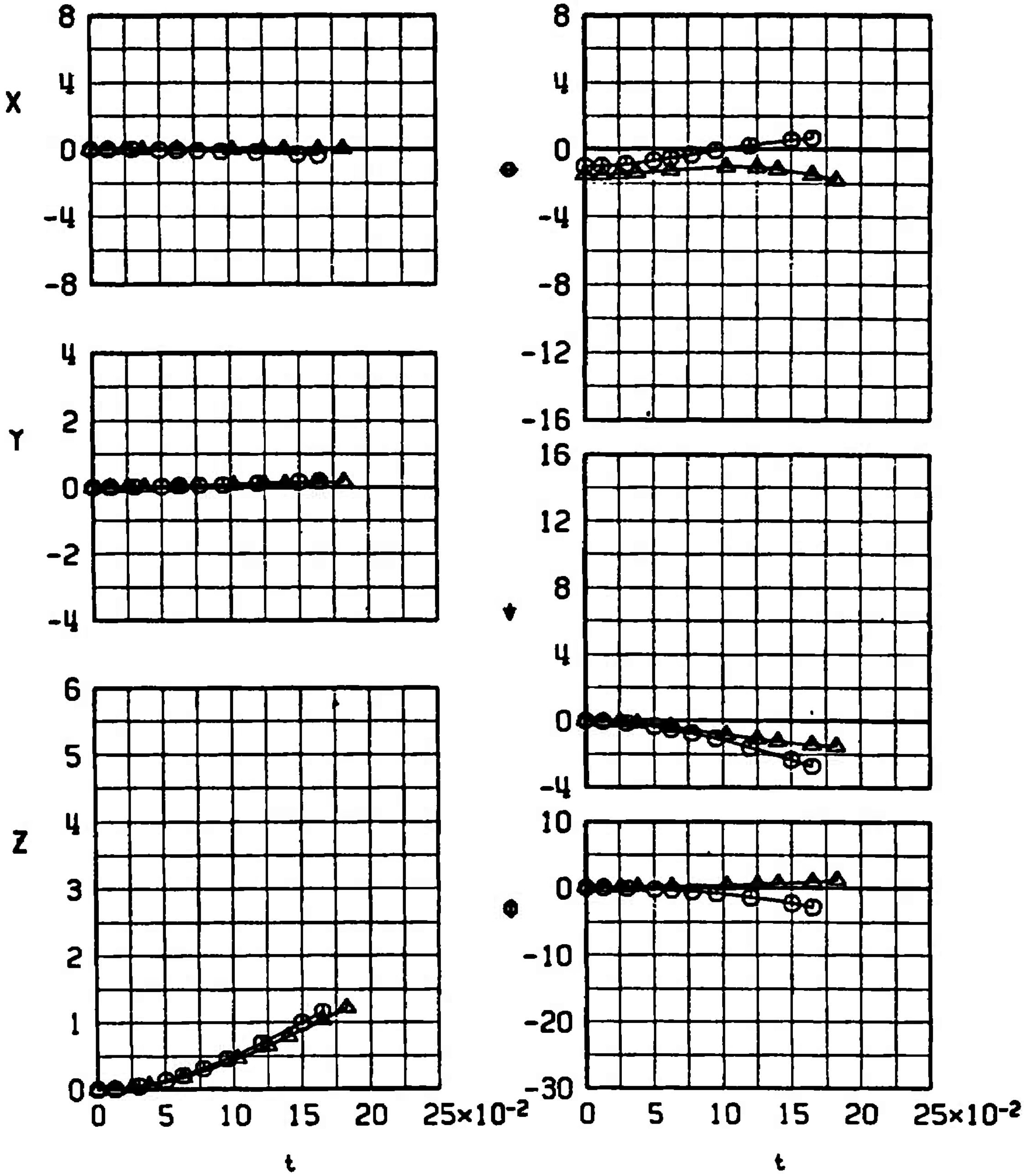

d. Configuration 13, M_∞ = 1.15
Fig. 27 Continued

SYMBOL	M_∞	α_p	γ	A_z
○	1.25	0.4	0	0
△	1.25	-0.6	60	0

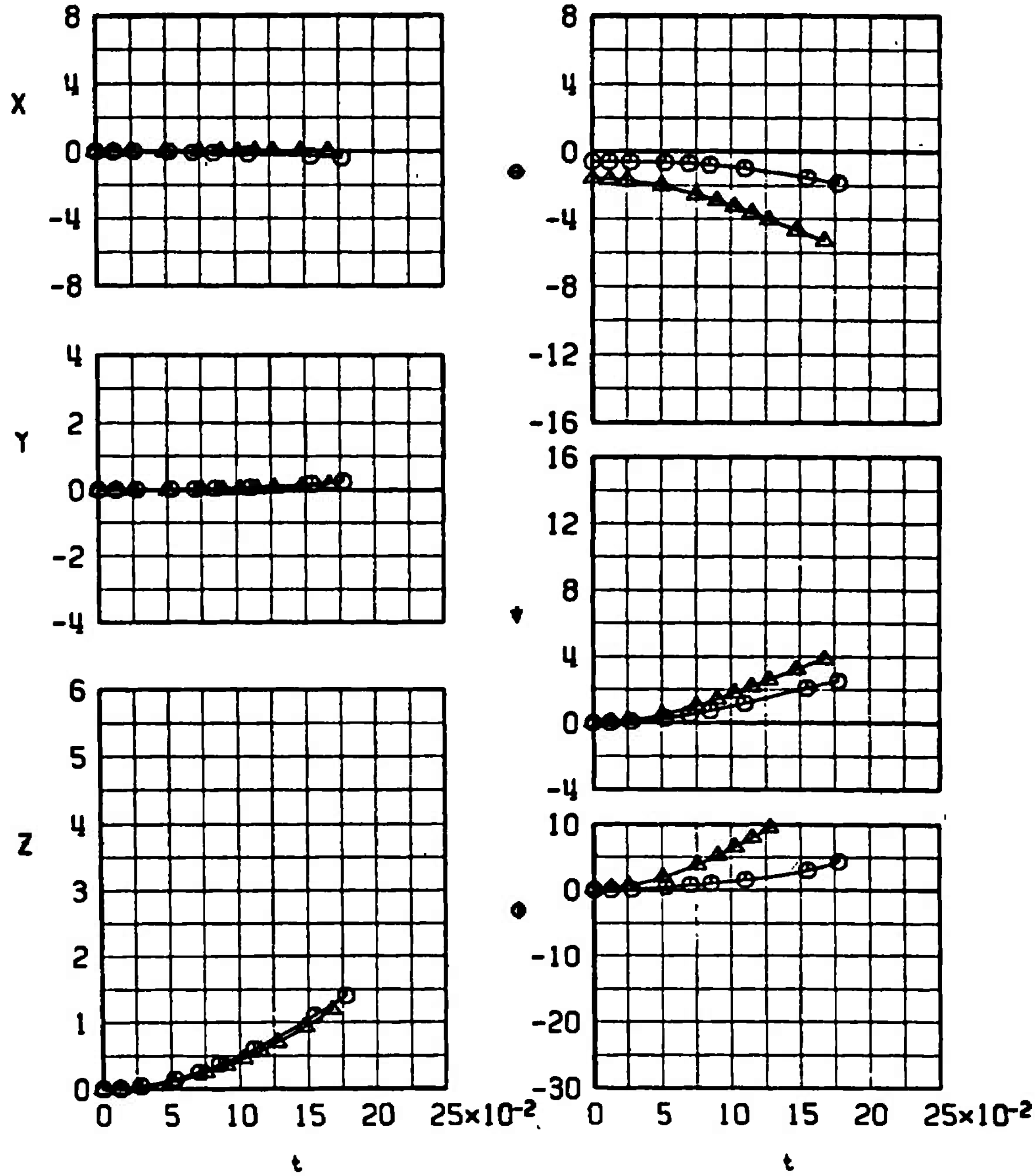

e. Configuration 13, M_∞ = 1.25
Fig. 27 Continued

SYMBOL	M_∞	α_p	γ	β_z
○	1.60	1.2	0	0
△	1.60	-0.3	60	0

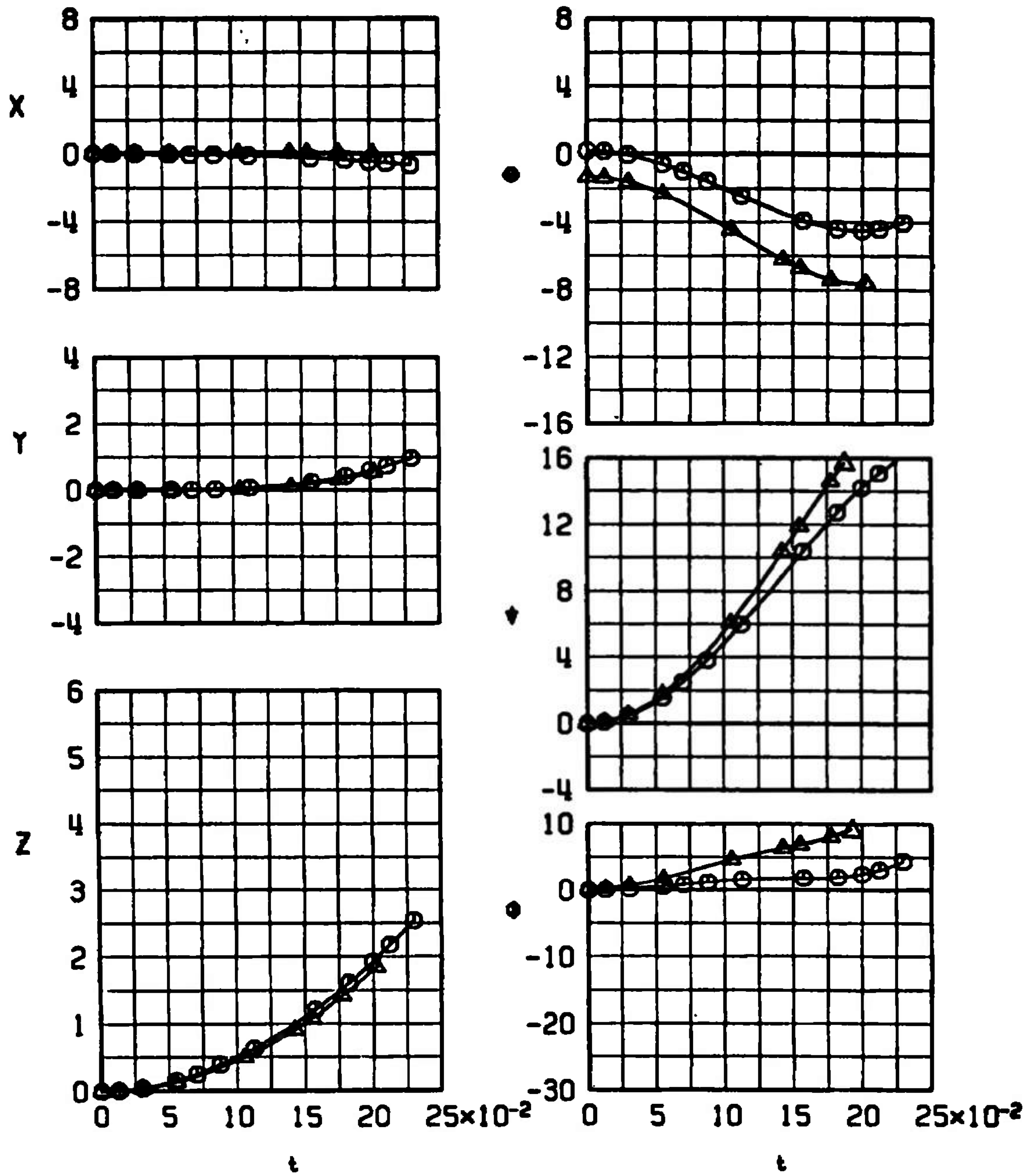

f. Configuration 13, M_∞ = 1.60
Fig. 27 Continued

SYMBOL	M_∞	α_p	γ	A_z
○	1.05	0	0	0
△	1.05	-0.4	60	0

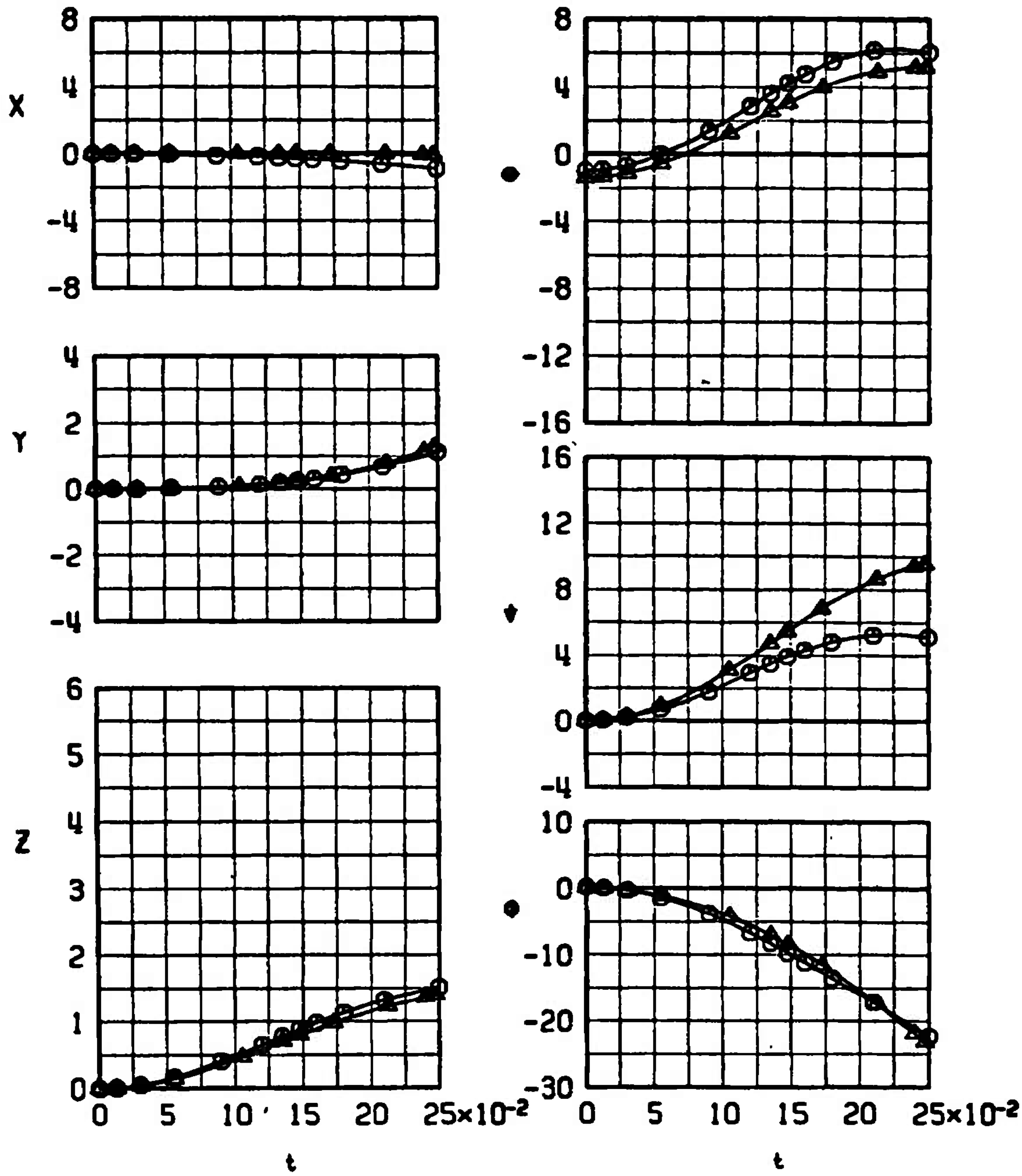

g. Configuration 14, M_∞ = 1.05
Fig. 27 Continued

SYMBOL	M_∞	α_p	γ	A_z
○	1.15	0	0	0
△	1.15	-0.5	60	0

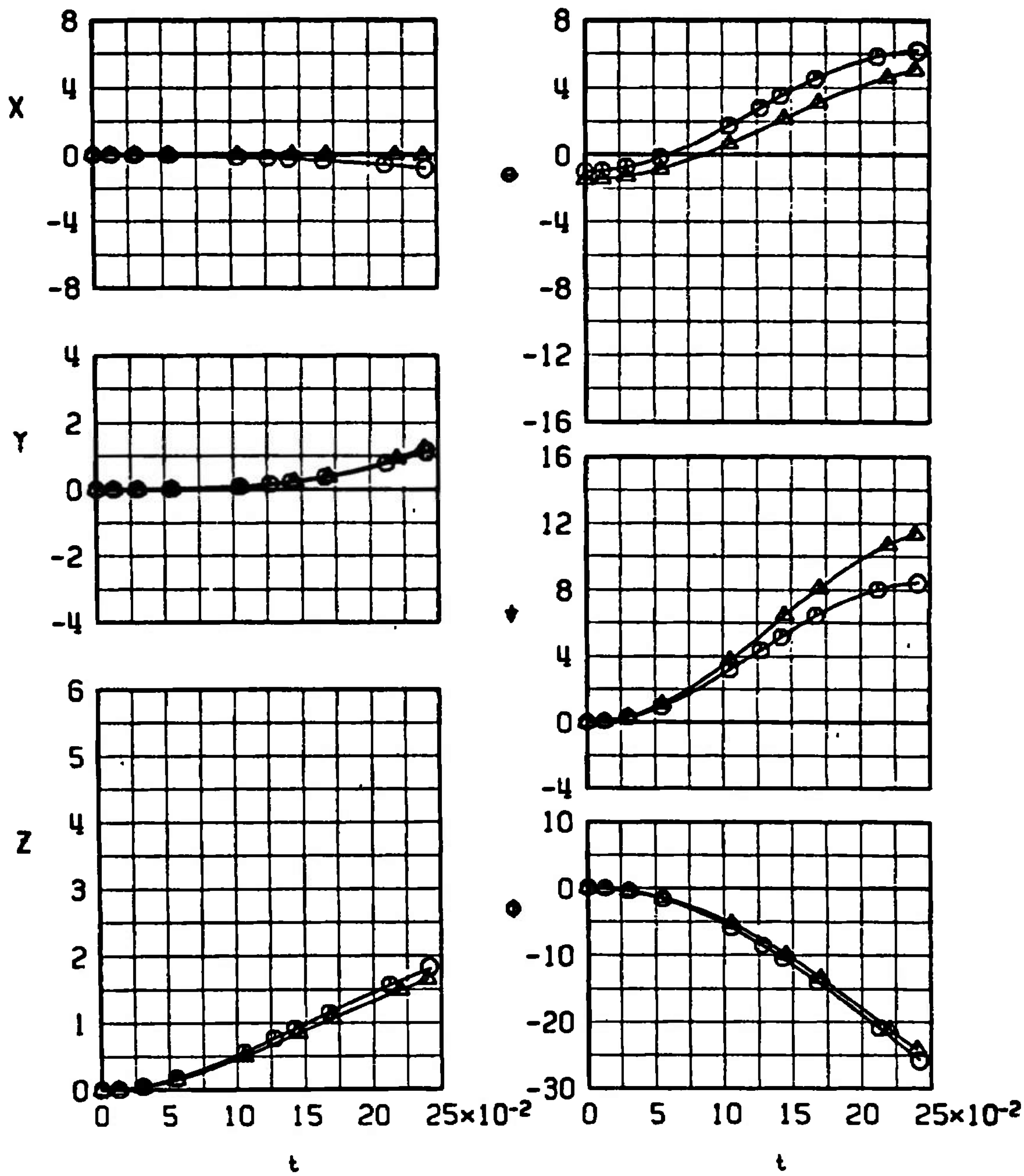

h. Configuration 14, M_∞ = 1.15
Fig. 27 Continued

SYMBOL	M_∞	α_p	γ	A_z
○	1.25	0.4	0	0
△	1.25	-0.6	60	0

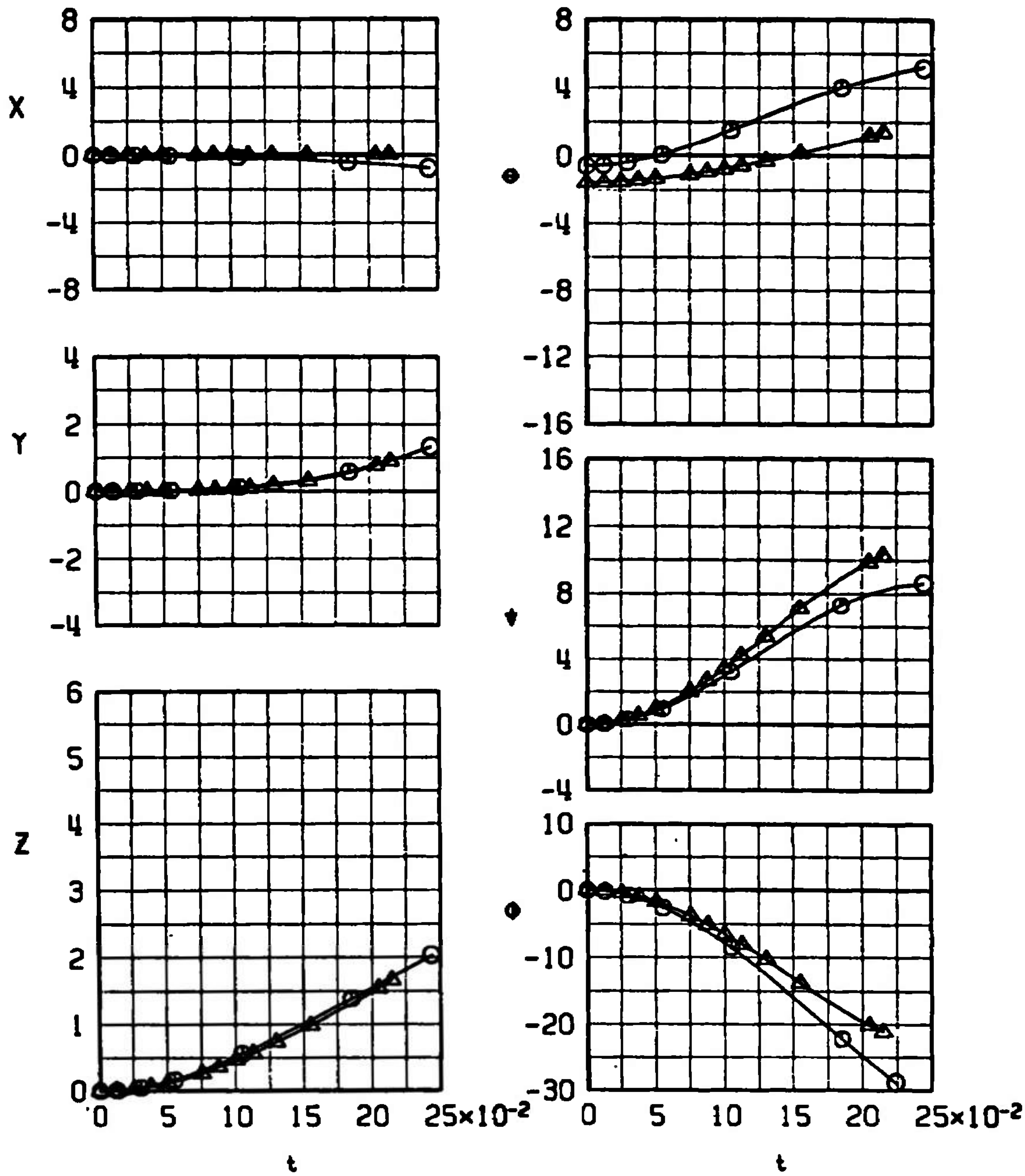

i. Configuration 14, M_∞ = 1.25
Fig. 27 Continued

SYMBOL	M_∞	α_p	γ	A_z
○	1.60	1.2	0	0
△	1.60	-0.3	60	0

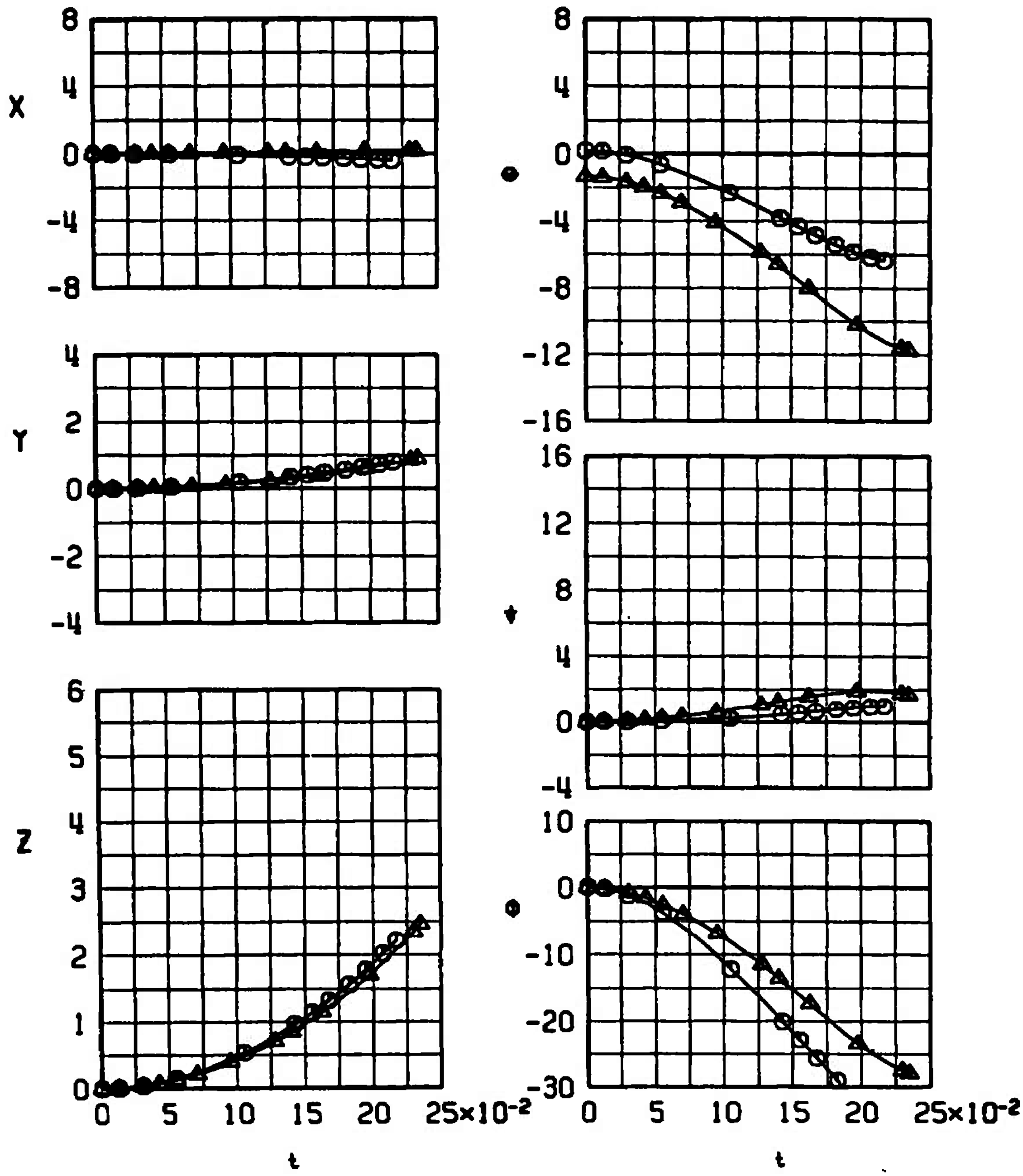

j. Configuration 14, M_∞ = 1.60
Fig. 27 Concluded

SYMBOL	M_∞	α_p	γ	A_z
○	1.05	0	0	0
△	1.05	-0.4	60	0

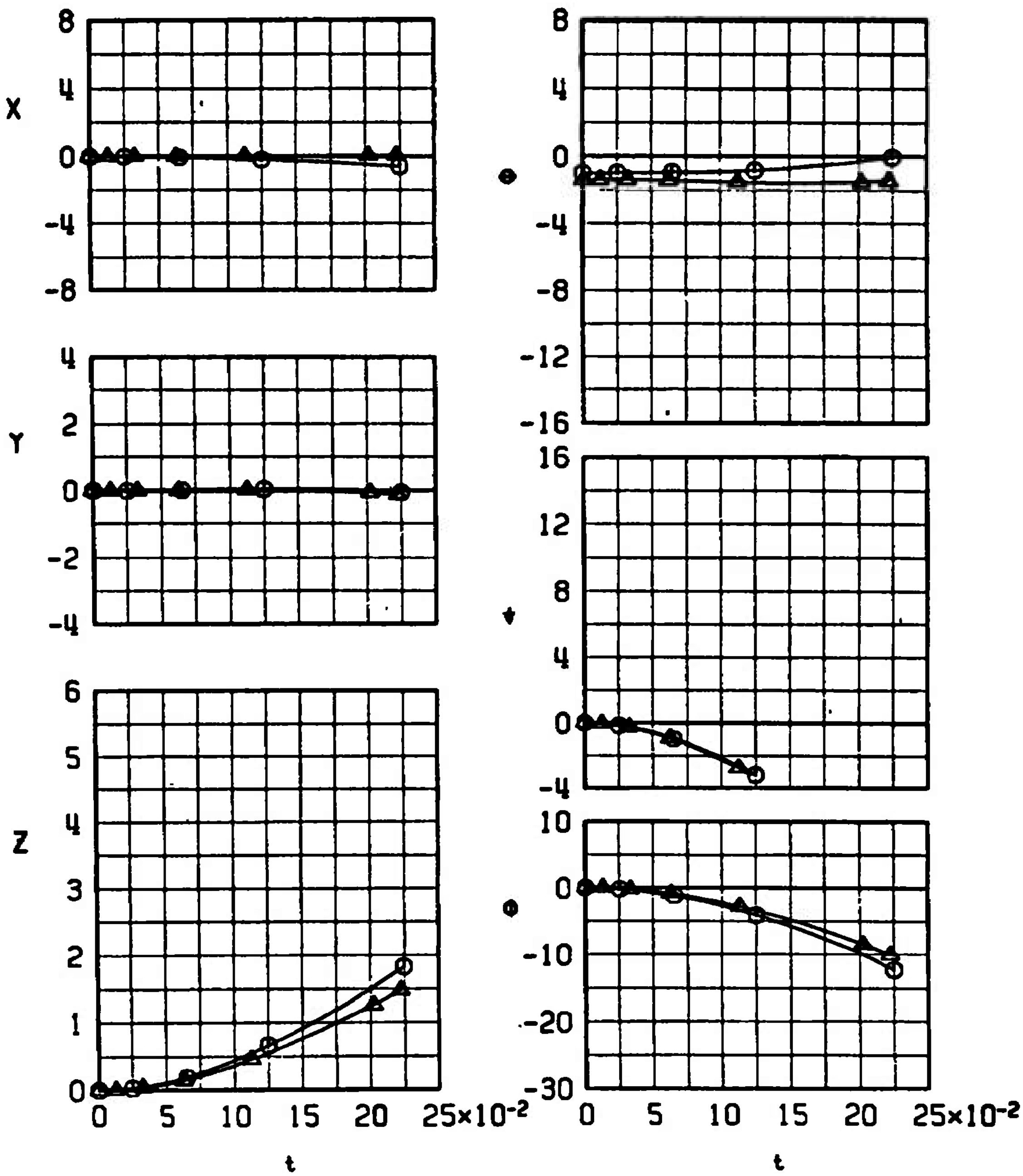

a. Configuration 15, M_∞ = 1.05
Fig. 28 Dive Angle Comparison of the MK-84 EOGB Launch Trajectories from the Inboard Pylon for Different Mach Numbers

SYMBOL	M_∞	α_p	γ	A_z
○	1.25	0.4	0	0
△	1.25	-0.6	60	0

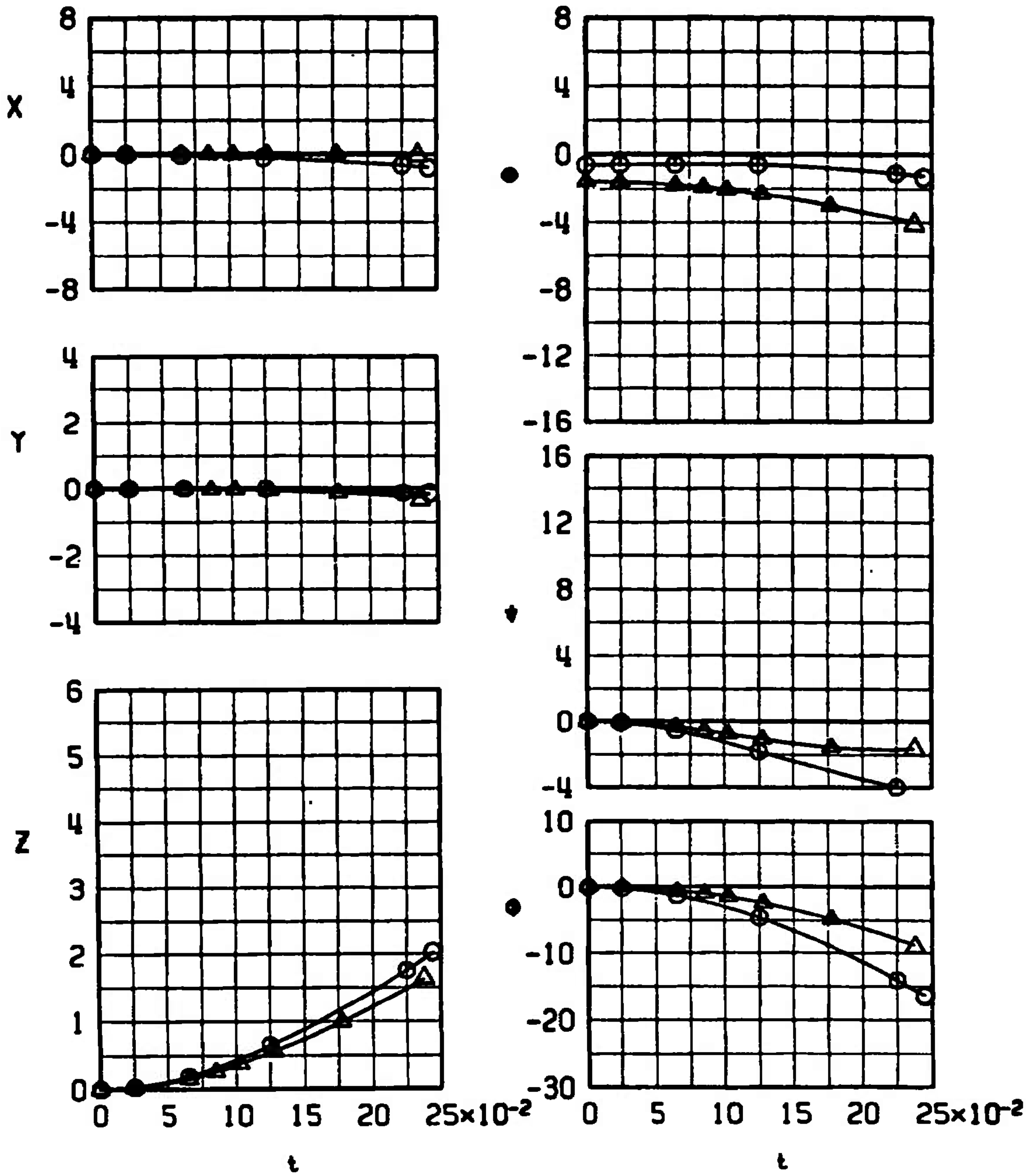

b. Configuration 15, M_∞ = 1.25
Fig. 28 Continued

SYMBOL	M_∞	α_p	γ	A_z
○	1.05	0	0	0
△	1.05	-0.4	60	0

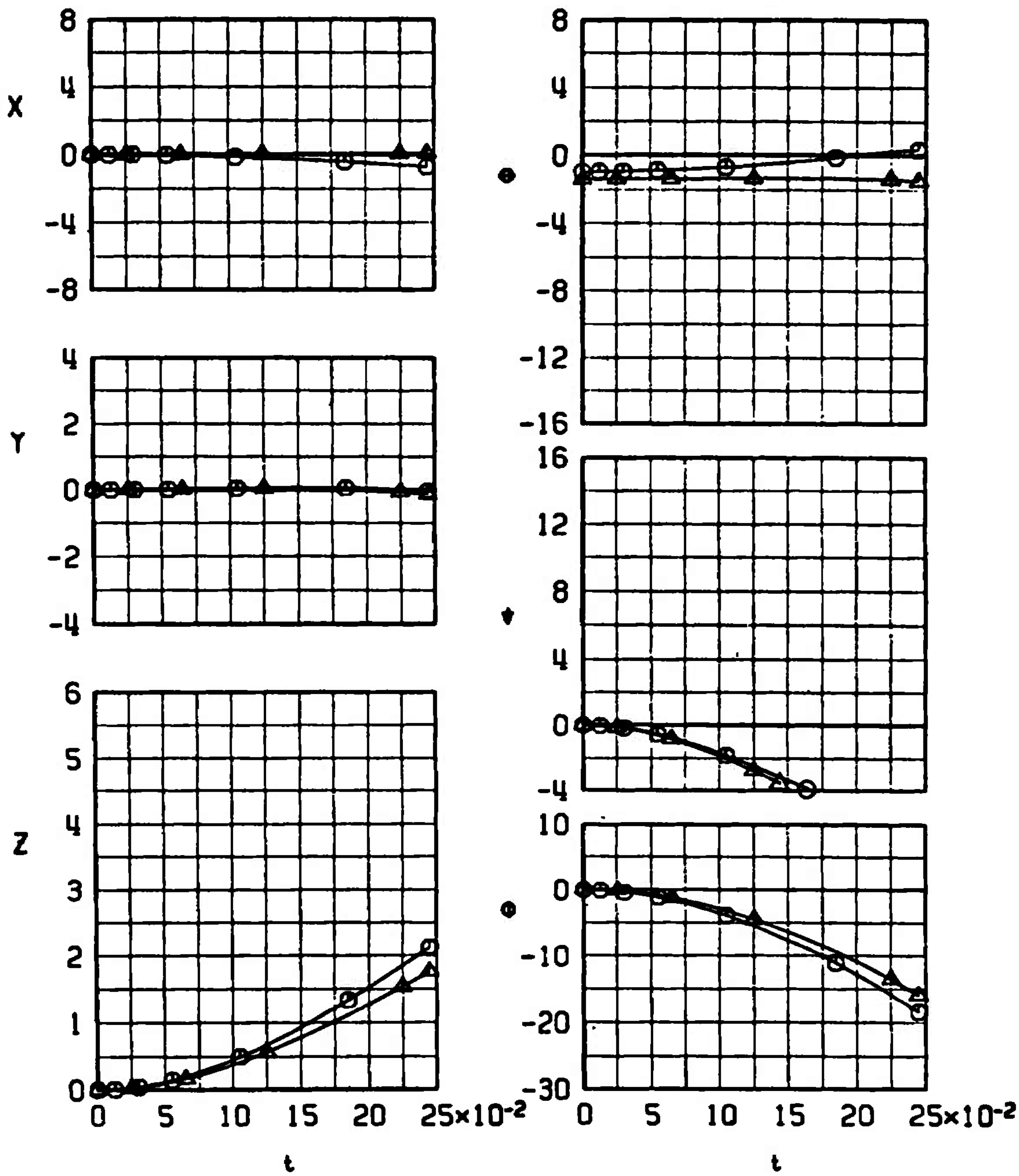

c. Configuration 16, M_∞ = 1.05
Fig. 28 Continued

SYMBOL	M_∞	α_p	γ	A_Z
○	1.15	0	0	0
△	1.15	-0.5	60	0

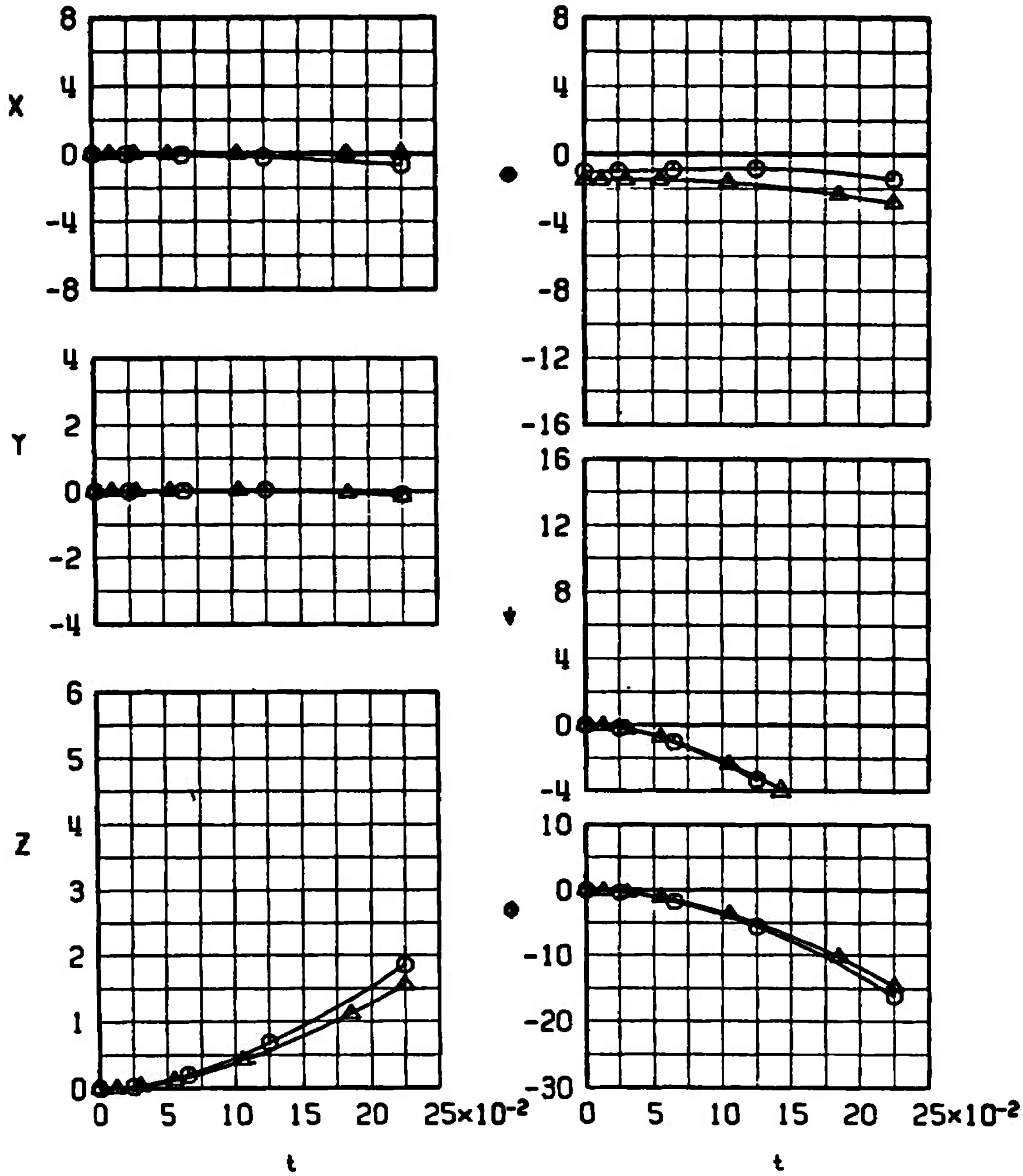

d. Configuration 16, M_∞ = 1.15
Fig. 28 Continued

SYMBOL	M_∞	α_p	γ	R_z
○	1.25	0.4	0	0
△	1.25	-0.6	60	0

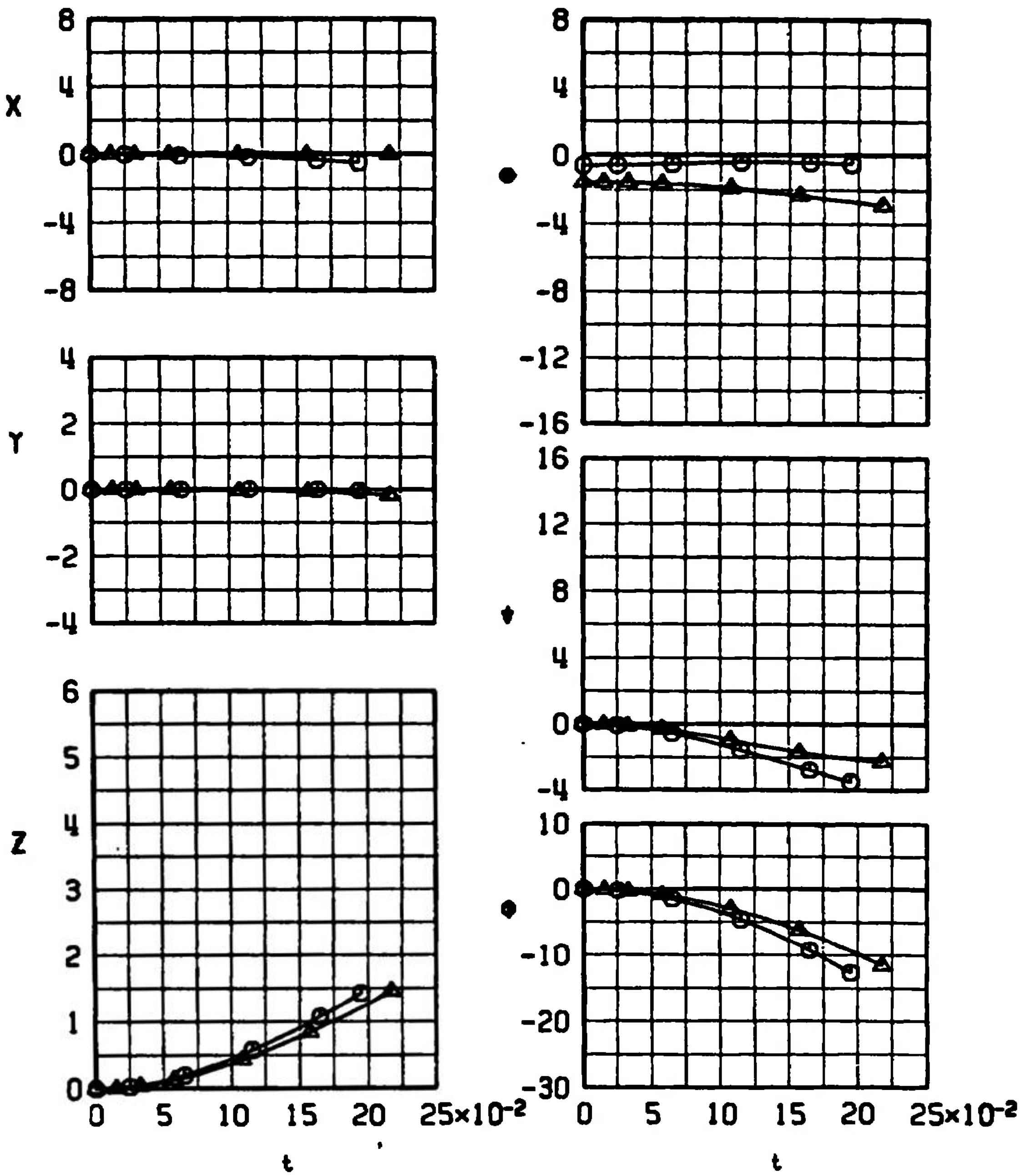

e. Configuration 16, M_∞ = 1.25
Fig. 28 Continued

SYMBOL	M_∞	α_p	γ	A_Z
○	1.60	1.2	0	0
△	1.60	-0.3	60	0

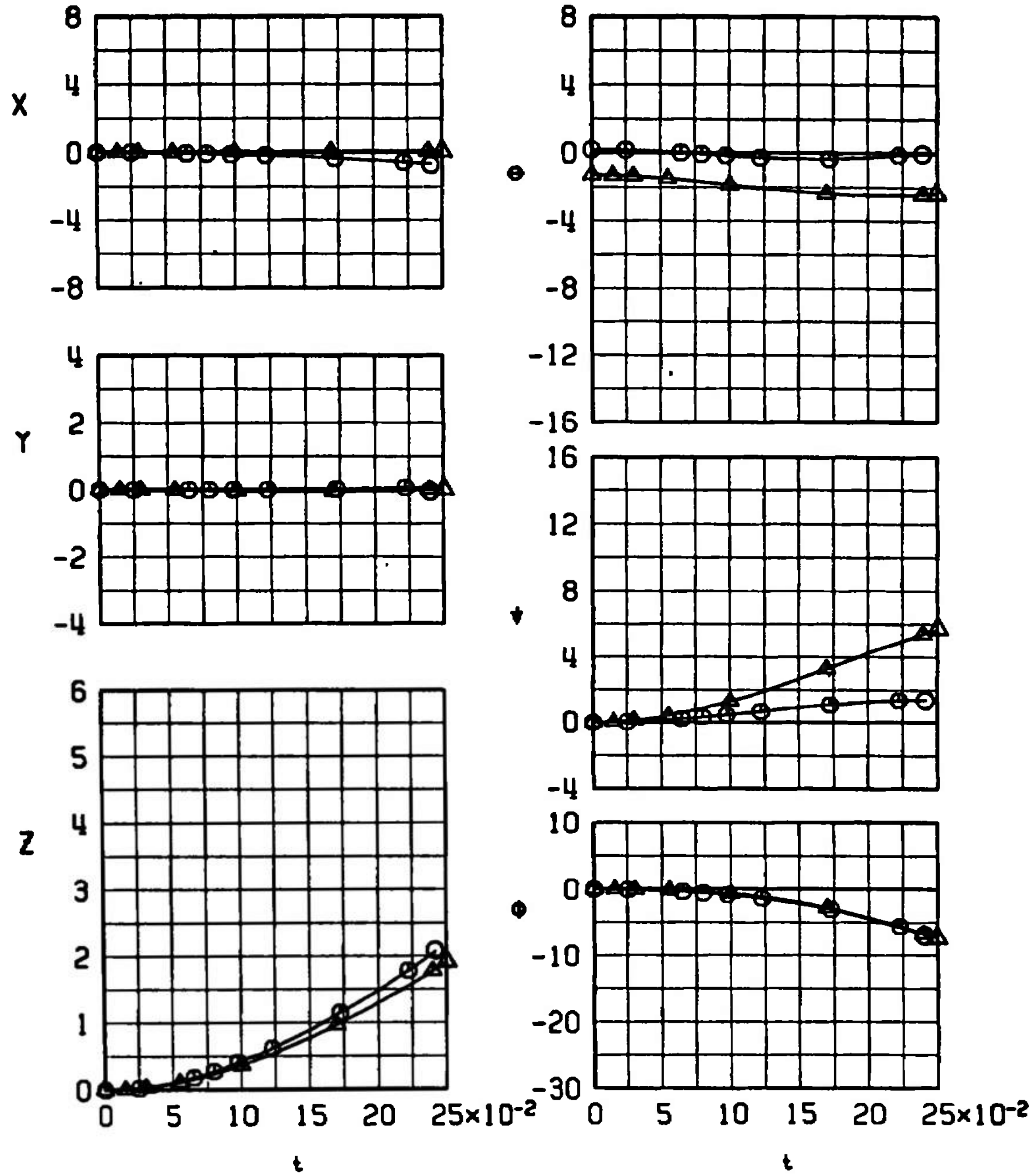

f. Configuration 16, M_∞ = 1.60
Fig. 28 Continued

SYMBOL	M_∞	α_p	γ	A_Z
○	1.05	0	0	0
△	1.05	-0.4	60	0

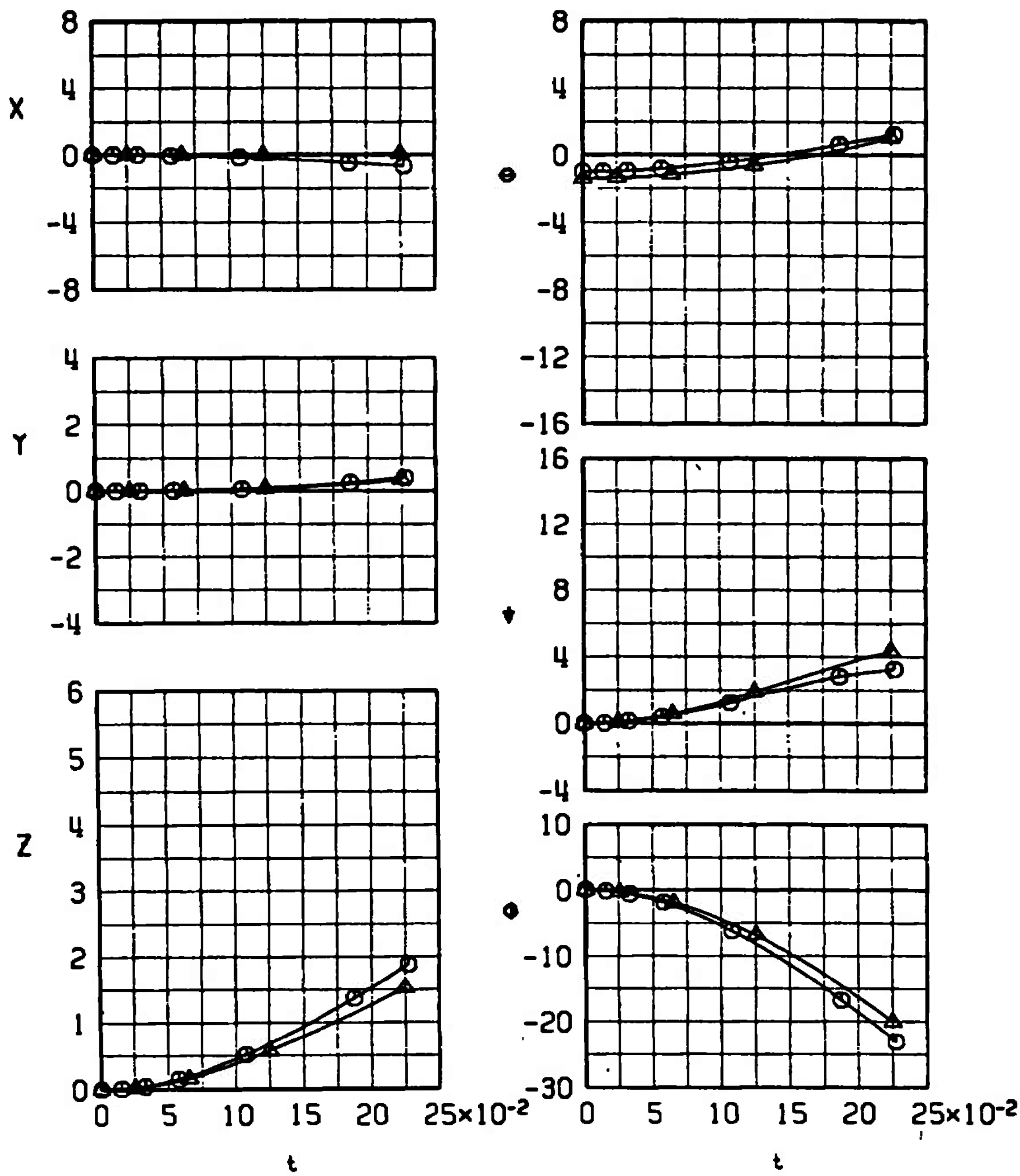

g. Configuration 17, M_∞ = 1.05
Fig. 28 Continued

SYMBOL	M_∞	α_p	γ	A_z
○	1.25	0.4	0	0
△	1.25	-0.6	60	0

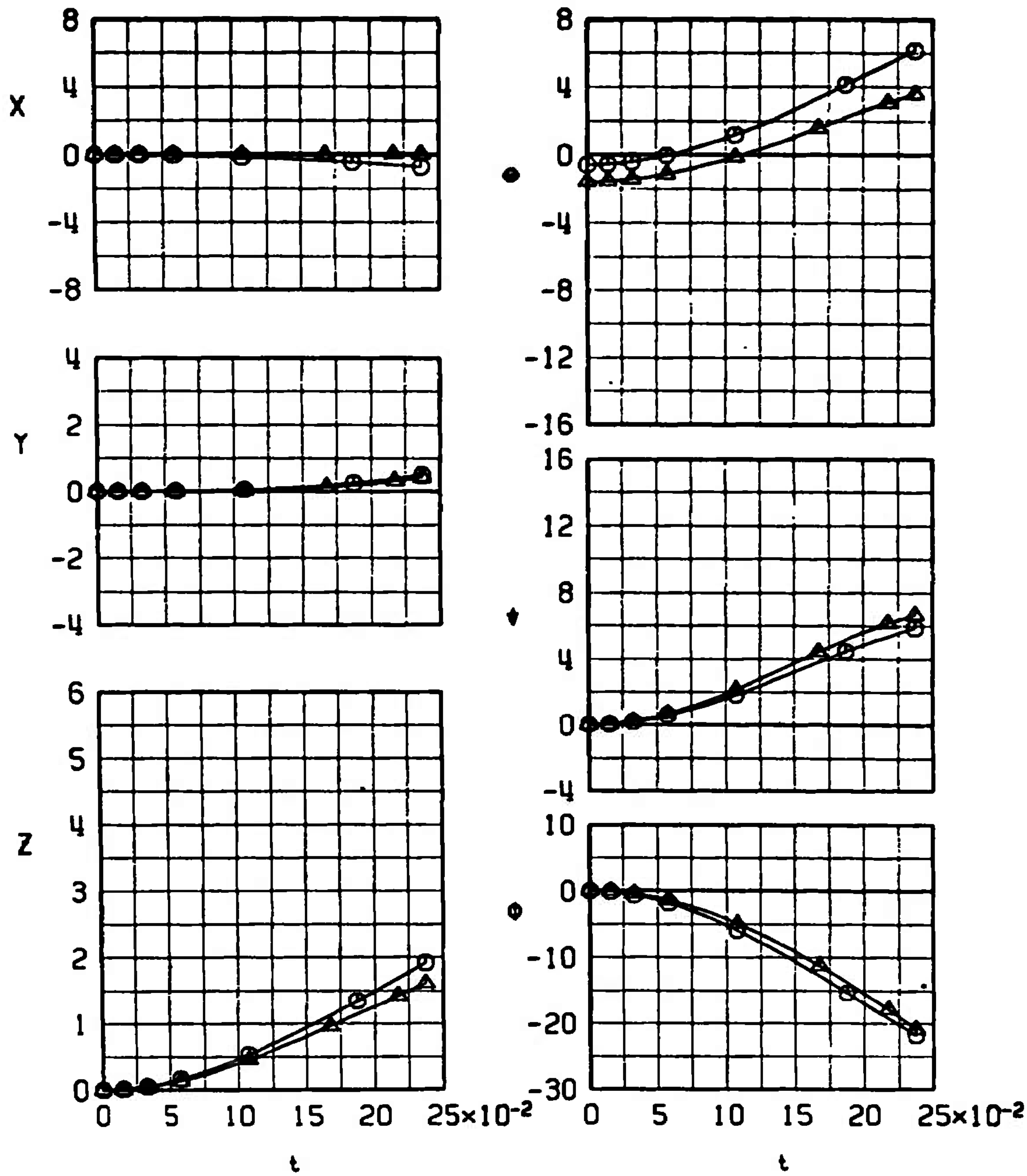

h. Configuration 17, M_∞ = 1.25
Fig. 28 Continued

SYMBOL	M_∞	α_p	γ	A_z
○	1.60	1.2	0	0
△	1.60	-0.3	60	0

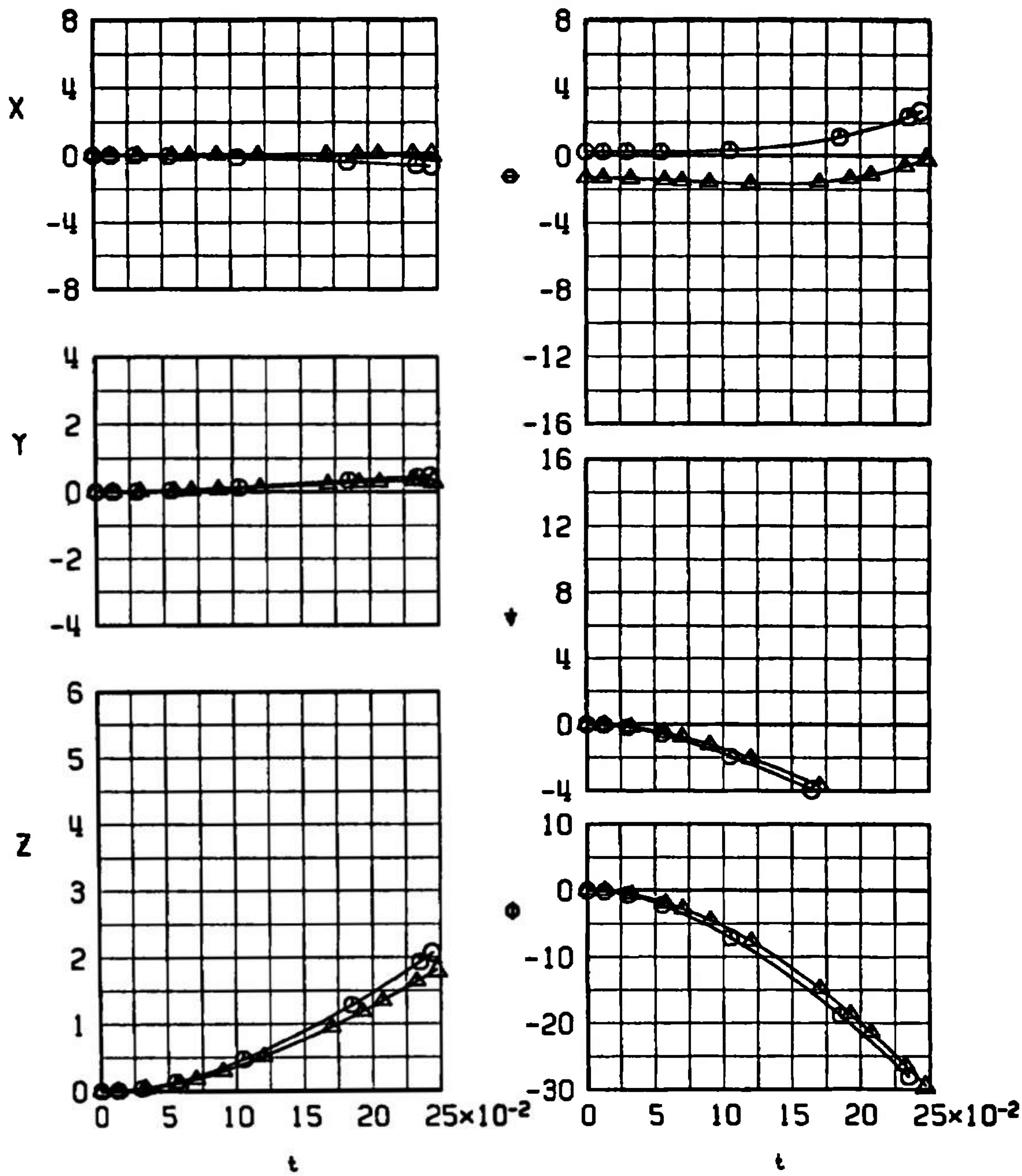

i. Configuration 17, M_∞ = 1.60
Fig. 28 Concluded

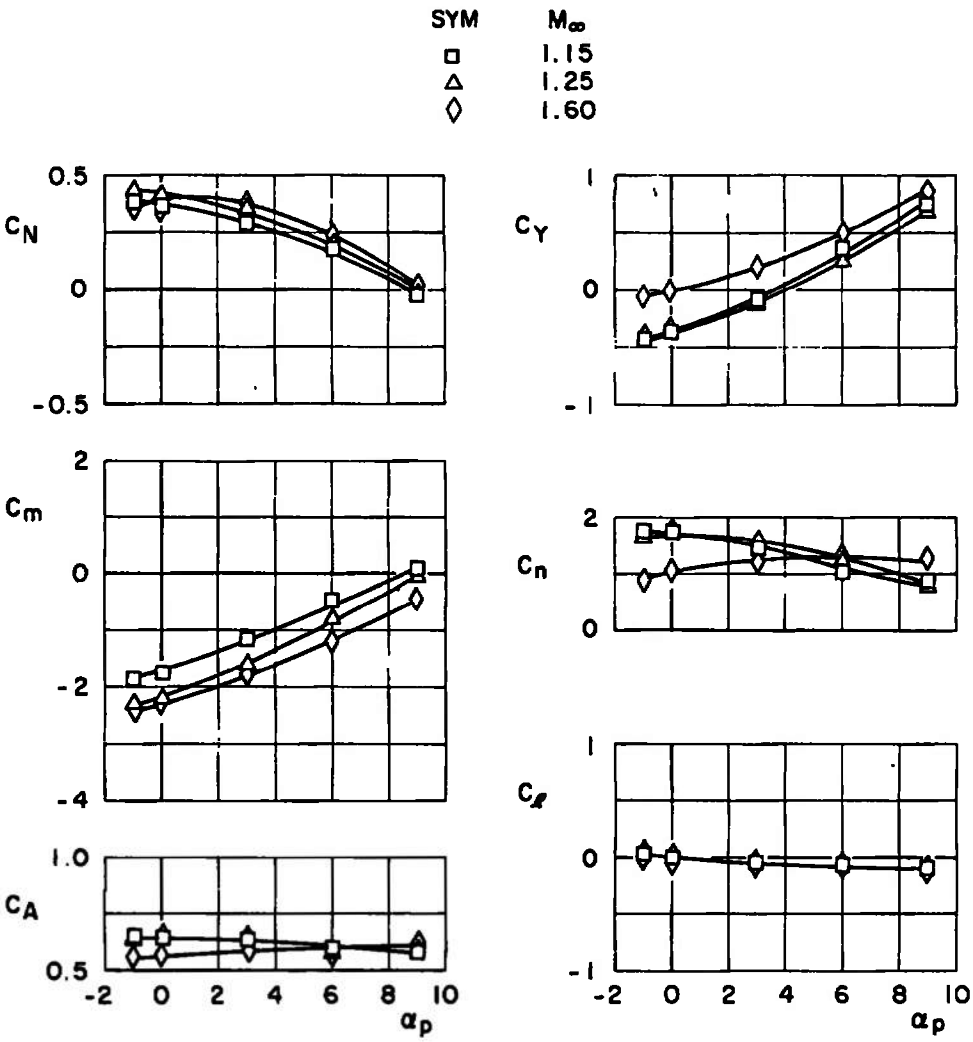

a. MK-84 GPB, Configuration 11

Fig. 29 Variation of the Aerodynamic Coefficients of the MK-84 Stores with Parent Angle of Attack Prior to Launch for Different Mach Numbers

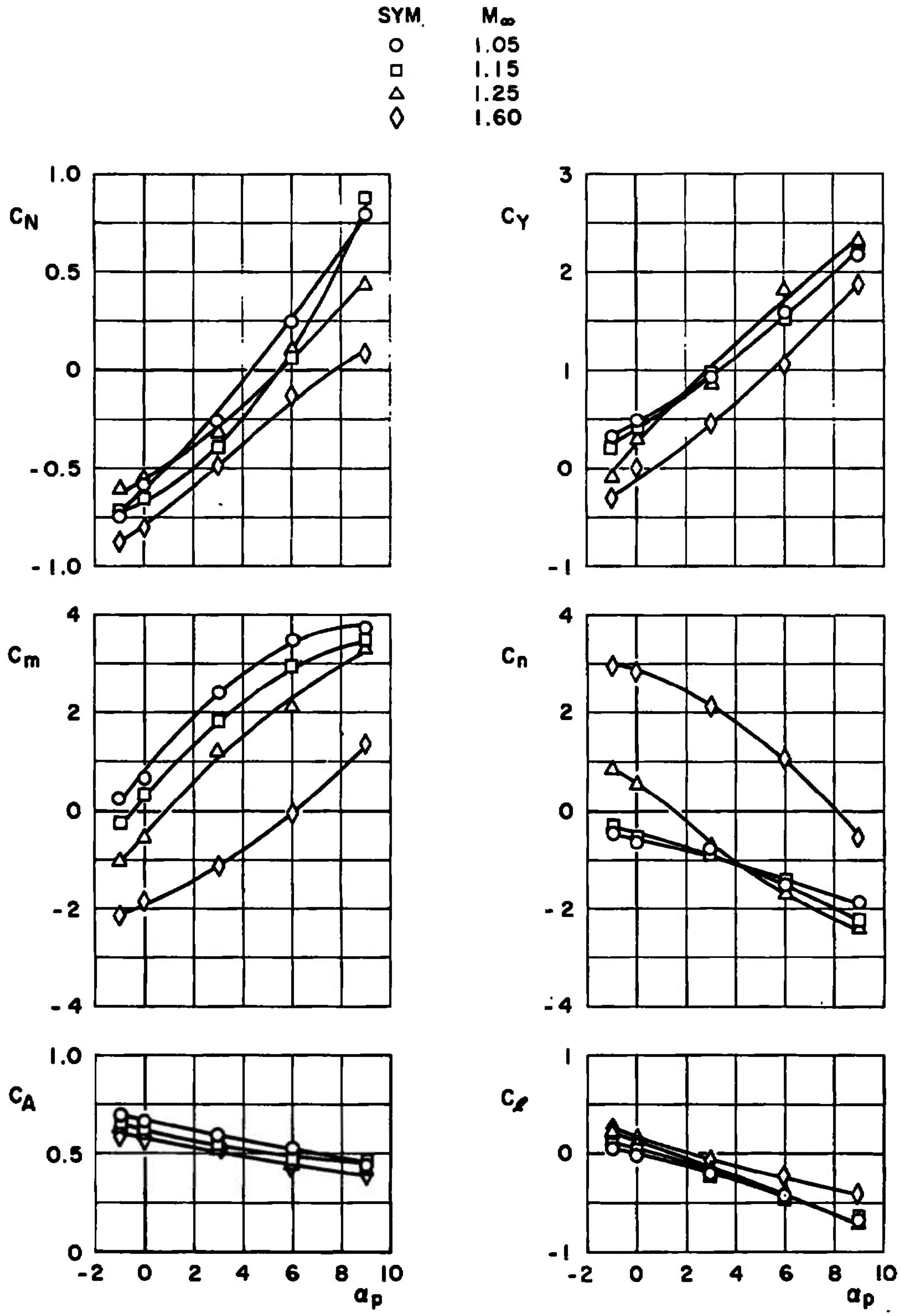

b. MK-84 LGB, Configuration 13
Fig. 29 Continued

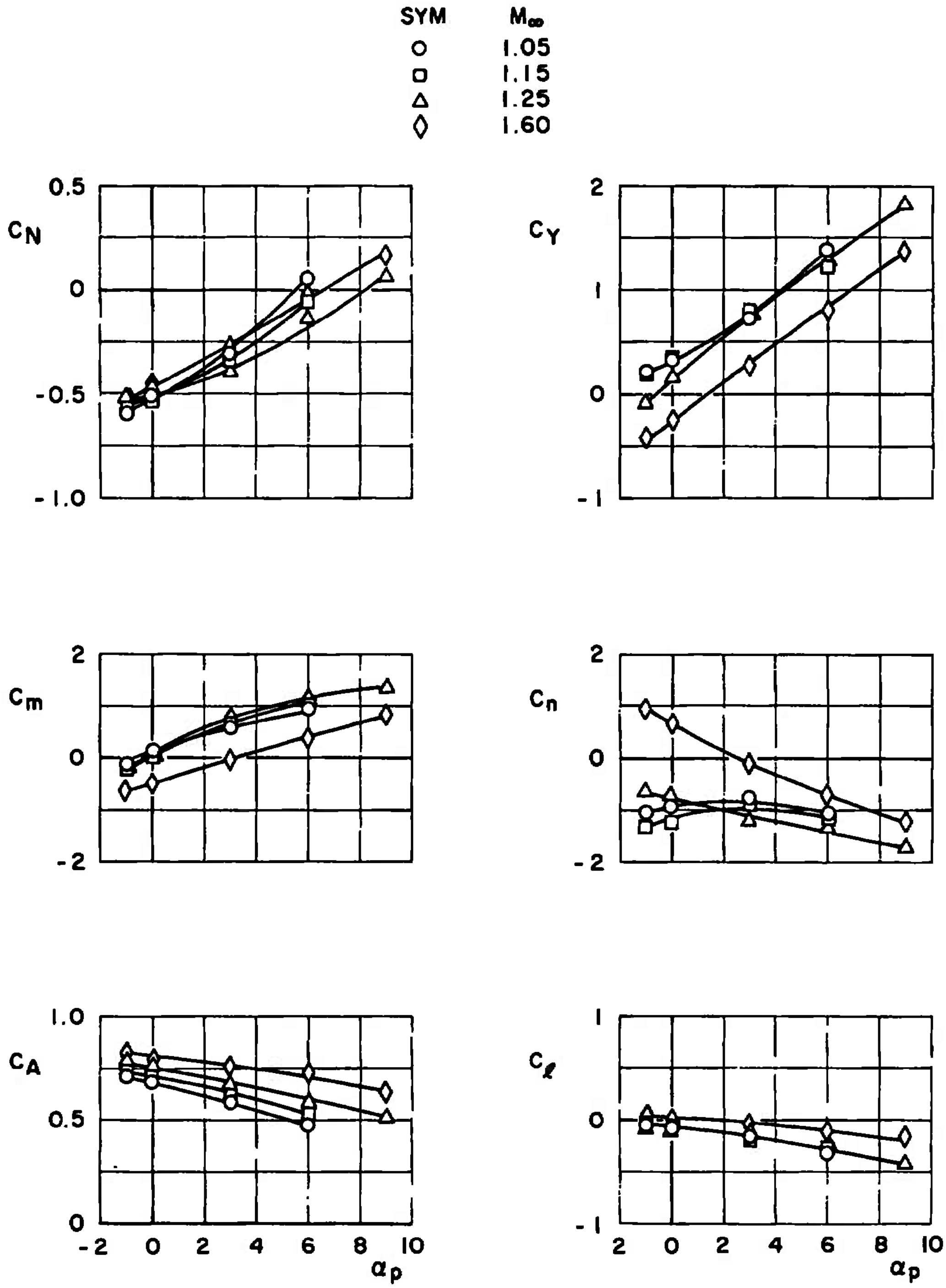

c. MK-84 EOGB, Configuration 16
Fig. 29 Concluded

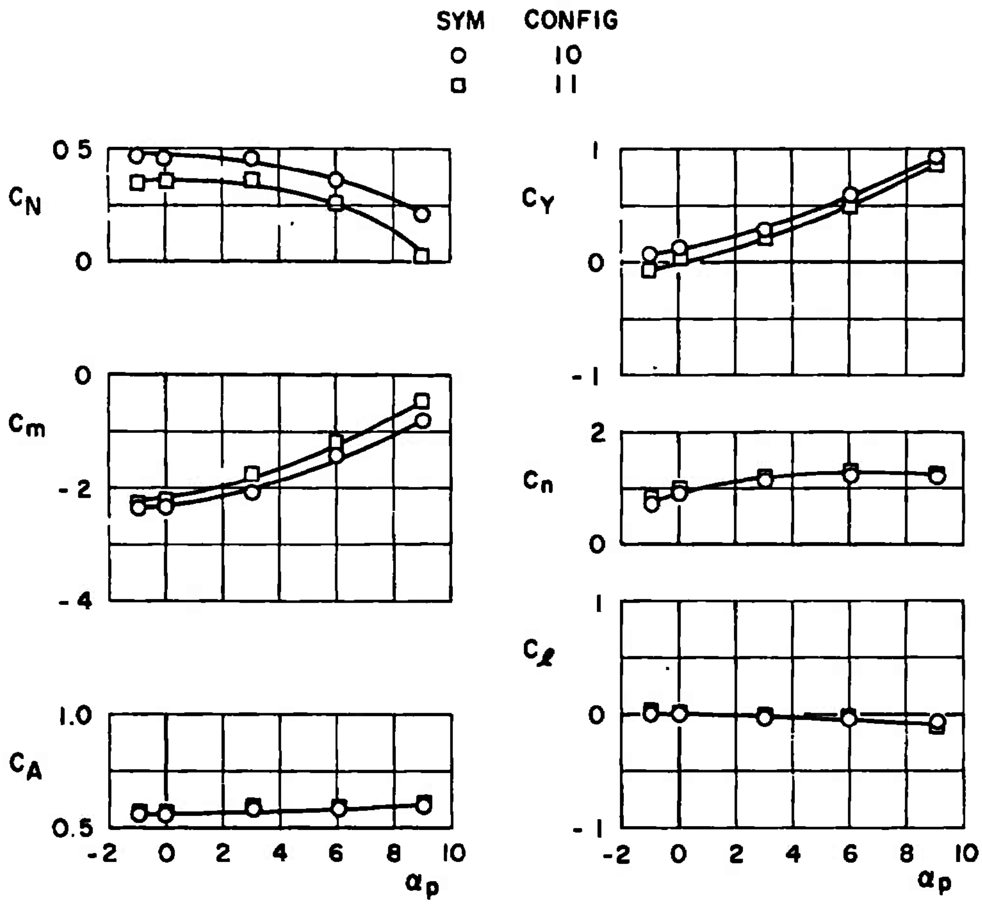

a. MK-84 GPB

Fig. 30 Variation of the Aerodynamic Coefficients of the MK-84 Stores with Parent Angle of Attack Prior to Launch for Different External Store Configurations, $M_\infty = 1.60$

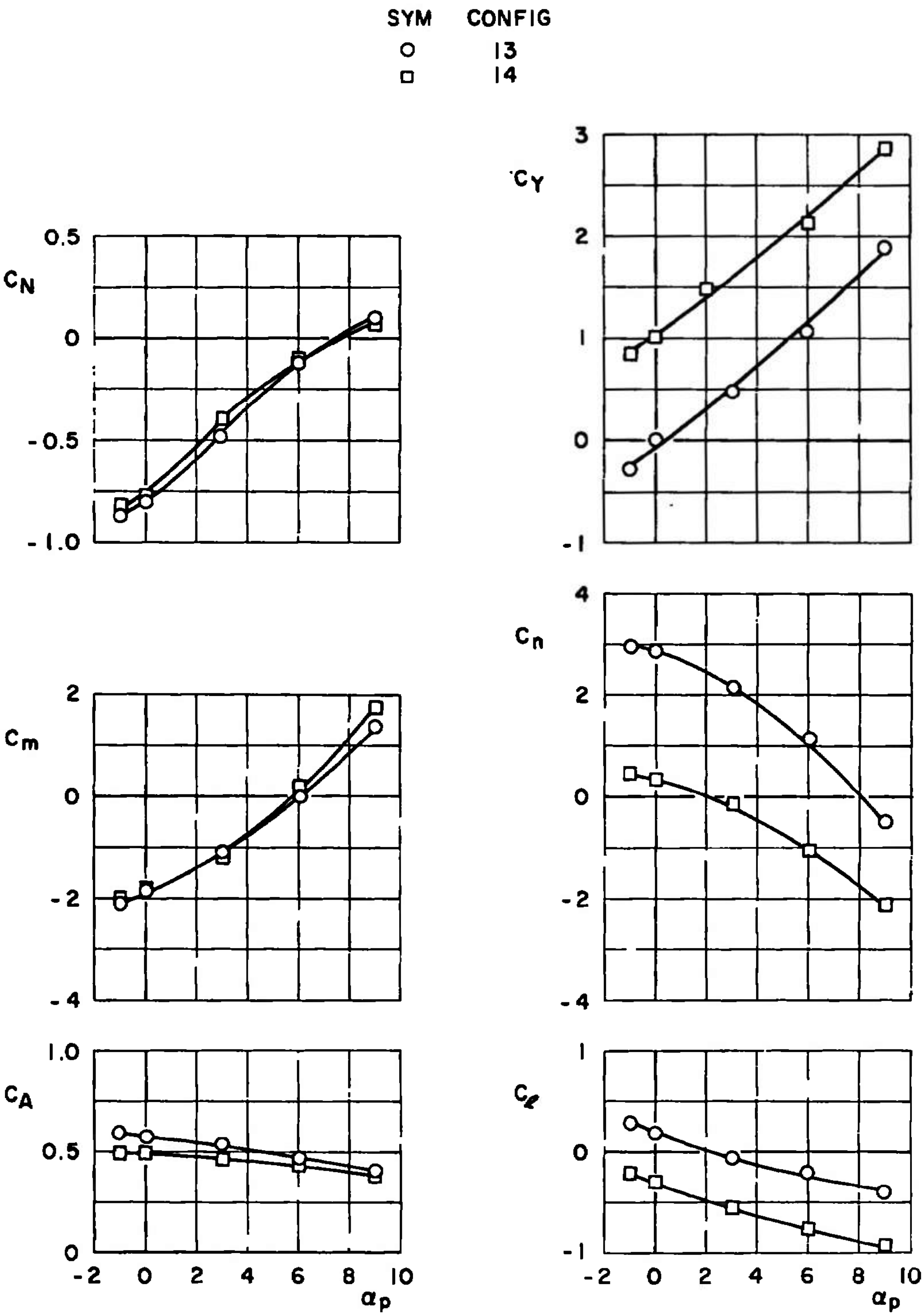

b. MK-84 LGB
Fig. 30 Continued

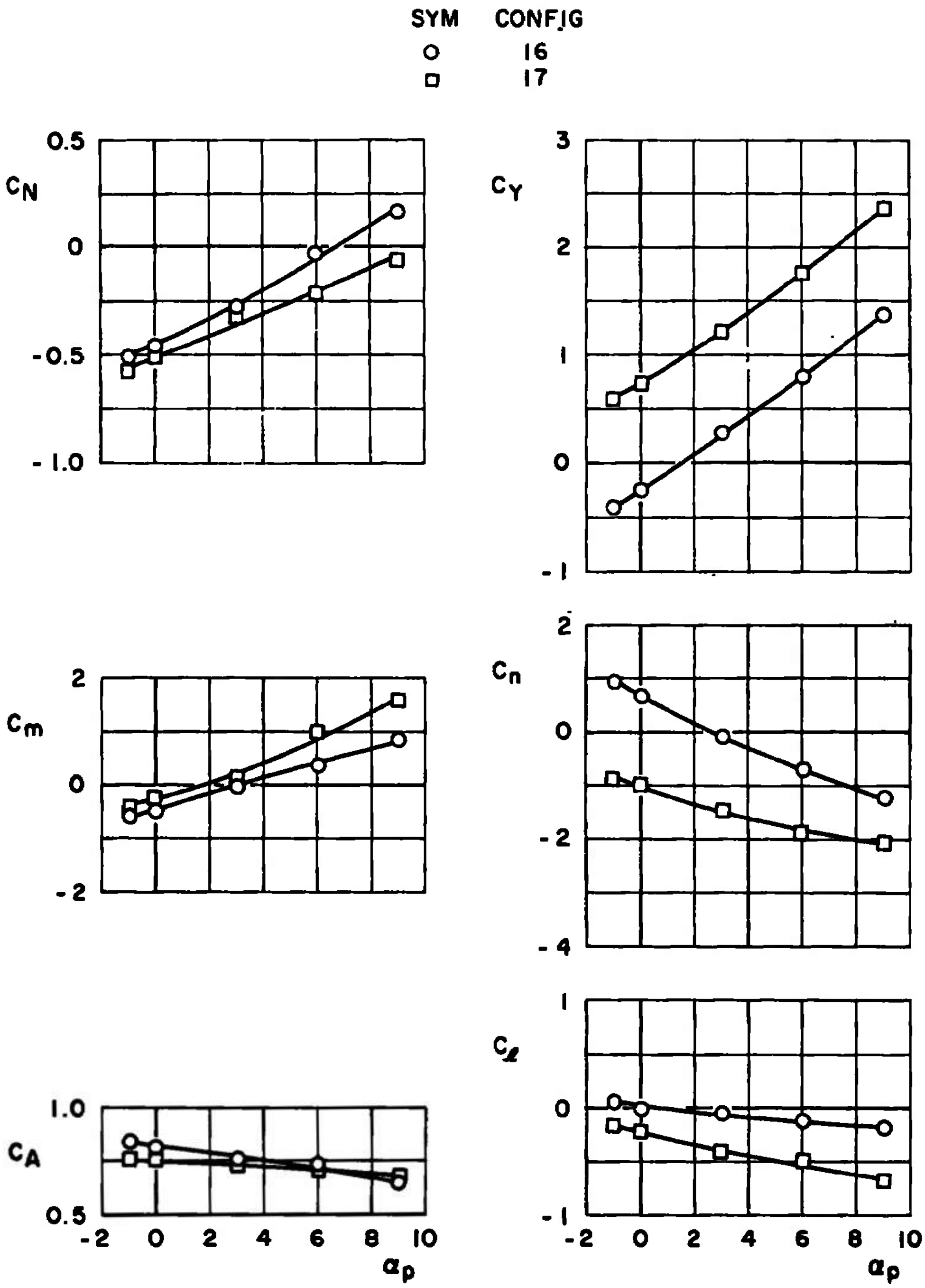

c. MK-84 EOGB
Fig. 30 Concluded

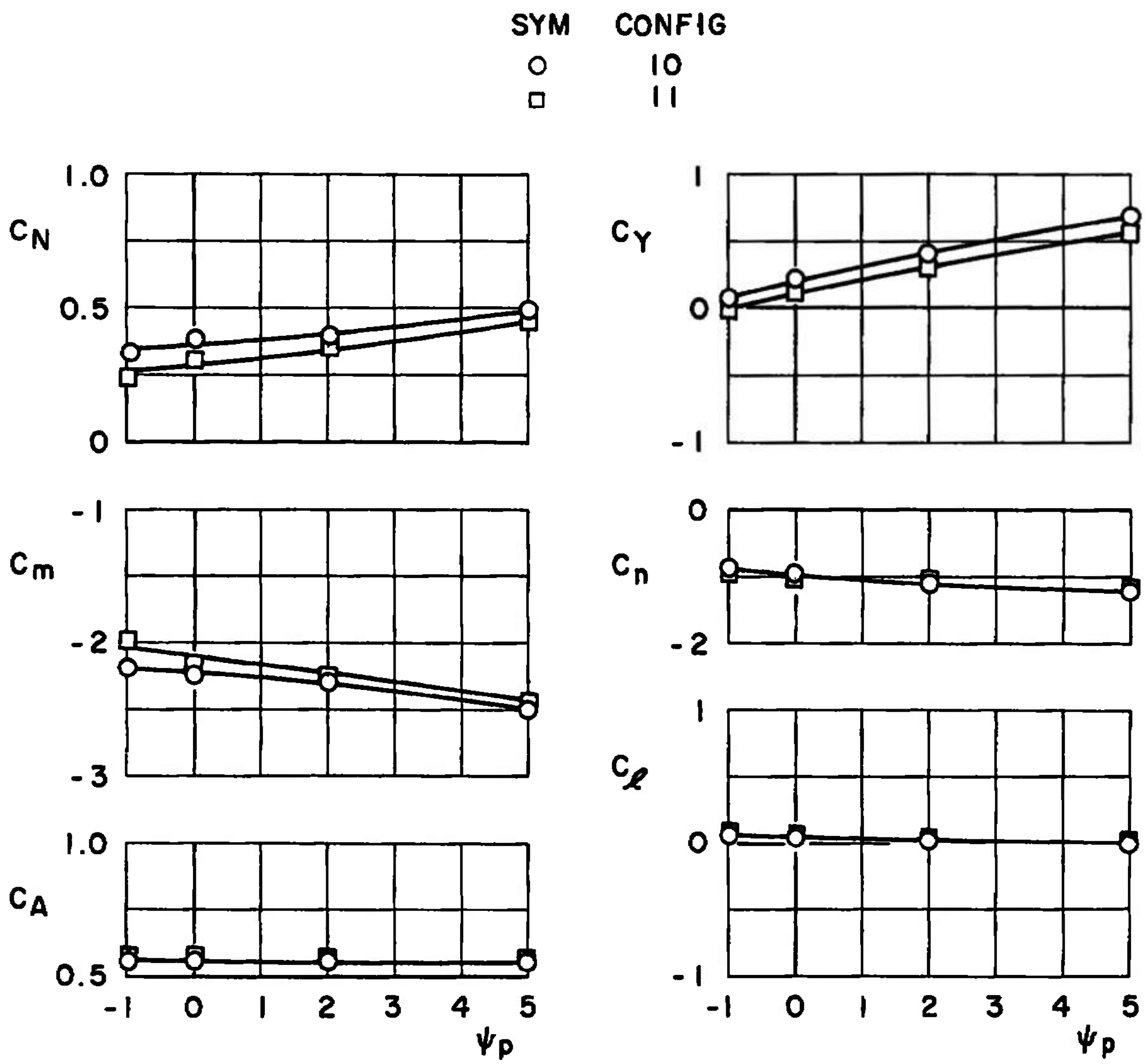

a. MK-84 GPB

Fig. 31 Variation of the Aerodynamic Coefficients of the MK-84 Stores with Parent Angle of Yaw Prior to Launch for Different External Store Configurations, M_∞ = 1.60

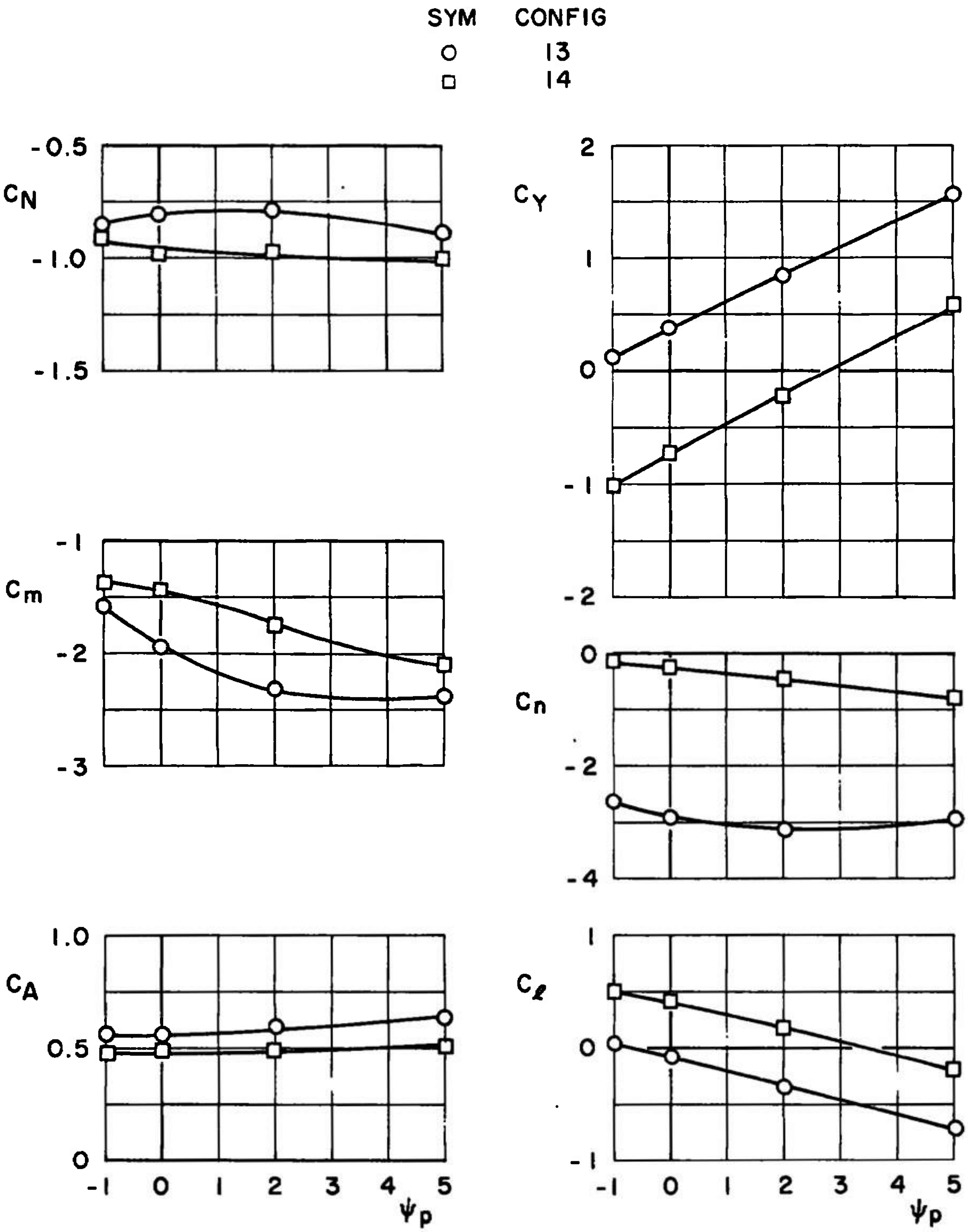

b. MK-84 LGB
Fig. 31 Continued

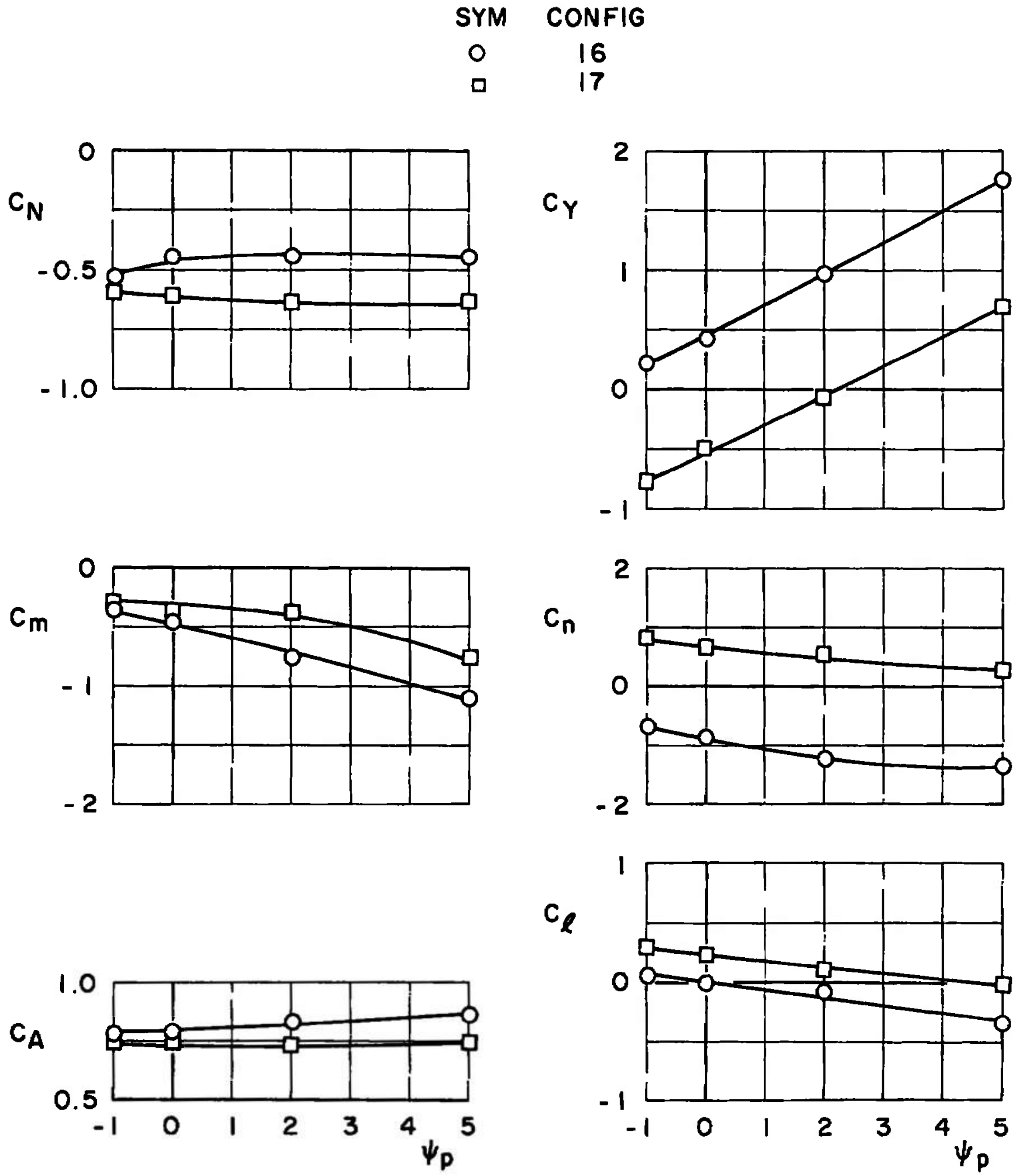

c. MK-84 EOGB
Fig. 31 Concluded

INB'D

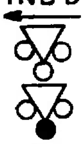

SYMBOL	M_∞	α_p	Λ_{LE}	EJECTOR	CONFIG
●	0.95	1.5	50	1	33
○	0.95	1.5	50	2	33
□	1.05	1.2	50	2	33

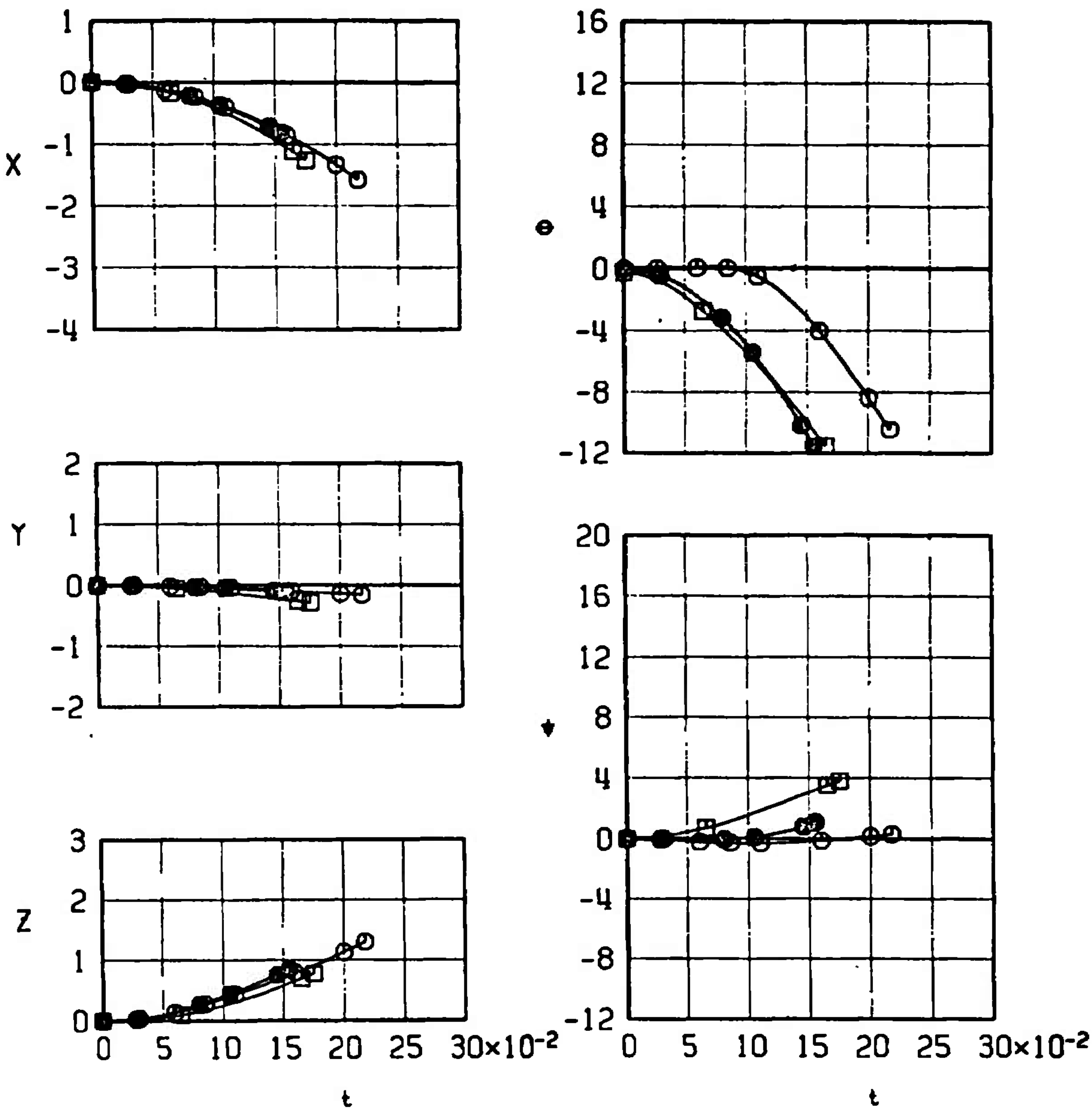

a. Configuration 33

Fig. 32 Mach Number Comparison of the SUU-30H/B Launch Trajectories from the F-111E for Different Ejector Forces, Λ_{LE} = 50 deg

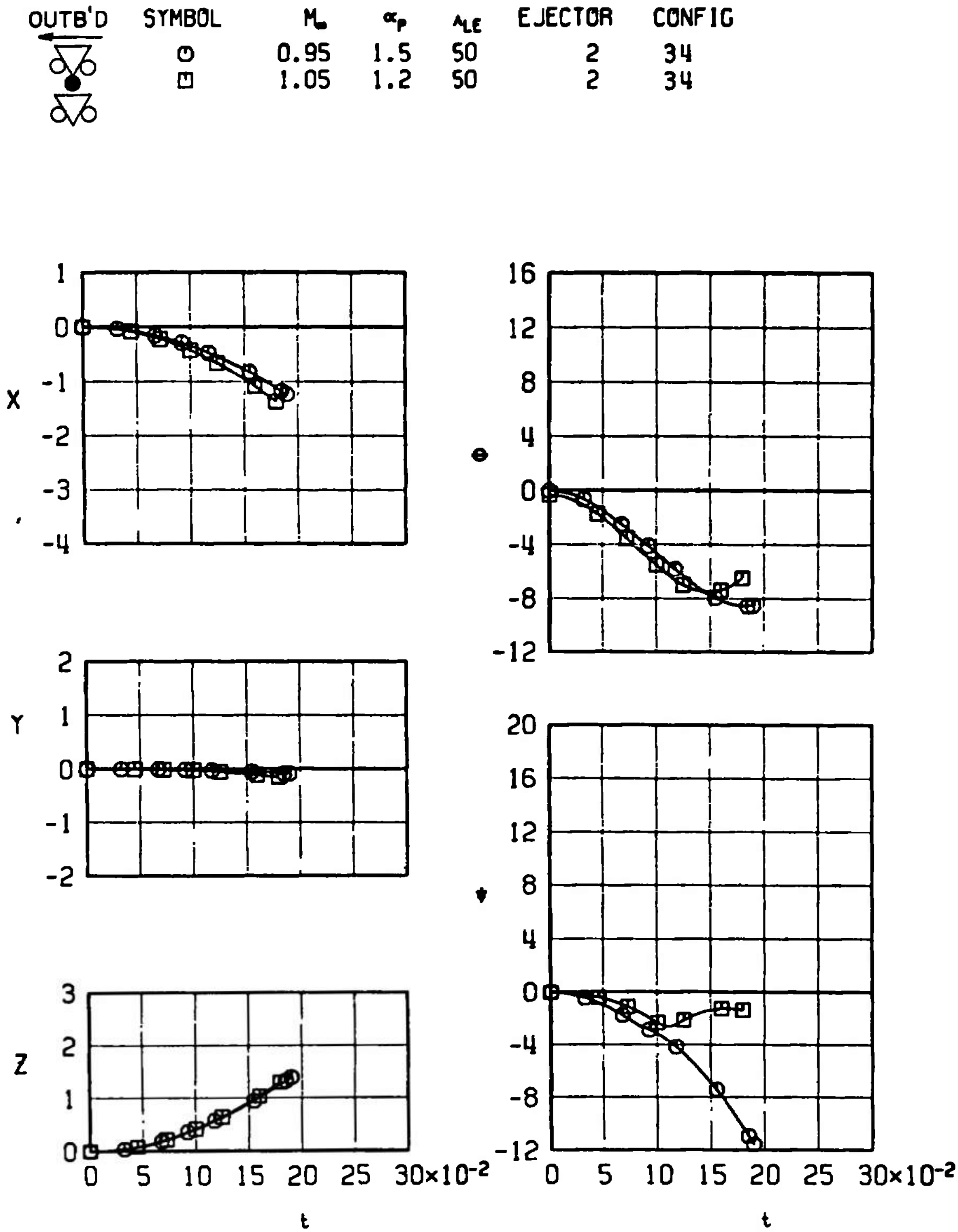

b. Configuration 34
Fig. 32 Continued

OUTB'D	SYMBOL	M_∞	α_p	Λ_{LE}	EJECTOR	CONFIG
	●	0.95	1.5	50	1	31
	○	0.95	1.5	50	2	31
	□	1.05	1.2	50	2	31

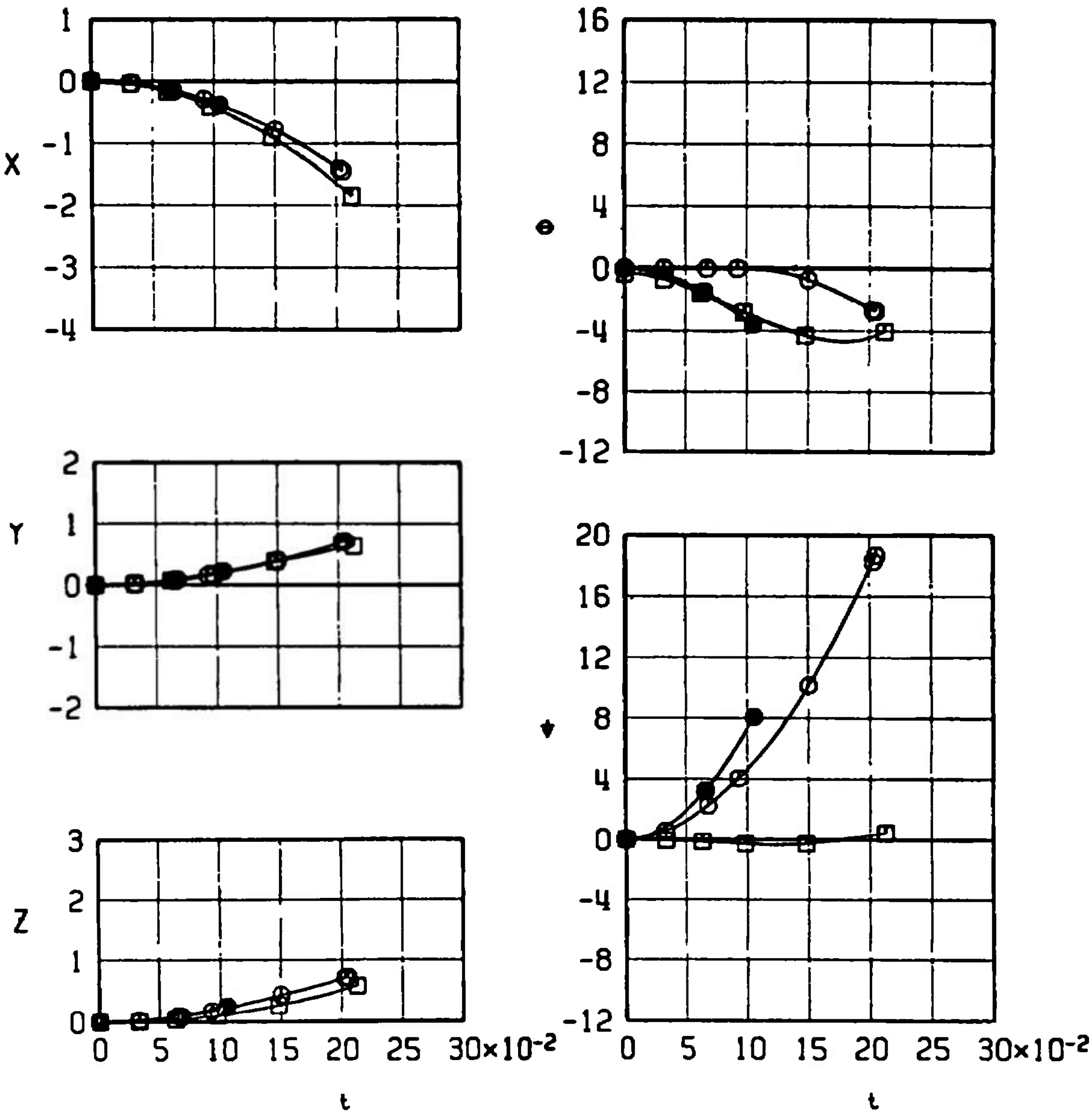

c. Configuration 31
Fig. 32 Continued

INB'D	SYMBOL	M_∞	α_p	Λ_{LE}	EJECTOR	CONFIG
	●	0.95	1.5	50	1	29
	○	0.95	1.5	50	2	29
	□	1.05	1.2	50	2	29

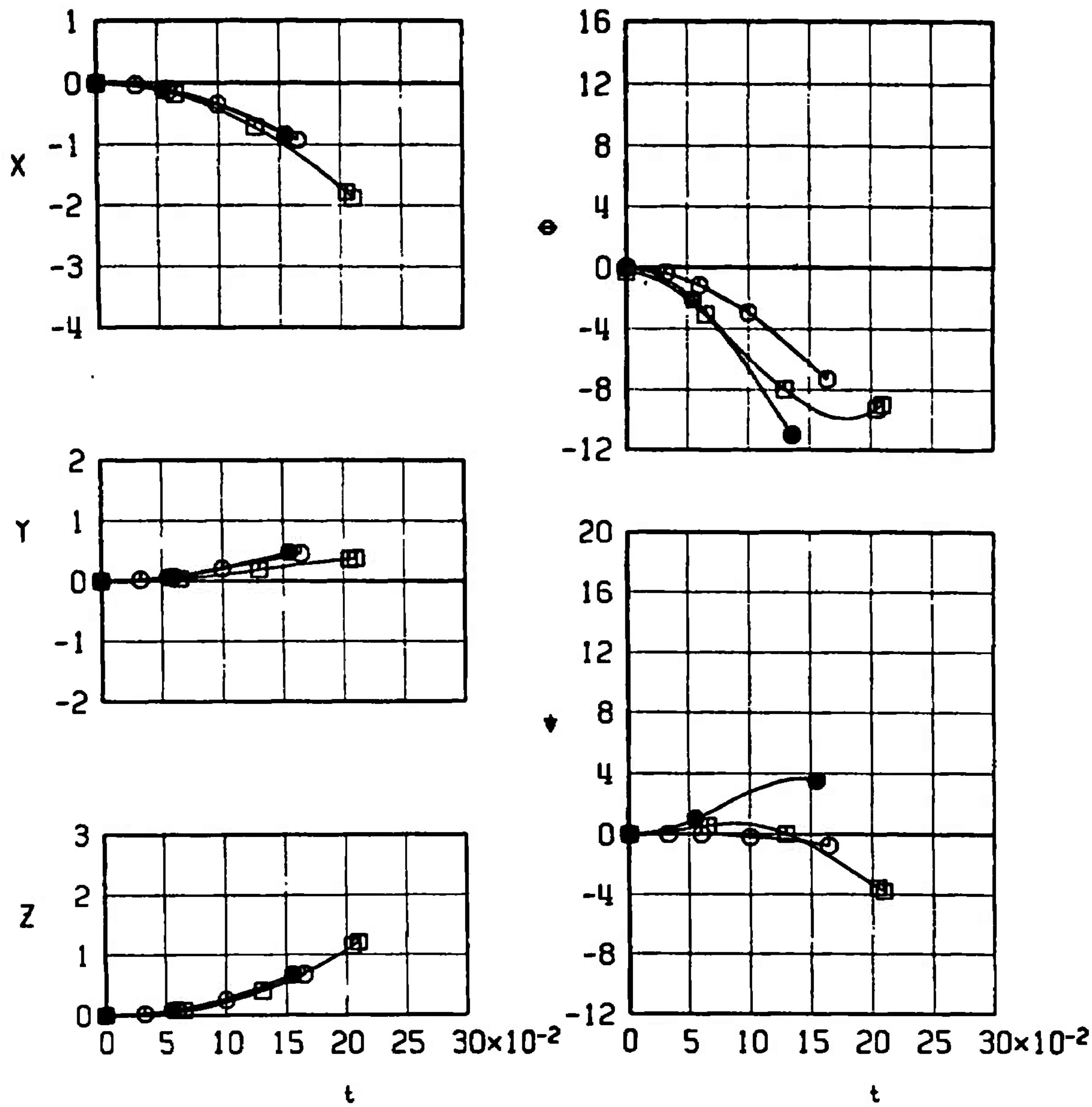

d. Configuration 29
Fig. 32 Continued

OUTB'D	SYMBOL	M_∞	α_p	Λ_{LE}	EJECTOR	CONFIG
	○	0.95	1.5	50	1	30
	□	1.05	1.2	50	1	30

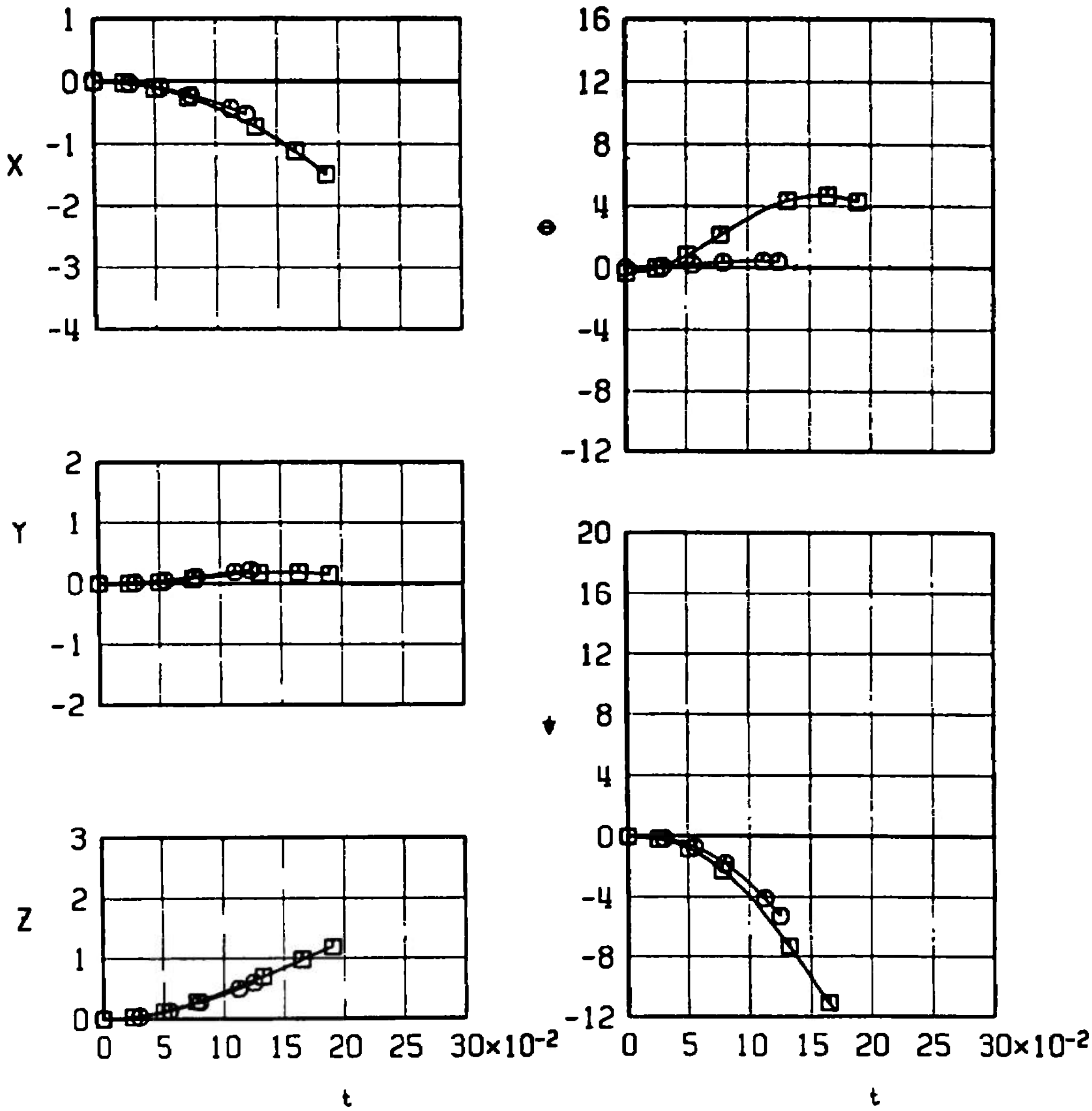

e. Configuration 30
Fig. 32 Continued

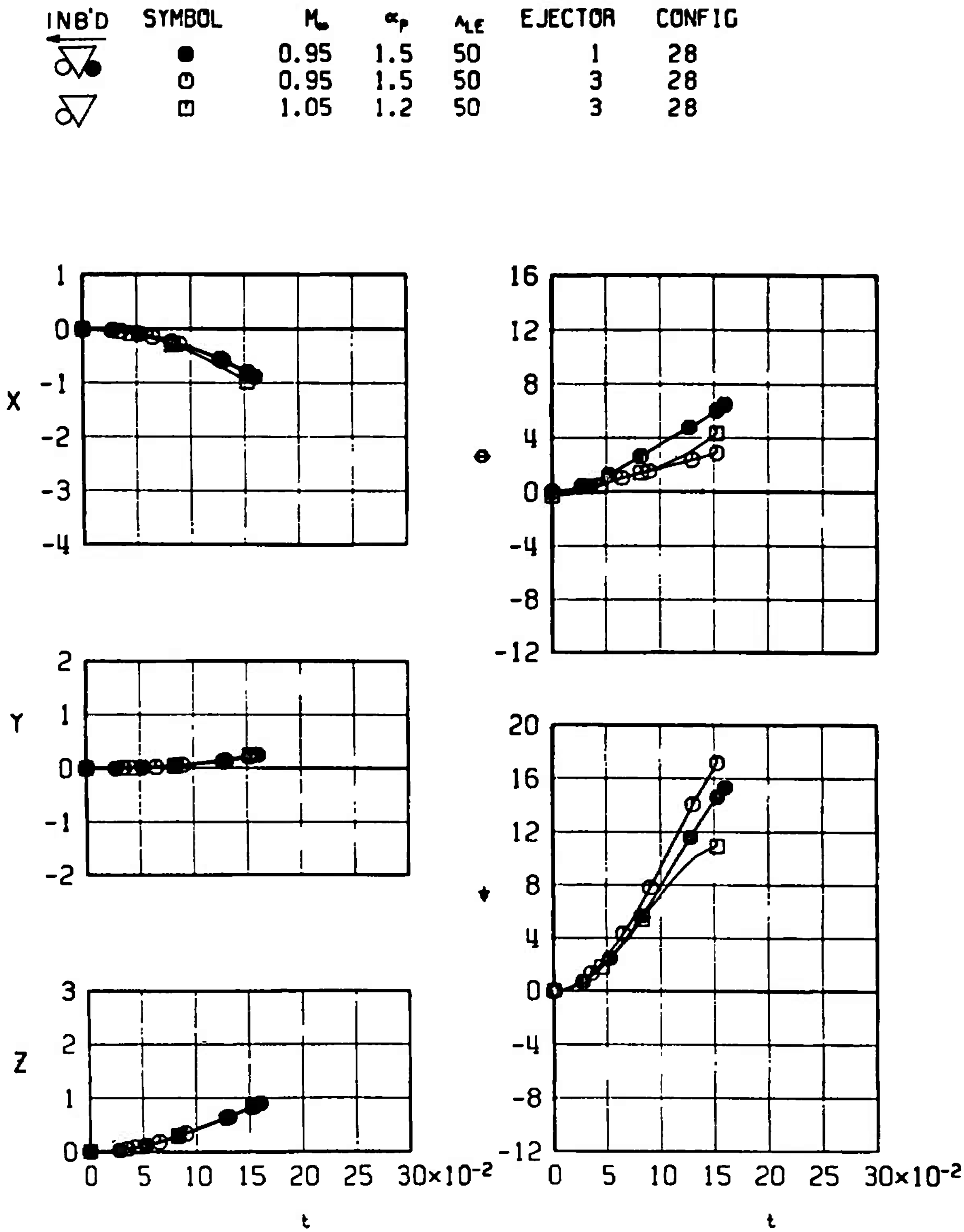

f. Configuration 28
Fig. 32 Continued

OUTB'D	SYMBOL	M_∞	α_p	Λ_{LE}	EJECTOR	CONFIG
	●	0.90	1.6	50	1	32
	△	0.90	1.6	50	2	32
	□	1.05	1.2	50	2	32

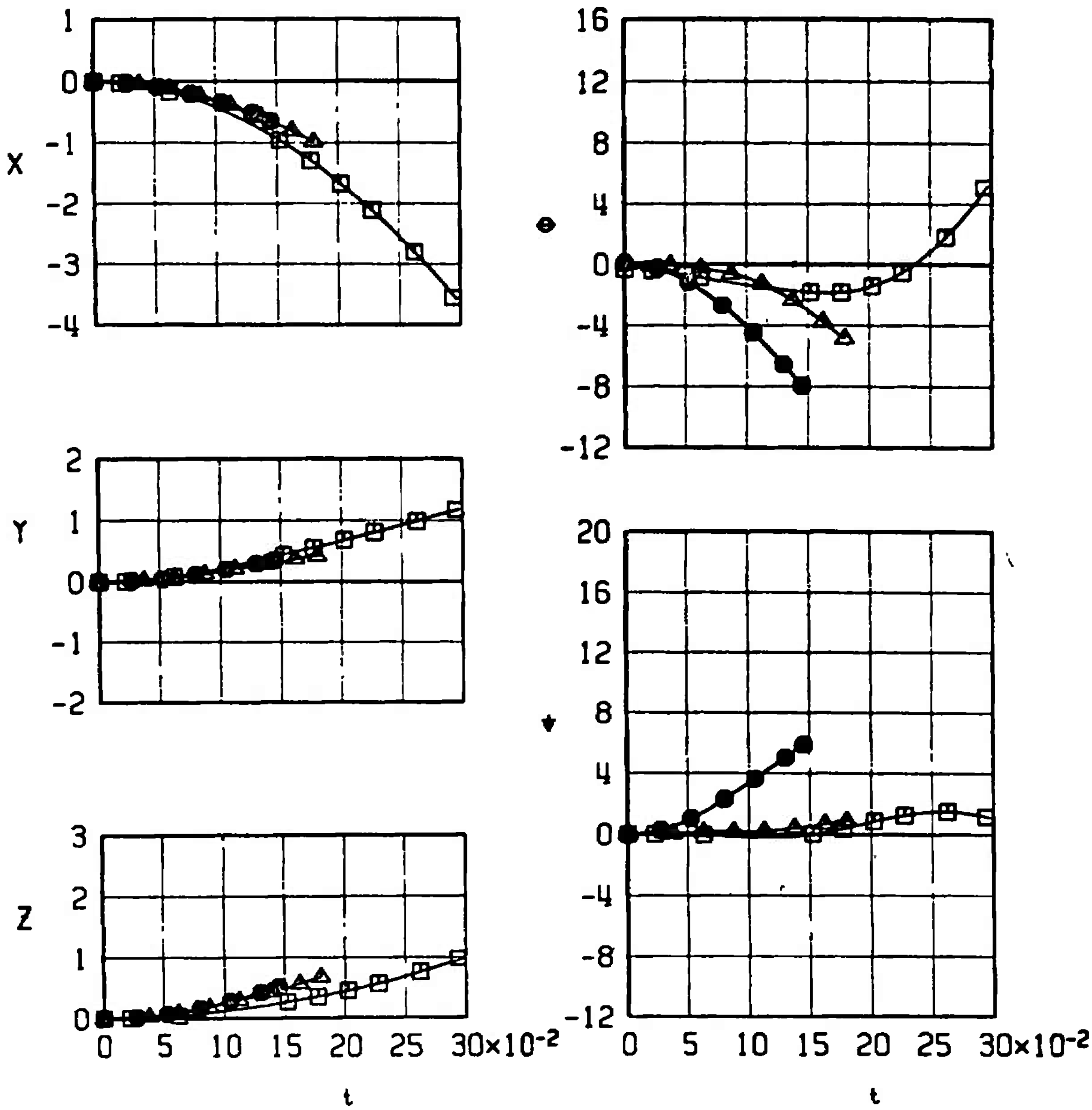

g. Configuration 32
Fig. 32 Continued

INB'D	SYMBOL	M_∞	α_p	Λ_{LE}	EJECTOR	CONFIG
	△	0.90	1.6	50	1	25
	□	1.05	1.2	50	1	25

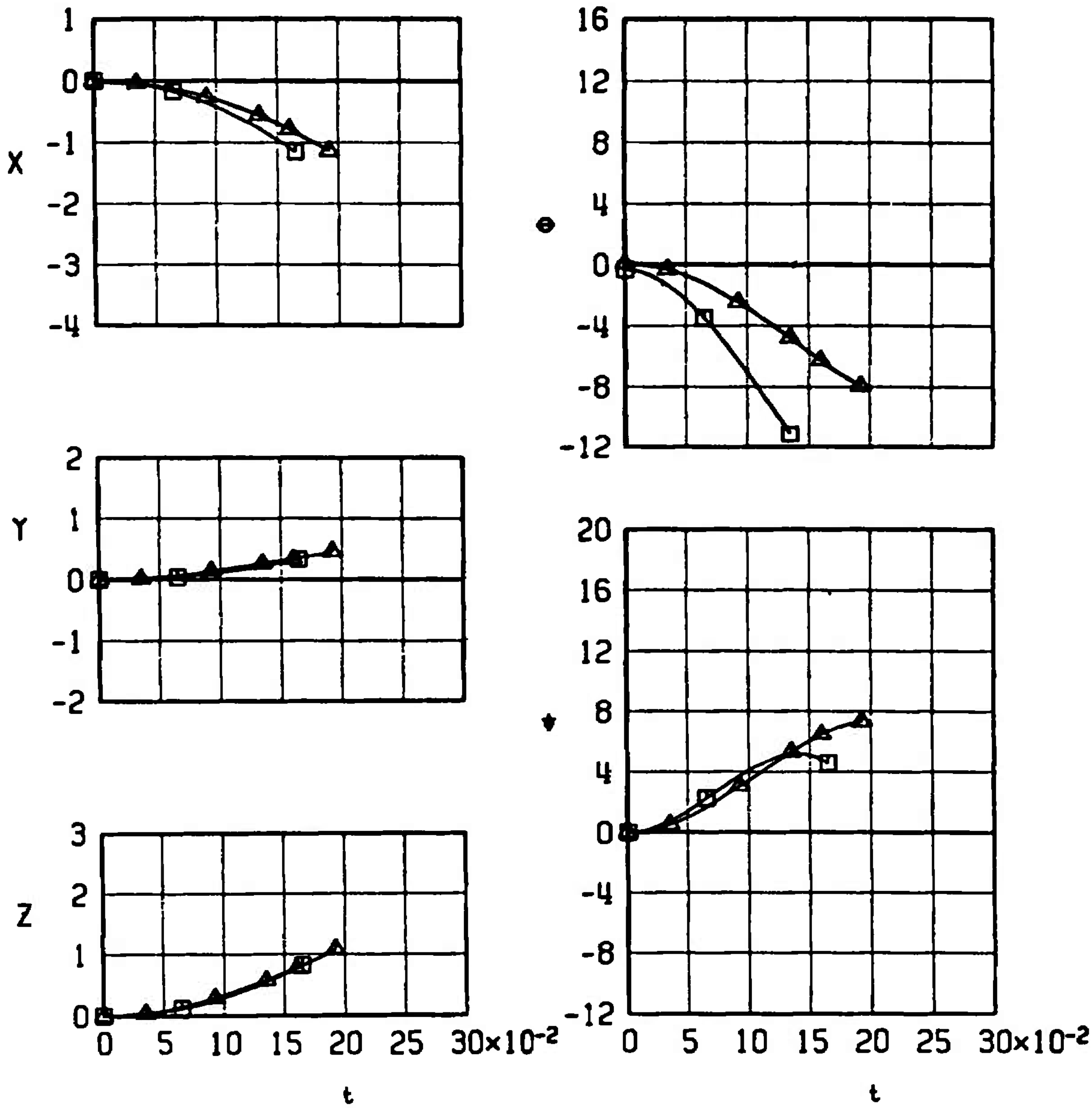

h. Configuration 25
Fig. 32 Continued

OUTB'D	SYMBOL	M_∞	α_p	Λ_{LE}	EJECTOR	CONFIG
	●	0.95	1.5	50	3	24
	○	0.95	1.5	50	1	24
	□	1.05	1.2	50	1	24

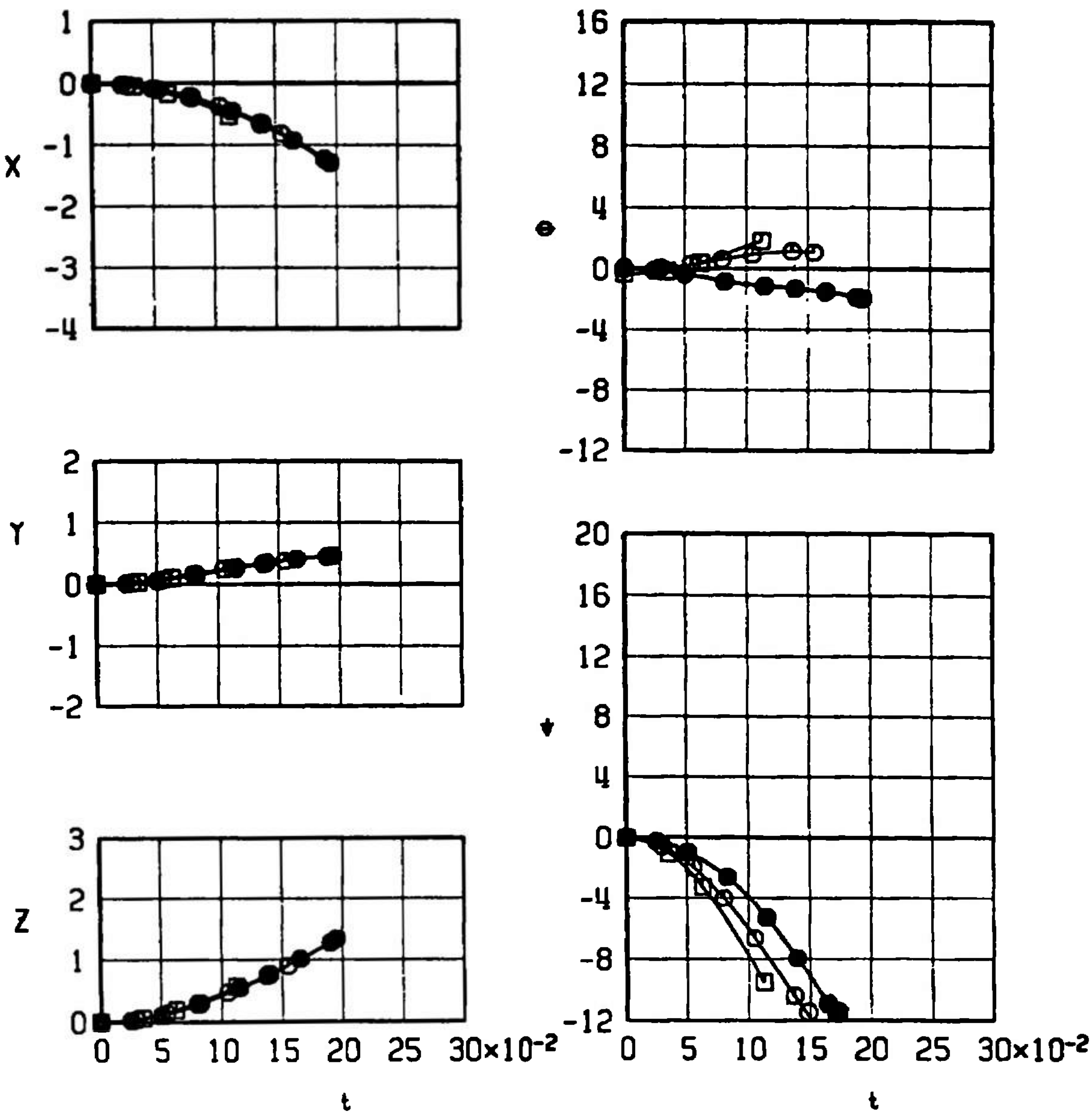

i. Configuration 24
Fig. 32 Continued

INB'D	SYMBOL	M_∞	α_p	Λ_{LE}	EJECTOR	CONFIG
▽●	○	0.95	1.5	50	1	23
	□	1.05	1.2	50	1	23
▽	●	0.95	1.5	50	3	23
	■	1.05	1.2	50	3	23

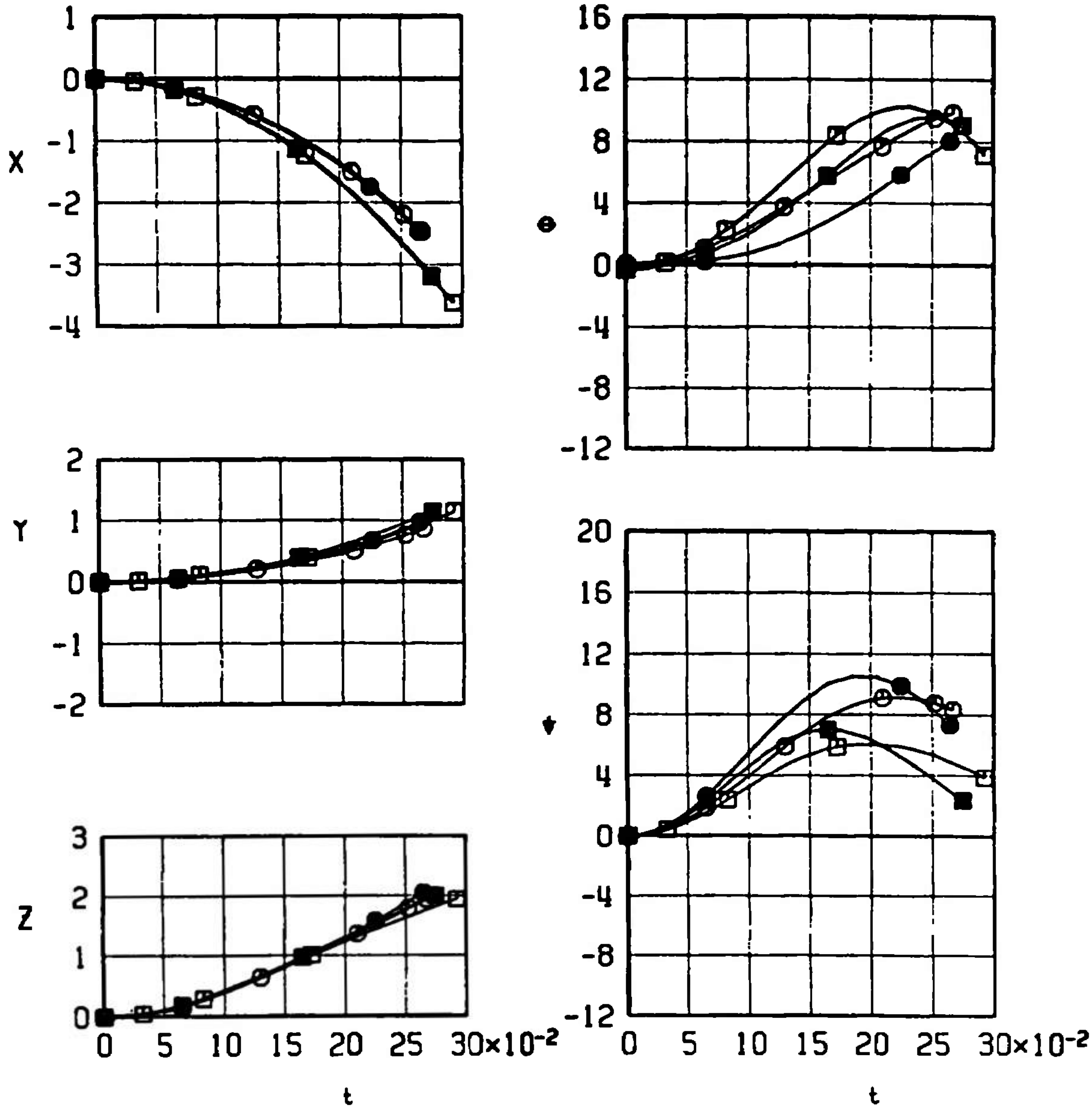

j. Configuration 23
Fig. 32 Continued

SYMBOL	M_∞	α_p	Λ_{LE}	EJECTOR	CONFIG
△	0.90	1.6	50	1	21
◁	1.20	1.4	50	1	21
✦	1.30	1.4	50	1	21

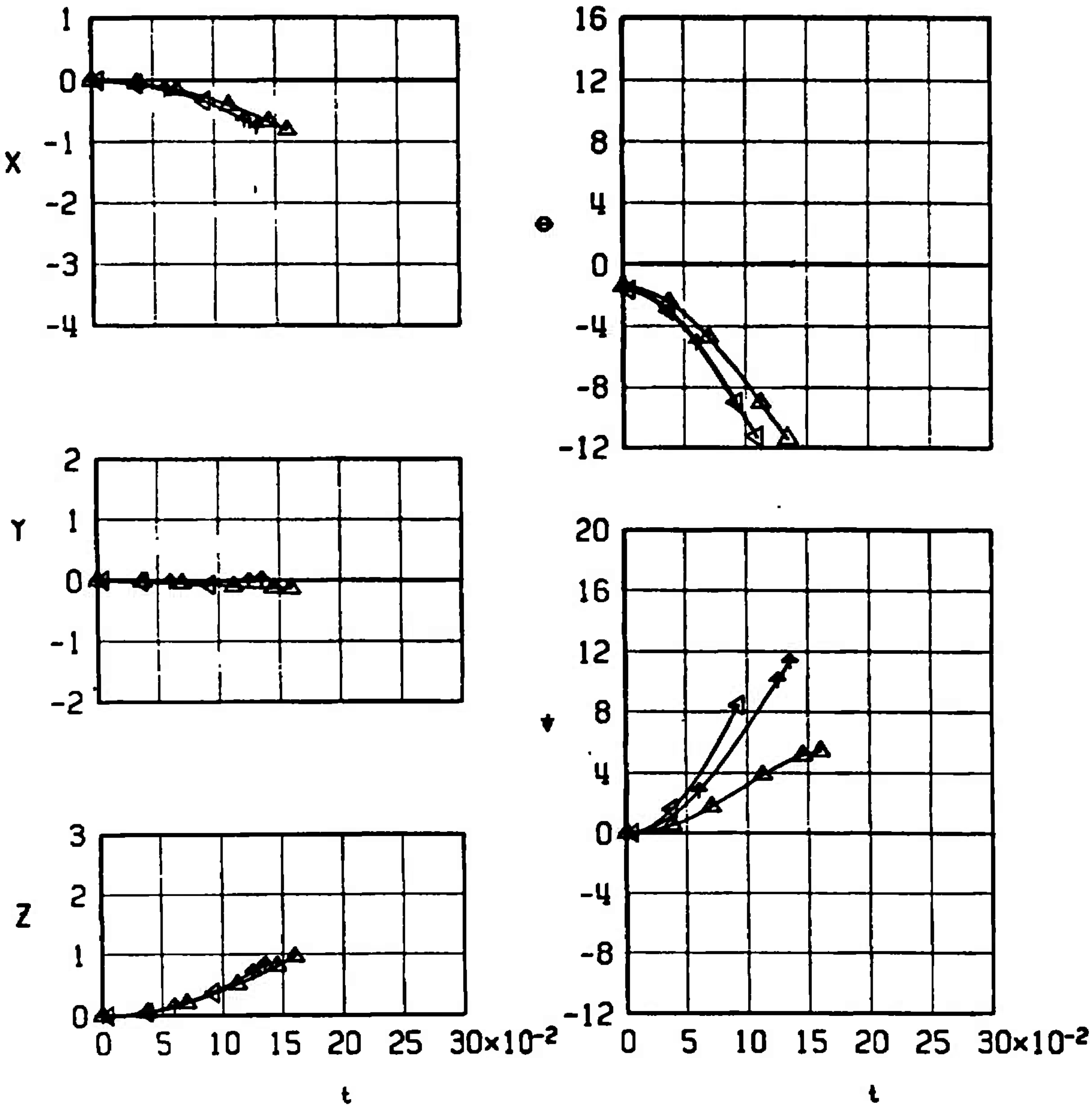

k. Configuration 21, Ejector 1
Fig. 32 Continued

SYMBOL	M_∞	α_p	Λ_{LE}	EJECTOR	CONFIG
△	0.90	1.6	50	2	21
□	1.05	1.2	50	2	21
◇	1.15	1.3	50	2	21

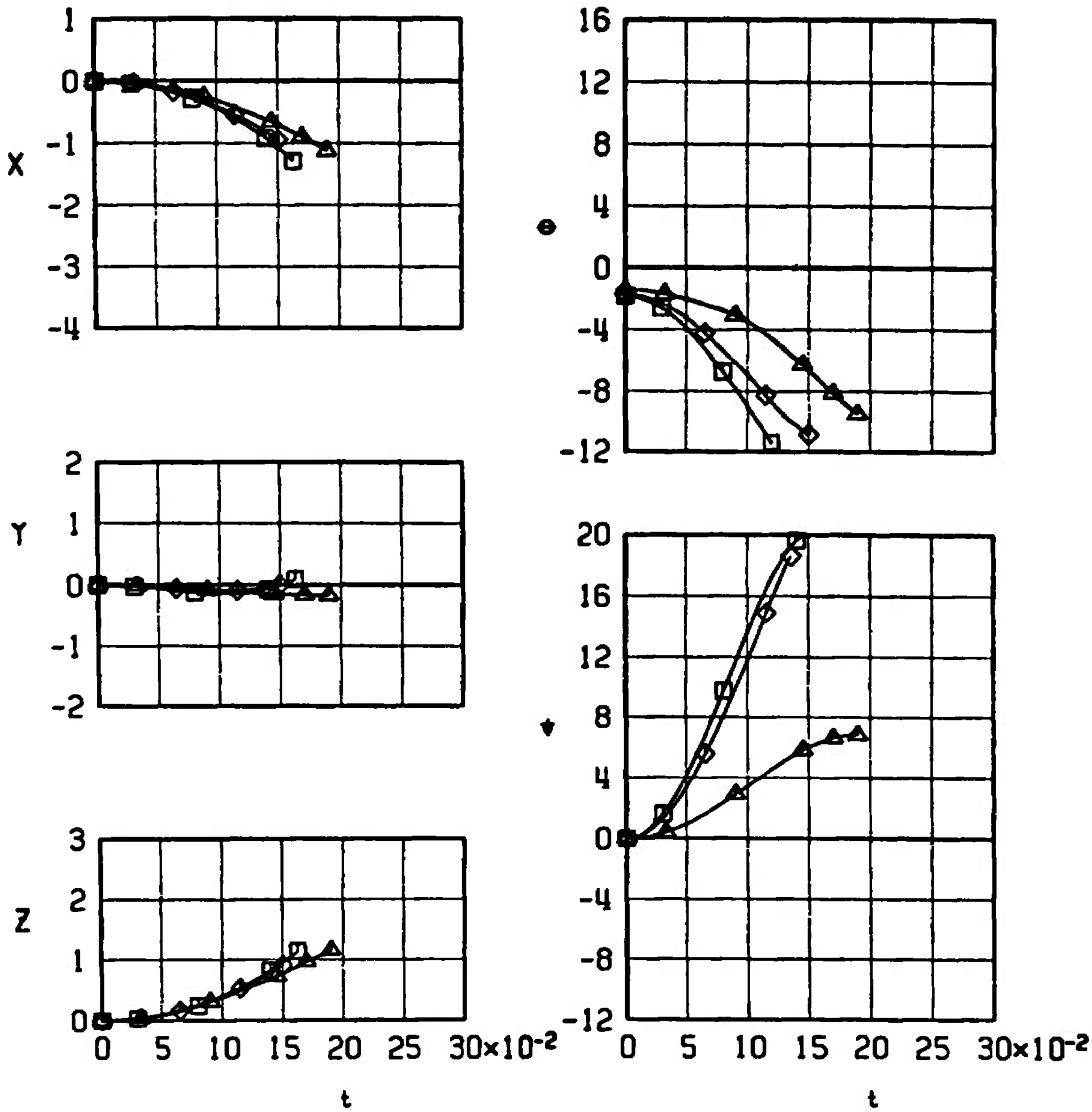

I. Configuration 21, Ejector 2
Fig. 32 Continued

SYMBOL	M_∞	α_p	Λ_{LE}	EJECTOR	CONFIG
△	0.90	1.6	50	1	22
◇	1.15	1.3	50	1	22
◁	1.20	1.4	50	1	22
◆	1.30	1.4	50	1	22

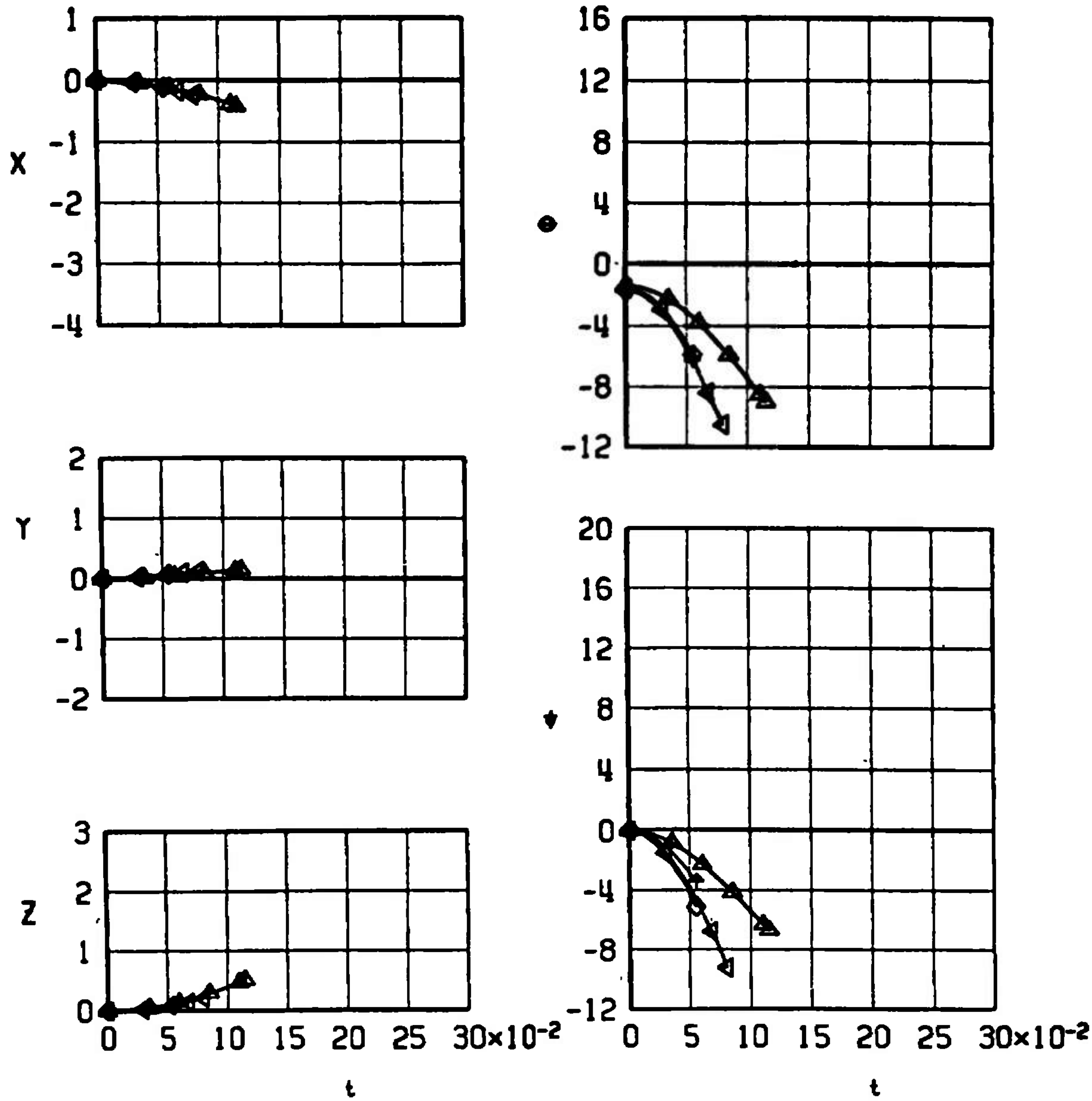

m. Configuration 22, Ejector 1
Fig. 32 Continued

SYMBOL	M_∞	α_p	Λ_{LE}	EJECTOR	CONFIG
△	0.90	1.6	50	2	22
□	1.05	1.2	50	2	22
◇	1.15	1.3	50	2	22

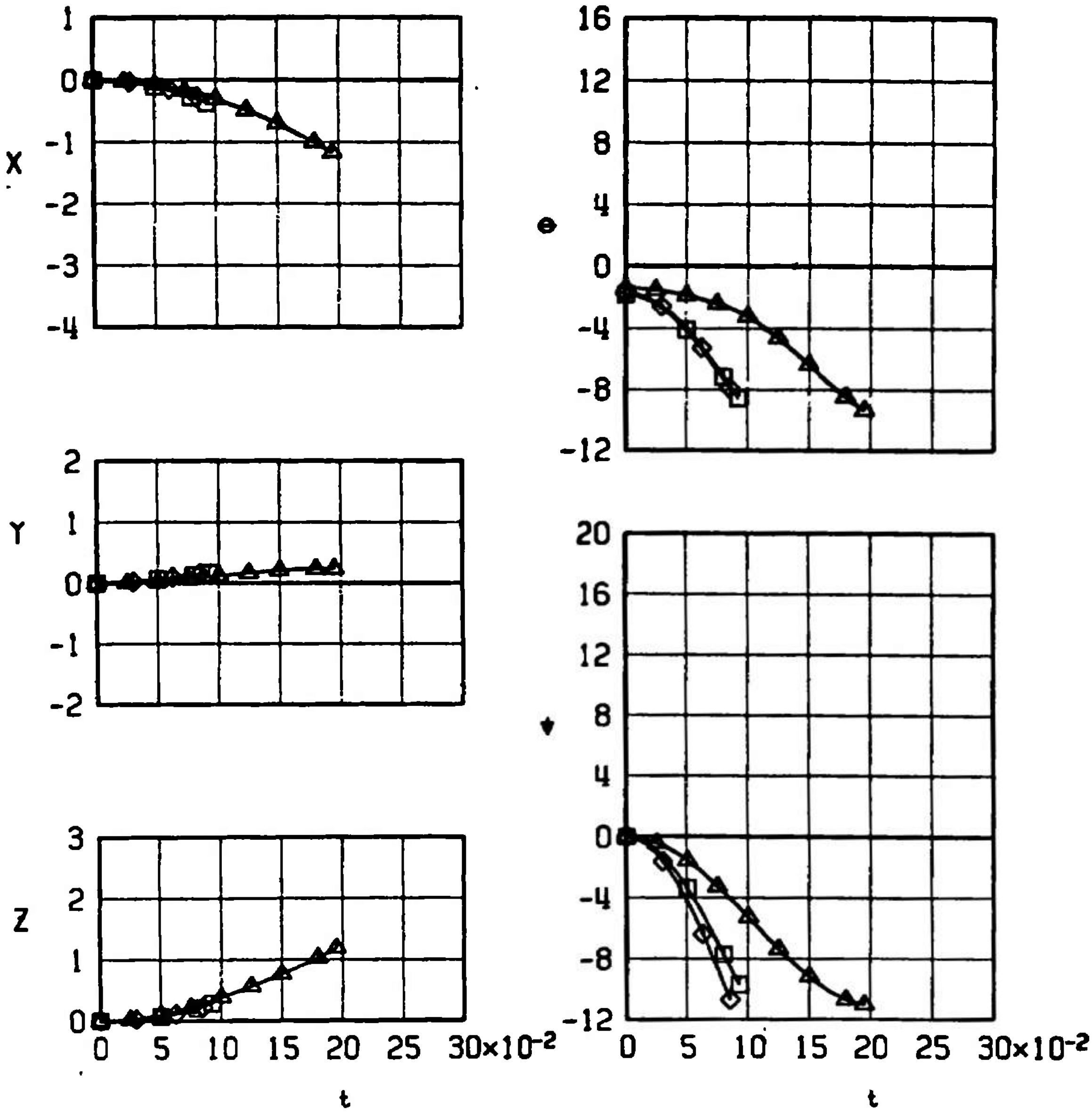

n. Configuration 22, Ejector 2
Fig. 32 Concluded

INB'D	SYMBOL	M_∞	α_p	Λ_{LE}	EJECTOR	CONFIG
	○	0.95	2.7	72.5	2	33
	□	1.05	2.1	72.5	2	33
	◇	1.15	1.5	72.5	2	33
	■	1.05	2.1	72.5	1	33

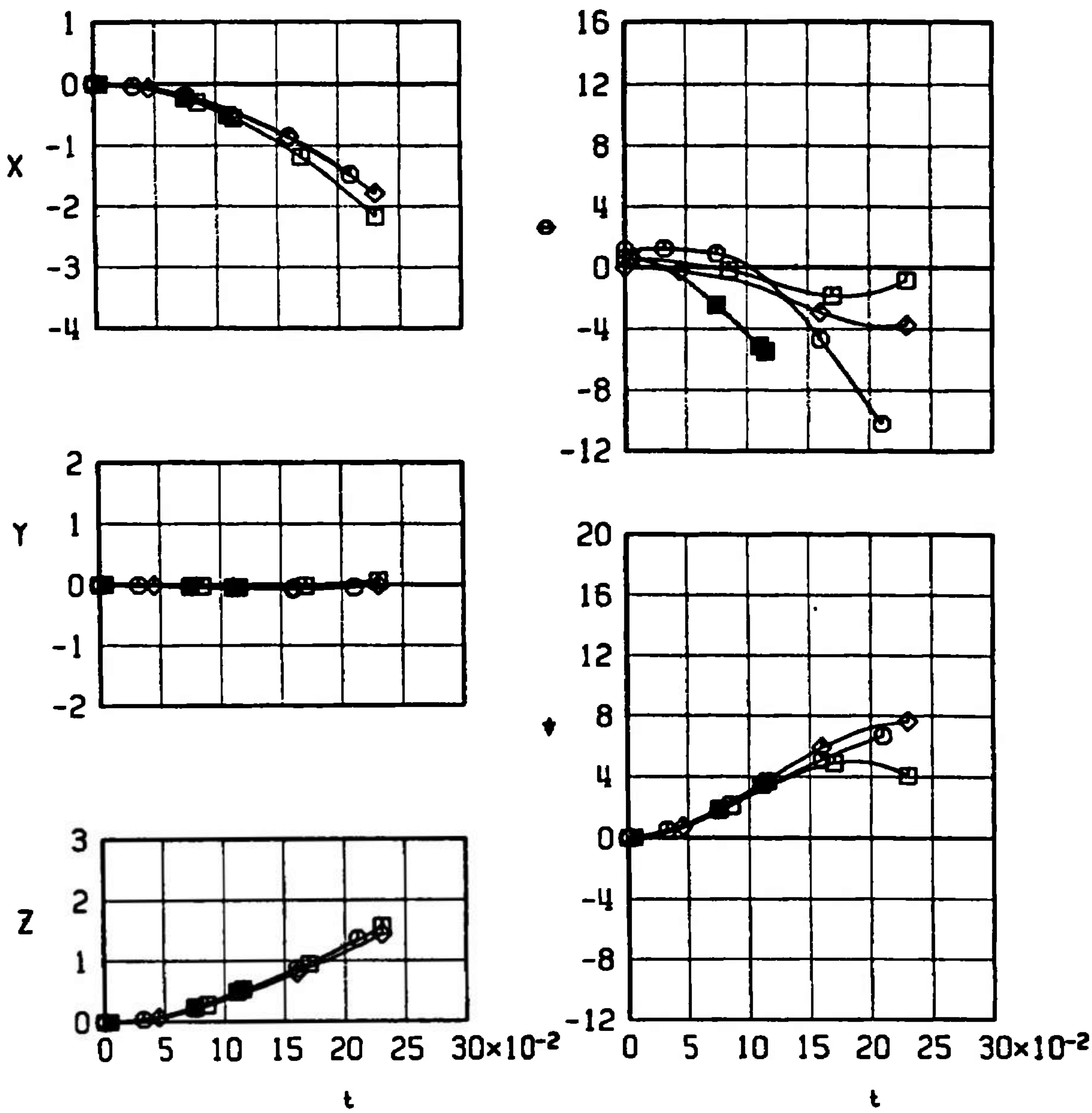

a. Configuration 33

Fig. 33 Mach Number Comparison of the SUU-30H/B Launch Trajectories from the F-111E for Different Ejector Forces, Λ_{LE} = 72.5 deg

OUTB'D	SYMBOL	M_∞	α_p	Λ_{LE}	EJECTOR	CONFIG
	○	0.95	2.7	72.5	2	34
	□	1.05	2.1	72.5	2	34
	◇	1.15	1.5	72.5	2	34

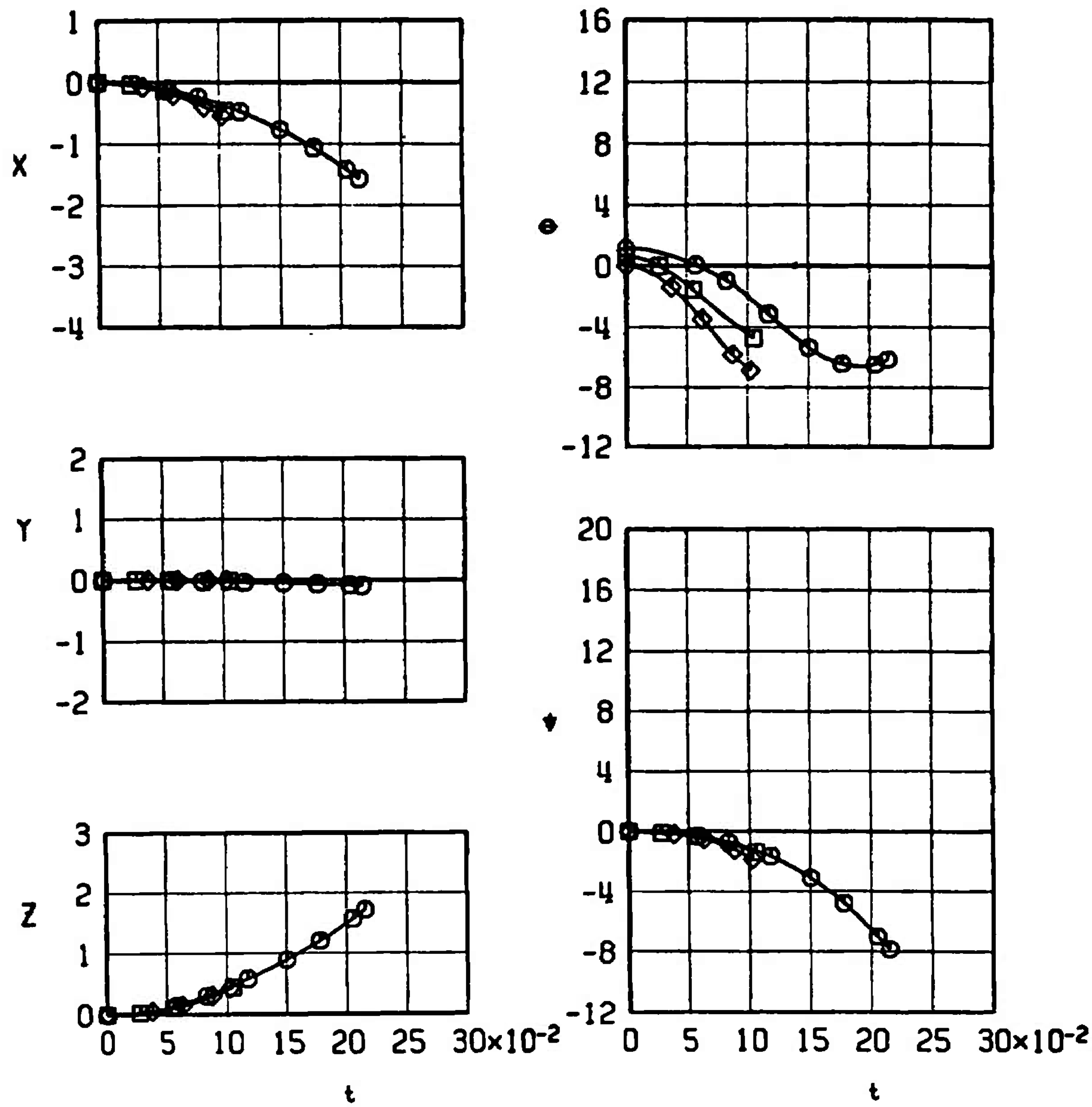

b. Configuration 34
Fig. 33 Continued

OUTB'D	SYMBOL	M_∞	α_p	Λ_{LE}	EJECTOR	CONFIG
	○	0.95	2.7	72.5	1	31
	▷	1.10	1.4	72.5	1	31
	◇	1.15	1.5	72.5	1	31

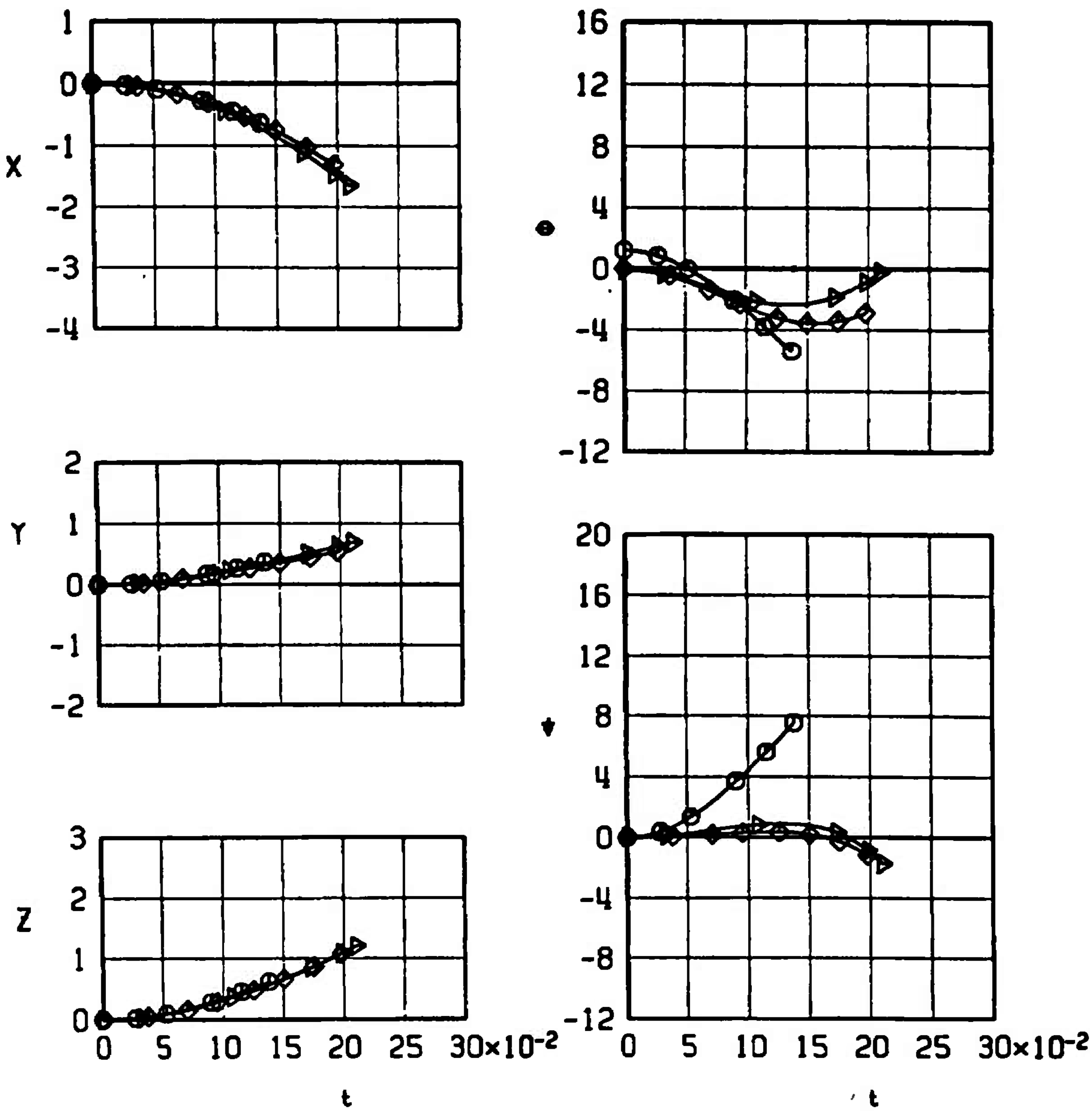

c. Configuration 31, Ejector 1
Fig. 33 Continued

OUTB'D	SYMBOL	M_∞	α_p	Λ_{LE}	EJECTOR	CONFIG
	○	0.95	2.7	72.5	2	31
	□	1.05	2.1	72.5	2	31
	▷	1.10	1.4	72.5	2	31
	◇	1.15	1.5	72.5	2	31
	◁	1.20	3.1	72.5	2	31

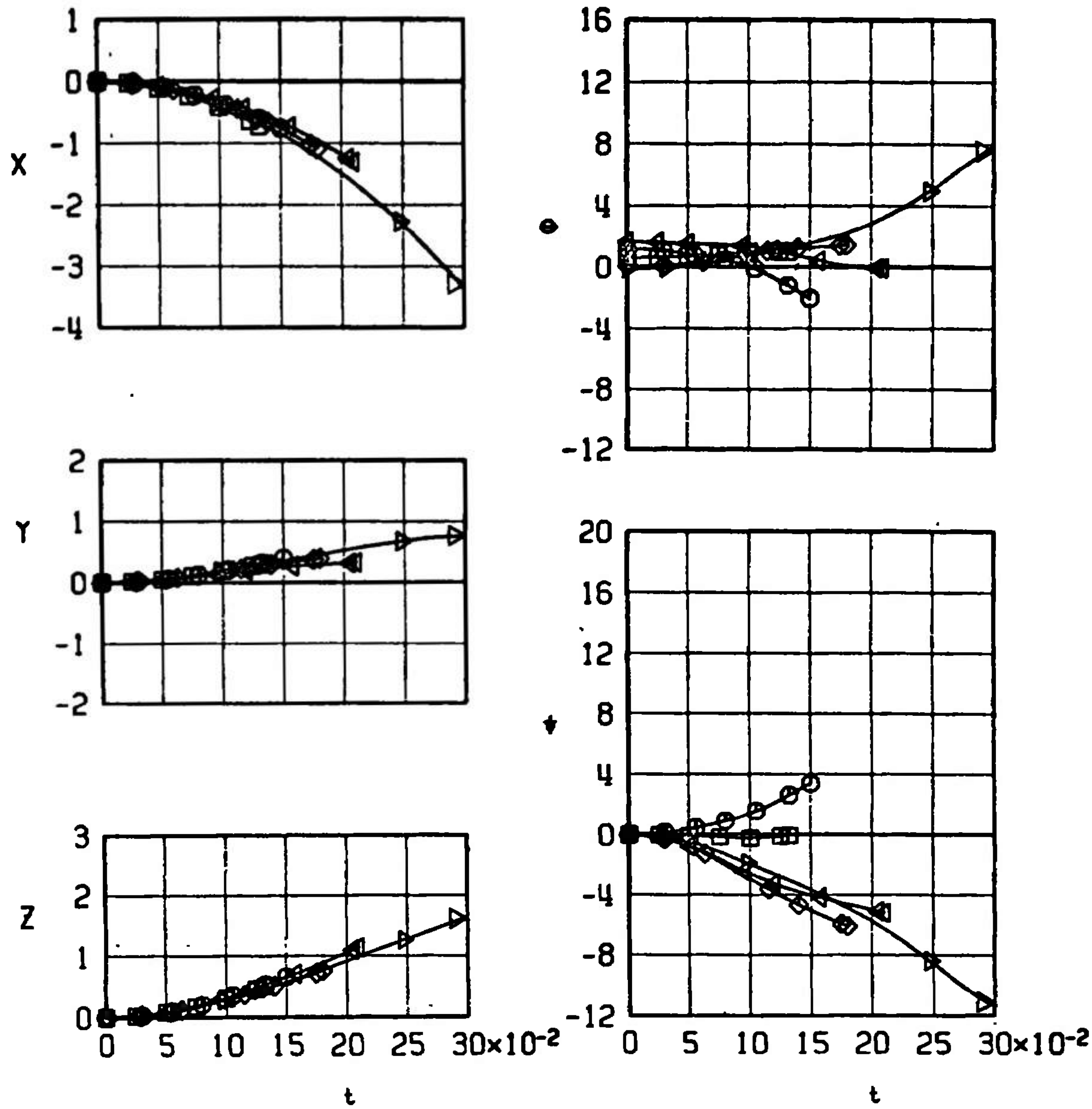

d. Configuration 31, Ejector 2
Fig. 33 Continued

INB'D	SYMBOL	M_∞	α_p	Λ_{LE}	EJECTOR	CONFIG
	○	0.95	2.7	72.5	1	29
	□	1.05	2.1	72.5	1	29
	▷	1.10	1.4	72.5	1	29
	◇	1.15	1.5	72.5	1	29
	◁	1.20	3.1	72.5	1	29
	■	1.05	2.1	72.5	2	29

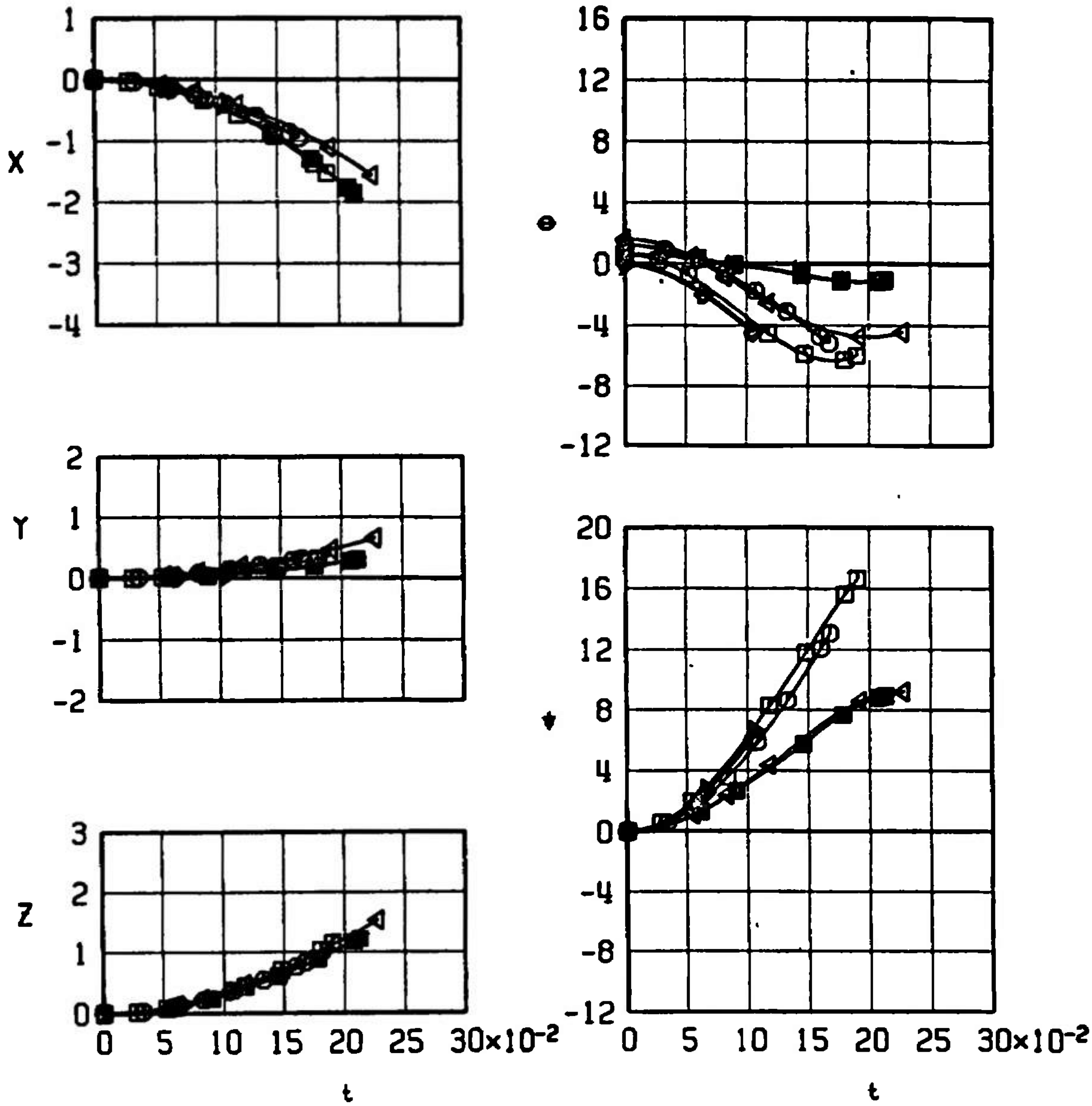

e. Configuration 29
Fig. 33 Continued

OUTB'D	SYMBOL	M_∞	α_p	Λ_{LE}	EJECTOR	CONFIG
	○	0.95	2.7	72.5	1	30
	◇	1.15	1.5	72.5	1	30

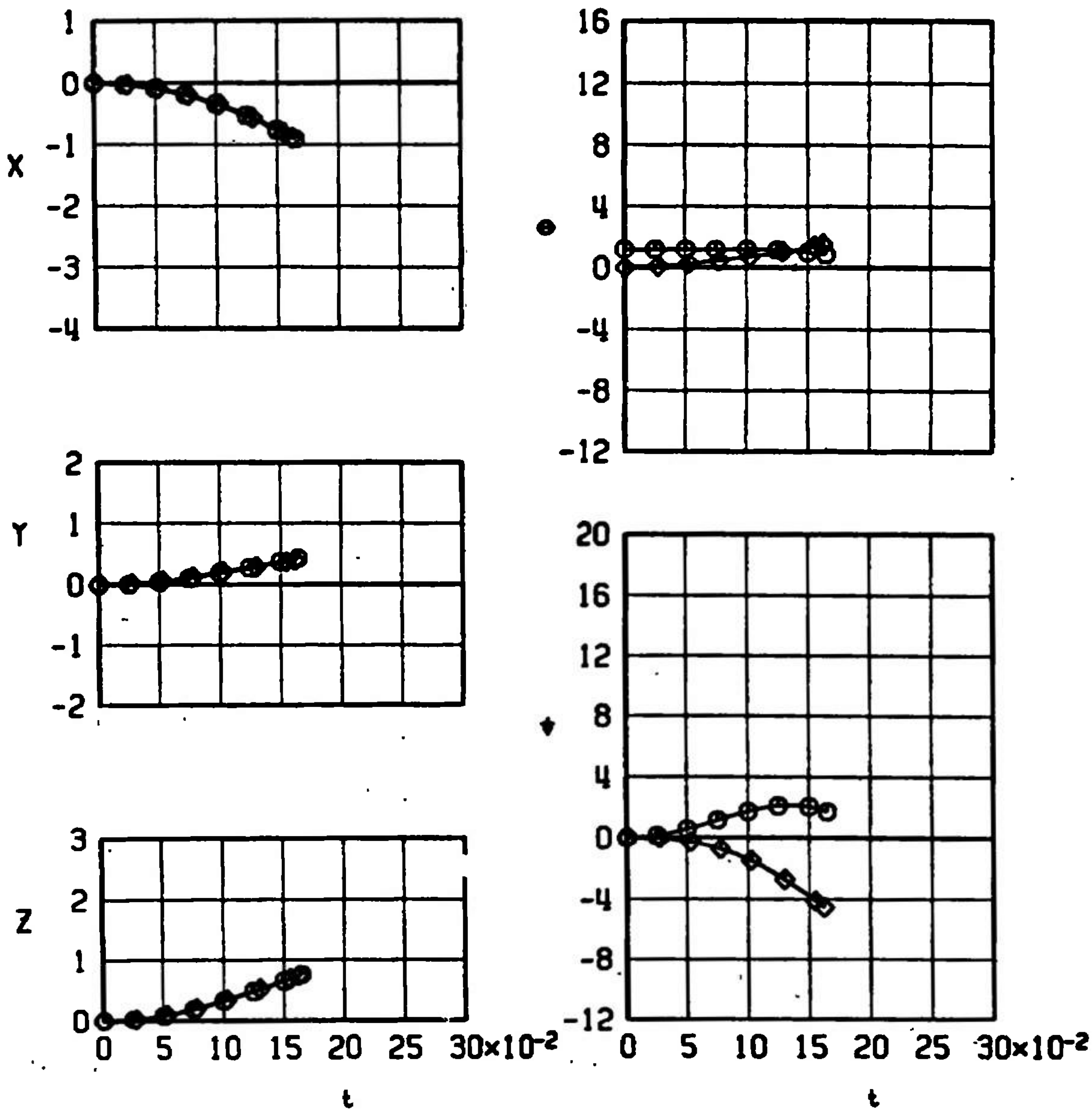

f. Configuration 30
Fig. 33 Continued

INB'D	SYMBOL	M_∞	α_p	Λ_{LE}	EJECTOR	CONFIG
	●	0.95	2.7	72.5	1	28
	○	0.95	2.7	72.5	3	28
	◇	1.15	1.5	72.5	3	28

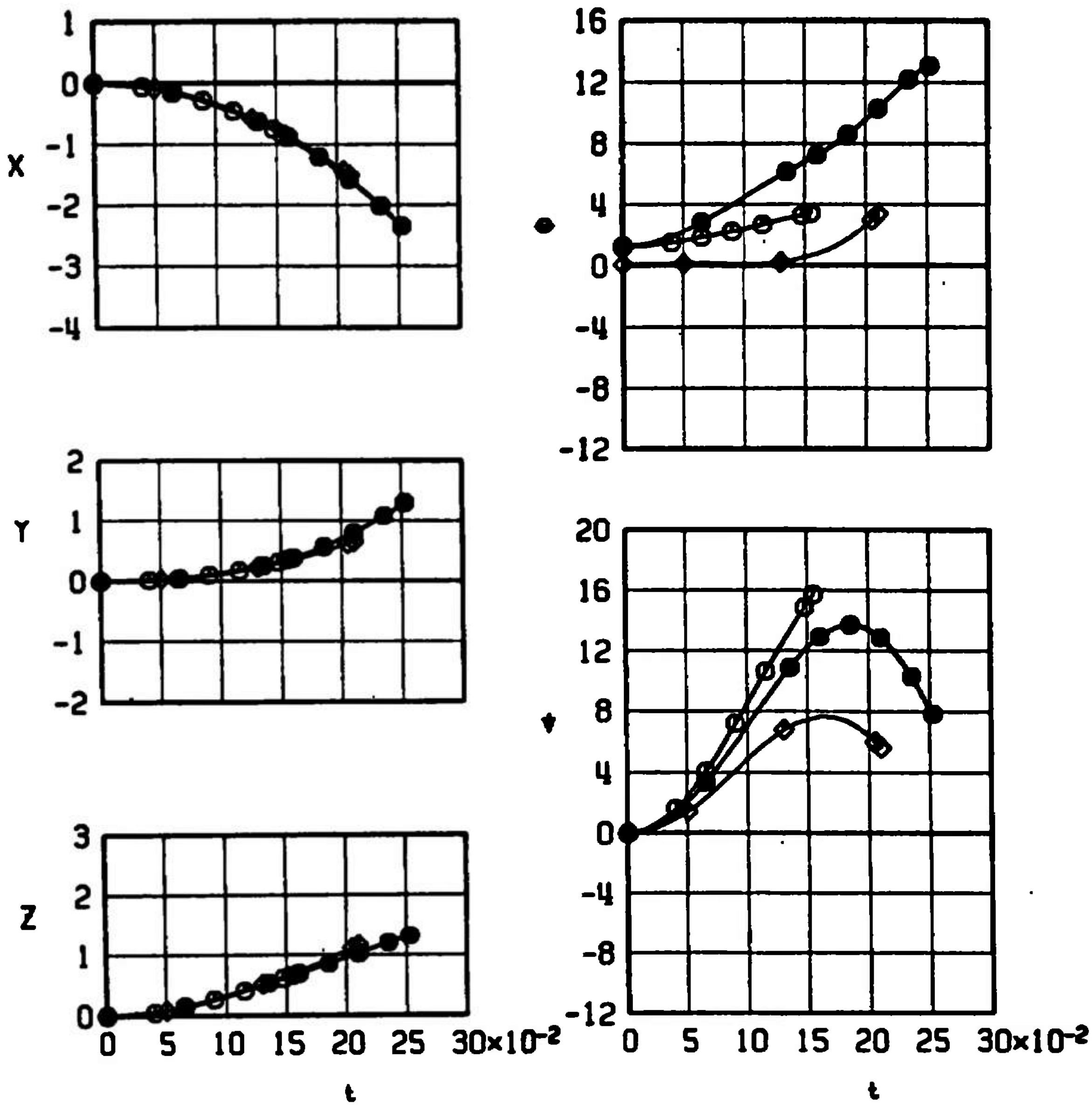

g. Configuration 28
Fig. 33 Continued

OUTB'D	SYMBOL	M_∞	α_p	Λ_{LE}	EJECTOR	CONFIG
	○	0.95	2.7	72.5	1	32
	□	1.05	2.1	72.5	1	32
	◇	1.15	1.5	72.5	1	32
	●	1.15	1.5	72.5	2	32

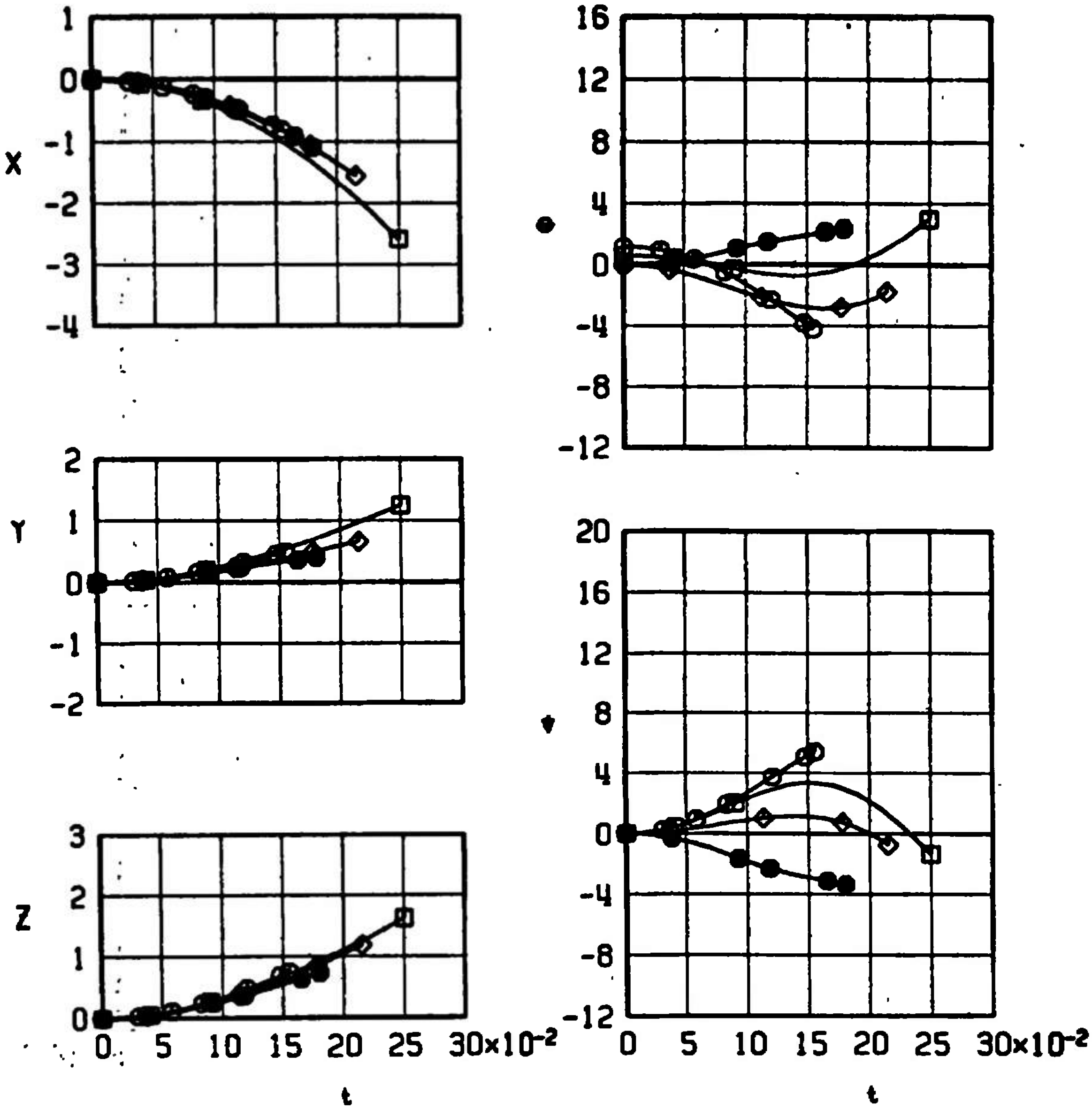

h. Configuration 32
Fig. 33 Continued

INB'D	SYMBOL	M_∞	α_p	Λ_{LE}	EJECTOR	CONFIG
	○	0.95	2.7	72.5	1	25
	□	1.05	2.1	72.5	1	25
	◇	1.15	1.5	72.5	1	25
	●	1.15	1.5	72.5	2	25

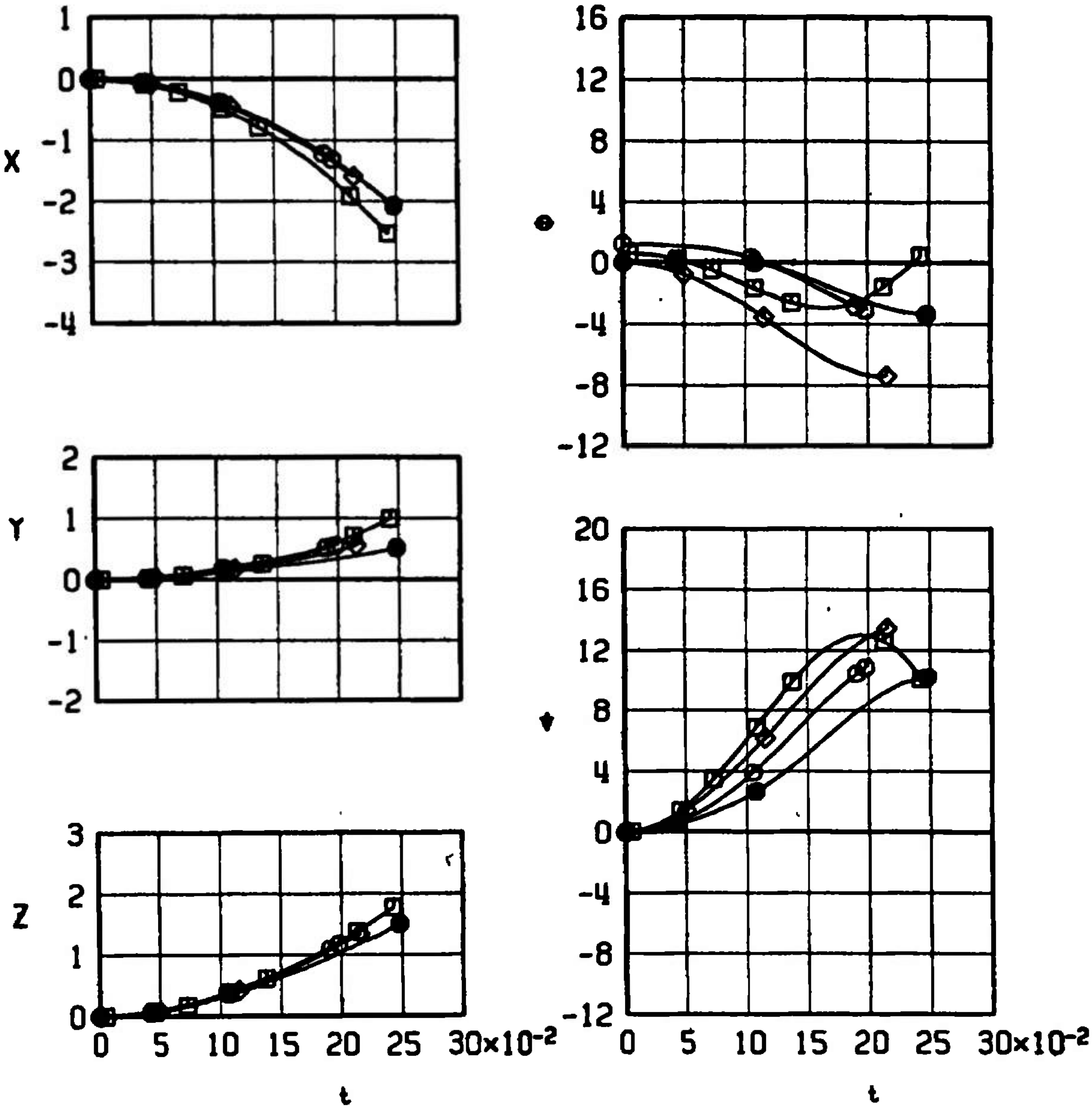

i. Configuration 25
Fig. 33 Continued

OUTB'D	SYMBOL	M_∞	α_p	Λ_{LE}	EJECTOR	CONFIG
	○	0.95	2.7	72.5	1	24
	◇	1.15	1.5	72.5	1	24

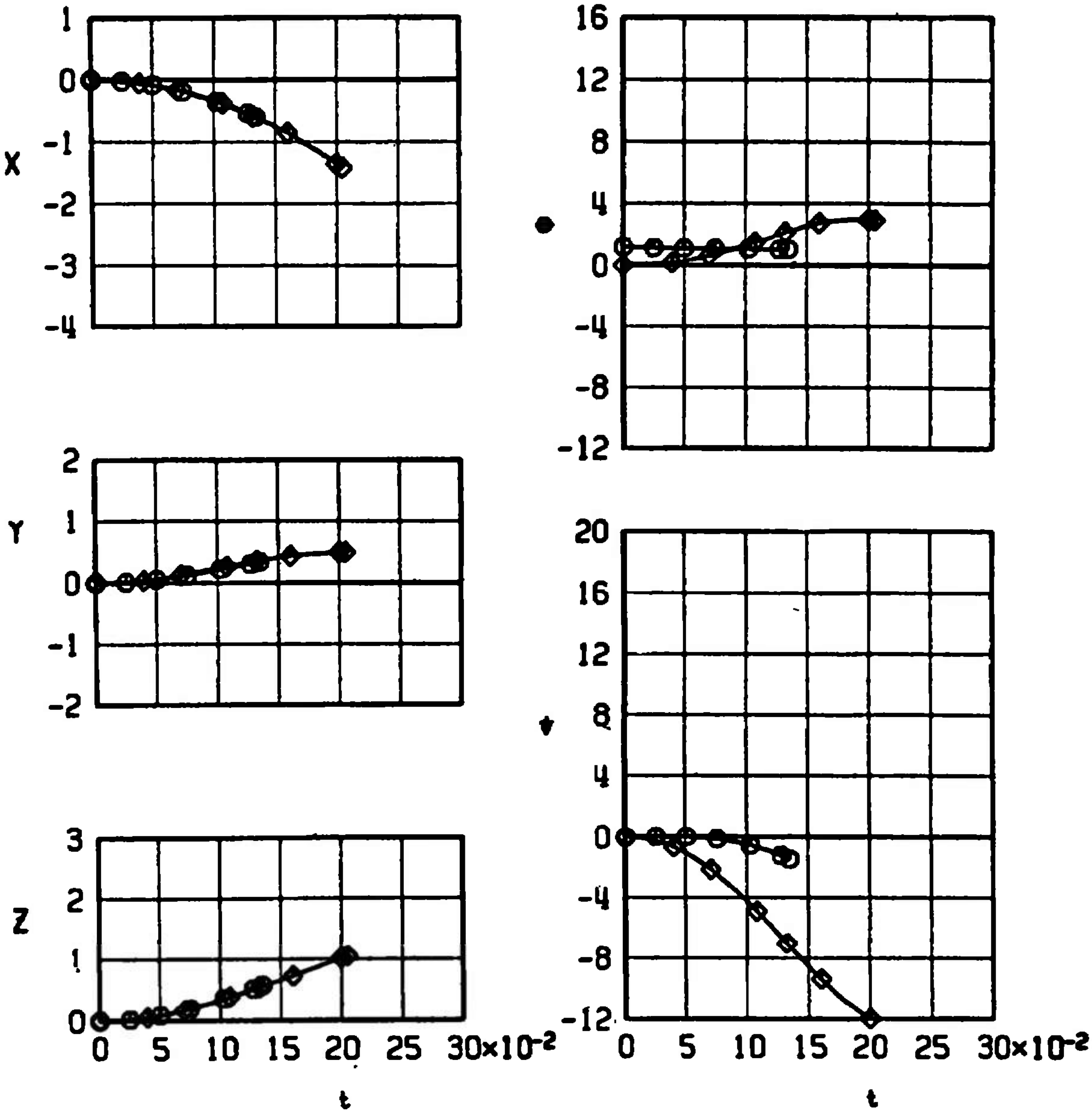

j. Configuration 24
Fig. 33 Continued

INB'D	SYMBOL	M_∞	α_p	Λ_{LE}	EJECTOR	CONFIG
	○	0.95	2.7	72.5	1	23
	□	1.05	2.1	72.5	1	23
	◇	1.15	1.5	72.5	1	23
	●	1.15	1.5	72.5	3	23

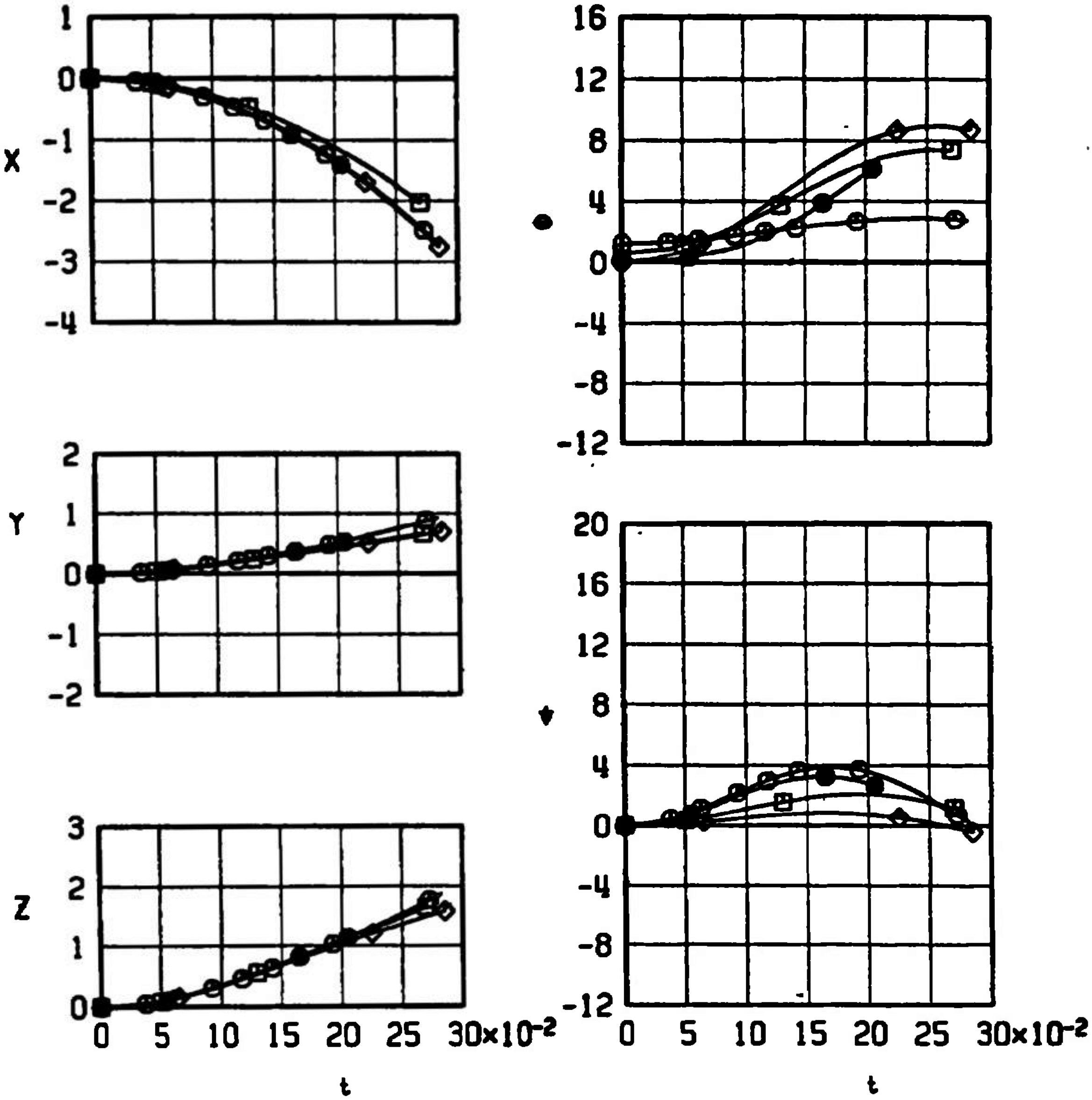

k. Configuration 23
Fig. 33 Continued

SYMBOL	M_∞	α_p	Λ_{LE}	EJECTOR	CONFIG
◇	1.15	2.1	72.5	2	21
♠	1.30	2.2	72.5	2	21

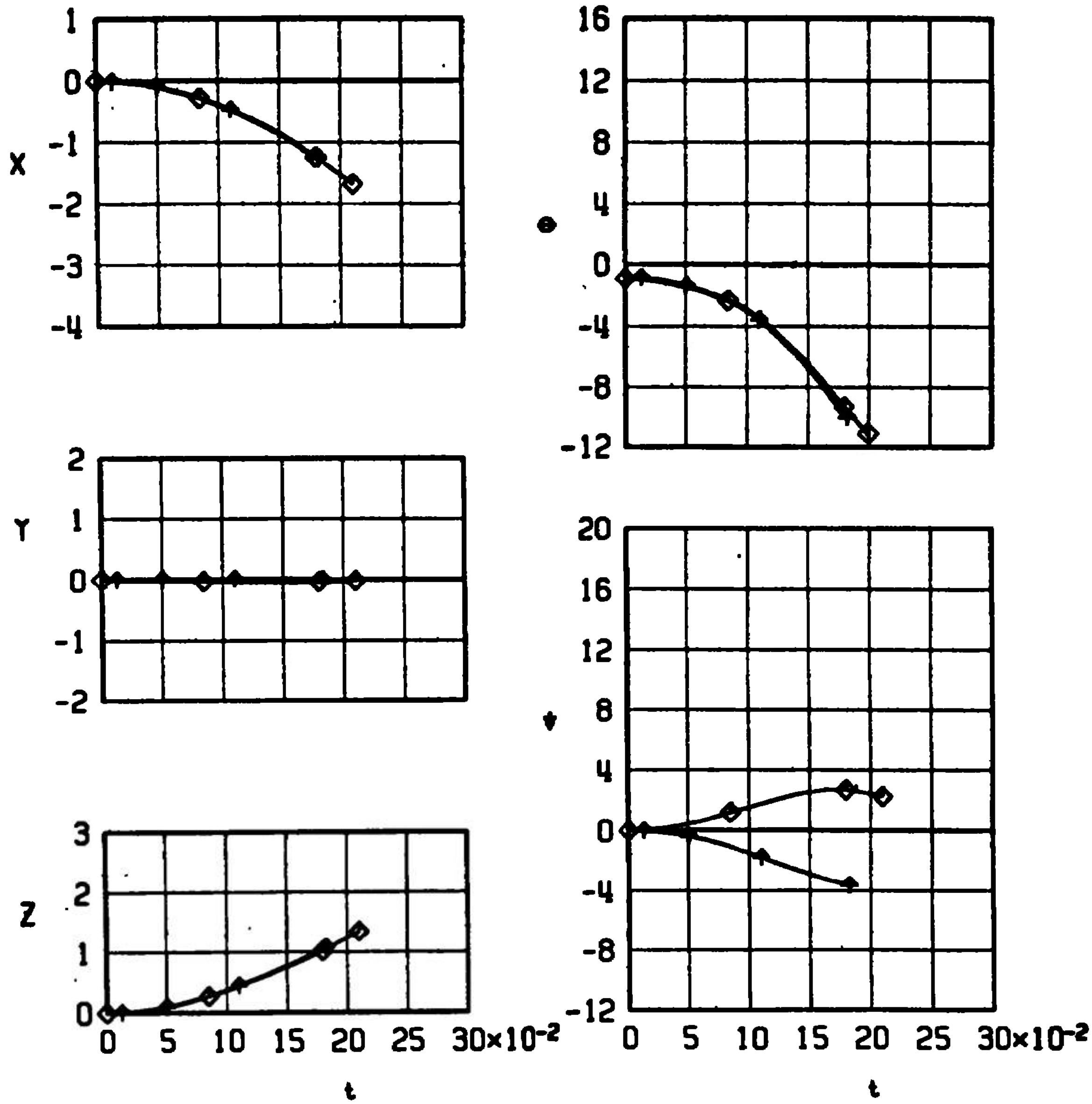

I. Configuration 21
Fig. 33 Continued

SYMBOL	M_∞	α_p	Λ_{LE}	EJECTOR	CONFIG
◇	1.15	2.1	72.5	2	22
✦	1.30	2.2	72.5	2	22

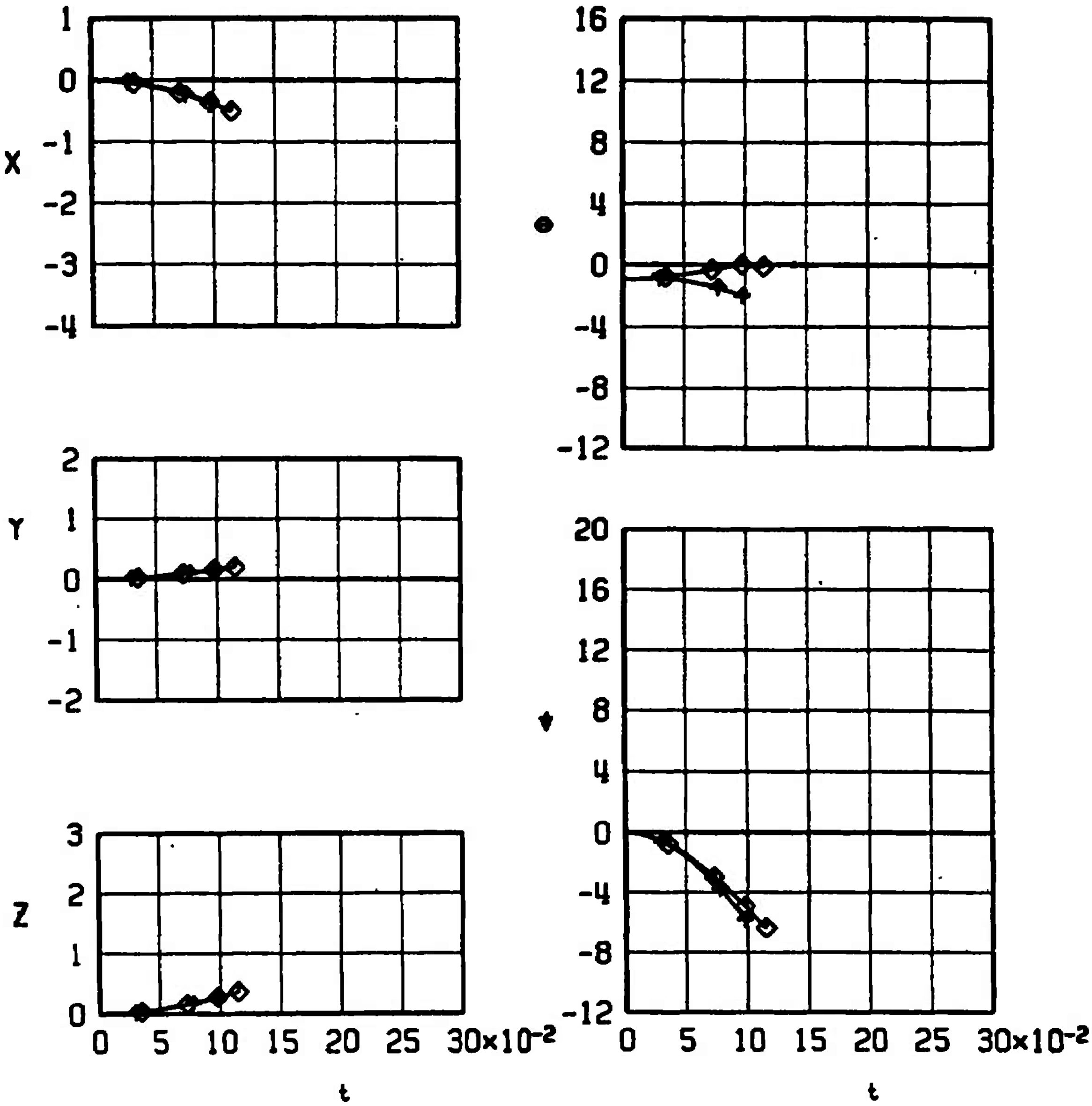

m. Configuration 22
Fig. 33 Concluded

TABLE I
FULL-SCALE STORE PARAMETERS USED IN TRAJECTORY CALCULATIONS

Parameter	MK 82 GPB	SUU 30 H/B (1/20 Scale)	MK-20	MK-84 GPB	MK-84 LGB	MK-84 EOGB	SUU-30 H/B (1/24 Scale)
Mass, $\bar{m}$, slugs	15.7	25.5	15.1	61.2	64.0	70.3	23.3
Center of gravity location, X_{cg}, ft	3.196	3.224 Fwd cg 3.393 Aft cg	3.725	5.000	8.216	6.604	3.267
Center-of-gravity location, Y_{cg}, ft	0	0	0	0	0	0	0
Center-of-gravity location, Z_{cg}, ft	0	0	0	0	0	0	0
Moment of inertia, I_{xx}, slug-ft^2	1.300	5.700	2.100	24.800	24.000	25.000	5.700
Moment of inertia, I_{yy}, slug-ft^2	37.50	60.35	49.80	360.00	416.000	524.000	57.00
Moment of inertia, I_{zz}, slug-ft^2	37.50	60.77	49.80	360.00	416.000	524.000	57.00
Product of inertia, I_{xz}, slug-ft^2	0	0	0	0	0	0	0
Store reference width, b, ft	0.895	1.343	1.106	1.500	1.500	1.500	1.343
Store reference area, S, ft^2	0.629	1.416	0.961	1.767	1.767	1.767	1.416
Location of forward ejector force, X_{L_1}, ft	-0.255	-0.380 Fwd cg -0.213 Aft cg	0.107	0.666	0.595	0.813	0.417
Location of aft ejector force, X_{L_2}, ft	---	---	---	-1.000	-0.071	-0.853	-0.750
Forward ejector force, lb	1100	1100	1100	1500	1500	1500	1) 900 2) 0 3) 1300
Aft ejector force, lb	---	-	---	1500	1500	1500	1) 500 2) 1300 3) 0
Pitch-damping derivative, C_{m_q}, per radian	-54	-54	-48	-120	-275	-110	-54
Yaw-damping derivative, C_{n_r}, per radian	-54	-54	-48	-120	-275	-110	-54
Roll-damping derivative, C_{ℓ_p}, per radian	-2	-2	-1	-10	-20	-10	-2
Ejector stroke length, ft	0.241	0.241	0.241	0.343	0.343	0.343	0.250

TABLE II
F-4C LOAD CONFIGURATIONS

Config.	Left Wing Outboard Pylon	Left Wing Inboard Pylon	Forward Left Missile Well Pylon	Centerline Pylon	Forward Right Missile Well Pylon	Right Wing Inboard Pylon	Right Wing Outboard Pylon
1-1	Empty*	Empty	Clean**	600-gal Fuel Tank	Clean	ALQ 119	MK-82 GPB
1-2	↓	↓	↓	↓	↓	↓	MK-82 GPB
1-3	↓	↓	↓	↓	↓	↓	MK-82 GPB
1-4	↓	↓	↓	↓	↓	↓	MK-82 GPB
1-5	↓	↓	↓	↓	↓	↓	MK-82 GPB
1-6	↓	↓	↓	↓	↓	↓	MK-82 GPB
1-7	↓	↓	↓	↓	↓	↓	MK-82 GPB
1-10	↓	↓	↓	↓	↓	↓	MK-82 GPB
2-6	↓	↓	↓	↓	↓	Empty	MK-82 GPB
2-7	↓	↓	↓	↓	↓	↓	MK-82 GPB
3-7	370-gal Fuel Tank	AGM 65	↓	SUU-30H/B	↓	AGM 65	370 gal Fuel Tank

* Empty denotes no store on pylon
** Clean denotes pylon removed

TABLE II (Continued)

Config.	Left Wing Outboard Pylon	Left Wing Inboard Pylon	Forward Left Missile Well Pylon	Centerline Pylon	Forward Right Missile Well Pylon	Right Wing Inboard Pylon	Right Wing Outboard Pylon
4-7	370-gal Fuel Tank	Empty	Clean	SUU-30H/B	Clean	ALQ 119	370-gal Fuel Tank
5-2		AGM 65		SUU-30H/B	ALQ 119	AGM 65	
5-3				SUU-30H/B			
5-4				SUU-30H/B			
5-5				SUU-30H/B			
5-6				SUU-30H/B			
5-7				SUU-30H/B			
6-7			ALQ 119	SUU-30H/B	Clean		
7-6		Empty	Clean	MK-20		ALQ 119	
8-1		AGM 65		MK-20	ALQ 119	AGM 65	
8-2				MK-20			
8-3				MK-20			

TABLE II (Concluded)

Config.	Left Wing Outboard Pylon	Left Wing Inboard Pylon	Forward Left Missile Well Pylon	Centerline Pylon	Forward Right Missile Well Pylon	Right Wing Inboard Pylon	Right Wing Outboard Pylon
8-4	370-gal Fuel Tank	AGM 65	Clean	MK-20 ●▽● ●▽	ALQ 119	AGM 65	370-gal Fuel Tank
8-5	↓	↓	↓	MK-20 ●▽ ●▽	↓	↓	↓
8-6	↓	↓	↓	MK-20 ●▽ ▽	↓	↓	↓
8-7	↓	↓	↓	MK-20 ▽● ▽	↓	↓	↓
9-6	↓	↓	ALQ 119	MK-20 ●▽ ▽	Clean	↓	↓
10	MK-84 GPB (Dummy)	Empty	Clean	600-gal Fuel Tank	↓	ALQ 119	MK-84 GPB (Launch)
11	↓	↓	↓	↓	↓	Empty	↓
12	370-gal Fuel Tank	MK-84 LGB (Dummy)	↓	Clean	ALQ 119	MK-84 LGB (Launch)	370-gal Fuel Tank
13	↓	↓	↓	↓	Clean	↓	↓
14	AGM 65	↓	↓	600-gal Fuel Tank	ALQ 119	↓	AGM 65
15	370-gal Fuel Tank	MK-84 EOGB (Dummy)	↓	Clean	↓	MK-84 EOGB (Launch)	370-gal Fuel Tank
16	↓	↓	↓	↓	Clean	↓	↓
17	AGM 65	↓	↓	600-gal Fuel Tank	ALQ 119	↓	AGM 65

TABLE III
F-111E LOAD CONFIGURATIONS*

Left Wing			Right Wing		
Config.	Pylon 3	Pylon 4	Config.	Pylon 5	Pylon 6
22	Empty	SUU-30H/B (Launch)	21	SUU-30H/B (Dummy)	SUU-30H/B (Launch)
24	SUU-30H/B 	Clean	23	Clean	SUU-30H/B 
32	SUU-30H/B 		25		SUU-30H/B 
30	SUU-30H/B 		28		SUU-30H/B 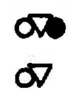
31	SUU-30H/B 		29		SUU-30H/B 
34	SUU-30H/B 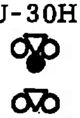		33		SUU-30H/B 

* Note: pylons 1, 2, 7, and 8 are clean for all configurations

UNCLASSIFIED
Security Classification

DOCUMENT CONTROL DATA - R & D

(Security classification of title, body of abstract and indexing annotation must be entered when the overall report is classified)

1 ORIGINATING ACTIVITY (Corporate author) Arnold Engineering Development Center Arnold Air Force Station, Tennessee 37389	2a. REPORT SECURITY CLASSIFICATION UNCLASSIFIED 2b. GROUP N/A

3 REPORT TITLE
SEPARATION CHARACTERISTICS OF SEVERAL MUNITIONS FROM THE F-4C AND F-111E AIRCRAFT AT MACH NUMBERS FROM 0.9 TO 1.6

4 DESCRIPTIVE NOTES (Type of report and inclusive dates)
Final Report - September 18, 1972 to June 14, 1973

5 AUTHOR(S) (First name, middle initial, last name)
J. B. Carman, ARO, Inc.

This document has been approved for public release its distribution is unlimited. Per TAB 76-4 13 Feb, 1976

6 REPORT DATE	7a. TOTAL NO. OF PAGES	7b. NO OF REFS
August 1973	173	2

8a. CONTRACT OR GRANT NO	9a. ORIGINATOR'S REPORT NUMBER(S) AEDC-TR-73-145 AFATL-TR-73-169
b. PROJECT NO 5613	
c. Program Element 64602F	9b. OTHER REPORT NO(S) (Any other numbers that may be assigned this report) ARO-PWT-TR-73-99
d.	

10 DISTRIBUTION STATEMENT ~~Distribution limited to U.S. Government agencies only; this report contains information on test and evaluation of military hardware; August 1973; other requests for this document must be referred to Air Force Armament Laboratory (AFATL/DLJA), Eglin AFB, FL 32542.~~

11 SUPPLEMENTARY NOTES	12 SPONSORING MILITARY ACTIVITY
Available in DDC	Air Force Armament Laboratory (DLJA), Eglin AFB, FL 32542

13. ABSTRACT Wind tunnel tests were conducted using 0.05- and 0.0416-scale models to study the separation characteristics of several munitions from the F-4C and F-111E aircraft, respectively. For the F-4C tests, separation trajectories of the MK-82 GPB, SUU-30H/B, MK-20 "Rockeye," MK-84 GPB, MK-84 LGB, and MK-84 EOGB stores were initiated from a multiple ejection rack (MER) on the right wing outboard and centerline pylons or from the right wing outboard and inboard pylons alone. Data were obtained at Mach numbers from 1.05 to 1.6 at simulated altitudes of 5,000 to 30,000 ft. Other simulated flight variables included dive angle (0 to 60 deg), parent aircraft acceleration (1 to 3 g), and store cg position. For the F-111E tests, separation trajectories of the SUU-30H/B store were initiated from a multiple rack (BRU-3A/A) on the numbers 3 and 6 pylons or from pylon numbers 4 and 6 alone. Data were obtained at Mach numbers from 0.9 to 1.3 at simulated altitudes of 5,000 to 20,000 ft. Other simulated flight variables included parent-aircraft wing sweep angle (50 and 72.5 deg) and different ejector forces.

~~Distribution limited to U.S. Government agencies only; this report contains information on test and evaluation of military hardware; August 1973; other requests for this document must be referred to Air Force Armament Laboratory (AFATL/DLJA), Eglin AFB, FL 32542.~~

DD FORM 1 NOV 65 1473

UNCLASSIFIED
Security Classification

14 KEY WORDS	LINK A		LINK B		LINK C	
	ROLE	WT	ROLE	WT	ROLE	WT
F-4C aircraft						
F-111E aircraft						
ammunition						
external stores						
MK-82 GPB						
SUU-30H/B						
MK-20 "Rockeye"						
MK-84 GPB						
MK-84 LGB						
MK-84 EOGB						
bomb trajectories						
transonic flow						
aerodynamic characteristics						
wind tunnel tests						

AFSC
Arnold AFS Tenn